A STUDY OF THE MAGNETIC AMPLIFIER

WILLIAM EELLS BETZER
WILLIAM RICHARD WERNER

Library
U. S. Naval Postgraduate School
Monterey, California

Mont 154
8854

Thesis
B48

A STUDY OF THE MAGNETIC AMPLIFIER

by

William Wells Betzer
Lieutenant Commander, United States Navy
B.S.
from the
United States Naval Academy
December 1941

and

William Richard Werner
Lieutenant Commander, United States Navy
B.S.
from the
United States Naval Academy
December 1941

Submitted in Partial Fulfillment of the Requirements

for the Degree of Master of Science

from the

Massachusetts Institute of Technology

Department of Electrical Engineering

September 1948

Thesis
B48

A STUDY OF THE MAGNETIC AMPLIFIER

by

William Nello Peterer
Lieutenant Commander, United States Navy
B.S.
From the
United States Naval Academy
December 1941

and

William Richard Werner
Lieutenant Commander, United States Navy
B.S.
From the
United States Naval Academy
December 1941

Submitted in Partial Fulfillment of the Requirements

for the Degree of Master of Science

from the

Massachusetts Institute of Technology

Department of Electrical Engineering

September 1948

ACKNOWLEDGMENT

The authors wish to extend their grateful appreciation to Professor Samuel H. Caldwell, who made the facilities of the M.I.T. No. 1 Differential Analyzer available for this study; to Mr. John L. C. Löf and Mr. Herbert P. Grossimon, who assisted in the Analyzer studies; to Mr. Harold B. Rex and Mr. Arthur O. Black, of the Bureau of Ordnance, Navy Department, who provided the ferromagnetic cores for use in the experimental investigations; and especially to Professor William H. Radford, who supervised the research.

11256

ACKNOWLEDGMENT

The authors wish to extend their grateful appreciation to Professor Samuel H. Caldwell, who made the facilities of the M.I.T. No. 1 Differential Analyzer available for this study; to Mr. John L. Ogg and Mr. Herbert P. Groseimon, who assisted in the Analyzer studies; to Mr. Herold B. Rex and Mr. Arthur O. Black, of the Bureau of Ordnance, Navy Department, who provided the ferromagnetic cores for use in the experimental investigations; and especially to Professor William H. Radford, who supervised the research.

TABLE OF CONTENTS

Page

ACKNOWLEDGMENT 2

ABSTRACT 5

CHAPTER I
INTRODUCTION

The Magnetic Amplifier 8

Elementary Theory of Operation 12

Nature of the Thesis Study 17

CHAPTER II
THE MAGNETIC CIRCUIT

Introduction 20

Selection of the Cores 20

Measurement of Magnetic Properties 30

Winding the Toroids. 37

CHAPTER III
EXPERIMENTAL STUDIES OF THE BASIC CIRCUIT

Introduction 45

The Experimental Circuit 45

Static Performance of the Basic Circuit. 48

Amplifier Dynamics Studied by Transient Response . . 73

Amplifier Dynamics Studied by Frequency Response . . 82

Summary. 99

CHAPTER IV
MATHEMATICAL ANALYSIS OF THE MAGNETIC AMPLIFIER

Introduction to the Analytical Problem 100

Formulation of the Equations 102

Preparation of the Differential Analyzer Problem . 108

Approximations, Limitations and Difficulties . . . 115

Nature of the Analytical Solutions 120

The Concept of Buildup of Flux Bias. 131

TABLE OF CONTENTS

ACKNOWLEDGMENT ii

ABSTRACT iii

CHAPTER I
INTRODUCTION

The Magnetic Amplifier 1

Elementary Theory of Operation 12

Nature of the Thesis Study 17

CHAPTER II
THE MAGNETIC CIRCUIT

Introduction 20

Selection of the Cores 20

Measurement of Magnetic Properties 30

Winding the Toroids. 37

CHAPTER III
EXPERIMENTAL STUDIES OF THE BASIC CIRCUIT

Introduction 41

The Experimental Circuit 43

Static Performance of the Basic Circuit. 49

Amplifier Dynamics Studied by Transient Response . . 73

Amplifier Dynamics Studied by Frequency Response . . 80

Summary. 94

CHAPTER IV
MATHEMATICAL ANALYSIS OF THE MAGNETIC AMPLIFIER

Introduction to the Analytical Problem 100

Formulation of the Equations 108

Preparation of the Differential Analysis Problem . 108

Approximations, Limitations and Difficulties . . . 113

Nature of the Analytical Solutions 130

The Concept of Building of Flux Time. 131

Page

The Analytical Steady-State Behavior 135

The Analytical Transient Behavior 148

Conclusions Regarding the Analytical Studies 166

CHAPTER V
REGENERATIVE FEEDBACK IN MAGNETIC AMPLIFIERS

The Use of Regenerative Feedback in Magnetic Amplifiers. 168

Theory of Regenerative Feedback in Magnetic Amplifiers. 169

Static Characteristics of Feedback Operation 174

Theory of Feedback Gain. 184

Dynamic Performance with Regenerative Feedback . . . 188

Analytical Equations for Regenerative Feedback . . . 191

CHAPTER VI
SUMMARY AND CONCLUSIONS

Summary of the Research 195

Results of the Research 196

Conclusions. 198

Suggestions for Further Work 201

APPENDIX
SAMPLE DESIGN PROCEDURE

Specifications 204

Flux Adjustment for Static Linear Operation. 204

Design for Dynamic Operation 205

Addition of Feedback Windings. 207

BIBLIOGRAPHY 208

Page

The Analytical Steady-State Behavior 132

The Analytical Transient Behavior 148

Conclusions Regarding the Analytical Results . . . 166

CHAPTER V

REGENERATIVE FEEDBACK IN MAGNETIC AMPLIFIERS

The Use of Regenerative Feedback in Magnetic Amplifiers. 186

Theory of Regenerative Feedback in Magnetic Amplifiers. 189

Static Characteristics of Feedback Operation . . . 194

Theory of Feedback Gain. 194

Special Performance with Regenerative Feedback . . . 210

Analytical Equations for Regenerative Feedback . . . 231

CHAPTER VI

SUMMARY AND CONCLUSIONS

Summary of the Research 251

Results of the Research 256

Conclusions. 264

Suggestions for Further Work 271

APPENDIX

MAGNETIC AMPLIFIER TERMINOLOGY

Specifications 274

Flux Adjustment for Static Linear Operation. . . . 284

Design for Pyramid Operation 288

Addition of Feedback Winding. 297

BIBLIOGRAPHY 308

A STUDY OF THE MAGNETIC AMPLIFIER

ABSTRACT

In this thesis an attempt has been made to determine the fundamentals of magnetic-amplifier performance both from experimental and theoretical studies. Although the steady-state behavior of the magnetic amplifier has been discussed in some detail in the literature, relatively little concrete information is available in regard to the dynamic performance. Studies have been made in the thesis to put circuit performance on a quantitative basis. Steady-state behavior has been expressed in the form of modulation characteristics and power-gain and power-output curves. The dynamics of the system are expressed in terms of effective characteristic time as determined by means of both transient and frequency-response data.

The major portion of the effort was directed towards the investigation of the basic-amplifier circuit without feedback. The nonlinear loop-equilibrium differential equations which describe this system were set up and solved by means of the M.I.T. Differential Analyzer No. 1. Solutions thus obtained were then compared with experimental data. Satisfactory agreement between analytic and experimental steady-state performance was observed. Significant differences were noted, however, between experimental and analytic transients. Although the control

A STUDY OF THE MAGNETIC AMPLIFIER

ABSTRACT

In this thesis an attempt has been made to determine the fundamental of magnetic-amplifier performance both from experimental and theoretical studies. Although the steady-state behavior of the magnetic amplifier has been discussed in some detail in the literature, relatively little concrete information is available in regard to the dynamic performance. Studies have been made in the thesis to put circuit performance on a quantitative basis. Steady-state behavior has been expressed in the form of modulation characteristics and power-gain and power-output curves. The dynamics of the system are expressed in terms of effective characteristic time as determined by means of both transient and frequency-response data.

The major portion of the effort was directed toward the investigation of the basic-amplifier circuit without feedback. The nonlinear loop-equilibrium differential equations which describe this system were set up and solved by means of the M.I.T. Differential Analyzer No. 1. Solutions thus obtained were then compared with experimental data. Satisfactory agreement between analytic and experimental steady-state performance was observed. Significant differences were noted, however, between experimental and analytic transients. Although the eventual

circuit appears to have been adequately described by the equations, the neglect of the functional dependence of core loss upon carrier-circuit constants and excitation introduced considerable error in the analytic transient. The value of the differential analyzer has not been confined to providing rapid solutions of difficult nonlinear equations, but is enhanced by giving a physical significance to the equations which is acquired from observation of the relative shaft motions which represent system variables.

Upon completion of the studies of the basic circuit, the remaining available time was allotted to experimental investigation of regenerative ampere-turn feedback. Careful balance of the feedback rectifier-bridge was found necessary to maintain symmetry in the carrier-current waveform. Further study of the feedback connection is indicated.

The magnetic-core material used in the saturable reactors was three-mil Allegheny Electrical Alloy #4750 which had been given a special magnetic anneal to produce high initial permeability and a sharp break at the knee of the magnetization curve. This was the best available material, although better cores now exist. The normal magnetization curve, which was measured by ballistic galvanometer techniques before winding the amplifier cores, was used in the machine solution as the nonlinear function

relating flux and magnetizing force.

The results of the amplifier studies indicate the way in which the various circuit parameters affect gain and bandwidth. It has been shown that a compromise between the two, consistent with the requirements of any specific application, must be sought. The principal limitation of this highly inductive device is its inherently narrow bandwidth. The use of positive feedback permits an improvement in the power gain by a factor of 100 or better, with an accompanying reduction of the pass-band. Further studies should indicate whether or not an overall gain-bandwidth improvement can be expected from the feedback connection.

A STUDY OF THE MAGNETIC AMPLIFIER

CHAPTER I

INTRODUCTION

The Magnetic Amplifier

Throughout the last thirty years, the use of the vacuum tube in all types of electrical circuitry has become widespread. The versatility and adaptability of this unique device has made it an indispensible part of the physical world, and its application has made possible scientific accomplishments which were undreamed of at the turn of the century. In 1925, however, the invention of the dry-disc rectifier by L. O. Grondahl marked the beginning of a period in which efforts were directed by many engineers toward the development of simple devices which would replace the vacuum tube in certain applications. This direction of interest into components which might compete with the vacuum tube, it should be remembered, occurred at a time when the use and application of the vacuum tube was in marked ascendancy, and it is obvious that a very small portion of the interest of the electrical engineering profession was directed into the more uninteresting competitive components when the triode and its variations seemed to supply most existing needs.

In the past decade, interest in vacuum-tube substitutes has achieved a new momentum marked by the practical use of germanium-diode and silicon-diode mixers and detectors in high-frequency-communications circuits, extensive utiliza-

A STUDY OF THE MAGNETIC AMPLIFIER

CHAPTER I

INTRODUCTION

The Magnetic Amplifier

Throughout the last thirty years, the use of the vacuum tube in all types of electrical circuitry has become widespread. The versatility and adaptability of this unique device has made it an indispensable part of the physical world, and its application has made possible scientific accomplishments which were undreamed of at the turn of the century. In 1907, however, the invention of the dry-disc rectifier by L. O. Grondahl marked the beginning of a period in which efforts were directed by many engineers toward the development of simple devices which would replace the vacuum tube in certain applications. This direction of interest into components which might compete with the vacuum tube, it should be remembered, occurred at a time when the use and application of the vacuum tube was in marked ascendancy, and it is obvious that a very small portion of the interest of the electrical engineering profession was directed into the more uninteresting competitive components when the triode and its variations seemed to supply most existing needs.

In the past decade, interest in vacuum-tube substitutes has achieved a new momentum marked by the practical use of germanium-diode and silicon-diode mixers and detectors in high-frequency-communications circuits, extensive utiliza-

tion of dry-disc rectifiers of the selenium type in power-supply circuits, the use of mechanical rectifiers in power circuits, the development and application of the magnetic amplifier, and very recently, the introduction of the Bell Laboratories' "transistor" amplifier. The inevitable replacement of the vacuum tube in many useful applications is a foregone conclusion, and undoubtedly the magnetic amplifier, when its dynamic and steady-state behavior is fully understood, will provide a useful addition to the tools of the electrical engineer.

Amplification is obtained in the magnetic amplifier through utilization of the saturation effects in an iron core under excitation by either an alternating current and a direct current, or by two alternating currents of different frequencies. The magnetic amplifier is a direct-current amplifying circuit of the carrier-frequency type in which the carrier is modulated by an input signal in a magnetically biased saturable-reactor unit. The amplified input signal is subsequently recovered in a demodulator system. The inductance of the magnetic circuit of this type is high, and an inherently slow time-response is associated with highly inductive devices of this type. Investigations of magnetic amplifier circuitry require attention to the improvement of either the gain or the time-response of the amplifier without undue sacrifice of the other factor.

The magnetic amplifier was originally developed in

successful form in 1912 by E. F. W. Alexanderson, of the General Electric Company, who used the device as an amplifier-modulator for voice-frequency amplitude-modulation of the output of a radio-frequency alternator. The magnetic amplifier enjoyed an early prominence in the field of wireless communications, but was soon superseded by the vacuum-tube amplifier as the triode was perfected and applied.

During the period between the great World Wars, various improvements of the magnetic amplifier appeared. The perfection of the dry-disc rectifier in 1925 provided the necessary component for the construction of a tubeless amplifier, the use of cascaded magnetic amplifiers, and the use of regenerative-feedback for the improvement of magnetic amplifier gain. In general, however, magnetic amplifier development was retarded because of the intense interest in vacuum-tube circuitry.

The nonlinear character of the inductance of the saturable core has made analytical study of the magnetic amplifier very difficult. Various methods of approach involving linear approximation of the magnetizing characteristic have been developed from the original method proposed by A. Boyajian in 1931. In general, however, most magnetic amplifiers have been designed from empirical considerations.

In the years preceding the outbreak of the recent war, German engineers recognized the fact that improvements in magnetic materials and in rectifier units gave the mag-

netic amplifier a new potential value. Extensive studies were conducted in Germany during the War, and the successes of these researches have been viewed with great interest in this country and in England.

The time-response problem has been studied rather extensively at the Servomechanisms Laboratory at the Massachusetts Institute of Technology. Degenerative-feedback techniques were applied to this problem, but results were not wholly encouraging, primarily because of the low quality magnetic materials from which the cores were constructed. The device has, however, proved to be a satisfactory servo-amplifier for limited applications when the period of cyclic variations of the system is long.

The magnetic amplifier is admirably suited to many military and industrial applications in which ruggedness and freedom from the need for frequent attention are of paramount importance. In contrast with the vacuum-tube amplifier, the magnetic device is totally shock and impact resistant, is not subject to deterioration with age or with use, and, with proper design, may display efficiencies of the order of 90%. The vacuum tube amplifier represents a variable ohmic resistance, and is, therefore, an inherently lossy device. The magnetic amplifier can be designed to be nearly purely reactive, and is, therefore, capable of theoretically lossless performance. Magnetic amplifiers are free from the need for complicated power supplies since all power is furnished by an a-c source. The magnetic

amplifier can provide high gains while maintaining compact construction.

The response of the vacuum-tube amplifier is essentially, within the designed band-width, independent of frequency. The magnetic amplifier, being a reactive device, is frequency dependent in response over a relatively narrow band. The inductive inertia of the magnetic amplifier has been a constant restraint against the use of the device. The nature of this inductive effect is discussed in this report.

The availability of new superior magnetic materials and efficient rectifier units has given the magnetic amplifier renewed prominence, and there is promise that the magnetic amplifier will soon find far wider acceptance and use.

Elementary Theory of Operation

The magnetic amplifier is a particular adaptation of the saturable-core reactor. Power magnification is obtained through utilization of the variation of the permeability of the core material of the reactor in the region of the knee of the normal magnetization curve. The incremental permeability of ferromagnetic coresmay be defined as the ratio of the incremental flux density in the material to the incremental value of the applied magnetizing force. Furthermore, the incremental inductance of a wire-wound core of this type is a function of the incremental permea-

bility. Figure 1-1 illustrates the variation of flux density and permeability with magnetizing force. It is clear, from the figure, that in the region of the knee of the normal magnetization curve there is a rapid change in permeability, and consequently of inductance, with relatively small changes in magnetizing force.

As shown in Figure 1-2, a typical magnetic amplifier consists of a pair of properly-wound toroidal cores. The alternating-current series circuit is composed of a high power a-c source, a load, and the a-c windings on the cores. The a-c source supplies essentially sinusoidal flux variations to the cores. The direct-current coils are connected in series opposition such that the induced fundamental alternating voltages in these coils are balanced out across the input windings. A source of low-level d-c or slowly fluctuating a-c power is supplied to the input terminals.

A slight change in the d-c control current will cause a large variation in the inductance of the a-c windings. This variation will effectively modify the total impedance presented to the a-c source in a manner related nonlinearly to the instantaneous magnitude of the control current. Such action will amplitude-modulate the voltage supplied by the a-c source with the signal applied to the control windings. The signal is then recovered from the carrier circuit in a system of dry-disc demodulators. Since the source voltage was applied at a much higher power-level

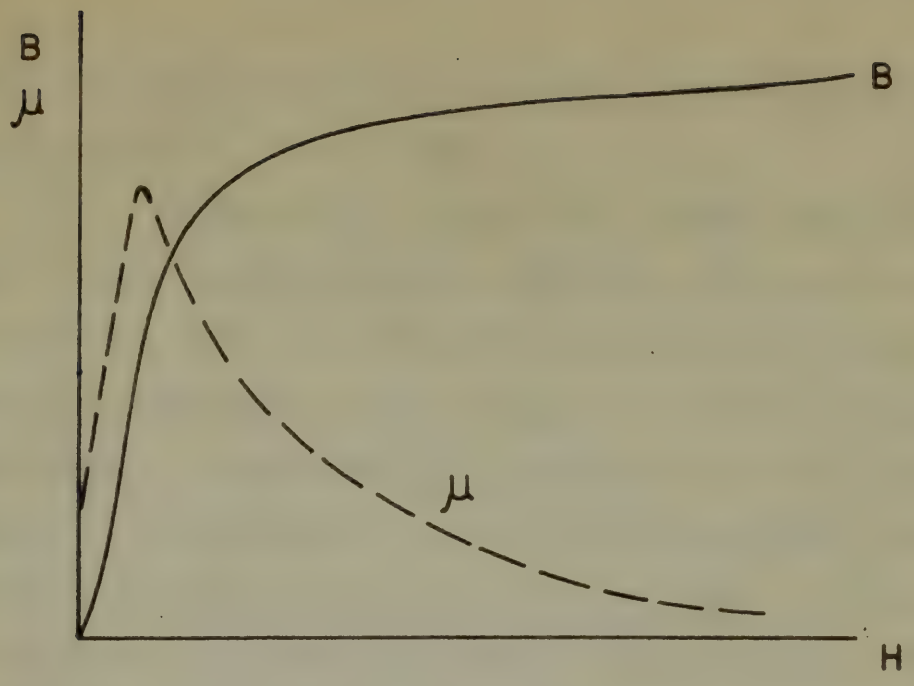

FIG. 1-1 NORMAL MAGNETIZATION CURVE.

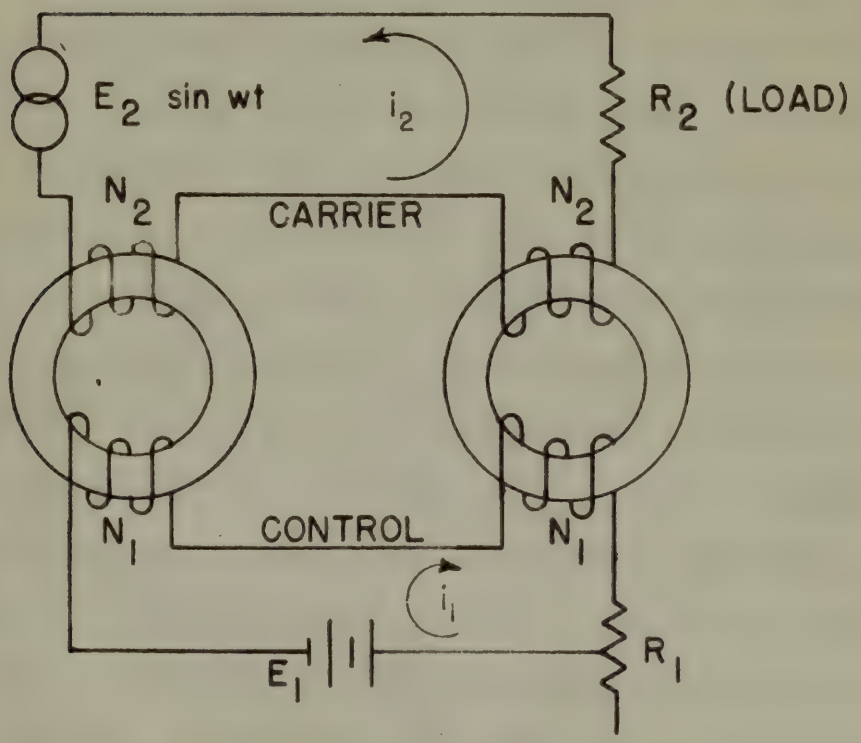

FIG. 1-2 BASIC MAGNETIC AMPLIFIER

ARCHIVE COPY

than the control current, overall amplification of the control signal is obtained.

Figure 1-3(a) depicts the normal magnetization curve of a typical magnetic amplifier under excitation of a sinusoidal flux as is shown in Figure 1-3(b), when a small control magnetizing force, NI_{dc}, is applied to the control windings. A simple graphical construction will give waveforms of the resultant a-c circuit magnetizing forces expressed in ampere-turns as shown in Figure 1-3(c). The use of harmonic analysis will permit the separation of the even and odd harmonic terms of the magnetizing currents. Such an analysis will indicate that the odd-harmonic terms are of the same magnitude and sign, while the even-harmonic terms are of equivalent magnitudes, but of opposite sign. These magnetizing forces are plotted in Figure 1-4. If the a-c coils of the amplifier are connected in series, and if the impedance of the d-c source is low, the phases of the harmonics will then be such that the even-harmonic currents will flow in the control circuit, while the odd-harmonic currents will flow as an output current in the a-c circuit. Actually, then, it is the odd-harmonic currents in the a-c circuit which are modulated by the applied control signals. Magnetization of the cores under these conditions is designated as "natural" magnetization. If, on the other hand, the cores are connected in series and the impedance of the d-c circuit is high to second-harmonic frequencies of the applied carrier, the second-harmonic currents are unable

11256

than the control current, overall amplification of the control signal is obtained.

Figure 1-3(a) depicts the normal magnetization curve of a typical magnetic amplifier under excitation of a sinusoidal flow as is shown in Figure 1-3(b), when a small control magnetizing force, NI_{dc}, is applied to the control windings. A simple graphical construction will give curve-forms of the resultant d-c circuit magnetizing forces expressed in ampere-turns as shown in Figure 1-3(c). The use of harmonic analysis will permit the separation of the even and odd harmonic terms of the magnetizing currents. Such an analysis will indicate that the odd-harmonic terms are of the same magnitude and sign, while the even-harmonic terms are of equivalent magnitudes, but of opposite sign. These magnetizing forces are plotted in Figure 1-4. If the d-c coils of the amplifier are connected in series, and if the impedance of the d-c source is low, the phases of the harmonics will then be such that the even-harmonic currents will flow in the control circuit, while the odd-harmonic currents will flow as an output current in the d-c circuit. Actually, then, it is the odd-harmonic currents in the d-c circuit which are modulated by the applied control signals. Magnetization of the cores under these conditions is designated as "natural" magnetization. If, on the other hand, the cores are connected in series and the impedance of the d-c circuit is high to second-harmonic frequencies of the applied carrier, the second-harmonic currents are unable

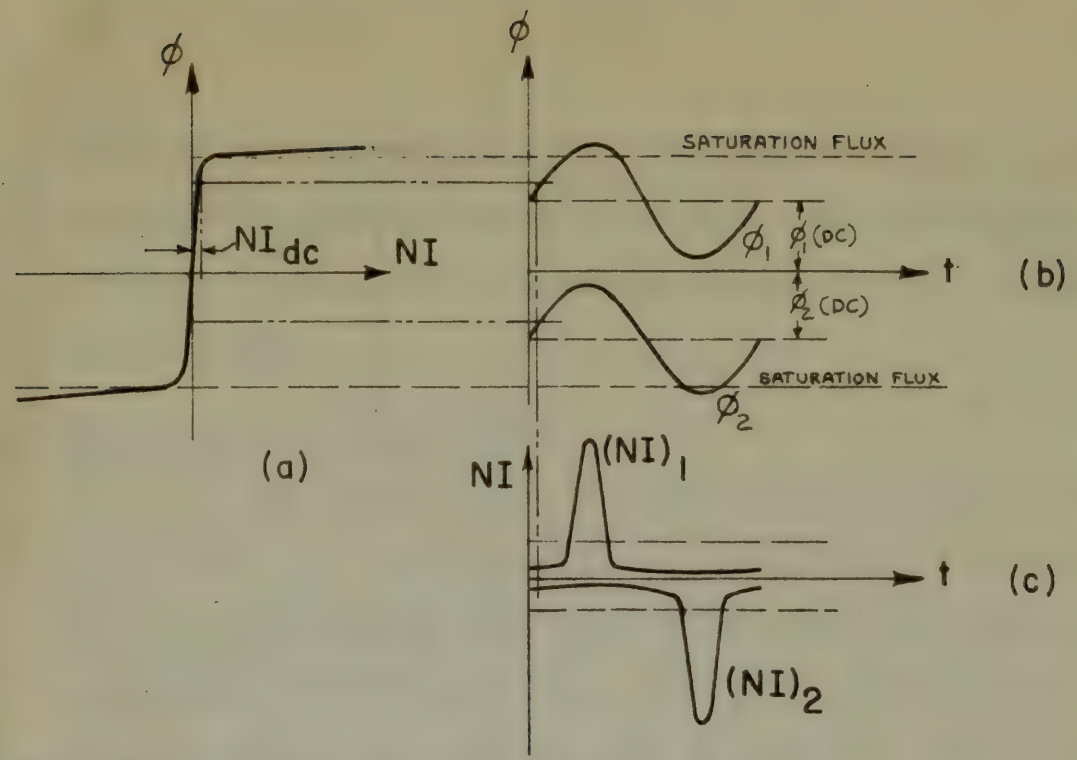

FIG. 1-3 (a) THE MAGNETIZATION CURVE.
(b) FLUX AS A FUNCTION OF TIME.
(c) MAGNETIZING FORCE AS A FUNCTION OF TIME.

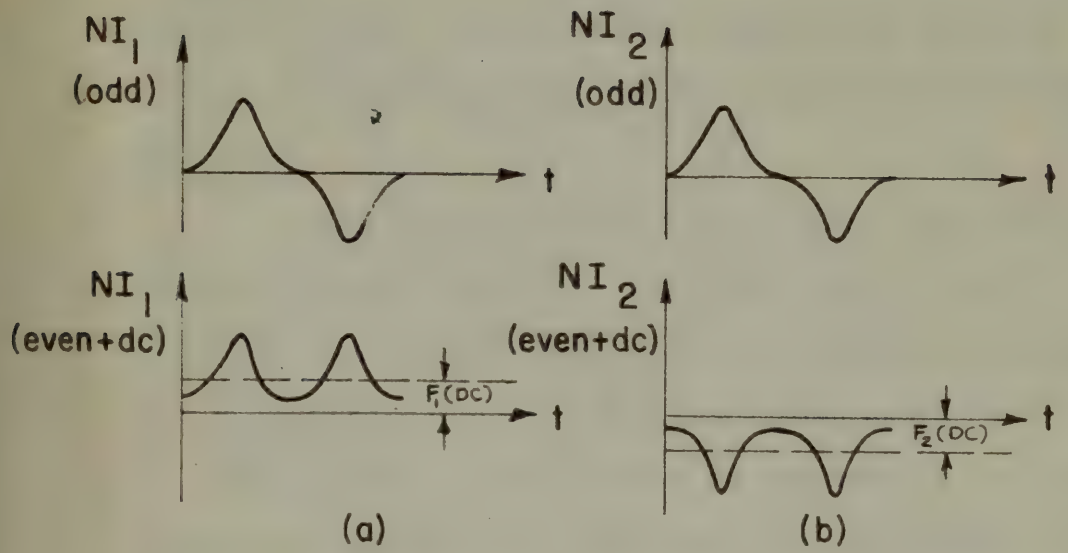

FIG. 1-4 (a) HARMONIC COMPONENTS OF MAGNETIZING FORCE IN CORE NO. 1.
(b) HARMONIC COMPONENTS OF MAGNETIZING FORCE IN CORE NO. 2.

to flow, and the condition of magnetization known as "constrained" magnetization will prevail. This report will deal primarily with the magnetic amplifier under "natural" magnetization.

Nature of the Thesis Study

The first phases of this study are devoted to investigations of the magnetic characteristics of magnetic-core materials which will present optimum performance in magnetic-amplifier circuitry. The performance of the amplifier is associated with the normal induction curve of the core-material and the performance is justified with mathematical relationships whenever linear approximations are possible. Comparison of available magnetic materials is made and the choice of the material from which the cores were constructed is justified by empirical and theoretical considerations. In connection with this phase of the work, magnetic characteristics of the available materials were measured.

The second phase of this investigation involves an experimental study of the basic magnetic-amplifier circuit. An experimental magnetic amplifier was designed, and an extensive series of laboratory tests were conducted on this circuit. The effects of the magnitudes of the load and input resistances, frequency and magnitude of the a-c source supply voltage, number of turns on the input and output circuits, and magnitude of the control current on

gain of the amplifier, power-output of the device, and dynamic response of the system were observed. Dynamic response of the amplifier was observed for both step-functions applied to the input circuit and for sinusoidal variations of the control voltage. Effects of the various parameters on gain and power output are based on steady-state operational considerations. The observed variations are correlated with theoretical considerations and explained, whenever possible, by the use of accepted formulae.

The third phase of this investigation is comprised of an analytic study of the magnetic amplifier based upon solution of the nonlinear equations of circuit operation on the #1 Differential Analyzer. A set of simultaneous differential equations describing the behavior of the amplifier circuit was prepared, and a series of analytical solutions to these equations was obtained mathematically on the analyzer. Circuit parameters for these theoretical solutions were made to closely approximate the actual experimental parameters under which laboratory observations were made. The analytical solution was found to be an invaluable aid to the understanding of circuit performance. The results of the analytical solutions are correlated with observed phenomena.

The use of positive, or regenerative, feedback was investigated in the fourth phase of this study. Again the effects of variations in the circuit parameters were

observed experimentally. Steady-state and dynamic characteristics of the feedback circuit are discussed and explained on the basis of information obtained on experimental and analytical studies of the basic circuit.

In the final phase of this study, certain design criteria are established. These criteria are based on analytical and empirical considerations of the performance of the magnetic-amplifier circuit. The nature of the gain, power output, and dynamic performance of the amplifier are correlated, and definite criteria for methods of design for a particular performance are formulated. In connection with these considerations, a typical magnetic-amplifier design is carried out. Finally, a series of suggestions for future work in this field is presented.

CHAPTER II

THE MAGNETIC CIRCUIT

Introduction

Since the action of the magnetic amplifier depends in a large measure upon the ferromagnetic properties of its saturable-reactor unit, the design of the magnetic circuit is of utmost importance. Considerations involved in the selection of the core material, the measurement of its properties, and the winding of the reactors will, therefore, be discussed in detail.

Selection of the Cores

The factors which must be investigated in choosing the magnetic circuit for magnetic-amplifier design are:

1. Normal magnetization curve,
2. Permeability,
3. Saturation flux density,
4. Core losses,
5. Core shape.

These will be discussed in order and their significance in relation to the amplifier design will be pointed out.

The normal magnetization curve of a ferromagnetic core is a qualitative sensitivity-index for a magnetic amplifier utilizing such cores. To achieve the highest amplifier sensitivity, the magnetization curve should have the idealized form shown in Figure 2-1, which exhibits a finite discontinuity at the origin. This idealized function is

often used in the literature as an approximation in the analysis of magnetic-amplifier performance.[1,2] Such a function implies, of course, infinite initial permeability and no hysteretic effects. The manner in which the magnetization curve indicates amplifier sensitivity can be seen by plotting the static permeability as a function of direct magnetizing force from the defining relation

$$\mu = \frac{B}{H} . \qquad (2\text{-}1)$$

For the idealized case this function is shown in Figure 2-2. The transfer characteristics of the amplifier depend upon the variation of inductance with direct magnetization, and hence upon the permeability, since the inductance is directly proportional to the permeability. The steeper the slope of the permeability function, the more sensitive will be the amplifier. Comparison of the ideal static-permeability function with the measured functions of two different magnetic materials, which are shown in Figures 2-9 and 2-10, reveals that the sensitivity of the practical amplifier is less than that of the ideal amplifier. This criterion is only of qualitative interest because the reactor inductance depends not upon the static permeability but upon the incremental permeability, there being no direct mathematical relation between the two. Although it is smaller than the static permeability, the incremental permeability exhibits, however, the same

---

1. Lamm, U., "The Transductor, a D.C. Pre-Saturated Reactor," (Stockholm, Esselte Aktiebolag, 1943).
2. Rex, H.B., "The Transductor," Instruments, 20, (1947), 1102-1109.

often used in the literature as an approximation in the analysis of magnetic-amplifier performance.[1,2] Such a function implies, of course, infinite initial permeability and no hysteretic effects. The manner in which the magnetization curve inside the amplifier sensitivity can be seen by plotting the static permeability as a function of direct magnetizing force from the defining relation

$$\mu_s = \frac{B}{H} \qquad (2\text{-}1)$$

For the idealized case this function is shown in Figure 2-2. The transfer characteristics of the amplifier depend upon the variation of inductance with direct magnetization, and hence upon the permeability, since the inductance is directly proportional to the permeability. The steeper the slope of the permeability function, the more sensitive will be the amplifier. Comparison of the ideal static-permeability function with the measured functions of two different magnetic materials, which are shown in Figures 2-9 and 2-10, reveals that the sensitivity of the practical amplifier is less than that of the ideal amplifier. This criterion is only of qualitative interest because the reactor inductance depends not upon the static permeability but upon the incremental permeability, there being no direct mathematical relation between the two. Although it is smaller than the static permeability, the incremental permeability exhibits, however, the same

1. Lamm, U., "The Transductor, a G.C. Pre-Saturated Reactor," (Stockholm, Gaseite Aktiebolag, 1943).
2. Das, S.A., "The Transductor," Instruments, 20, (1947), 1108-1109.

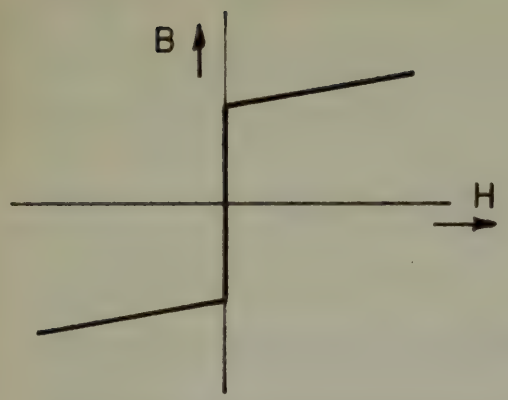

FIG. 2–1

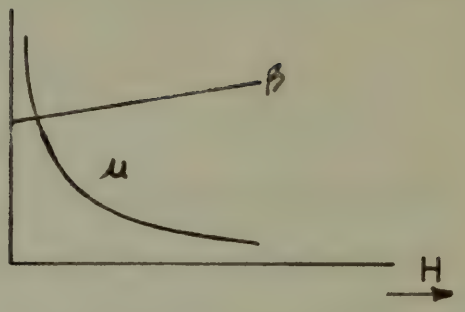

FIG. 2–2

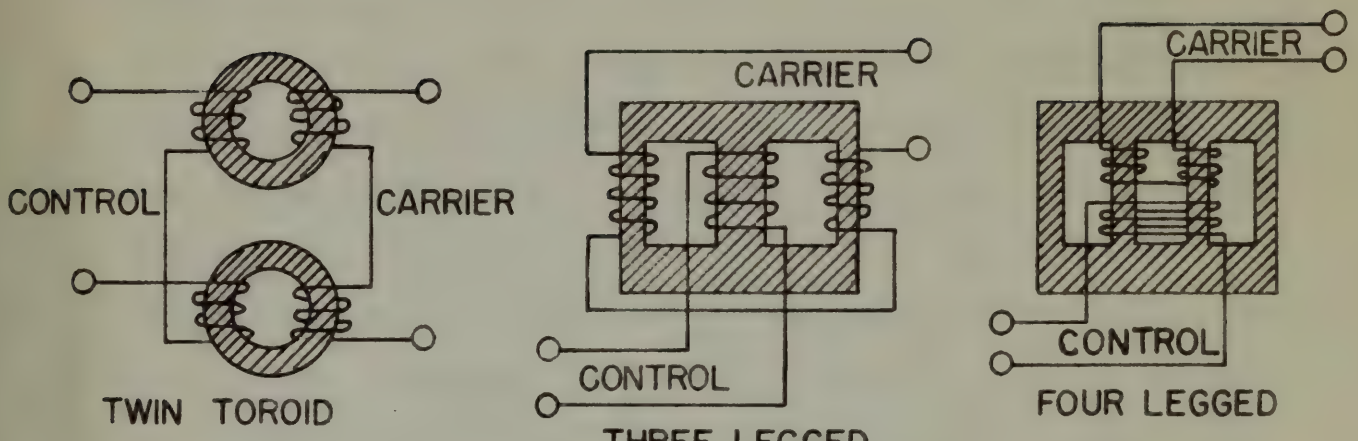

SATURABLE REACTORS

FIG. 2–3

general trend for a given alternating flux-density amplitude, and renders the above-cited criterion of practical interest. This criterion is particularly valuable as a guide to the metallurgist seeking to improve the properties of core materials for magnetic-amplifier design. Several ways of defining incremental permeability appear in engineering literature.[1,2] It may be defined as

$$\mu_{ac} = \frac{B_{rms}}{H_{rms}} \qquad (2\text{-}2)$$

in which the root-mean-square values of alternating induction and magnetization are taken. If one of these quantities is assumed sinusoidal, the other will not have a sinusoidal waveform because of the nonlinearity of the magnetization curve. Incremental permeability, therefore, is merely a definition which has meaning only in the sense in which defined, in this case being the ratio of the root-mean-square values of the alternating components of B and H.

The saturation flux-density is of importance in determining the relation between the cross-sectional core area, the carrier voltage, the carrier frequency, and the number of turns in the carrier winding. The carrier circuit power supply is a sinusoidal-voltage source which gives rise to an alternating sinusoidal flux in the cores provided the impedance of the input circuit of the induced even-harmonic voltages is kept low. Under this condition, the magnetization is natural. If the impedance of the input circuit to these

---

1. Lamson, H.W., "Alternating-Current Measurements of Magnetic Properties," I.R.E. Proc., 36, (1948), 266-277.
2. M.I.T. Staff, "Magnetic Circuits and Transformers," (New York, John Wiley & Sons, 1943), 198.

general trend for a given alternating flux-density amplitude, and renders the above-cited criterion of practical interest. This criterion is particularly valuable as a guide to the metallurgist seeking to improve the properties of core materials for magnetic-amplifier design. Several ways of defining incremental permeability appear in engineering literature.[1,2] It may be defined as

$$\mu_{ac} = \frac{B_{rms}}{H_{rms}} \qquad (2\text{-}2)$$

in which the root-mean-square values of alternating induction and magnetization are taken. If one of these quantities is assumed sinusoidal, the other will not have a sinusoidal waveform because of the nonlinearity of the magnetization curve. Incremental permeability, therefore, is merely a definition which has meaning only in the sense in which defined, in this case being the ratio of the root-mean-square values of the alternating components of B and H.

The saturation flux-density is of importance in determining the relation between the cross-sectional core area, the carrier voltage, the carrier frequency, and the number of turns in the carrier winding. The carrier circuit power supply is a sinusoidal-voltage source which gives rise to an alternating sinusoidal flux in the cores provided the impedance of the input circuit of the induced even-harmonic voltages is kept low. Under this condition, the magnetization is natural. If the impedance of the input circuit to these

---

1. Lamson, H.W., "Alternating-Current Measurements of Magnetic Properties," I.R.E. Proc., 36, (1948), 266-277.
2. M.I.T. Staff, "Magnetic Circuits and Transformers," (New York, John Wiley & Sons, 1943), 198.

even-harmonic voltages is high, the magnetization is constrained and the core flux is not sinusoidal.[1] The present studies involve only natural magnetization, a high-pass filter being shunted across the input windings such that it offers a high impedance to the signal-frequency currents and yet insures a low-impedance path for the even-harmonics of the carrier frequency. Under these conditions the flux in the core may be derived from the law of induction,

$$e = -N_2 \frac{d\phi}{dt} \qquad (2\text{-}3)$$

$$\phi = \beta A = -\frac{1}{N_2}\int e\, dt \qquad (2\text{-}4)$$

$$\beta = -\frac{1}{N_2 A}\int E \sin\omega_2 t\, dt \qquad (2\text{-}5)$$

$$\beta = \frac{E}{\omega_2 N_2 A} \cos\omega_2 t \qquad (2\text{-}6)$$

where

e is the voltage across the carrier winding of one reactor,

ϕ is the flux in webers,

β is the flux density in webers/sq. meter,

A is the cross-sectional core area in sq. meters,

ω_2 is the angular carrier frequency,

N_2 is the number of carrier turns on one core.

With zero direct magnetization and with the carrier windings connected in series, the alternating voltage across one reactor will very nearly equal one-half of the carrier voltage, the difference being a result of the voltage drop in the load caused by the exciting current. For best amplifier

---

1. Rex, H.B., "The Transductor," Instruments, 20, (1947), 1102-1109

even-harmonic voltages is high, the magnetization is constrained and the core flux is not sinusoidal.[1] The present studies involve only natural magnetization, a high-pass filter being shunted across the input windings such that it offers a high impedance to the signal-frequency currents and yet insures a low-impedance path for the even-harmonics of the carrier frequency. Under these conditions the flux in the core may be derived from the law of induction,

$$e = -N_2 \frac{d\phi}{dt} \qquad (2\text{-}3)$$

$$\phi = \beta A = -\frac{1}{N_2}\int e\,dt \qquad (2\text{-}4)$$

$$\beta = -\frac{1}{N_2 A}\int e \sin\omega_2 t\,dt \qquad (2\text{-}5)$$

$$\beta = \frac{1}{\omega_2 N_2 A}\cos\omega_2 t \qquad (2\text{-}6)$$

where

e is the voltage across the carrier winding of one reactor,

ϕ is the flux in webers,

β is the flux density in webers/sq. meter,

A is the cross-sectional core area in sq. meters,

ω_2 is the angular carrier frequency,

N_2 is the number of carrier turns on one core.

With zero direct magnetization and with the carrier windings connected in series, the alternating voltage across one reactor will very nearly equal one-half of the carrier voltage, the difference being a result of the voltage drop in the load caused by the emitting current. For best amplifier

1. Hun, E.A., "The Transductor," Instruments, 20, (1947), 1103-1107

performance, the flux density in the cores should be so adjusted that for no direct magnetization the flux-density amplitude just reaches the knee of the magnetization curve. If the flux-density amplitude is chosen too large, the exciting current will be excessive. If too small an amplitude is chosen, the linear portion of the modulation characteristic will be severely restricted. These effects may be seen by referring to the modulation characteristics shown in Chapters III and V. The circuit parameters which may be adjusted to achieve this condition, consistent with other considerations such as power output, space and weight, bandwidth, and linearity, are A, N_2, E_2, and ω_2.

Because it is a variable reactance, the magnetic amplifier is ideally a lossless circuit in contrast with the electronic amplifier, which is a variable resistance, and inherently dissipative. For efficient operation, the core and copper losses in the magnetic amplifier should be minimized. Or, stated in another fashion, it is desirable to minimize the exciting current of the saturable reactors and to obtain a coil with as high a Q as possible. Exciting current which flows in the load when no signal is applied represents a useless component of load power. It has the further disadvantage of causing cumulative saturation when magnetic-amplifier stages are cascaded. If the demodulated exciting-current output of the first stage were fed to a second stage of amplification, a signal would flow in the second stage tending to saturate this stage even though no

signal had been applied to the first stage. This cumulative-saturation effect in cascaded amplifiers must usually be compensated for by one method or another.[1]

The core-loss is made up of two components, hysteresis and eddy-current loss. Hysteresis loss may usually be expressed by the relation

$$P_h = \eta V f \beta_m^n \qquad (2\text{-}7)$$

where:

P_h is the hysteresis power loss,

n is the Steinmetz coefficient,

η is a constant of the material,

V is the core volume,

f is the alternating-current frequency,

β_m is the maximum flux density.

This formula is strictly applicable only to a core which is in the symmetrically cyclically magnetized condition.[2] Since the magnetic amplifier is asymmetrically magnetized by virtue of the superposed direct magnetization, the validity of this formula applied to a magnetic-amplifier circuit is open to question. It serves to point out, however, that the hysteresis loss is a function of both the frequency and the quality of the core material. Since the carrier frequency will be limited by the available alternating-current source or by bandwidth requirements, hysteresis can be minimized by proper selection of core material. Another manner in which

---

1. Fitzgerald, A.S., "Magnetic Amplifier Circuits-Neutral Type," J.F.I., 244, (1947), 249-265.
2. M.I.T. Staff, "Magnetic Circuits and Transformers," (New York, John Wiley & Sons, 1943), 129-130.

signal had been applied to the first stage. This cumulative-saturation effect in cascaded amplifiers must usually be compensated for by one method or another.[1]

The core-loss is made up of two components, hysteresis and eddy-current loss. Hysteresis loss may usually be expressed by the relation

$$P_h = \mu V f \beta_m^n \qquad (8\text{-}7)$$

where:

P_h is the hysteresis power loss,

n is the Steinmetz coefficient,

μ is a constant of the material,

V is the core volume,

f is the alternating-current frequency,

β_m is the maximum flux density.

This formula is strictly applicable only to a core which is in the symmetrically cyclically magnetized condition.[2] Since the magnetic amplifier is asymmetrically magnetized by virtue of the superposed direct magnetization, the validity of this formula applied to a magnetic-amplifier circuit is open to question. It serves to point out, however, that the hysteresis loss is a function of both the frequency and the quality of the core material. Since the carrier frequency will be limited by the available alternating-current source or by bandwidth requirements, hysteresis can be minimized by proper selection of core material. Another manner in which

1. FitzGerald, A.M., "Magnetic Amplifier Circuits-Neutral Type," J.F.I., 244, (1947), 249-258.
2. M.L.T. Kauff, "Magnetic Circuits and Transformers," (New York, John Wiley & Sons, 1947), 129-130.

hysteresis might be reduced is by making use of the Elmen effect.[1] If an electromagnetic device is excited by current of a given frequency, it is possible to reduce the hysteresis loop for the low frequency by the superposition of a second alternating-current of considerably higher frequency, the effect being that the high-frequency current supplies most of the hysteresis loss. This method of approach to the hysteresis-reduction problem, however, would require an additional alternating-current source of higher frequency than the carrier. If such additional windings were used, the available window space would be reduced. Effects of intermodulation also would have to be considered.

The other component of core loss is that of eddy-current dissipation. This may be written to a first approximation[2] as

$$P_e = k_e f^2 \tau^2 \beta_m^2 V$$

where

P_e is the eddy-current power loss,

k_e is a constant of the material,

f is the alternating-current frequency,

τ is the lamination thickness,

β_m is the maximum flux density,

V is the core volume.

To minimize eddy-current loss it is apparent that the core should be kept small, the material should possess as high a

---

1. Elmen, G.W., "High-Frequency Detector," U.S. Patent 1,289,418, (1918).
2. M.I.T. Staff, "Magnetic Circuits and Transformers," (New York, John Wiley & Sons, 1943), 132-138.

resistivity as possible consistent with the magnetic properties, the material should be as thinly laminated as practicable, and the interlaminar insulation should be efficient. Spirally-wound tapes of one-mil thickness are now commercially available, and the processing of even thinner tapes is in the developmental stage.

A further effect of the eddy currents is to distort the flux by reducing the field at the center of the laminations. This effect increases with frequency as the skin depth of the eddy currents decreases. This effect, known as eddy-current shielding, reduces the effective cross-sectional area of the core.

The shape of the magnetic circuit is, likewise, an important consideration. Currently used configurations include the twin-toroidal, the three-legged, and the four-legged saturable reactor units, illustrated in Figure 2-3. As previously discussed, the permeability must be maximized for optimum performance, and hence the presence of even a minute air gap must be avoided. This requirement indicates that dust cores or interleaved punchings should be avoided. Stacked annular laminations or spirally-wound tapes are preferred. Since it is desirable to keep the coupling between the windings as high as possible, the leakage flux must be minimized. The toroidal-core reactor, in which each winding is distributed over the entire periphery, offers the best solution to this problem. The advantage of the three and

four-legged reactors over the twin-toroidal type is that no fundamental or odd harmonic voltage is induced in the control windings, whereas in the latter type these voltages are actually induced, although bucked out by the connection of the two windings in series opposition. Since these induced voltages may be high enough under certain conditions to cause breakdown, the three or four-legged reactor may be preferred in some designs.

Magnetic materials which are now being used in magnetic-amplifier design include permenorm 5000-Z, Alleghany Electrical Alloy Steel #4750, mumetal, permalloy, hipernik, and silicon steel. The requisite magnetic properties are not ensured by alloy composition alone. Such metallurgical processes as grain orientation and magnetic annealing are most essential in determining the performance of the specimen. The most outstanding among these magnetic materials is permenorm 5000-Z, which is a very recent development of the Naval Ordnance Laboratory and attributed to G.W. Elmen and E.A. Gaugler.[1] Characterized by a maximum permeability of about 300,000 and a saturation flux density of about 15 kilogauss, the most distinctive feature is its almost rectangular hysteresis loop. From a performance viewpoint, silicon steel is the poorest choice for magnetic-amplifier reactors, although the cost is much less than the nickel alloys. The recent work of Minihera, however, indicates that much better performance may be obtained from silicon-iron, if properly

---

1. Rockett, Frank, "Improved Material for Magnetic Amplifiers," Electronics, (August 1948), 128-130.

treated.[1]

Measurement of Magnetic Properties.

Four matched toroidal cores of Allegheny Electrical Alloy #4750 and four matched toroidal cores of Allegheny Mumetal were available for this study. The former type cores, shown in Figure 2-4, are spirally-wound metallic tapes of three mil thickness whose convolutions are separated by a magnesium-oxide insulating layer. The latter type cores, shown in Figure 2-5, are assembled from three-mil annular stampings. In order to evaluate magnetic circuit performance and to check the consistency of magnetic properties among the samples, the normal magnetization curve and typical hysteresis loops were measured with a Leeds and Northrup type P-2239-D ballistic galvanometer using standard techniques.[2] The results are shown in Figure 2-6 for the Allegheny Electrical Alloy #4750, and in Figure 2-7 for the Allegheny Mumetal. The approximately rectangular hysteresis loop of the Allegheny #4750 is contrasted with the more conventional curvature of the mumetal loop. This rectangular effect is achieved by reducing impurities to a minimum in the original melt, by annealing the spiral tapes in a hydrogen atmosphere, and by cooling slowly in a magnetic field applied in the direction of rolling. Ferromagnetic materials are well-known to be magnetically anisotropic, that is, they have a direction of easiest magnetization. For a single crystal of

---

1. Target Report X-34N (unclassified), U. S. Naval Technical Mission to Japan, "Magnetic Development in Japan during World War II, (1946).
2. Ricker and Tucker, "Electrical Engineering Laboratory Experiments," (New York, McGraw-Hill, 1940), 91-100.

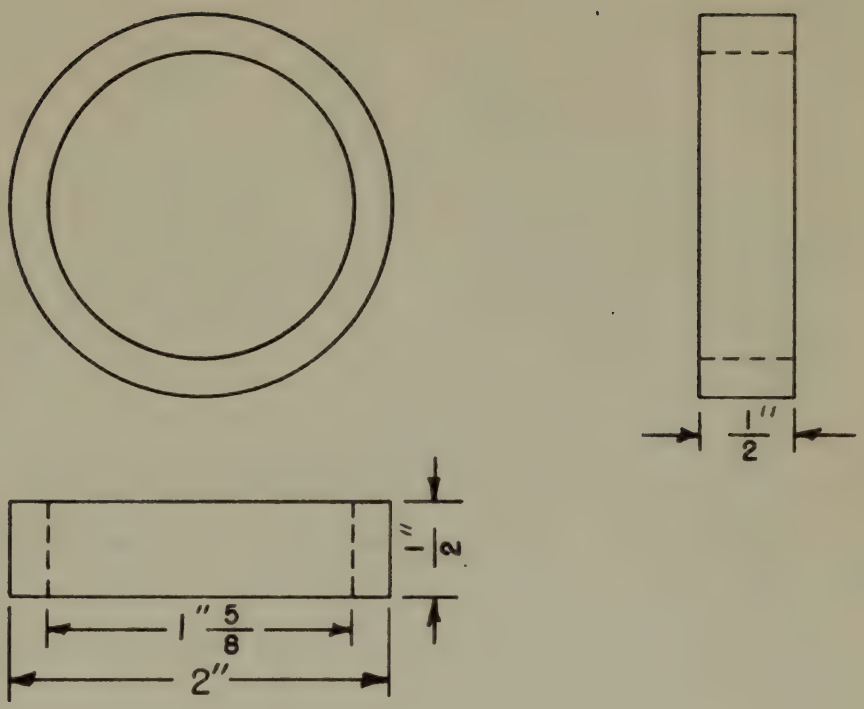

CORE CONSTRUCTION

48 SPIRALLY WOUND TURNS OF ALLEGHENY LUDLUM NO. 4750 ALLOY OF 0.003 INCHES THICKNESS. MAGNESIUM OXIDE INSULATION APPLIED DURING WINDING. CORES HEAT-ANNEALED IN HYDROGEN ATMOSPHERE BY NAVAL ORDNANCE LABORATORY OF WHITE OAK, MARYLAND.

WINDING DATA

7200 TURNS OF NO. 30 FORMVAR ENAMELED COPPER WIRE, TAPPED EACH 200 TURNS.

FIG. 2-4 SPECIFICATIONS FOR NO. 4750 CORES

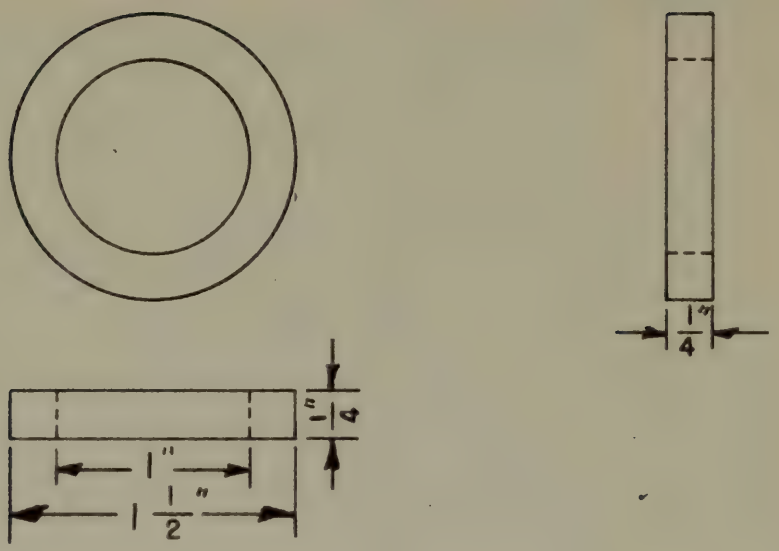

CORE CONSTRUCTION

70 LAMINATIONS OF ALLEGHENY LUDLUM MUMETAL OF 0.003 INCHES THICKNESS, STACKED AS SHOWN. HEAT TREATED BY ALLEGHENY LUDLUM.

WINDING DATA

2000 TURNS OF NO. 36 MAGNETIC WIRE, TAPPED EACH 200 TURNS.

FIG. 2-5 SPECIFICATIONS FOR MUMETAL CORES

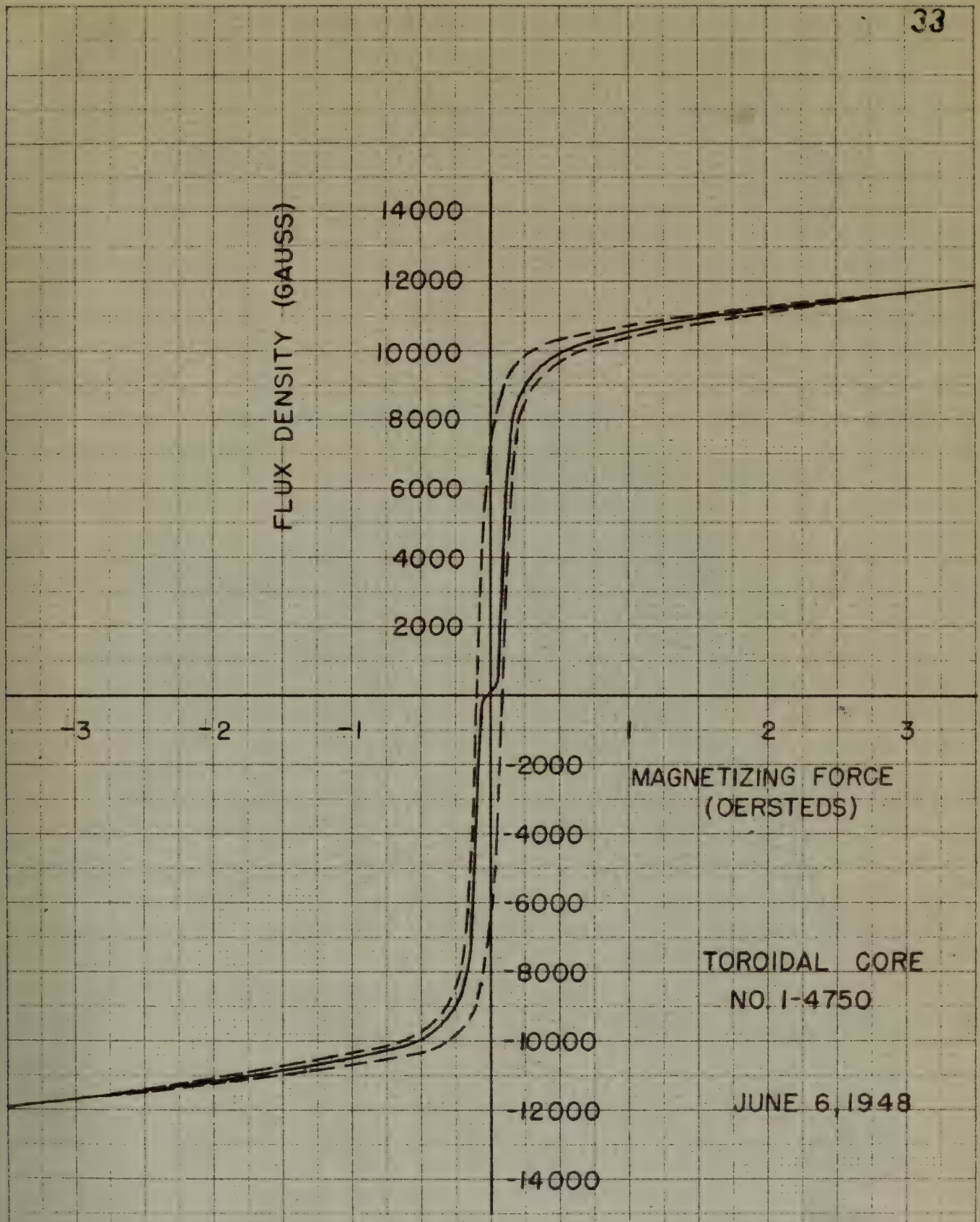

FIG. 2-6 NORMAL MAGNETIZATION CURVE AND TYPICAL HYSTERESIS LOOP FOR ALLEGHENY LUDLUM NO. 4750 MAGNETIC ALLOY

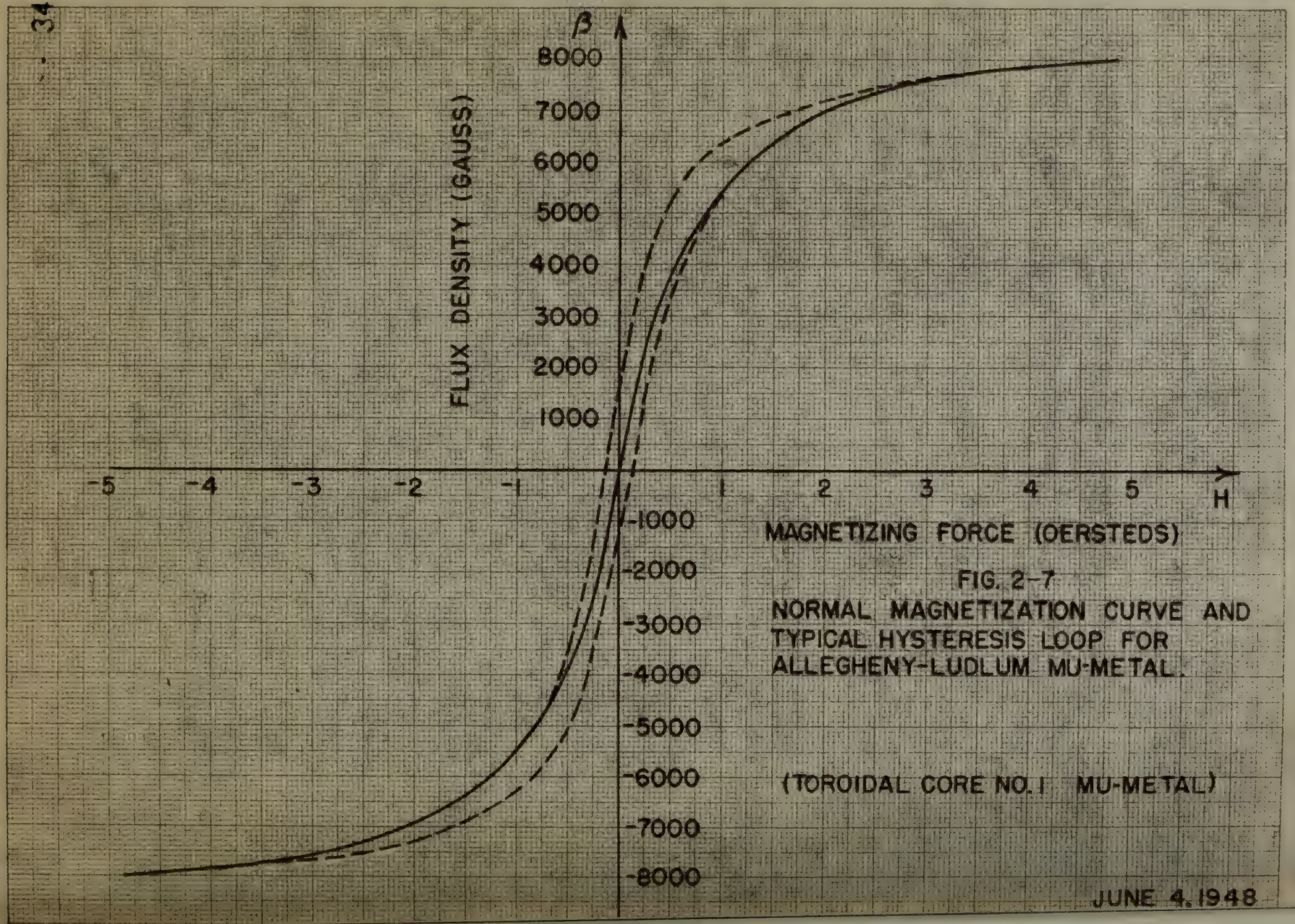

FIG. 2-7
NORMAL MAGNETIZATION CURVE AND TYPICAL HYSTERESIS LOOP FOR ALLEGHENY-LUDLUM MU-METAL.

(TOROIDAL CORE NO. 1 MU-METAL)

JUNE 4, 1948

fifty percent nickel-iron this is the crystal edge or the 1,0,0 axis. In this direction the electron spins can be aligned with minimum energy. In grain-oriented material, achieved by rolling in the 1,0,0 plane, the crystal lattice of the grains is aligned such that the entire mass exhibits magnetic behavior similar to a single crystal. The magnetic anneal, on the other hand, orients the domains by means of internal magnetostrictive forces without changing the crystal alignment. The effects of domain growth and rotation in the direction of an applied alternating magnetic field are thereby eliminated, leaving only the sudden 180-degree reversals of the electron spins as the direction of the field is changed. This results in a rectangular hysteresis loop. As seen from Figure 2-6, this effect is achieved to considerable degree in the Allegheny #4750 cores which were given a magnetic anneal by the Naval Ordnance Laboratory at White Oak, Maryland.

The consistency of the magnetic properties between the various samples of Allegheny #4750 was found to be quite good, as shown in Figure 2-8. The control of the complex metallurgical processes to produce uniformity in magnetic properties between different lots of material, or even between different samples of the same melt, is one of the most difficult problems in the manufacture of core materials. Lack of uniformity of the core properties in a magnetic amplifier will produce an unbalanced current-waveform.

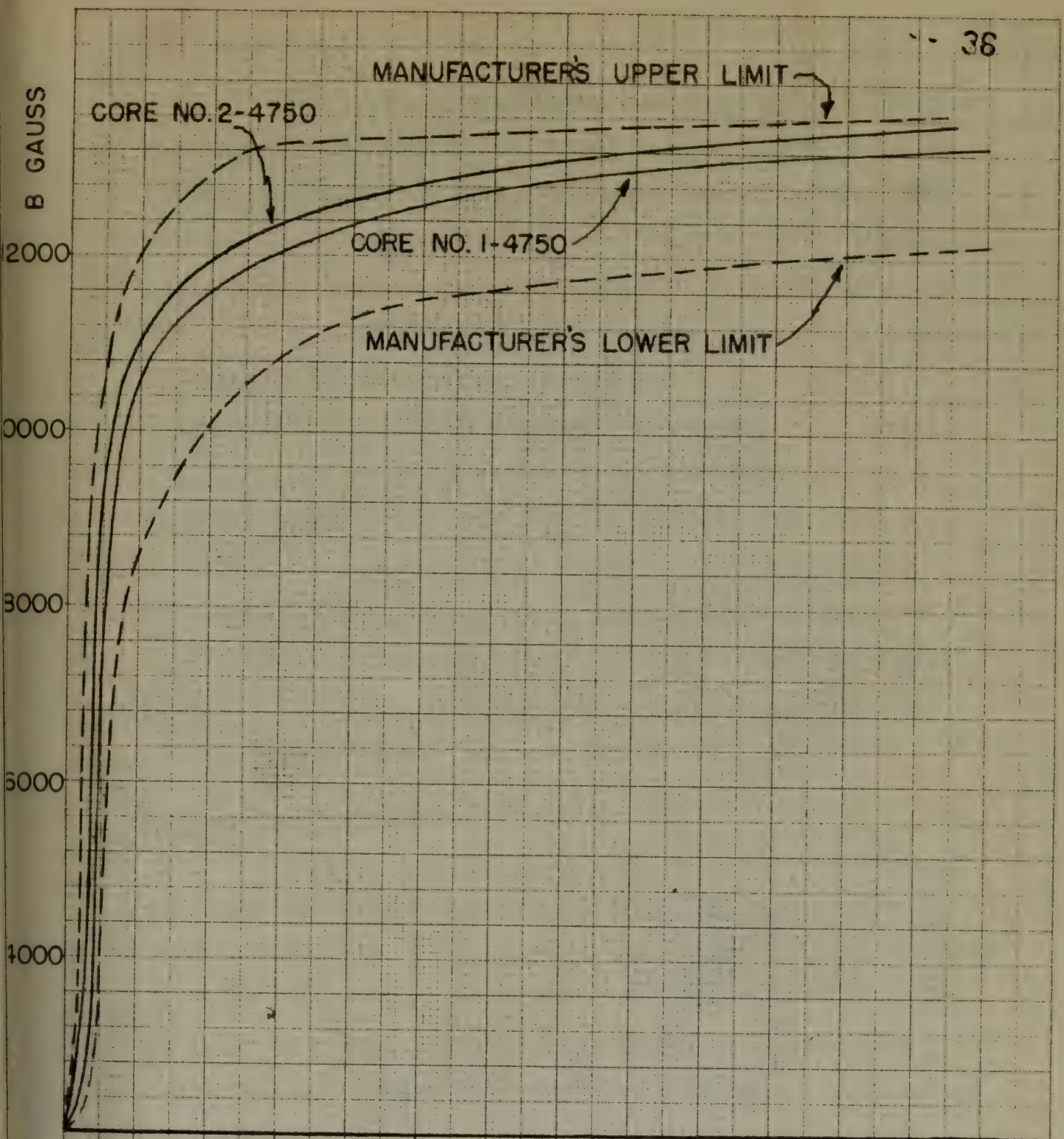

FIG. 2-8 COMPARISON OF MEASURED NORMAL MAGNETIZATION CURVES FOR CORES NO. 1-4750 AND 2-4750

The static permeability was computed as a function of direct magnetizing force and plotted in Figure 2-9 for a #4750 sample and in Figure 2-10 for a mumetal sample. The maximum static permeability of the Allegheny #4750 is seen to be much higher than for the mumetal. This indicates that a #4750 reactor would have a higher magnetizing inductance and a lower exciting current than one using mumetal. Furthermore, the rate of change of inductance with direct magnetization, being proportional to the slope of the permeability function, is observed to be much greater in the case of the Allegheny #4750. Magnetic amplifiers using Allegheny #4750 reactors would, therefore, be expected to give higher sensitivity. Since time limitations precluded a study of both type cores, those of Allegheny #4750 were chosen for this study.

Winding the Toroids.

A pair of #4750 cores were wound using a toroidal-core winding machine. When winding ferromagnetic cores of high permeability, it is necessary to enclose them in protective insulating containers, such as linen-covered bakelite, in order to relieve the cores of any mechanical strains caused by the winding procedure.[1] The containers should fit loosely enough to insure that no external magnetostrictive forces are applied, while at the same time fitting snugly enough to hold the cores securely in place. The application of a magnetic field to a ferromagnetic body disturbs the

---

1. Burton, E.T., "Transformer," U.S. Patent #1,880,412 (1930).

The static permeability was computed as a function of direct magnetizing force and plotted in Figure 6-9 for a 4750 sample and in Figure 6-10 for a nonetal sample. The maximum static permeability of the Allegheny 4750 is seen to be much higher than for the nonetal. This indicates that a 4750 reactor would have a higher magnetizing inductance and a lower exciting current than one using nonetal. Furthermore, the rate of change of inductance with direct magnetization, being proportional to the slope of the permeability function, is preserved to be much greater in the case of the Allegheny 4750. Magnetic amplifiers using Allegheny 4750 reactors would, therefore, be expected to give higher sensitivity. Since line limitations prevented a study of both type cores, those of Allegheny 4750 were chosen for this study.

Winding the Cores.

A pair of 4750 cores were made using a toroidal-core winding machine. When winding ferromagnetic cores of high permeability, it is necessary to deform them in protective insulating containers, such as linen-covered bakelite, in order to relieve the cores of any mechanical strains caused by the winding pressure.[1] The containers should fit loosely enough to insure that no external magnetostrictive forces are applied, while at the same time fitting snugly enough to hold the cores securely in place. The application of a magnetic field to a ferromagnetic body disturbs the

1. Burton, C.T., "Transformer," U.S. Patent #1,860,412 (1930).

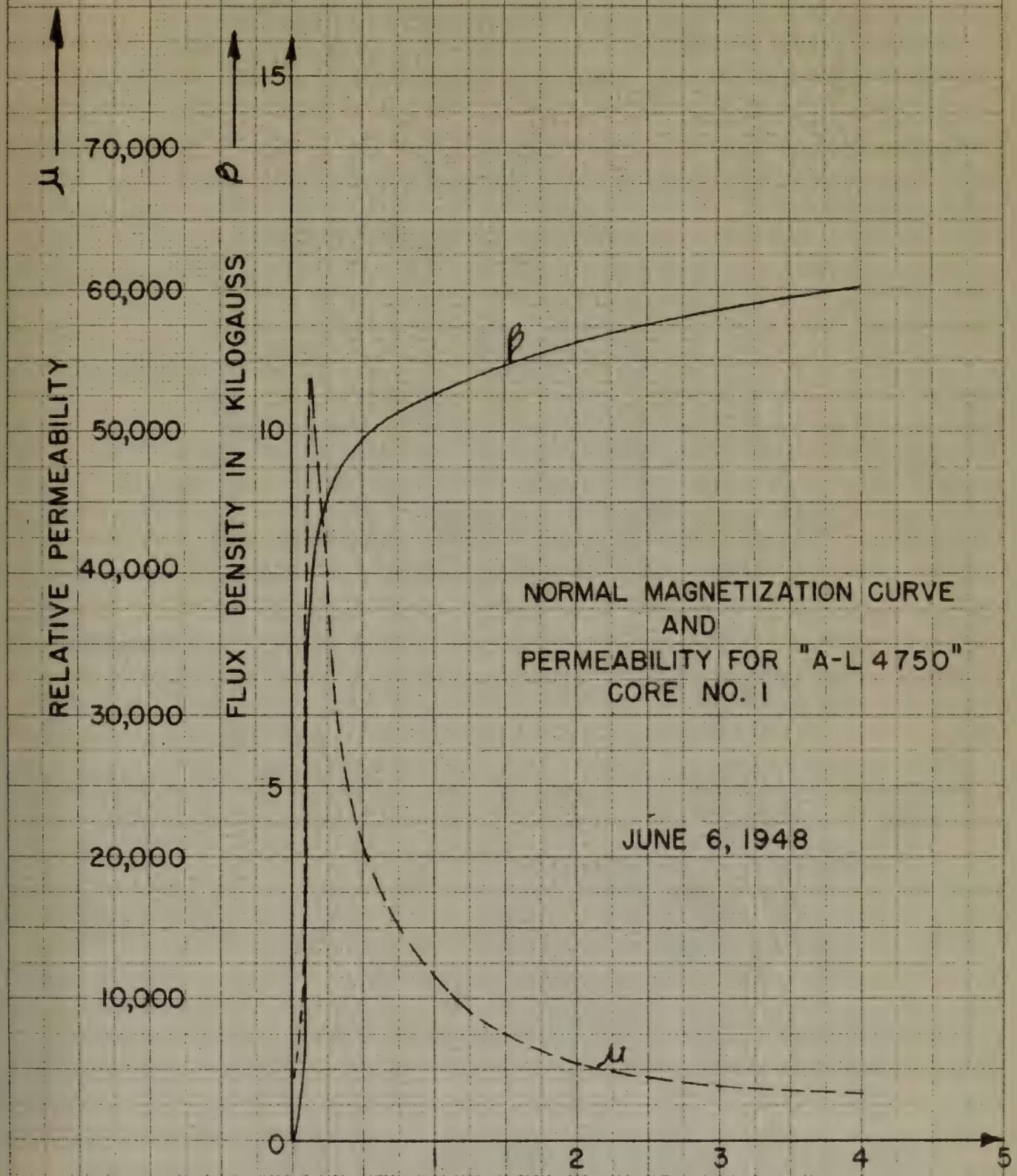

FIG. 2-9 MAGNETIZING FORCE IN OERSTEDS

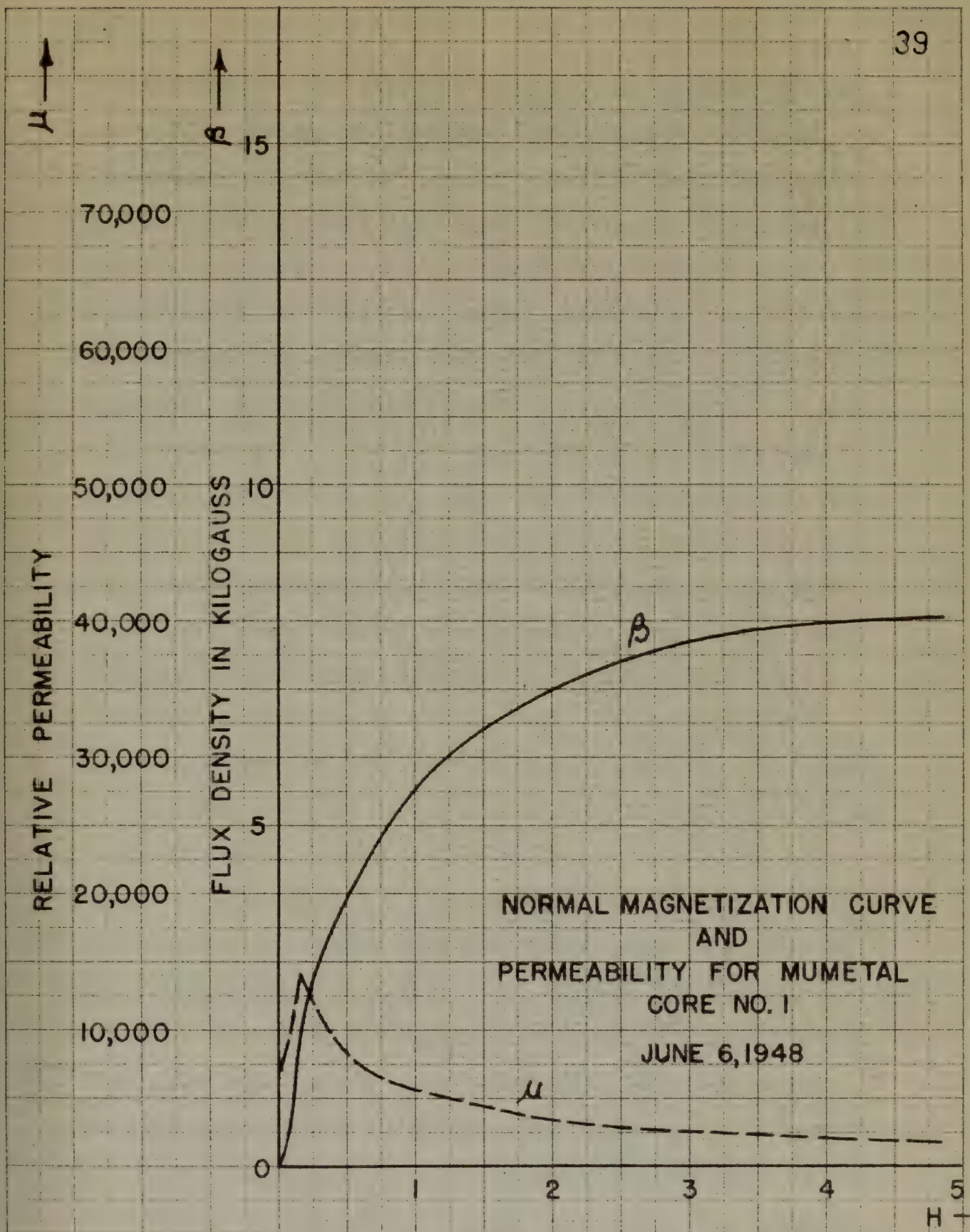

FIG. 2-10 MAGNETIZING FORCE IN OERSTEDS

balance between the internal electric and magnetic forces, and hence, changes the physical dimensions of the body. Conversely, a mechanical strain resulting from the application of an external mechanical stress will alter the magnetic properties. These effects are referred to as magnetostriction. It is apparent, therefore, that in order to preserve the magnetic properties of a given ferromagnetic specimen, provision must be made for the natural expansion and contraction of the core under the influence of magnetizing forces. Another consideration in the design of the containers is that they should be constructed as small as possible consistent with mechanical rigidity in order to prevent undue loss of window space. Accordingly, the Allegheny #4750 cores were provided with linen-covered bakelite boxes, shown in Figure 2-11. The mumetal cores were also provided with similar boxes, shown in Figure 2-12, in the event that it became feasible to include them in the study of magnetic-amplifier circuits.

The pair of Allegheny #4750 cores which had been selected for the study were each wound with 7200 turns of #30 Formvar enameled copper wire. During the winding process, caution must be exercised to prevent scraping the insulation and thereby short-circuiting adjacent turns. Shorted turns result in lowering the Q of the coil because of the copper loss caused by the high short-circuit currents induced. A low Q reduces the efficiency of the amplifier and increases the exciting current.

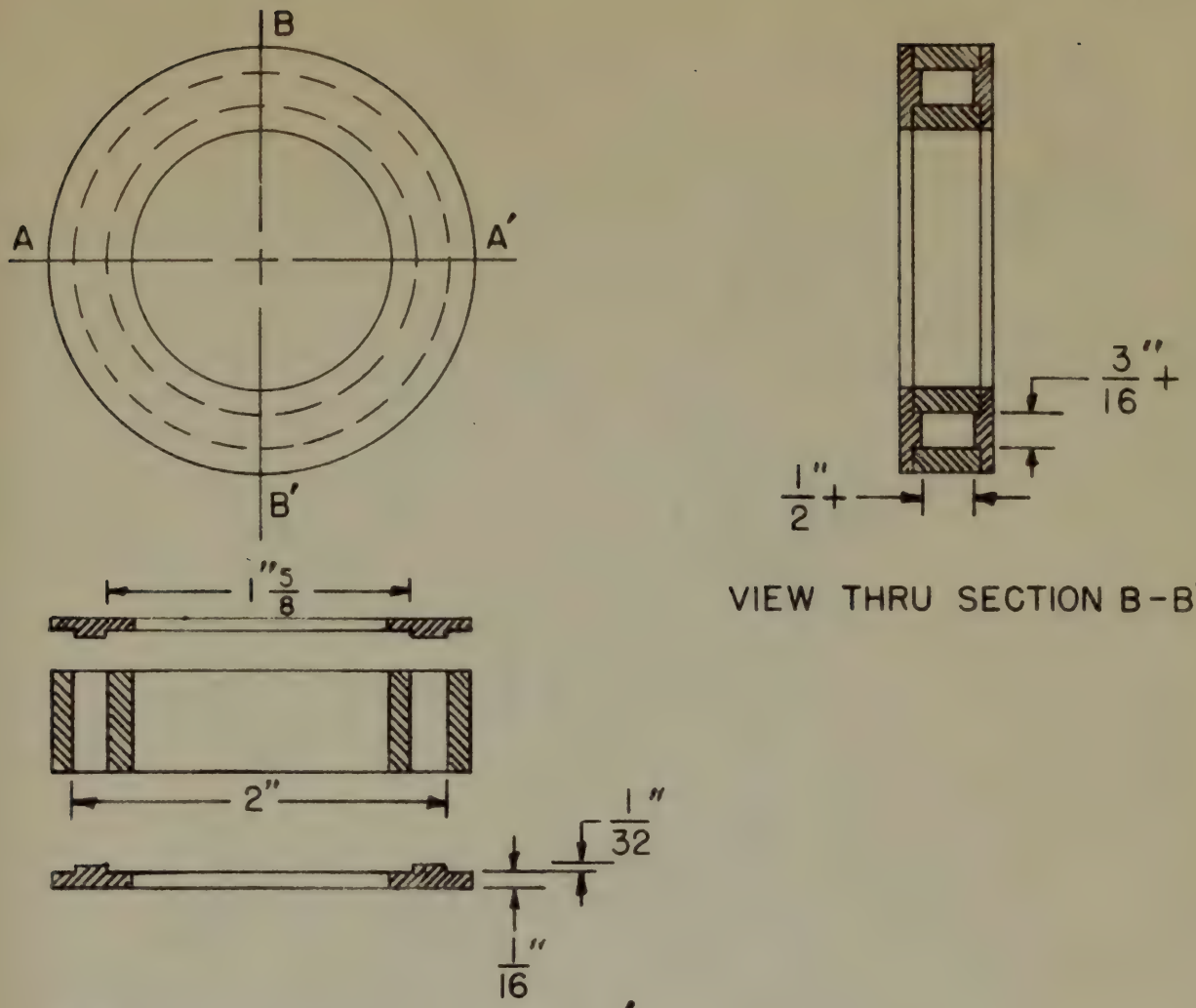

MATERIAL – LINEN COVERED BAKELITE

NOTE – INSIDE DIMENSIONS OF THE BOX ARE VERY SLIGHTLY GREATER THAN THE OUTSIDE DIMENSIONS OF THE CORE IN ORDER TO AVOID PLACING ANY MECHANICAL STRAIN ON THE CORES WHEN WINDINGS ARE APPLIED.

FIG. 2-11 SPECIFICATIONS FOR SPECIAL INSULATING BOXES FOR NO. 4750 CORES

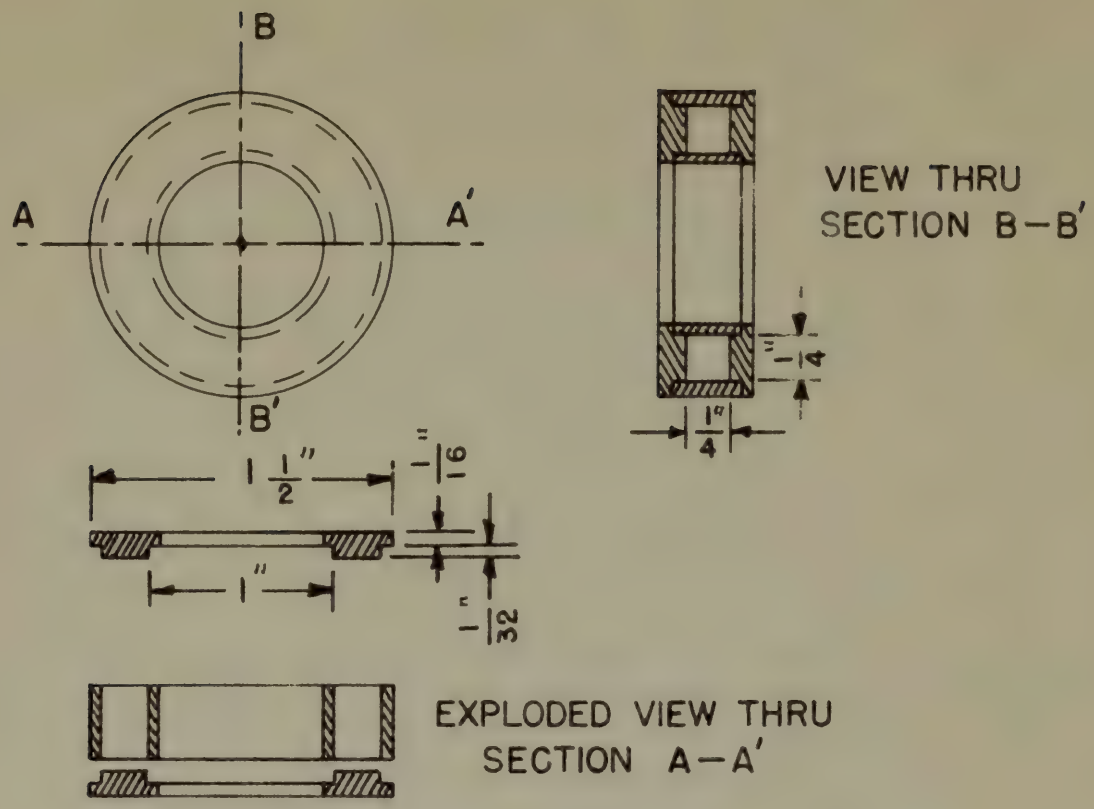

MATERIAL— LINEN COVERED BAKELITE

NOTE — INSIDE DIMENSIONS OF THE BOX ARE VERY SLIGHTLY GREATER THAN THE OUTSIDE DIMENSIONS OF THE CORE IN ORDER TO AVOID PLACING ANY MECHANICAL STRAIN ON THE CORES WHEN WINDINGS ARE APPLIED.

FIG. 2-12 SPECIFICATIONS FOR SPECIAL INSULATING BOXES FOR MUMETAL CORES.

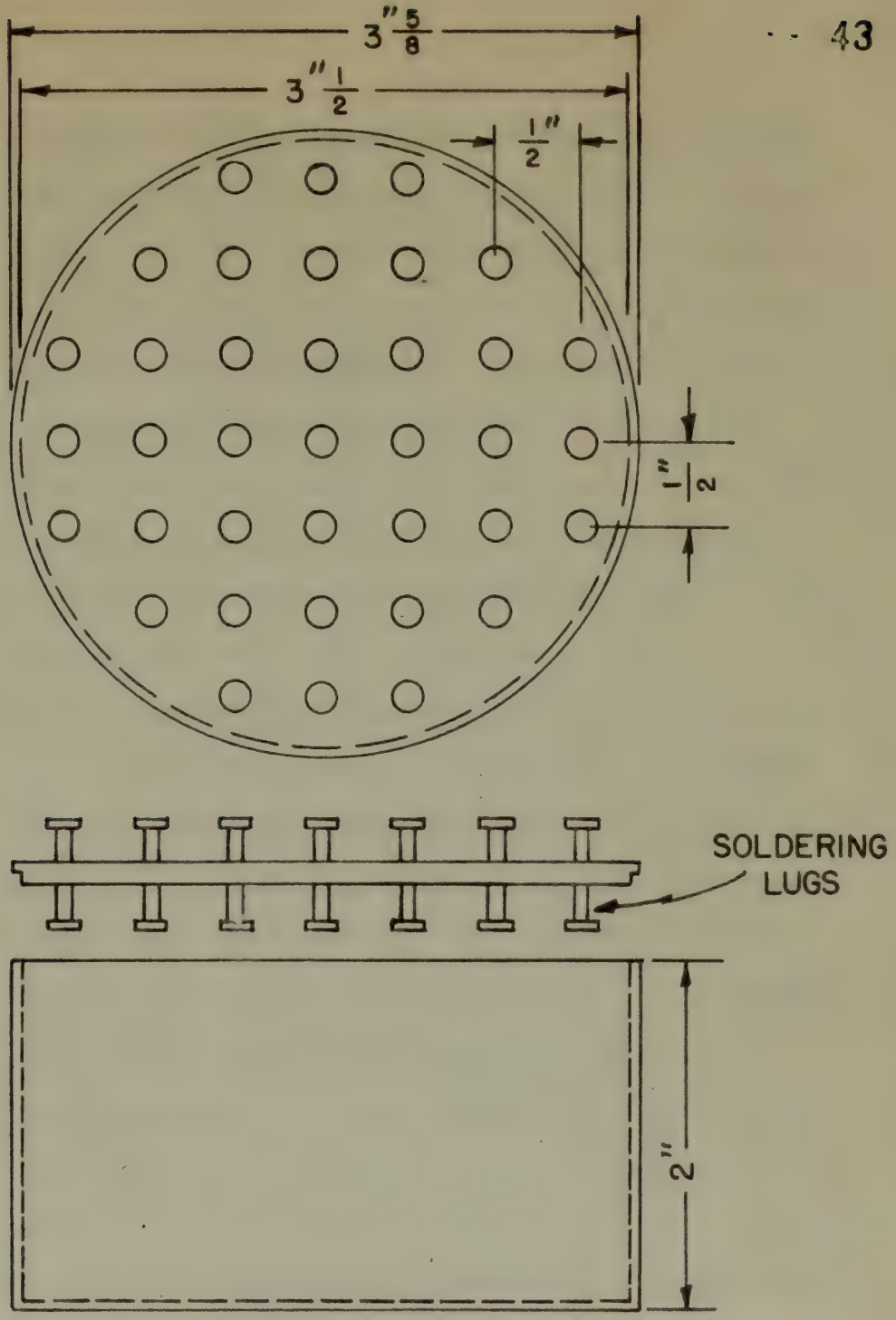

MATERIALS – LINEN COVERED BAKELITE AND STANDARD SOLDERING LUGS.

NOTE – THE 37 SOLDERING LUGS ARE CONNECTED TO TAPS ON THE CORE WINDINGS EVERY 200 TURNS, PROVIDING A CONVENIENT METHOD FOR CHANGING THE ARRANGEMENT OF THE VARIOUS WINDINGS.

FIG. 2-13 SPECIFICATIONS FOR TEST COIL BOXES.

To achieve maximum coupling between the various windings it is necessary to minimize leakage flux. It is desirable, therefore, that each of the several windings required by the amplifier design be distributed around the entire circumference of the toroid. In order to reduce capacitance parasitics, the cores should be wound such that large potential differences between turns are avoided whenever possible. The separation of the windings from the metallic cores by means of the protective boxes is an additional aid in reducing stray capacity.

All reactor windings were tapped every 200 turns in order to provide a ready means for changing the number of turns. Each finished coil was then enclosed in a cylindrical container. As shown in Figure 2-13, the covers of these containers were provided with 35 soldering lugs to which the various coil taps were attached in a systematic manner and labeled to permit easy identification. The coils were then impregnated with Ceresine Wax to improve the insulation and exclude moisture. The convenience with which the number of turns could be adjusted in the various windings was of great value while conducting experimental studies.

CHAPTER III

EXPERIMENTAL STUDIES OF THE BASIC CIRCUIT

Introduction

Although the basic magnetic-amplifier circuit, whose properties will be discussed in this chapter, is not the case of most practical interest, conclusions drawn from its study will provide certain fundamental concepts as to the static and dynamic performance of the magnetic amplifier. Because the problem of designing magnetically-biased saturable reactors involves nonlinear differential equations, the usual approach has been to approximate mathematically the empirically determined nonlinear functions, or to carry out experimental investigations on a prototype.[1,2] A third method of attack, which to the knowledge of the authors has not yet been applied to the problem, is the solution of the system equations by machine methods. This latter method has been carried out using the M.I.T. Differential Analyzer Number One. The analytic results obtained therefrom are compared in Chapter IV with the experimental results set forth in the present chapter.

The Experimental Circuit

The basic magnetic-amplifier circuit studied in this chapter is the series-connected saturable reactor with a direct-current input and an alternating-current power

---

1. M.I.T. Staff, "Magnetic Circuits and Transformers," (New York, John Wiley & Sons, 1943), 199.
2. Lamm, U., "The Transductor, A D.C. Pre-Saturated Reactor," (Stockholm, Esselte Aktiebolag, 1943).

CHAPTER III

EXPERIMENTAL STUDIES OF THE BASIC CIRCUIT

Introduction

Although the basic magnetic-amplifier circuit, whose properties will be discussed in this chapter, is not the case of most practical interest, conclusions drawn from its study will provide certain fundamental concepts as to the static and dynamic performance of the magnetic amplifier. Because the problem of designing magnetically-biased saturable reactors involves nonlinear differential equations, the usual approach has been to approximate mathematically the empirically determined nonlinear functions, or to carry out experimental investigations in a prototype.[1,2] A third method of attack, which is the knowledge of the authors has not yet been applied to the problem, is the solution of the system equations by machine methods. This latter method has been carried out using the M.I.T. Differential Analyzer Number One. The analytic results obtained therefrom are compared in Chapter IV with the experimental results set forth in the present chapter.

The Experimental Circuit

The basic magnetic-amplifier circuit studied in this chapter is the series-connected saturable reactor with a direct-current input and an alternating-current power

1. M.I.T. Staff, "Magnetic Circuits and Transformers," (New York, John Wiley & Sons, 1943), 193.
2. Lamm, U., "The Transductor, A D.C. Pre-Saturated Reactor," (Stockholm, Reseite Aktiebolag, 1941).

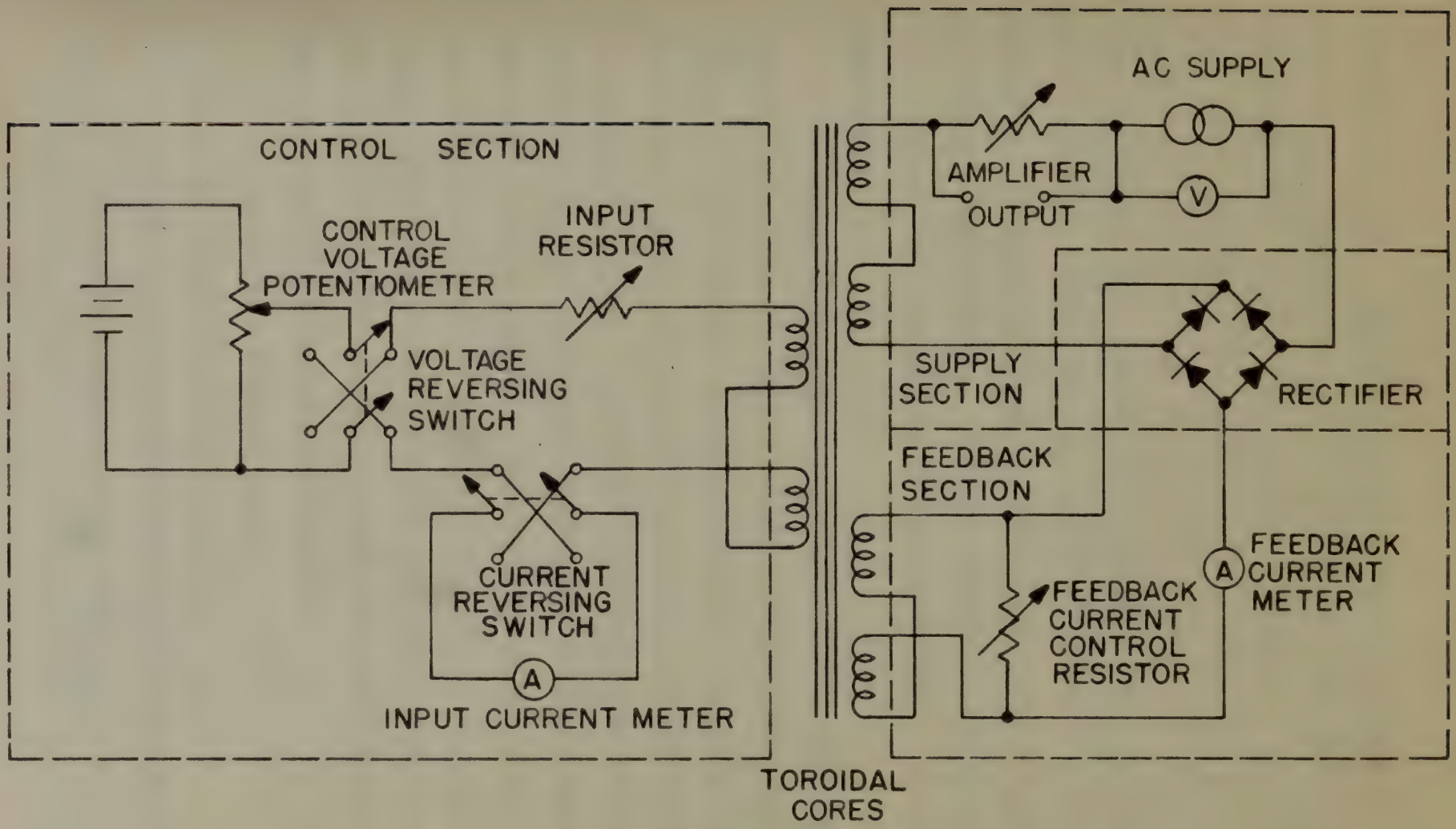

FIG. 3-1 BREADBOARD CIRCUIT FOR EXPERIMENTAL MAGNETIC AMPLIFIER STUDIES.

supply and load. The circuit arrangement is shown in Figure 3-1, disregarding the feedback section, which is not applicable to the basic circuit and will be discussed in a later chapter. The purpose of the experimental study is to show the effect of the various circuit elements on both the static and dynamic performance of the magnetic amplifier with a view towards establishing certain design criteria. A thorough study of these effects in a prototype amplifier permits the use of model theory in scaling the size and winding data of the reactors to meet a specific application.

Because the magnetic amplifier is a nonlinear circuit, its behavior cannot be characterized by a system function, or transform, as in the case of a linear device. The system itself, more specifically the circuit inductance, is a function of the excitation. The nonlinearity is attributable to the saturation phenomenon of the ferromagnetic core which is prescribed by the magnetization curve. Since the amplifier cannot be analyzed as a linear system, this chapter will discuss the empirical approach, based upon experimental data, for optimizing the following excitation variables and lumped-circuit parameters:

1. the control current, i_1,
2. the control-circuit resistance, R_1,
3. the number of turns in the control winding, N_1,
4. the carrier-excitation voltage, E_2,

supply and load. The circuit arrangement is shown in Figure 3-1, disregarding the feedback section, which is not applicable to the basic circuit and will be discussed in a later chapter. The purpose of the experimental study is to show the effect of the various circuit elements on both the static and dynamic performance of the magnetic amplifier with a view towards establishing certain design criteria. A thorough study of these effects in a prototype amplifier permits the use of model theory in scaling the size and winding data of the reactors to meet a specific application.

Because the magnetic amplifier is a nonlinear circuit, its behavior cannot be characterized by a system function, or transform, as in the case of a linear device. The system itself, more specifically the circuit inductance, is a function of the excitation. The nonlinearity is attributable to the saturation phenomenon of the ferromagnetic core which is prescribed by the magnetization curve. Since the amplifier cannot be analyzed as a linear system, this chapter will discuss the empirical approach, based upon experimental data, for optimizing the following excitation variables and lumped-circuit parameters:

1. the control current, i_1,
2. the control-circuit resistance, R_1,
3. the number of turns in the control winding, N_1,
4. the carrier-excitation voltage, E_2,

5. the carrier-excitation frequency, f_2,

6. the load resistance, R_2, and

7. the number of turns in the carrier winding, N_2.

The response variable will be considered to be the carrier current, i_2, from which the ampere-turn sensitivity, the power output, and power gain can be readily computed.

Static Performance of the Basic Circuit.

The modulation characteristic, or functional relationship between the control current and the average-carrier current, is the most useful transfer curve for describing the static behavior of the magnetic amplifier. This characteristic is more significant when average output ampere-turns are plotted as a function of input ampere-turns, giving the relationship between control and carrier magnetizing forces. For the ideal case of infinite initial permeability, this relationship would be a straight line through the origin having a forty-five degree slope; that is, the average carrier ampere-turns would equal the control ampere-turns within the amplifying range of control excitation. In the practical case, this relationship is closely approximated and has been discussed in detail by Buchhold.[1] Because of the exciting current which is required to furnish the no-load core losses in the practical amplifier, the average carrier ampere-turns exceed the control ampere-turns in the lower control range, whereas in

1. Rex, H.B., "The Transductor," Instruments, 20, (1947), 1102-1109.

5. the carrier-excitation frequency, f_c,

6. the load resistance, R_L, and

7. the number of turns in the carrier winding, N_c.

The response variable will be considered to be the carrier current, i_c, from which the ampere-turn sensitivity, the power output, and power gain can be readily computed.

Static Performance of the Basic Circuit.

The modulation characteristic, or functional relationship between the control current and the average-carrier current, is the most useful transfer curve for describing the static behavior of the magnetic amplifier. This characteristic is more significant when average output ampere-turns are plotted as a function of input ampere-turns, giving the relationship between control and carrier magnetizing forces. For the ideal case of infinite initial permeability, this relationship would be a straight line through the origin having a forty-five degree slope; that is, the average carrier ampere-turns would equal the control ampere-turns within the amplifying range of control excitation. In the practical case, this relationship is closely approximated and has been discussed in detail by Bernhold.[1] Because of the exciting current which is required to furnish the no-load core losses in the practical amplifier, the average carrier ampere-turns exceed the control ampere-turns in the lower control range, whereas in

1. Bee, R.G., "The Transductor," Instruments, 30, (1957), 1106-1128.

the higher control range they fall off and become less than the control ampere-turns. A modulation characteristic is plotted in Figure 3-2 for constant voltage across the reactors, a case of no practical interest because it implies the absence of load resistance. The manner in which this characteristic arises is explained by reference to Figure 3-3, which shows the relation between the flux and the ampere-turns in the cores. Only the action of one core need be given. As long as the peak excursions of the flux lie below the saturation line, the ampere turns are small and essentially constant in amplitude, as shown by Figure 3-3, (1) and (2). As the peak flux-excursions begin to exceed the saturation line, linear amplifying action takes place. The end of the linear range, point (4) of Figure 3-2, occurs when the direct flux biases the alternating flux to the saturation line shown in Figure 3-3 (5). As the input increases beyond this point, the characteristic begins to flatten out, becoming horizontal when the direct flux is so large that the entire excursion of the alternating flux lies above the saturation line shown in Figure 3-3 (5). Regardless of further increases of the control current, the carrier current will remain constant by virtue of the fact that the core is now completely saturated at all times with respect to the alternating components.

In the practical magnetic amplifier the voltage across the reactor is not constant, but falls off as the voltage-drop across the load resistor rises with increasing

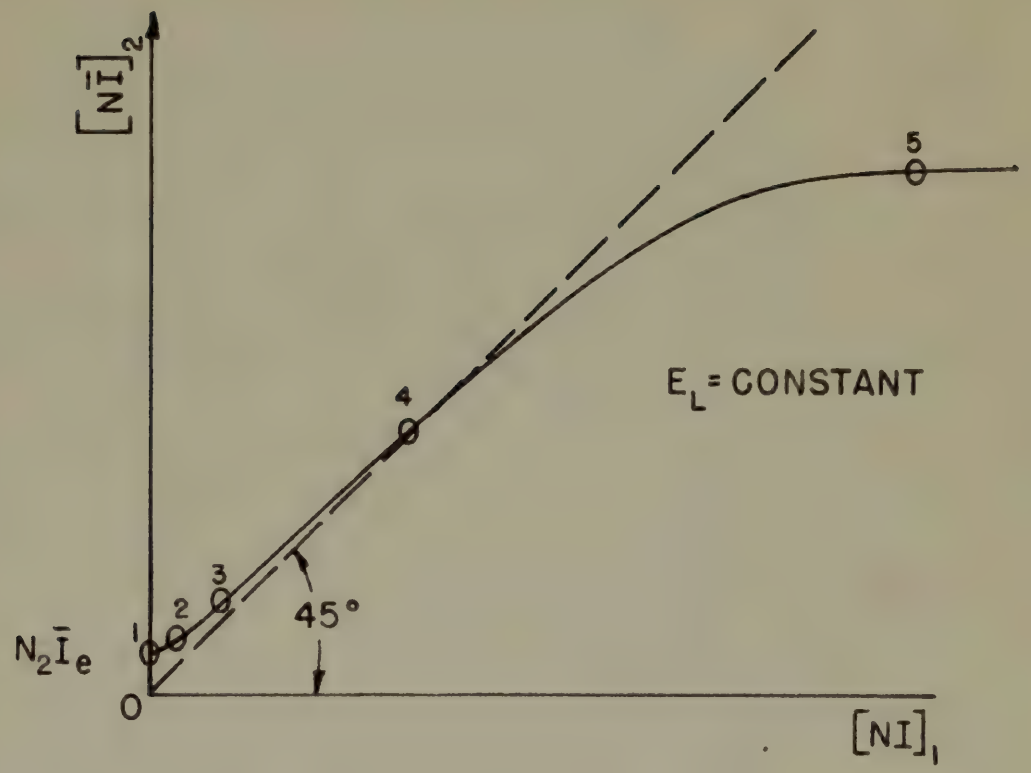

FIG. 3–2 MODULATION CHARACTERISTIC.

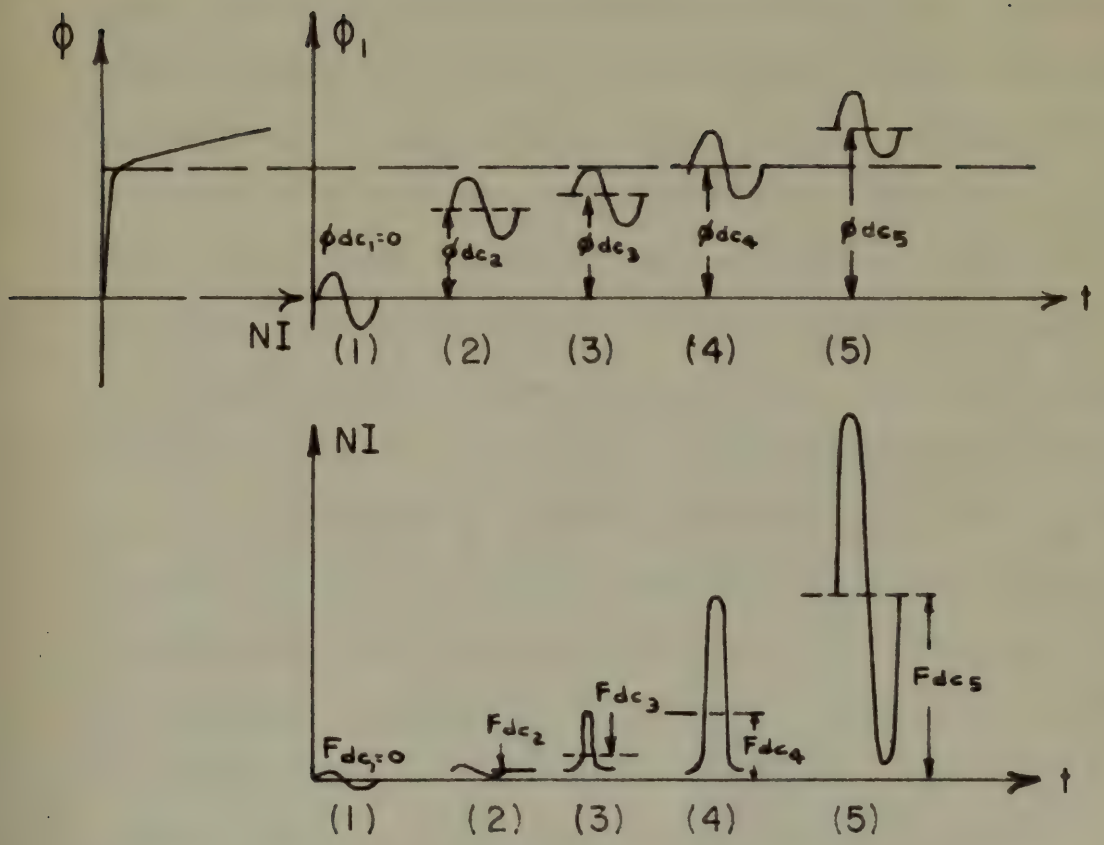

FIG.3-3 FLUX AND MAGNETIZING FORCE FOR VARIOUS VALUES OF DIRECT EXCITATION.

carrier current, and hence the actual modulation characteristic flattens out somewhat sooner. The observed effect of the circuit variables upon the modulation characteristic will be taken up and explained individually in order. A Western-Electric type 142A amplifier fed by a Hewlett-Packard model 205AG audio-frequency generator was used as the carrier-power supply. The load voltage was read from a Hewlett-Packard model 400A vacuum-tube voltmeter whose deflection is proportional to the average value of the voltage although calibrated to read the root-mean-square value of a sine wave. The average value of the carrier current was then computed from Ohm's law, knowing the value of the load resistance and the average value of the load voltage. The value of input current was read directly from a direct-current milliammeter.

The control circuit parameters, R_1 and R_1, were observed to have no effect upon the modulation characteristic. R_1 was taken from a minimum value of 165 ohms, the resistance of the input winding, to a maximum value of about 10,000 ohms. No effect would be anticipated unless the impedance of the control circuit to the induced even-harmonic carrier currents is high. If, for example, a choke coil were placed in series with the control windings, the flow of the even harmonics would be restricted and the magnetization of the cores would be constrained. The flux, as explained by Buchhold,[1] would no longer be sinusoidal and the waveform of the carrier current would be altered. To ensure natural magnetization, and

---

1. Rex, H.B., "The Transductor," Instruments, 20, (1947), 1102-1109.

carrier current, and hence the actual modulation characteristic flattens out somewhat sooner. The observed effect of the circuit variables upon the modulation characteristic will be taken up and explained individually in order. A Western-Electric type 1[illegible] amplifier fed by a Hewlett-Packard model [illegible] audio-frequency generator was used as the carrier-power supply. The load voltage was read from a Hewlett-Packard model [illegible] vacuum-tube voltmeter whose deflection is proportional to the average value of the voltage although calibrated to read the root-mean-square value of a sine wave. The average value of the carrier current was then computed from Ohm's law, knowing the value of the load resistance and the average value of the load voltage. The value of input current was read directly from a direct-current milliammeter.

The control circuit parameters, R_2 and R_1, were observed to have no effect upon the modulation characteristic. R_1 was taken from a minimum value of 1[illegible] ohms, the resistance of the input winding, to a maximum value of about 10,000 ohms. No effect could be anticipated unless the impedance of the control circuit to the induced even-harmonic carrier currents is high. If, for example, a choke coil were placed in series with the control windings, the flow of the even harmonics would be restricted and the magnetization of the cores would be constrained. The flow, as explained by Buchhold,[1] would no longer be sinusoidal and the waveform of the carrier current would be altered. To ensure natural magnetization, and

1. Rec, S.S., "The Transductor," Instruments, 20, (1947), 1105-1109.

sinusoidal flux, a capacitor should be shunted across the control-current windings of a magnetic amplifier. This filter should present a low impedance to the even-harmonic frequencies of the carrier, and a high impedance to the signal frequencies.

While the control circuit has little effect upon the modulation characteristic, the carrier-circuit variables were all observed to have quite a pronounced effect. The effect of the load resistor, R_2, will first be considered.

The effect of R_2 is to reduce the alternating voltage which appears across the carrier windings of the saturable reactors as a result of the voltage drop in the load, thereby reducing the magnitude of the alternating-flux amplitude in the cores. If, for the moment, the carrier current is assumed sinusoidal, an assumption which is quantitatively invalid because of the high odd-harmonic content of this current, linear-impedance concepts, based on sinusoidal excitation and response, may be used to give a qualitative picture of the effect of load resistance on the modulation characteristic. Figure 3-4 may be taken as the equivalent carrier circuit where L_2 is an inverse function of the control current. The core losses are lumped into R_2 for convenience. The ratio of the voltage, E_L, across the reactors to the carrier-supply voltage, E_2, is obtained as follows:

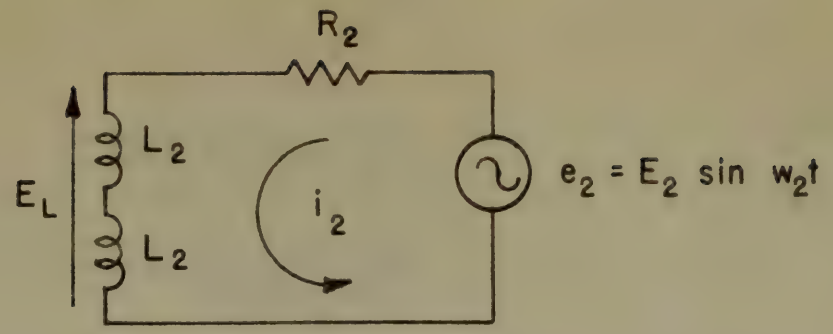

FIG. 3-4 EQUIVALENT CARRIER CIRCUIT

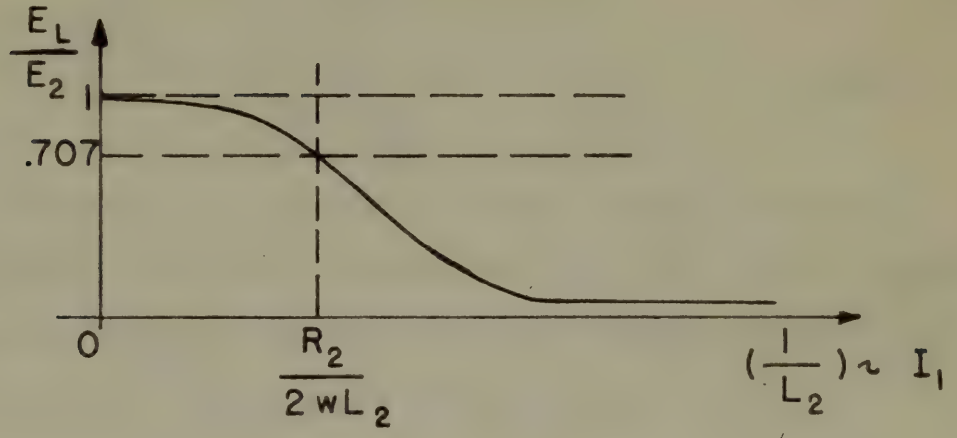

FIG. 3-5 $\frac{E_L}{E_2}$ AS A FUNCTION OF I_1

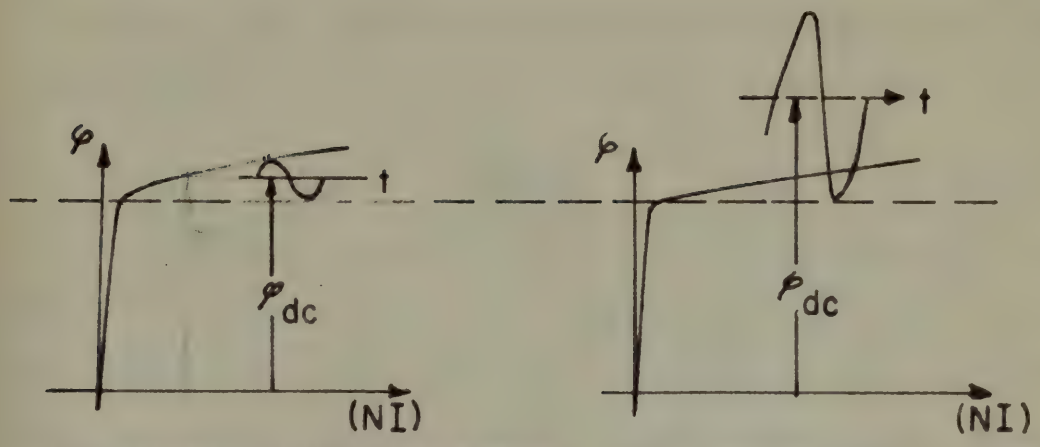

(a) SMALL FLUX AMPLITUDE. (b) LARGE FLUX AMPLITUDE.

FIG. 3-6

$$E_L = I_2 X_2 = \frac{E_2}{Z_2} X_2 \qquad (3\text{-}1)$$

$$= \frac{E_2 (2j\omega_1 L_2)}{R_2 + 2j\omega_1 L_2} \qquad (3\text{-}2)$$

$$\frac{E_L}{E_2} = \frac{1}{1 - j\left(\frac{R_2}{2\omega_1 L_2}\right)} \qquad (3\text{-}3)$$

$$\left|\frac{E_L}{E_2}\right| = \frac{1}{\sqrt{1 + \left[\frac{R_2}{2\omega_1 L_2}\right]^2}} \qquad (3\text{-}4)$$

Since, for zero I_1, L_2 is very large, ideally infinite, the ratio is initially unity, or nearly so. As I_1 increases and L_2 decreases, the ratio falls off and approaches zero for small L_2. The ratio is down 3 db when

$$\frac{R_2}{2\omega_1 L_2} = 1 \qquad (3\text{-}5)$$

The E_L/E_2 function is plotted in Figure 3-5. For higher load resistances, therefore, the ratio drops from unity at a higher rate. Since the alternating flux-density amplitude is given by

$$\mathcal{B} = \frac{\frac{1}{2} E_L}{\omega_2 N_2 A} \qquad (3\text{-}6)$$

the alternating component of core-flux experiences the same rate of change of amplitude with I_1 as does the voltage E_L. The modulation characteristic, therefore, tends to flatten out for lower values of input ampere-turns as the R_2 is made larger. This effect may be pictured physically by reference to Figure 3-6, from which it is seen that a smaller value of direct flux is needed to bias the entire alternating flux

$$E_L = I_2 X_2 = \frac{E_2}{R_2} X_2 \qquad (3\text{-}1)$$

$$= \frac{E_2 (2j\omega L_2)}{R_2 + 2j\omega L_2} \qquad (3\text{-}2)$$

$$\frac{E_L}{E_2} = \frac{1}{1 - j\left(\frac{R_2}{2\omega L_2}\right)} \qquad (3\text{-}3)$$

$$\left|\frac{E_L}{E_2}\right| = \frac{1}{\sqrt{1 + \left[\frac{R_2}{2\omega L_2}\right]^2}} \qquad (3\text{-}4)$$

Since, for zero I_1, L_2 is very large, ideally infinite, the ratio is initially unity, or nearly so. As I_1 increases and L_2 decreases, the ratio falls off and approaches zero for small L_2. The ratio is down 3 db when

$$\frac{R_2}{2\omega L_2} = 1 \qquad (3\text{-}5)$$

The E_L/E_2 function is plotted in Figure 3-5. For higher load resistances, therefore, the ratio drops from unity at a higher rate. Since the alternating flux-density amplitude is given by

$$\beta = \frac{\frac{1}{2}E_L}{\omega_2 R_2 A} \qquad (3\text{-}6)$$

the alternating component of core-flux experiences the same rate of change of amplitude with I_1 as does the voltage E_L. The modulation characteristic, therefore, tends to flatten out for lower values of input ampere-turns as the R_2 is made larger. This effect may be pictured physically by reference to Figure 3-6, from which it is seen that a smaller value of direct flux is needed to bias the entire alternating flux

above the saturation line with a small flux amplitude as compared with a large flux amplitude. This effect was observed experimentally, as shown by Figures 3-7, 3-13 and 3-16.

The manner in which E_2 affects the modulation characteristic can best be explained by again referring to the ratio E_L/E_2 which is expressed by Equation 3-4 and shown in Figure 3-5. E_2 does not affect the rate at which E_L falls off with I_1, but does control its magnitude. Thus, for higher E_2 there exists a larger core-flux amplitude from the Equation 3-6, and the modulation characteristic tends to flatten out for higher values of control ampere-turns. This effect was observed as shown in Figures 3-8, 3-14 and 3-17. Another effect which should be pointed out is that if, with no control current applied, the value of the alternating-flux amplitude is such that it exceeds the saturation line, an excessive exciting current is drawn. As stated in Chapter II, the flux should be so adjusted that it just fails to exceed the saturation line when no control current is applied. A good illustration of excessive exciting current as a result of incorrect alternating-flux adjustment is the E_2 = 80 volts (rms.) curve at a carrier frequency of 100 cycles per second, shown in Figure 3-14.

Unlike the effects of E_2 and R_2, the carrier frequency, f_2, affects both the core flux and the carrier-circuit impedance. The flux-density amplitude is seen from Equation

above the saturation line with a small flux amplitude as compared with a large flux amplitude. This effect was observed experimentally, as shown by Figures 3-7, 3-13 and 3-15.

The manner in which E_2 affects the modulation characteristic can best be explained by again referring to the ratio E_L/E_2 which is expressed by Equation 3-4 and shown in Figure 3-5. E_2 does not affect the rate at which E_L falls off with I_1, but does control its magnitude. Thus, for higher E_2 there exists a larger core-flux amplitude from the Equation 3-6, and the modulation characteristic tends to flatten out for higher values of control amperetures. This effect was observed as shown in Figures 3-6, 3-14 and 3-17. Another effect which should be pointed out is that if, with no control current applied, the value of the alternating-flux amplitude is such that it exceeds the saturation line, an excessive exciting current is drawn. As stated in Chapter II, the flux should be so adjusted that it just fails to exceed the saturation line when no control current is applied. A good illustration of excessive exciting current as a result of incorrect alternating-flux adjustment is the E_2 = 50 volts (rms.) curve at a carrier frequency of 100 cycles per second, shown in Figure 3-14.

Unlike the effects of E_2 and E_3, the carrier frequency, f_2, affects both the core flux and the carrier-circuit impedance. The flux-density amplitude is seen from Equation

3-6 to be inversely proportional to the frequency. If the frequency is raised, the flux-density amplitude is lowered and the modulation characteristic would be expected to flatten out for lower I_1 by reason of the effect pointed out in Figure 3-6. The E_L/E_2 ratio, however, would fall off at a slower rate for the higher frequency tending to counteract the former effect. Experimental results plotted in Figure 3-9 show that the lowering of the flux-density amplitude is the more significant effect, since the modulation characteristics flatten out sooner at higher frequencies.

The final system parameter to be considered is N_2. Similar to the effect of f_2, N_2 affects both the core flux and the carrier-circuit impedance. A larger number of turns would decrease the core flux, as shown by Equation 3-6, and the modulation characteristic would tend to flatten out at a smaller value of I_1 from this consideration. The way in which N_2 affects the carrier-circuit inductance is indicated by the relation

$$L_2 = k N_2^2 \mu_{ac} \qquad (3\text{-}8)$$

In the case of the frequency effect, the reactance went up directly with the frequency, whereas with N_2, the reactance goes up as the square of the number of turns. The E_L/E_2 ratio has considerably more effect here than in the case of the frequency variation. For larger N_2 the effect of this ratio is to cause the modulation characteristic to flatten out at higher values of I_1. These two effects, as in the case of the frequency variation, tend to oppose one another,

3-6 to be inversely proportional to the frequency. If the frequency is raised, the flux-density amplitude is lowered and the modulation characteristic would be expected to flatten out for lower L_1 by reason of the effect pointed out in Figure 3-6. The R_L/R_2 ratio, however, would fall off at a slower rate for the higher frequency tending to counteract the former effect. Experimental results plotted in Figure 3-9 show that the lowering of the flux-density amplitude is the more significant effect, since the modulation characteristics flatten out sooner at higher frequencies.

The final system parameter to be considered is R_2. Similar to the effect of L_2, R_2 affects both the core flux and the carrier-circuit impedance. A larger number of turns would decrease the core flux, as shown by Equation 3-6, and the modulation characteristic would tend to flatten out at a smaller value of L_1 from this consideration. The way in which R_2 affects the carrier-circuit impedance is indicated by the relation

$$L_2 = k R_2^2 \mu_{ac} \qquad (3\text{-}8)$$

In the case of the frequency effect, the reactance went up directly with the frequency, whereas with R_2, the reactance goes up as the square of the number of turns. The R_L/R_2 ratio has considerably more effect here than in the case of the frequency variation. For larger R_2 the effect of this ratio is to cause the modulation characteristic to flatten out at higher values of L_1. These two effects, as in the case of the frequency variation, tend to oppose one another,

but because of the squared relation there is an optimum value of N_2 to be sought such that the modulation characteristic follows along a forty-five degree slope as long as possible before tending to flatten out. The fact that an optimum N_2 exists can be seen by examination of Figures 3-10, 3-11, 3-12, 3-15 and 3-16.

From this qualitative discussion it is seen that two factors must be kept in mind when predicting a modulation characteristic, namely: the initial value of the flux-density amplitude and the rate at which this amplitude falls off with respect to increasing control current. As stated at the beginning of this discussion, these concepts are only of a qualitative nature because the impedance concept itself is based upon the assumption that the carrier current is sinusoidal, an assumption which is highly approximate, as can be seen by reference to the actual waveforms encountered, as illustrated in Chapter IV.

From a knowledge of the modulation characteristics of a given circuit, the values of power output and power gain may be obtained directly by computation. Since the exciting current which flows in the load when no signal is applied does not represent useful power, it is usually compensated for in the practical case by one method or another.[1] If I_e represents the root-mean-square value of the exciting current, the power output is then obtained from the expression

---

1. Fitzgerald, A.S., "Magnetic Amplifier Characteristics - Neutral Type," J.F.I., 244, (1947), 415-439.

but because of the squared relation there is an optimum value of N_g to be sought such that the modulation characteristic follows along a forty-five degree slope as long as possible before tending to flatten out. The fact that an optimum N_g exists can be seen by examination of Figures 3-10, 3-11, 3-12, 3-13 and 3-16.

From this qualitative discussion it is seen that two factors must be kept in mind when predicting a modulation characteristic, namely: the initial value of the flux-density amplitude and the rate at which this amplitude falls off with respect to increasing control current. As stated at the beginning of this discussion, these contents are only of a qualitative nature because the Lagrangian concept itself is based upon the assumption that the carrier current is sinusoidal, an assumption which is highly approximate, as can be seen by reference to the actual waveforms encountered, as illustrated in Chapter IV.

From a knowledge of the modulation characteristics of a given circuit, the values of power output and power gain may be obtained directly by computation. Since the exciting current which flows in the load when no signal is applied does not represent useful power, it is usually compensated for in the practical case by one method or another.[1] If I_c represents the root-mean-square value of the exciting current, the power output is then obtained from the expression

---

1. Fitzgerald, A.R., "Magnetic Amplifier Characteristics - Neutral Type," A.F.L., 23A, (1947), 410-433.

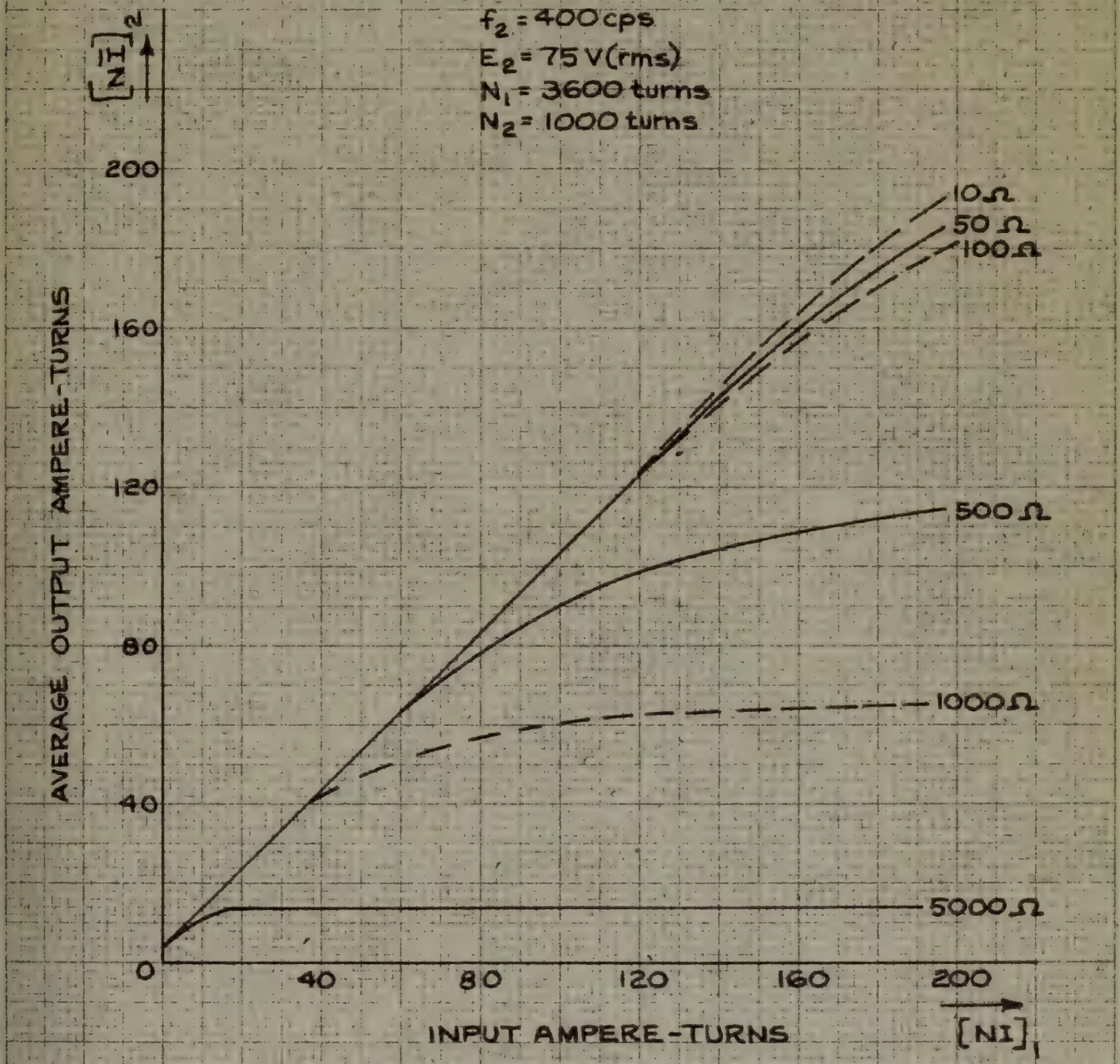

FIG. 3-7 MODULATION CHARACTERISTIC OF THE BASIC MAGNETIC AMPLIFIER SHOWING EFFECT OF LOAD RESISTANCE.

JUNE 29, 1948

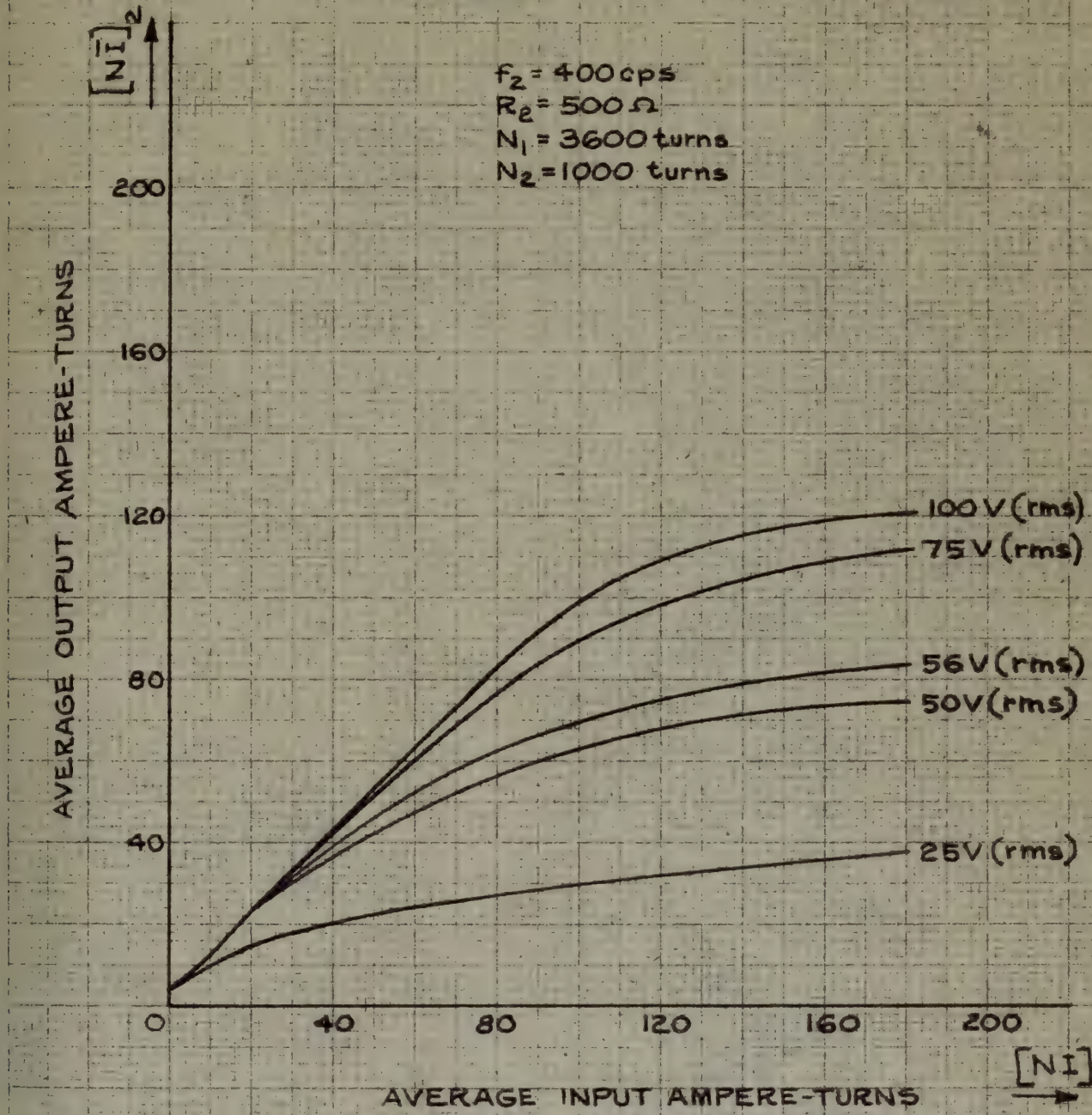

FIG. 3-8 MODULATION CHARACTERISTIC OF BASIC MAGNETIC AMPLIFIER SHOWING EFFECT OF ALTERNATING-CURRENT VOLTAGE.

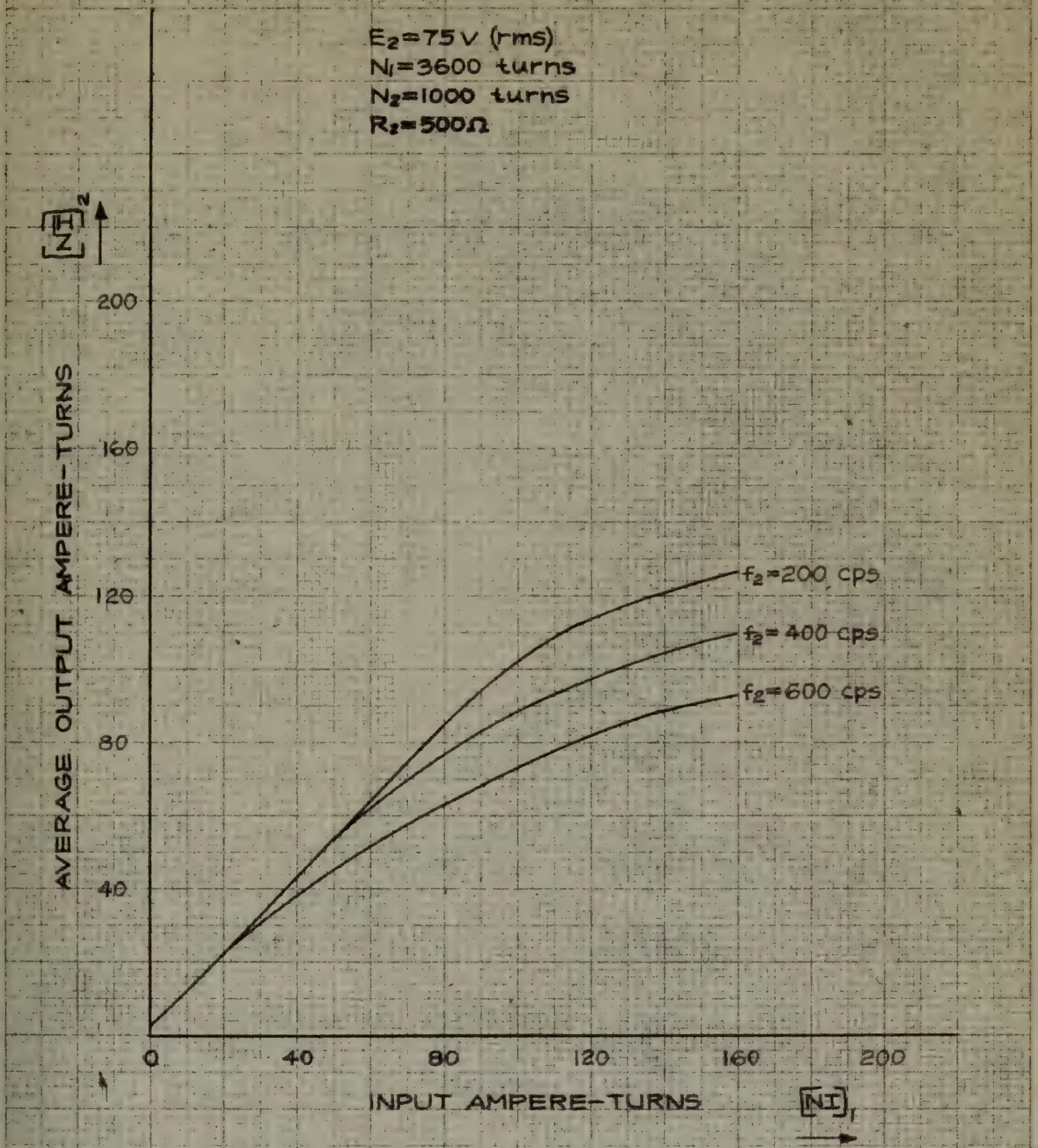

FIG. 3-9 MODULATION CHARACTERISTIC OF THE BASIC MAGNETIC AMPLIFIER SHOWING THE EFFECT OF CARRIER FREQUENCY

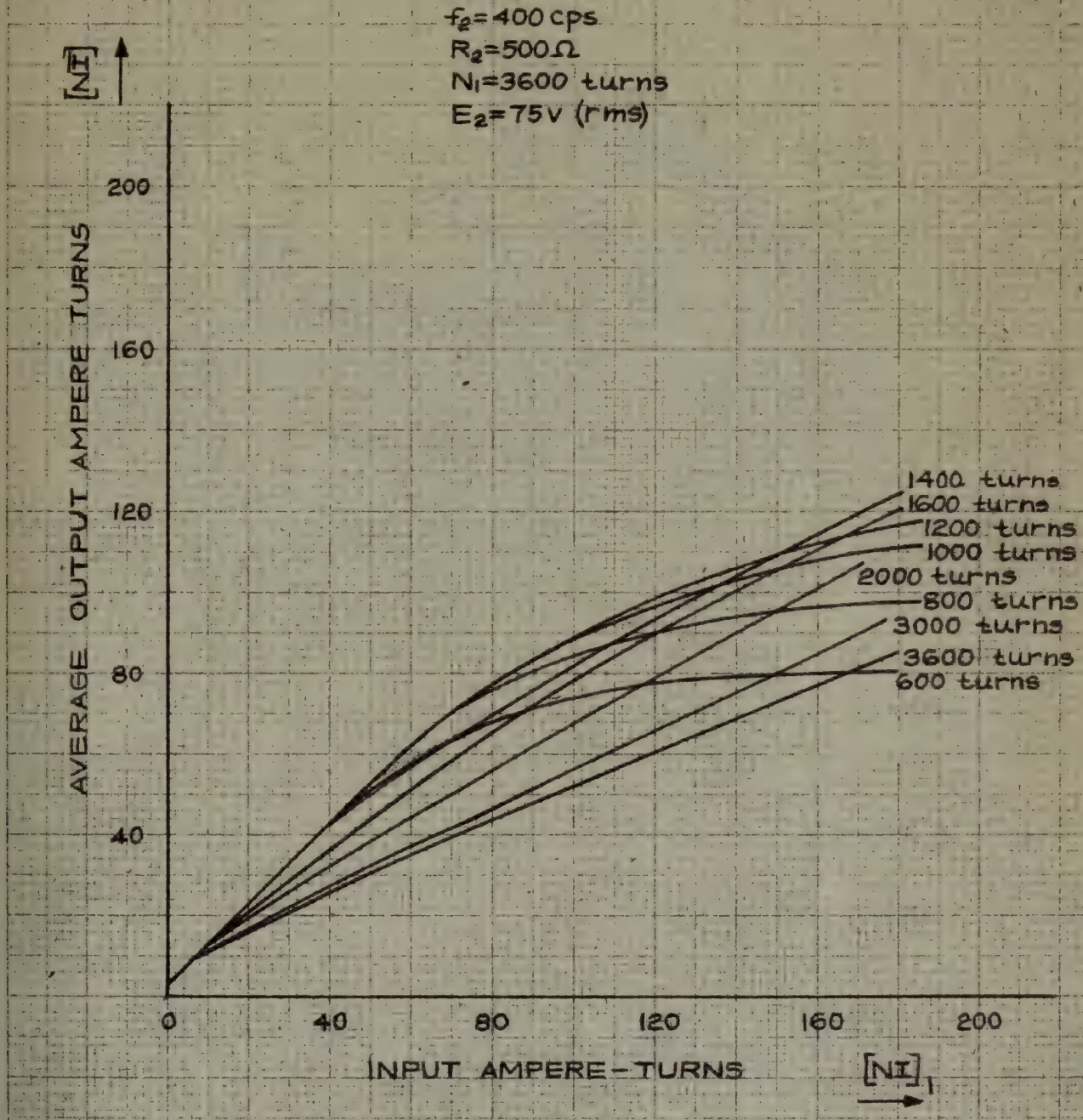

FIG. 3-10 MODULATION CHARACTERISTIC OF THE BASIC MAGNETIC AMPLIFIER SHOWING THE EFFECT OF OUTPUT TURNS

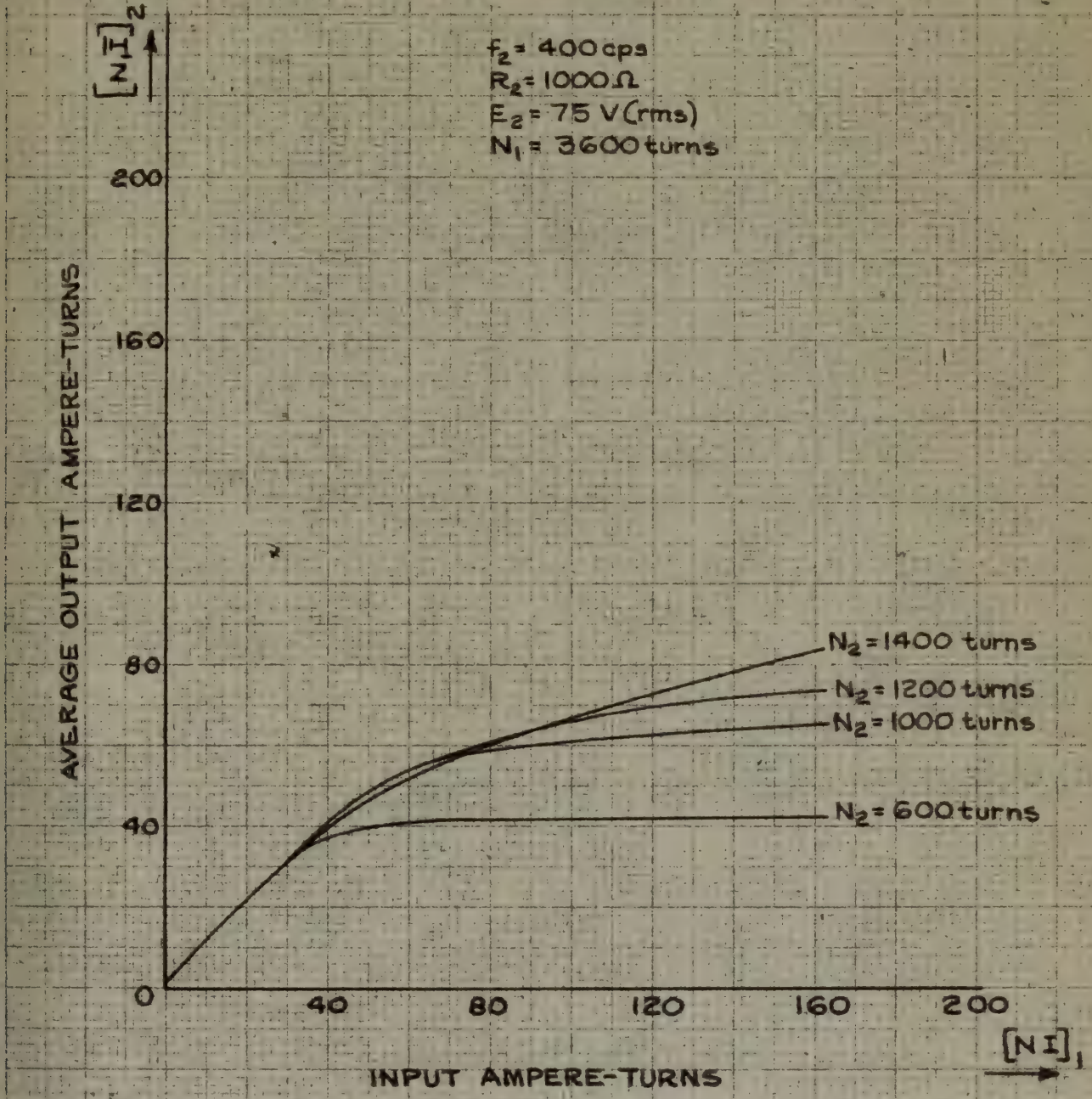

FIG. 3-11 MODULATION CHARACTERISTIC OF THE BASIC MAGNETIC AMPLIFIER SHOWING THE EFFECT OF OUTPUT TURNS.

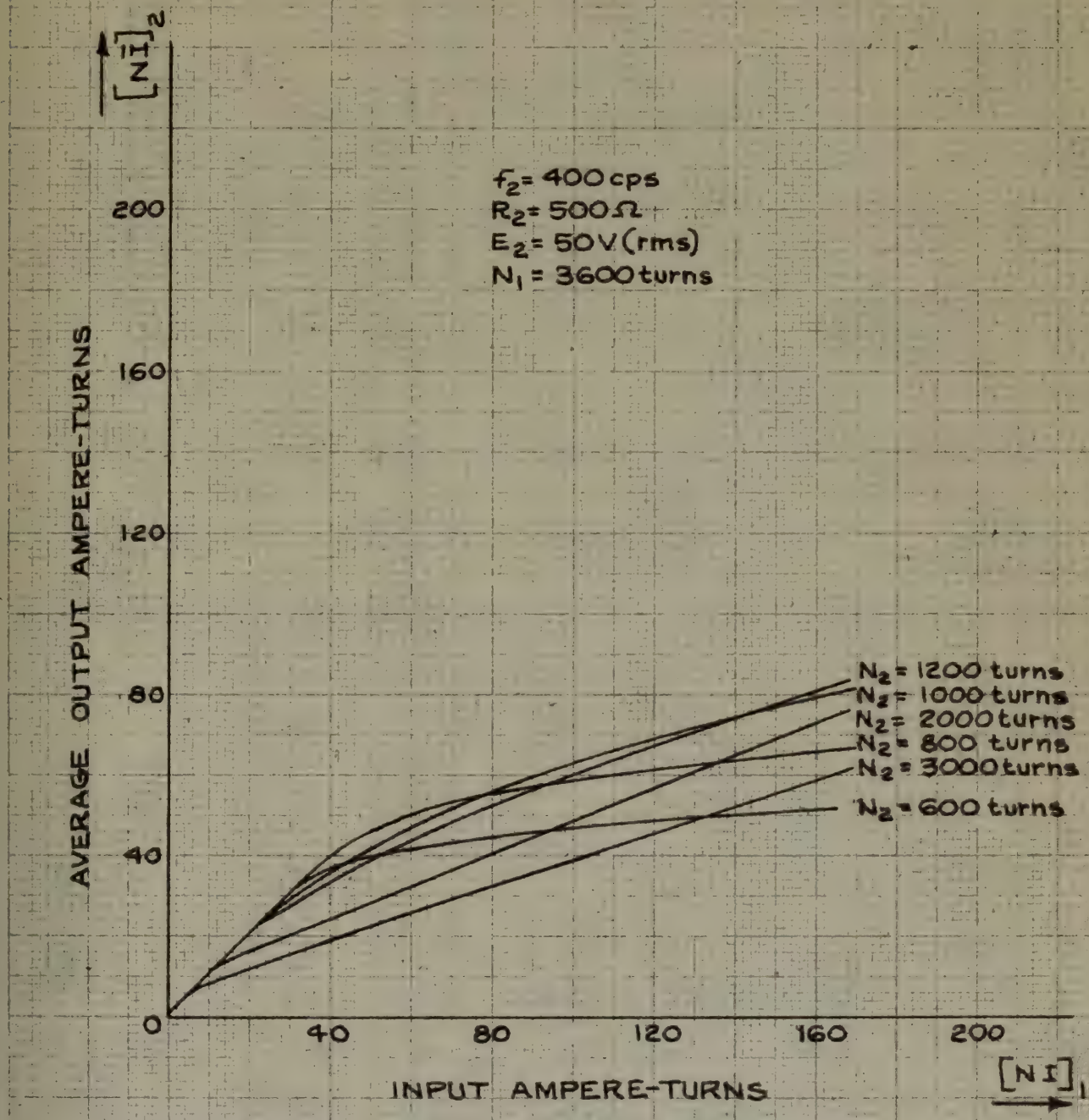

FIG. 3-12 MODULATION CHARACTERISTIC OF THE BASIC MAGNETIC AMPLIFIER SHOWING THE EFFECT OF OUTPUT TURNS.

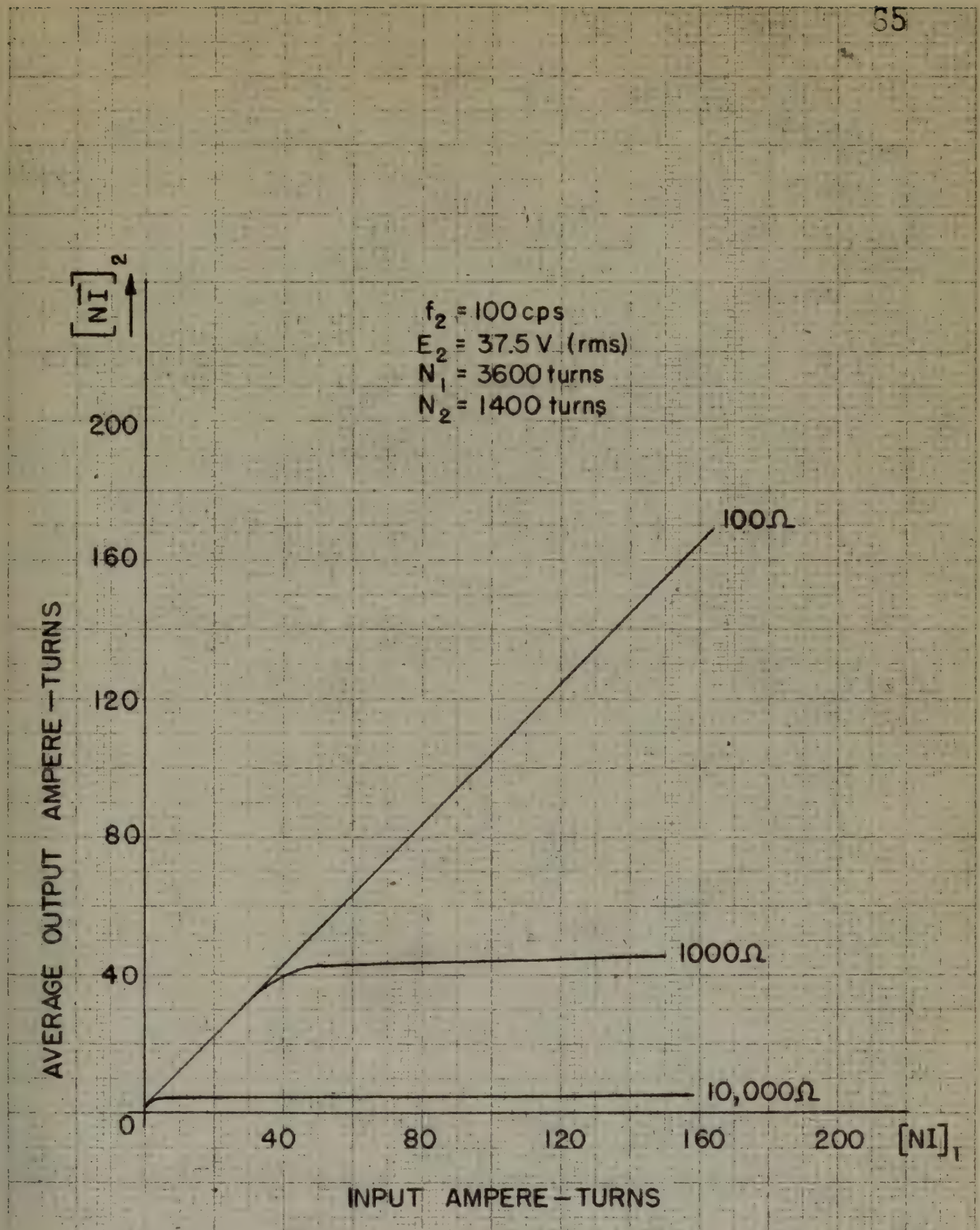

FIG. 3-13 MODULATION CHARACTERISTIC OF BASIC MAGNETIC AMPLIFIER SHOWING EFFECT OF LOAD RESISTANCE.

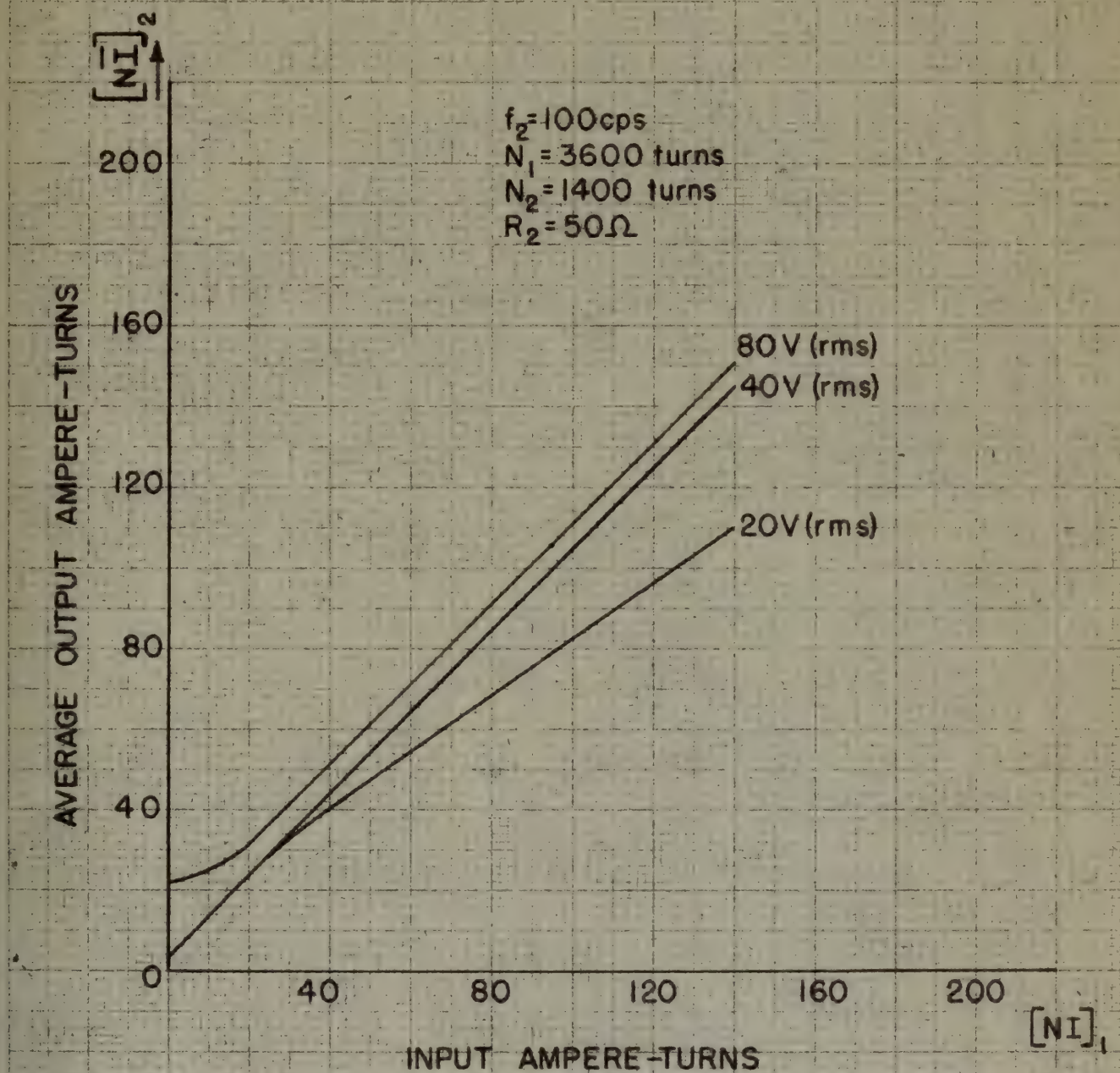

FIG. 3-14 MODULATION CHARACTERISTIC OF BASIC MAGNETIC AMPLIFIER SHOWING EFFECT OF ALTERNATING CURRENT VOLTAGE.

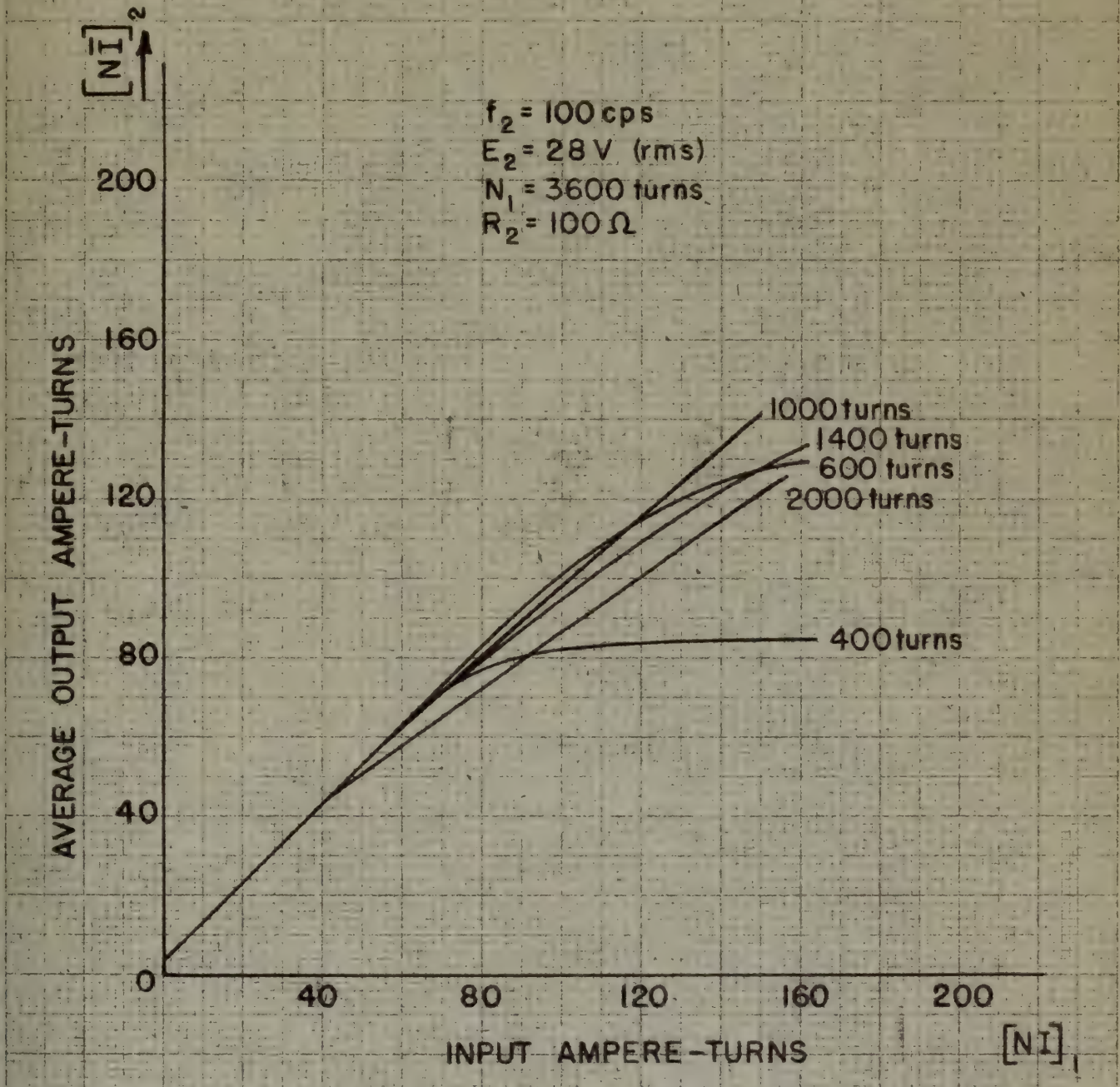

FIG. 3-15 MODULATION CHARACTERISTIC OF BASIC MAGNETIC AMPLIFIER SHOWING EFFECT OF OUTPUT TURNS.

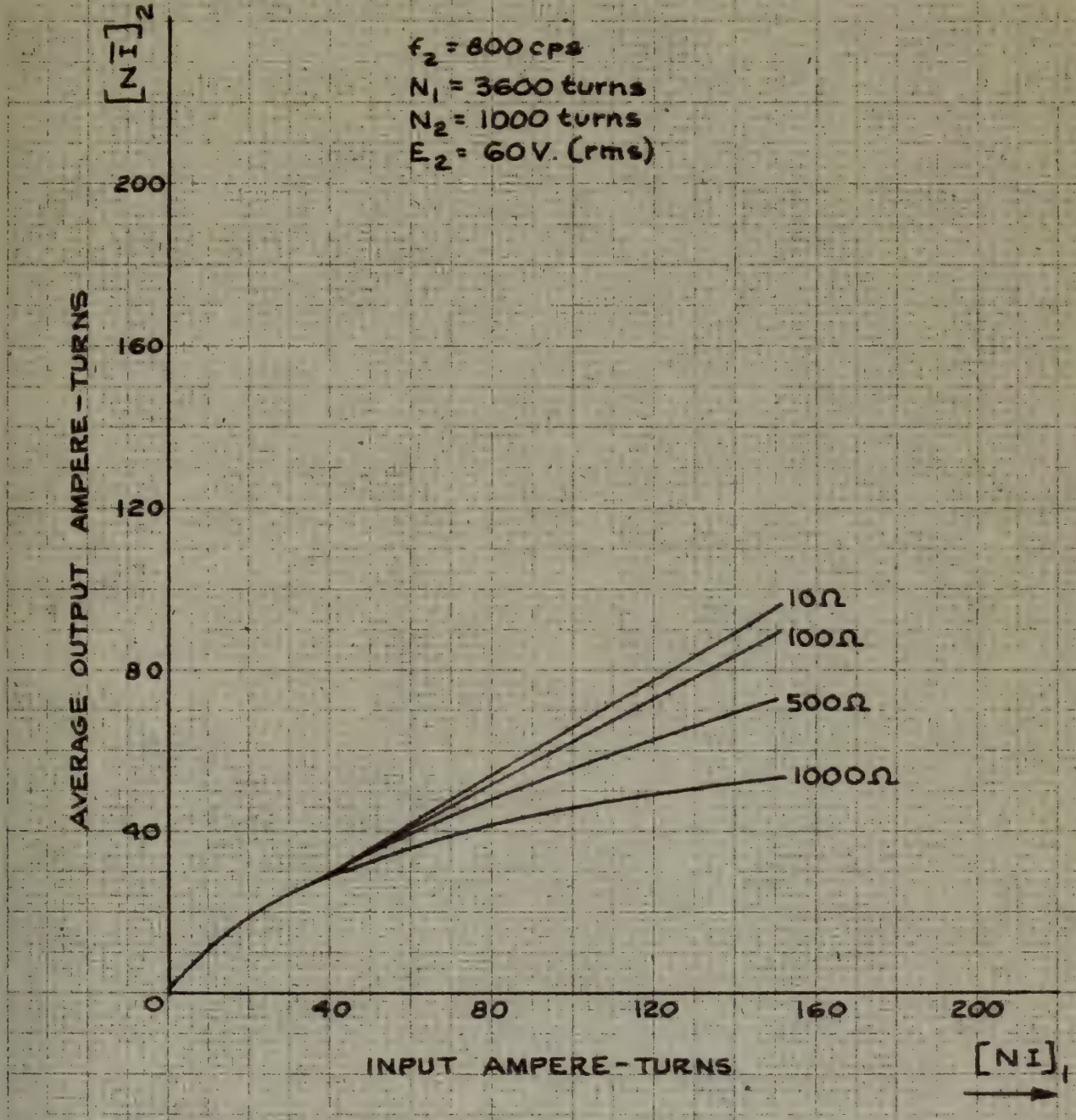

FIG. 3-16 MODULATION CHARACTERISTIC OF THE BASIC MAGNETIC AMPLIFIER SHOWING EFFECT OF LOAD RESISTANCE.

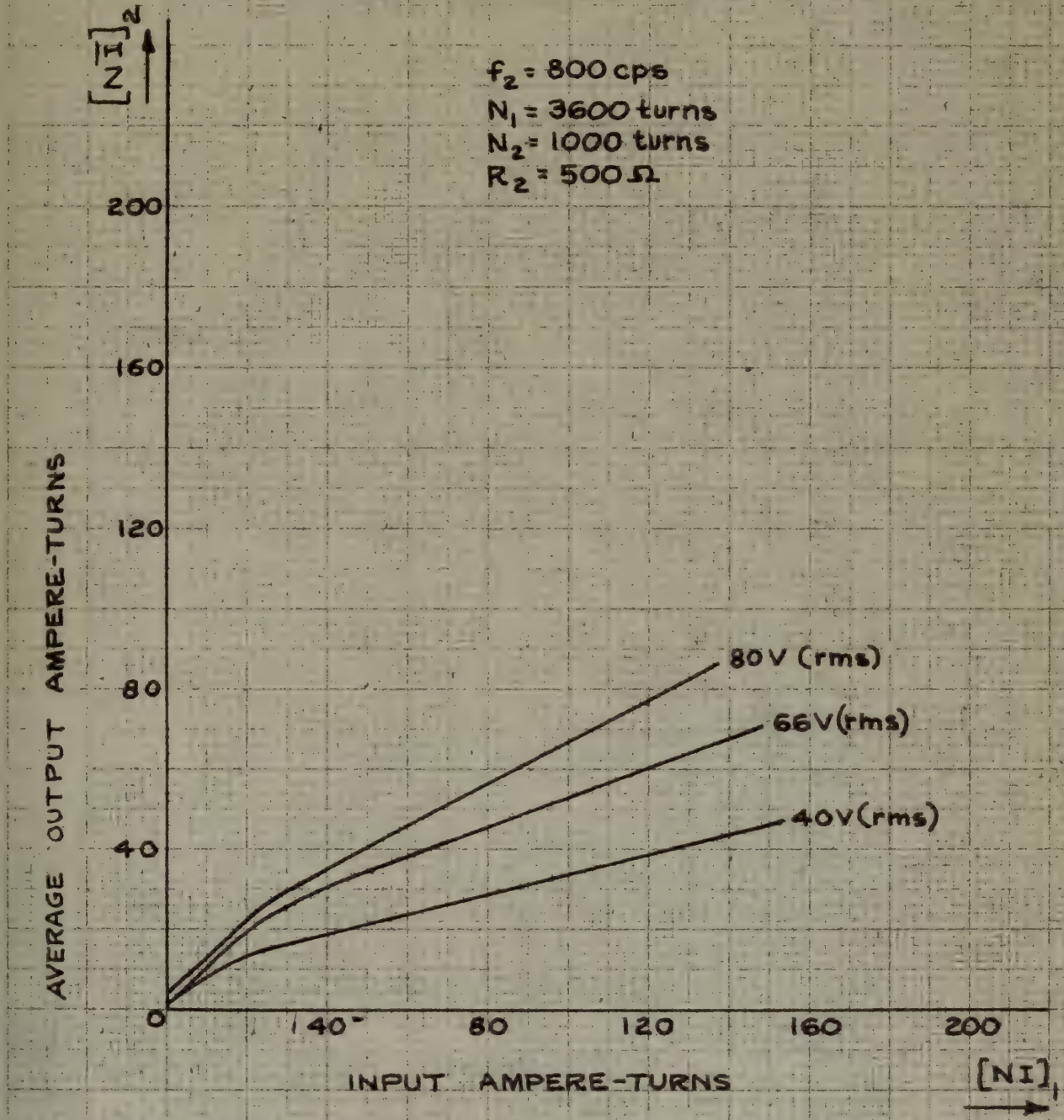

FIG. 3-17 MODULATION CHARACTERISTIC OF THE BASIC MAGNETIC AMPLIFIER SHOWING EFFECT OF ALTERNATING CURRENT VOLTAGE.

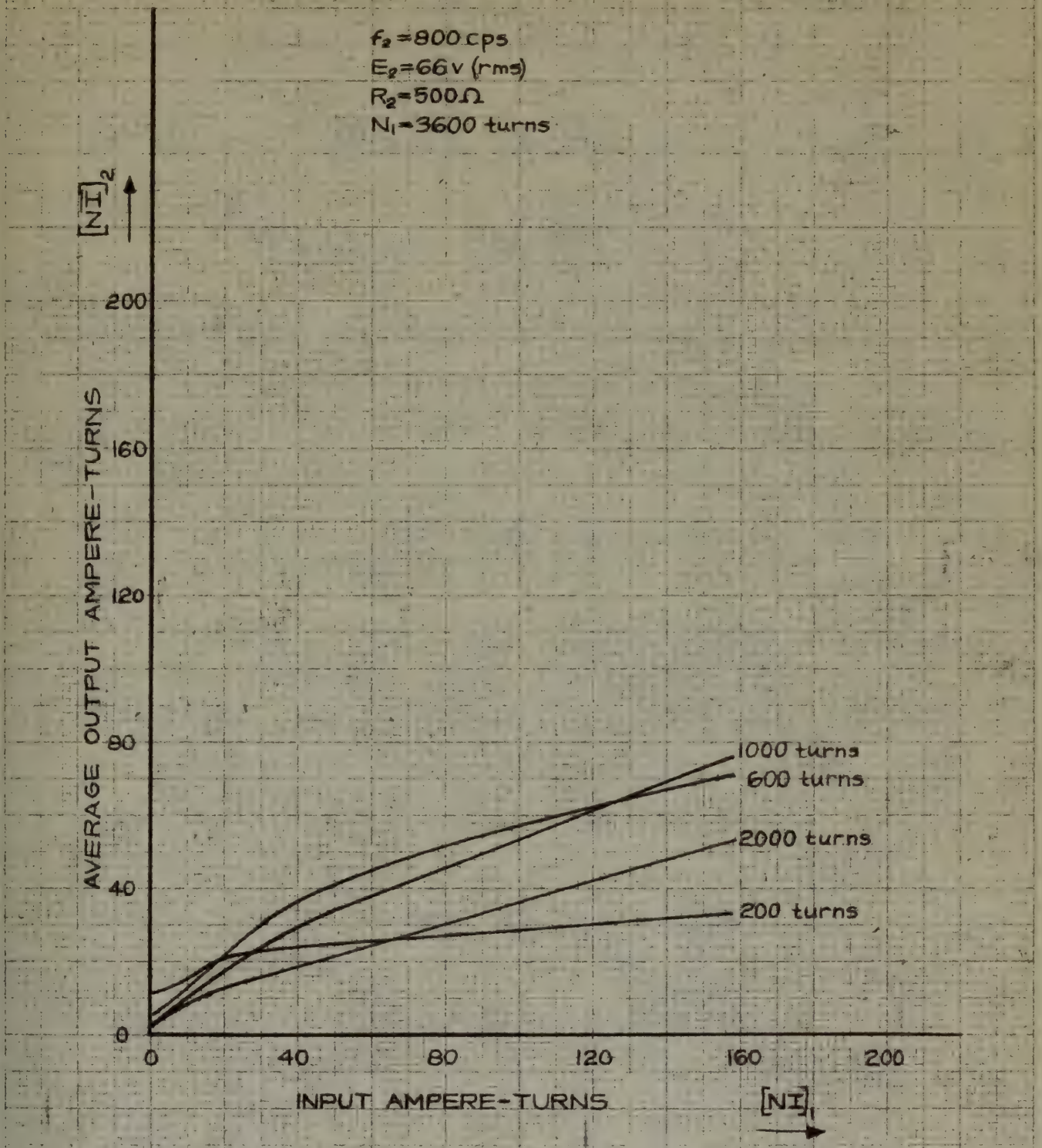

FIG. 3-18 MODULATION CHARACTERISTIC OF THE BASIC MAGNETIC AMPLIFIER SHOWING THE EFFECT OF OUTPUT TURNS.

$$P_2 = (I_2 - I_e)^2 R_2 \qquad (3\text{-}9)$$

The power input may be obtained from the relation

$$P_1 = I_1^2 R_1 \qquad (3\text{-}10)$$

From these two expressions, the power gain may be defined as

$$K_p = P_2/P_1 = \frac{(I_2 - I_e)^2 R_2}{I_1^2 R_1} \qquad (3\text{-}11)$$

From these relations power output and power gain may be plotted as a function of power input, or more conveniently, as functions of I_1^2, in order that the choice of R_1, based on dynamic considerations, may be made independently. Figure 3-19 shows P_2 and $(R_1 K_p)$ plotted as functions of I_1^2. The parameter is chosen as R_2, since the choice of f_2 has been assumed fixed by bandwidth or power-supply requirements, and the value of N_2 has been assumed optimized from studies of the modulation characteristic. These families of curves reveal that the value of R_2 chosen is a compromise between power gain, power output, and linear range. As will be shown in the discussion of circuit dynamics, a higher R_1 decreases the response time, but also lowers the gain. The actual design must, therefore, be a compromise between power output, power gain, linearity, and response time.

An approximate formula for estimating the power gain of a magnetic amplifier without feedback may be developed using the relation

$$N_1 I_1 \cong N_2 I_2 \qquad (3\text{-}12)$$

$$\mathrm{g}^{\mu\nu}\mathrm{I}_{\mu}\mathrm{I}_{\nu} = \mathrm{I}^{2} \qquad (3\text{-}13)$$

acloped using the relation

$$\mathrm{I}^{\mu} = \mathrm{I}^{\nu}_{\mathrm{o}}\,\mathrm{g}^{\mu} \qquad (3\text{-}10)$$

Two observers, who have their clocks and measuring rods coupled by a suitable coupling function, will not necessarily agree on the length of time between two events, but will agree on the length of a proper time interval, because their clocks, as a consequence of the relativity principle, run at the same rate. The proper time interval $\mathrm{d}\tau$ between two events is the time measured by an observer who is present at both events, and is given by the relation

$$\mathrm{d}\tau^{2} = \mathrm{g}_{\mu\nu}\mathrm{dI}^{\mu}\mathrm{dI}^{\nu} = \frac{\mathrm{dI}^{\mu}\,\mathrm{dI}^{\nu}}{(\mathrm{I}^{\mathrm{o}} - \mathrm{I}^{\mathrm{o}})^{2}_{\mathrm{o}}\,\mathrm{c}^{2}} \qquad (3\text{-}12)$$

Figure 3-13 shows I^{μ} and $(\mathrm{I}^{\mu} + \mathrm{dI}^{\mu})$ plotted as functions of $\mathrm{I}^{\mu}_{\mathrm{o}}$. The increment in time dI^{μ} minus the units of $\mathrm{I}^{\mu}_{\mathrm{o}}$ has been examined first by mathematically identifying dI^{μ} as the value of I^{μ} for which $\mathrm{I}^{\mu}_{\mathrm{o}} = 0$, and then examining the value of I^{μ} for which $\mathrm{I}^{\mu}_{\mathrm{o}} = 1$. Since I^{μ} is a contravariant vector, and since $\mathrm{I}^{\mu}_{\mathrm{o}}$ is a contravariant vector, it follows that the value of I^{μ} for which $\mathrm{I}^{\mu}_{\mathrm{o}} = 1$ is a contravariant vector. Since I^{μ} is a contravariant vector, it follows that the value of I^{μ} for which $\mathrm{I}^{\mu}_{\mathrm{o}} = 0

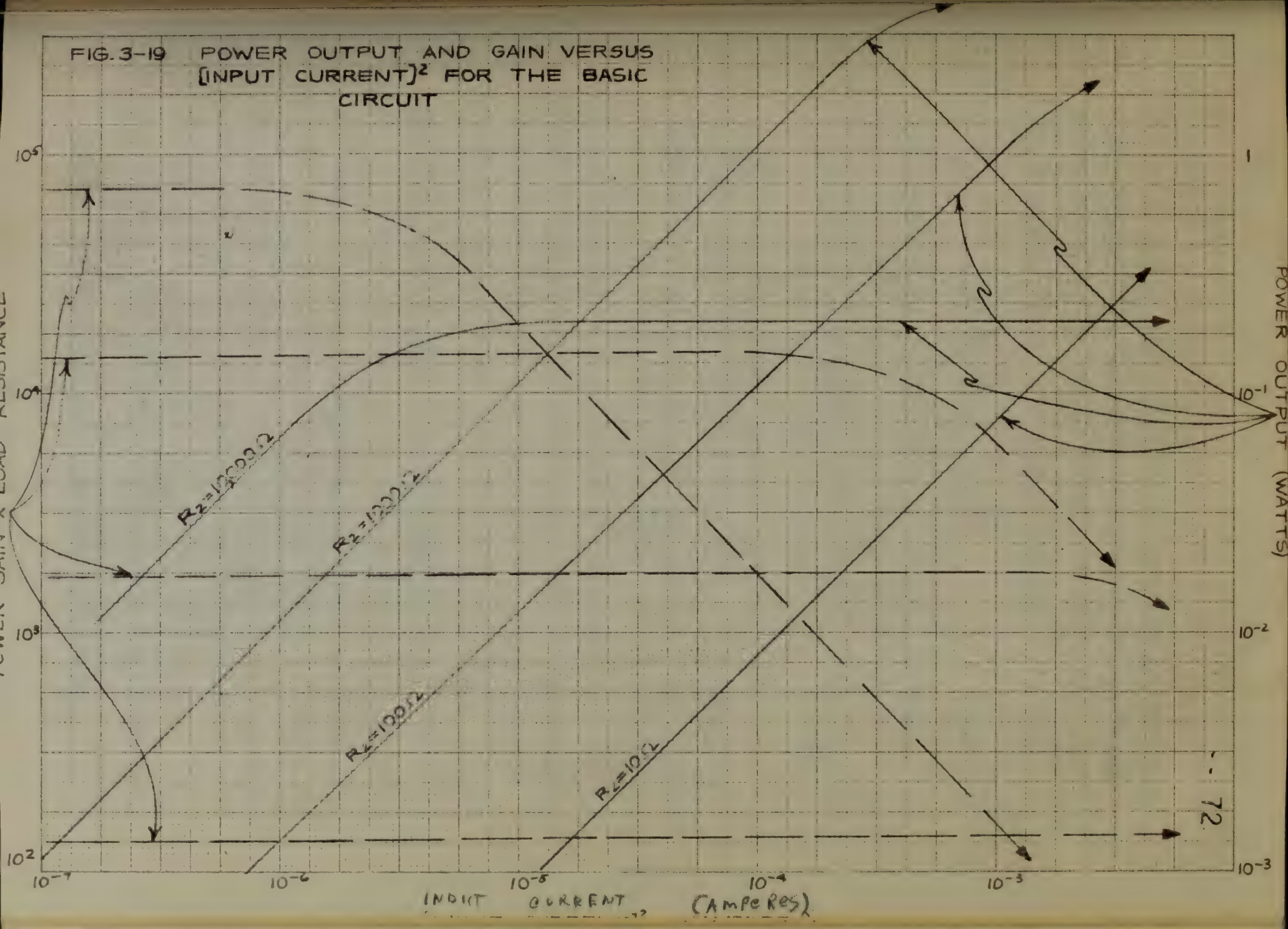
FIG. 3-19 POWER OUTPUT AND GAIN VERSUS [INPUT CURRENT]² FOR THE BASIC CIRCUIT
POWER GAIN X LOAD RESISTANCE
POWER OUTPUT (WATTS)
INPUT CURRENT (AMPERES)
10^5
10^4
10^3
10^2
1
10^{-1}
10^{-2}
10^{-3}
10^{-7}
10^{-6}
10^{-5}
10^{-4}
10^{-3}
$R_L = 1200\,\Omega$
$R_L = 1200\,\Omega$
$R_L = 1200\,\Omega$
$R_L = 10\,\Omega$

which is a fairly good approximation over the region where excitation current, I_e, is small and where the modulation characteristic has a slope of approximately 45 degrees. The power gain may be developed as follows:

$$\frac{\bar{I}_2}{I_1} \cong \frac{N_1}{N_2} \qquad (3\text{-}13)$$

$$I_2 \cong 1.11\ \bar{I}_2 \qquad (3\text{-}14)$$

$$\frac{I_2}{I_1} \cong \frac{N_1}{1.11\ N_2} \qquad (3\text{-}15)$$

$$K_p \cong \frac{I_2^2\ R_2}{I_1^2\ R_1} \qquad (3\text{-}16)$$

$$K_p \cong \left(\frac{N_1}{1.11\ N_2}\right)^2 \frac{R_2}{R_1} \qquad (3\text{-}17)$$

This relation shows which factors are most important for consideration in obtaining high gains with the basic amplifier circuit, assuming that the alternating flux has been properly adjusted by correct choice of E_2 and f_2.

Amplifier Dynamics Studied by Transient Response

Although a great deal of material has appeared in engineering literature concerning the static characteristics of the magnetic amplifier, very little detailed analysis of the transient behavior has been published. In 1943, Buchhold established that the speed of response was proportional to the ratio of input-circuit inductance to input-circuit resistance.[1] Lamm, in the same year, published a transient

1. Buchhold, T., "On the Theory of the Magnetic Amplifier," Archiv fur Elektrotechnik, 37, (1943), 197-211.

1. Woodward, J., "On the Theory of the Magnetic Modulator," Wireless Engr. (1943), 20, 141-147.

The power gain may be developed as follows:

$$\frac{I_2^2}{I_1^2} \approx \frac{R_2}{R_1} \qquad (3\text{-}13)$$

$$I_2 \approx 1.11\, I_1^2 \qquad (3\text{-}14)$$

$$\frac{I_1^2}{I_2^2} \approx \frac{1.11\, R_1^2}{R_1^2} \qquad (3\text{-}15)$$

$$K_p \approx \frac{I_2^2 R_2}{I_1^2 R_1^2} \qquad (3\text{-}16)$$

$$K_p \approx \left(\frac{1.11\, R_1^2}{R_1^2}\right)^2 \frac{R_2}{R_1} \qquad (3\text{-}17)$$

Practically optimum design values may be obtained for the linear element, assuming that the saturating flux does not appreciably affect the permeability. In [6], Woodward points out the importance of the ratio of inductance to inductance-plus-resistance, $\frac{L}{L+R}$, known, in the case here, as the quality factor, Q. Woodward's [2] use of the quality factor, in the case of the magnetic modulator, was limited to the consideration of the maximum value of Q and $\frac{L}{R}$.

Modifier Parameter Optimization

Although a great deal of material has been published in the literature concerning the various characteristics of the magnetic modulator, very little detailed analysis of the transient behavior has been attempted. In [6], Woodward established that the theory of inductance was fundamentally the ratio of flux-linkage to flux-current, $\frac{L}{R}$, and further established that the theory of reactance was fundamentally the ratio of flux-linkage to flux-current, $\frac{L}{R}$, known, in the case here, as the quality factor, Q. Woodward's [2] use of the theory of the magnetic modulator, was limited to the consideration of the maximum value of Q and $\frac{L}{R}$.

Although a great deal of material has been published in the literature concerning the various characteristics of the magnetic modulator, very little detailed analysis of the transient behavior has been attempted. In [6], Woodward established that the theory of inductance was fundamentally the ratio of flux-linkage to flux-current, $\frac{L}{R}$, known, in the case here, as the quality factor, Q. Woodward's [2] use of the theory of the magnetic modulator, was limited to the consideration of the maximum value of Q and $\frac{L}{R}$.

Modifier Parameter Optimization

Although a great deal of material has been published in the literature concerning the various characteristics of the magnetic modulator, very little detailed analysis of the transient behavior has been attempted. In [6], Woodward established that the theory of inductance was fundamentally the ratio of flux-linkage to flux-current, $\frac{L}{R}$, known, in the case here, as the quality factor, Q. Woodward's [2] use of the theory of the magnetic modulator, was limited to the consideration of the maximum value of Q and $\frac{L}{R}$.

Although a great deal of material has been published in the literature concerning the various characteristics of the magnetic modulator, very little detailed analysis of the transient behavior has been attempted. In [6], Woodward established that the theory of inductance was fundamentally the ratio of flux-linkage to flux-current, $\frac{L}{R}$, known, in the case here, as the quality factor, Q. Woodward's [2] use of the theory of the magnetic modulator, was limited to the consideration of the maximum value of Q and $\frac{L}{R}$.

Modifier Parameter Optimization

Although a great deal of material has been published in the literature concerning the various characteristics of the magnetic modulator, very little detailed analysis of the transient behavior has been attempted. In [6], Woodward established that the theory of inductance was fundamentally the ratio of flux-linkage to flux-current, $\frac{L}{R}$, known, in the case here, as the quality factor, Q. Woodward's [2] use of the theory of the magnetic modulator, was limited to the consideration of the maximum value of Q and $\frac{L}{R}$.

Although a great deal of material has been published in the literature concerning the various characteristics of the magnetic modulator, very little detailed analysis of the transient behavior has been attempted. In [6], Woodward established that the theory of inductance was fundamentally the ratio of flux-linkage to flux-current, $\frac{L}{R}$, known, in the case here, as the quality factor, Q. Woodward's [2] use of the theory of the magnetic modulator, was limited to the consideration of the maximum value of Q and $\frac{L}{R}$.

Modifier Parameter Optimization

Although a great deal of material has been published in the literature concerning the various characteristics of the magnetic modulator, very little detailed analysis of the transient behavior has been attempted. In [6], Woodward established that the theory of inductance was fundamentally the ratio of flux-linkage to flux-current, $\frac{L}{R}$, known, in the case here, as the quality factor, Q. Woodward's [2] use of the theory of the magnetic modulator, was limited to the consideration of the maximum value of Q and $\frac{L}{R}$.

Although a great deal of material has been published in the literature concerning the various characteristics of the magnetic modulator, very little detailed analysis of the transient behavior has been attempted. In [6], Woodward established that the theory of inductance was fundamentally the ratio of flux-linkage to flux-current, $\frac{L}{R}$, known, in the case here, as the quality factor, Q. Woodward's [2] use of the theory of the magnetic modulator, was limited to the consideration of the maximum value of Q and $\frac{L}{R}$.

analysis of a three-phase saturable-reactor in which he states that the response time is proportional to the carrier frequency.[1] In 1946, Grafinger pointed out that the magnetic amplifier could be characterized by a first-order time constant.[2] Therkelsen confirmed this observation from frequency-response studies, showing the time constant to be essentially the ratio of inductance to resistance in the input circuit.[3] The purpose of the present study is to extend these investigations in order to establish the effect of all circuit parameters upon the dynamics of the amplifier.

Because the magnetic amplifier is a nonlinear system, it is inherently incorrect to characterize its dynamic performance by means of a time constant unless additional defining restrictions are imposed. Since the input inductance is a function of the degree of saturation of the core, which is, in turn, a function of the excitation current, any time constant defined in terms of the ratio of input inductance to input resistance is, in reality, a variable. If, however, a sinusoidal signal is superimposed upon a biasing-current level, the amplifier response has the characteristics of a first-order system as first shown by Therkelsen and extended later in this chapter.

The speed of response will be studied in this section in terms of the time required for the amplifier to respond to an applied step voltage. Because the system is

---

1. Lamm, U., "The Transductor, A D.C. Pre-Saturated Reactor," (Stockholm, Esselte Aktiebolag, 1943).
2. Grafinger, L.N., "A Study of Magnetic Amplifiers for Servomechanisms," E.E. Thesis (M.I.T., 1946).
3. Therkelsen, E.B., "A Low-Power Magnetic Amplifier for Servomechanisms," E.E. Thesis (M.I.T., 1946).

analysis of a three-phase saturable-reactor in which he states that the response time is proportional to the carrier frequency.[1] In 1946, Grafinger pointed out that the magnetic amplifier could be characterized by a first-order time constant.[2] Thorkelsen confirmed this observation from frequency-response studies, showing the time constant to be essentially the ratio of inductance to resistance in the input circuit.[3] The purpose of the present study is to extend these investigations in order to establish the effect of all circuit parameters upon the dynamics of the amplifier.

Because the magnetic amplifier is a nonlinear system, it is inherently incorrect to characterize its dynamic performance by means of a time constant unless additional defining restrictions are imposed. Since the input inductance is a function of the degree of saturation of the core, which is, in turn, a function of the excitation current, any time constant defined in terms of the ratio of input inductance to input resistance is, in reality, a variable. If, however, a sinusoidal signal is superimposed upon a biasing-current level, the amplifier response has the characteristics of a first-order system as first shown by Thorkelsen and extended later in this chapter.

The speed of response will be studied in this section in terms of the time required for the amplifier to respond to an applied step voltage. Because the system is

---

1. Lamm, G., "The Transductor, A D.C. Pre-Saturated Reactor," (Stockholm, Gazette Aktiebolag, 1947).
2. Grafinger, L.R., "A Study of Magnetic Amplifiers for Servomechanisms," M.E. Thesis (M.I.T., 1946).
3. Thorkelsen, S.B., "A Low-Power Magnetic Amplifier for Servomechanisms," E.E. Thesis (M.I.T., 1946).

nonlinear, the term, time constant, will not be used. A more appropriate expression is effective characteristic time, (CT), which will be defined as that time required for the output to rise or fall through 63% of the total change in response to a step-function input.[1] This concept is based on an analogy with the simple exponential curve which characterizes a first-order linear system, in which the time constant is defined as the time for the step-function response to rise or fall through (1-1/e), or 63%, of the total change. Thus, the characteristic time of the nonlinear system is analogous to the time constant of the linear system. The characteristic time will, therefore, be the index used in specifying the speed of response of the magnetic amplifier.

The laboratory technique used to measure (CT) involved the application of a step voltage to the input terminals and observation of the carrier-current transient on a calibrated oscilloscope. A DuMont type 215 low-frequency linear time-base generator was used to furnish the sweep voltage to a DuMont type 208 cathode-ray oscilloscope which was modified by the substitution of a high-persistence cathode-ray tube. The time for the carrier envelope to rise or fall from its initial value through 63% of the total change could be read directly from the oscilloscope once the horizontal sweep had been calibrated in milliseconds. The step voltage

---

1. Draper, C.S. and McKay, W., "Instrument Analysis," M.I.T., 1946.

nonlinear, the term, time constant, will not be used. A more appropriate expression is effective characteristic time, (07), which will be defined as that time measured for the output to rise or fall through 63% of the total change in response to a step-function input.[1] This concept is based on an analogy with the simple exponential curve which characterizes a first-order linear system, in which the time constant is defined as the time for the step-function response to rise or fall through (1-1/e), or 63%, of the total change. Thus, the characteristic time of the nonlinear system is analogous to the time constant of the linear system. The characteristic time will, therefore, be the index used in specifying the speed of response of the magnetic amplifier.

The laboratory procedure used to measure (07) involved the application of a step voltage to the input terminals and observation of the carrier-current transient on a calibrated oscilloscope. A Dumont type 315 low-frequency linear time-base generator was used to furnish the sweep voltage to a Dumont type 208 cathode-ray oscilloscope which was modified by the substitution of a high-persistence cathode-ray tube. The time for the carrier envelope to rise or fall from its initial value through 63% of the total change could be read directly from the oscilloscope once the horizontal sweep had been calibrated in milliseconds. The step voltage

1. Cooper, D.G. and Mayer, W., "Instrument Analysis," M.I.T., 1945.

was applied by means of a switch in the input circuit whose closure also triggered the sweep.

Circuit conditions were chosen as nearly identical as possible with those used on the differential analyzer in order that a comparison of analytic and experimental transient data could be made. A standard condition was selected and the circuit parameters were varied one at a time in order to observe their effect upon the transient.

The effects of changes in the control-circuit parameters, R_1, I_1, and M_1, were investigated first. The results indicate that (CT) varies inversely with R_1. This conclusion is drawn from the fact that when (CT) is plotted as a function of R_1 on logarithmic coordinates, the function has a negative slope of unity. The experimental data is shown in Figure 3-20. This result confirms the observations of previous experimenters. The effect of the input current upon the transient response showed that (CT) varies inversely as the square-root of I_1, as can be seen from the negative slope of one-half which the function exhibits on the logarithmic plot in Figure 3-20. When the effect of input turns was examined, (CT) was observed to vary directly as N_1, the logarithmic plot of Figure 3-20 having a positive slope of unity. Pease has shown that the reactor inductance is inversely proportional to the control current to a first approximation.[1] On this basis, the following relation holds,

---

1. Pease, W.M., "Design of a 400 Cycle Servomechanism," E.E. Thesis, (M.I.T., 1943).

was applied by means of a switch in the input circuit whose closure also triggered the sweep.

Circuit conditions were chosen as nearly identical as possible with those used on the differential analyzer in order that a comparison of analytic and experimental transient data could be made. A standard condition was selected and the circuit parameters were varied one at a time in order to observe their effect upon the transient.

The effects of changes in the control-circuit parameters, R_1, L_1, and R_2, were investigated first. The results indicate that (CT) varies inversely with R_1. This conclusion is drawn from the fact that when (CT) is plotted as a function of R_1 on logarithmic coordinates, the function has a negative slope of unity. The experimental data is shown in Figure 3-20. This result confirms the observations of previous experimenters. The effect of the input current upon the transient response showed that (CT) varies inversely as the square-root of L_1, as can be seen from the negative slope of one-half which the function exhibits on the logarithmic plot in Figure 3-20. When the effect of input turns was examined, (CT) was observed to vary directly as R_2, the logarithmic plot of Figure 3-20 having a positive slope of unity. These has shown that the reactor inductance is inversely proportional to the control current to a first approximation.[1] On this basis, the following relation holds,

1. Pemm, G.G., "Design of a 400 Cycle Servomechanism," E.E. Thesis, (S.I.T., 1943).

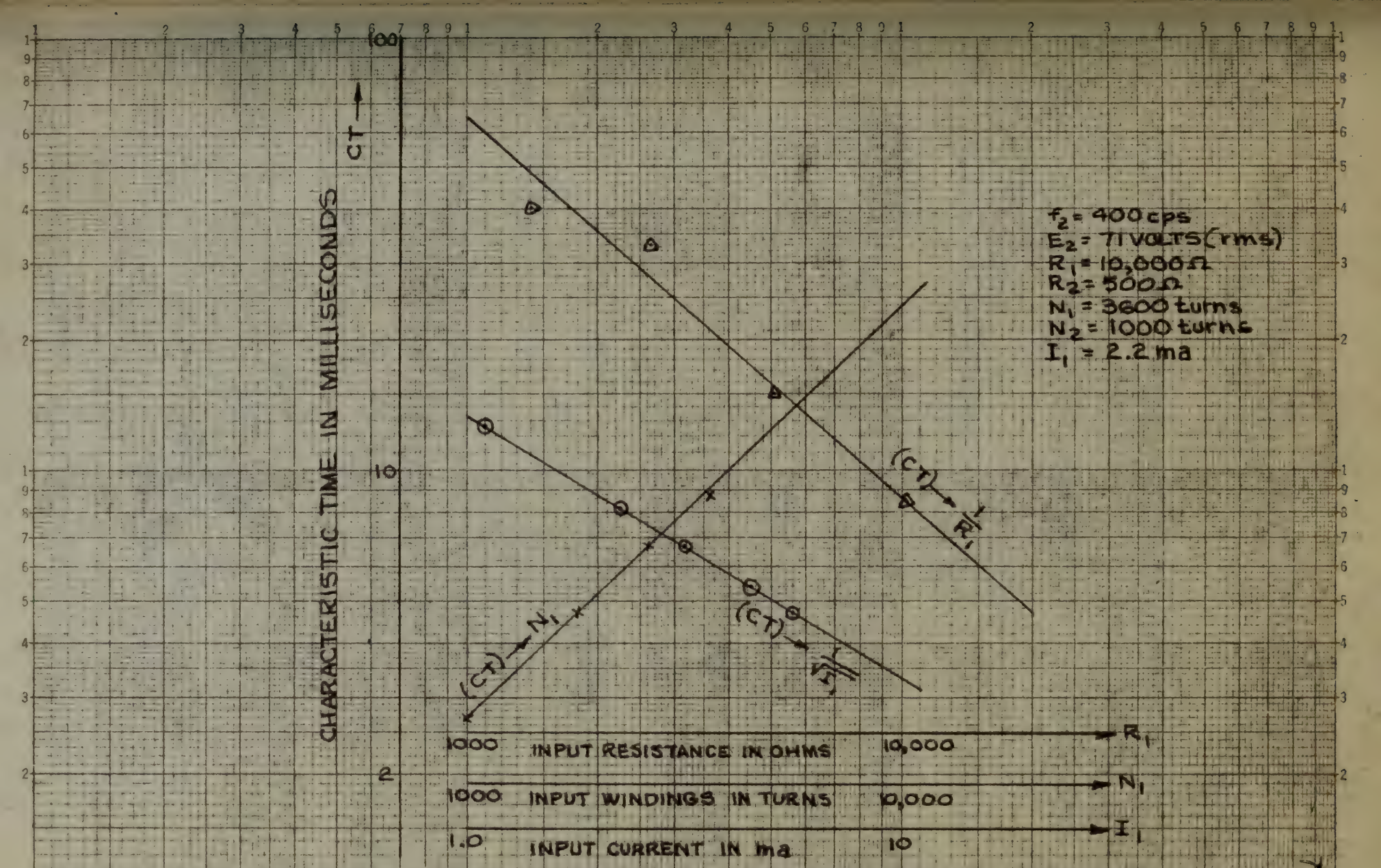

FIG. 3-20 EFFECT OF CONTROL-CIRCUIT PARAMETERS AND EXCITATION UPON THE CHARACTERISTIC TIME AS OBTAINED FROM EXPERIMENTAL TRANSIENT DATA.

$$L_1(I_1) \cong \frac{k' N_1^2}{I_1} \qquad (3\text{-}18)$$

in which k' is a constant of proportionality, and L_1, because it is a function of I_1, is identified by the additional subscript, (I_1). The following relations can be seen:

$$(CT) \rightarrow \frac{N_1}{R_1 \sqrt{I_1}} \rightarrow \frac{1}{R_1} \left[\frac{N_1^2}{I_1}\right]^{\frac{1}{2}} \qquad (3\text{-}19)$$

or

$$(CT) \rightarrow \frac{\sqrt{L_1(I_1)}}{R_1} \qquad (3\text{-}20)$$

It is concluded, therefore, that the characteristic time is directly proportional to the square-root of the final value of the input inductance, and inversely proportional to the input resistance.

The effects of the carrier-circuit parameters, R_2, N_2, E_2, and f_2, were next observed. As shown in Figure 3-21, the effect of R_2 was found to be negligible. E_2 and f_2 had only slight effect, while N_2 produced a pronounced variation. From empirical data over the region examined, (CT) has the following functional relation with respect to the carrier circuit:

$$(CT) \rightarrow \frac{(E_2)^{\frac{1}{5}}}{(f_2)^{\frac{1}{10}} (N_2)^{\frac{1}{2}}} \qquad (3\text{-}21)$$

These effects are difficult to explain because of the nonlinear nature of the energy-storage elements, the saturable reactors. Since the analytic results, discussed in Chapter IV, do not confirm the experimental data for the variation

$$L_1(I_1) = \frac{k' N_1^2}{I_1} \qquad (3\text{-}18)$$

in which k' is a constant of proportionality, and L_1, because it is a function of I_1, is identified by the additional subscript, (I_1). The following relations can be seen:

$$(CT) \leftarrow \frac{N_1}{R_1 \sqrt{I_1}} \leftarrow \frac{1}{R_1}\left[\frac{N_1^2}{I_1}\right]^{\frac{1}{2}} \qquad (3\text{-}19)$$

or

$$(CT) \leftarrow \frac{\sqrt{L_1(I_1)}}{R_1} \qquad (3\text{-}20)$$

It is concluded, therefore, that the characteristic time is directly proportional to the square-root of the final value of the input inductance, and inversely proportional to the input resistance.

The effects of the carrier-circuit parameters, R_2, M_2, E_2, and f_2, were next observed. As shown in Figure 3-21, the effect of R_2 was found to be negligible. E_2 and f_2 had only slight effect, while M_2 produced a pronounced variation. From empirical data over the region examined, (CT) has the following functional relation with respect to the carrier circuit:

$$(CT) \leftarrow \frac{(E_2)^{\frac{1}{2}}}{(f_2)^{\frac{1}{10}}\,(M_2)^{\frac{1}{2}}} \qquad (3\text{-}21)$$

These effects are difficult to explain because of the non-linear nature of the energy-storage elements, the saturable reactors. Since the analytic results, discussed in Chapter IV, do not confirm the experimental data for the variation

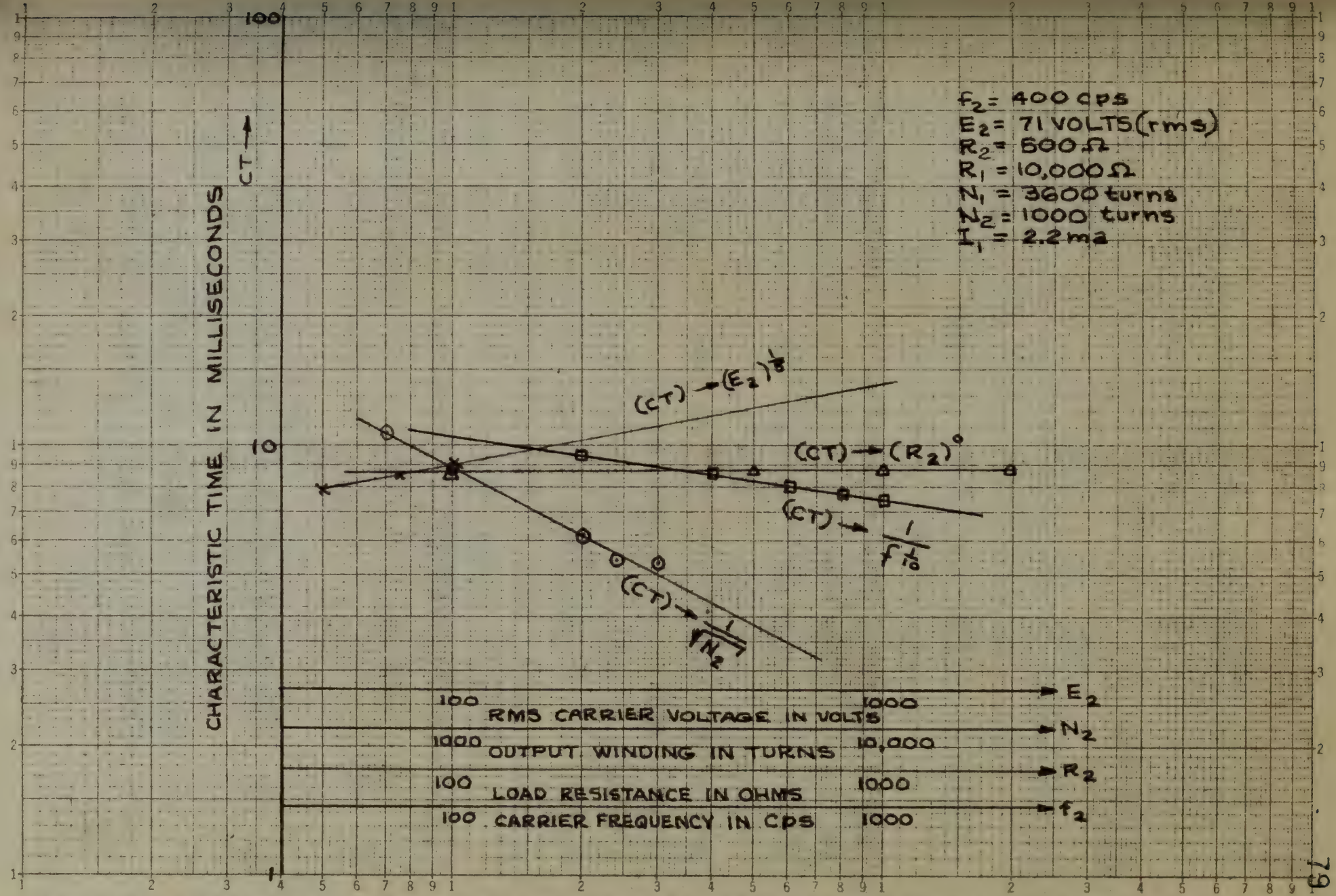
CHARACTERISTIC TIME IN MILLISECONDS
CT
100
10
1
f_2 = 400 cps
E_2 = 71 VOLTS (rms)
R_2 = 500 Ω
R_1 = 10,000 Ω
N_1 = 3600 turns
N_2 = 1000 turns
I_1 = 2.2 ma
(CT) → $(E_2)^{\frac{1}{3}}$
(CT) → $(R_2)^0$
(CT) → $\frac{1}{f^{\frac{1}{10}}}$
(CT) → $\frac{1}{\sqrt{N_2}}$
100 RMS CARRIER VOLTAGE IN VOLTS 1000 → E_2
1000 OUTPUT WINDING IN TURNS 10,000 → N_2
100 LOAD RESISTANCE IN OHMS 1000 → R_2
100 CARRIER FREQUENCY IN CPS 1000 → f_2

FIG. 3-21 EFFECT OF CARRIER-CIRCUIT PARAMETERS AND EXCITATION UPON THE CHARACTERISTIC TIME AS OBTAINED FROM EXPERIMENTAL TRANSIENT DATA.

of (CT) with the carrier-circuit parameters, some effect not taken into account in the formulation of the system equations for the analytic study must be responsible for the discrepancy between the two. This discrepancy is attributed to the fact that the functional dependence of core loss was neglected in establishing the analytic equations. The analytic solution assumed the eddy-current and copper losses to be lumped into the resistance R_2, while hysteresis was neglected entirely by using the normal magnetization curve as the functional relation between flux and magnetizing force. Although these assumptions, as will be shown in Chapter IV, satisfy the steady-state solution and correctly describe the transient effects of the control circuit, they appear to misrepresent the transient effects which take place in the carrier circuit. The relation of the core loss to the carrier-circuit constants and excitation will be developed in order to point out the effects which were neglected. For symmetrical alternating-magnetization, eddy-current and hysteresis loss can be expressed by

$$P_e = k_1 f_2^2 \beta^2_{max} \qquad (3\text{-}22)$$

$$P_h = k_2 f_2 \beta^{\eta}_{max} \qquad (3\text{-}23)$$

where is the Steinmetz coefficient, and k_1 and k_2 constants of proportionality.

As discussed in Chapter II, these formulae do not necessarily hold for asymmetrical magnetization such

as occurs in magnetically-biased saturable reactors. In the absence of more accurate loss functions, these relations will be assumed to describe the total core loss which is the sum of its two components

$$P_T = P_e + P_h \qquad (3\text{-}24)$$

$$P_T = k_1 f^2 \beta^2_{max} + k_2 f \beta^{\eta}_{max} \qquad (3\text{-}25)$$

From the induction law the following equation expresses the flux amplitude for peak sinusoidal induction voltage, $\hat{E}$

$$\beta_{max} = \frac{\hat{E}}{2 f_2 N_2} \qquad (3\text{-}26)$$

Eliminating the flux amplitude in Equation 3-25 by means of the Equation 3-26, the following expression for total core loss is obtained

$$P_T = k_3 \left(\frac{\hat{E}}{N_2}\right)^2 + k_4 \left(\frac{\hat{E}}{N_2}\right)^{\eta} \frac{1}{[f_2]^{(\eta-1)}} \qquad (3\text{-}27)$$

where k_3 and k_4 are constants of proportionality. This relation clearly shows that the equivalent core-loss resistor is a function of the coil induction voltage, the carrier frequency, and the number of turns in the carrier windings. Although the core loss in the experimental reactors has been minimized by careful design, it is still appreciable and is believed to be intimately related to the effect of the carrier circuit upon the transient response, and hence should be accounted for in the differential equations of the system if the analytic solution is to reveal these carrier-circuit transient effects.

Before leaving this discussion of transient effects, the fact that (CT) measured by opening the switch

in the control circuit is somewhat less than measured when closing the switch should be mentioned. This phenomenon occurs because the response envelope is not a simple exponential, but builds up or decays at a slower rate for lower values of control current. It, therefore, takes a shorter time for the carrier envelope to fall through 63% of the total change than it does to rise through the same percentage. This would explain the differences in "time off" and "time on" noted by Fitzgerald.[1]

Amplifier Dynamics Studied by Frequency Response

The practical value of the magnetic amplifier for many applications depends upon its ability to behave as a linear amplifier in spite of the inherent nonlinearity of the circuit. A study of the frequency response of a system to a sinusoidal driving function yields information both as to the static and dynamic behavior of the system. As mentioned earlier in the chapter, Therkelsen pointed out that the magnetic amplifier had a frequency response similar to that of a first order system. It will be the objective of this section to investigate in greater detail the nature of the frequency response as a function of the various amplifier parameters, and from the study correlate the observed frequency characteristics with observed transient behavior. The laboratory arrangement for these frequency studies was essentially the same as that used for the measurement of the static characteristics, with

---

1. Fitzgerald, A.S., "Magnetic Amplifier Characteristics-Neutral Type," J.F.I., 244, (1947), 415-439.

in the control circuit is somewhat less than measured when closing the switch should be mentioned. This phenomenon occurs because the response envelope is not a simple exponential, but builds up or decays at a slower rate for lower values of control current. It, therefore, takes a shorter time for the carrier envelope to fall through 63% of the total change than it does to rise through the same percentage. This would explain the differences in "time off" and "time on" noted by Fitzgerald.[1]

Amplifier Dynamics Studied by Frequency Response

The practical value of the magnetic amplifier for many applications depends upon its ability to behave as a linear amplifier in spite of the inherent nonlinearity of the circuit. A study of the frequency response of a system to a sinusoidal driving function yields information both as to the static and dynamic behavior of the system. As mentioned earlier in the chapter, Thorbaldson pointed out that the magnetic amplifier had a frequency response similar to that of a first order system. It will be the objective of this section to investigate in greater detail the nature of the frequency response as a function of the various amplifier parameters, and from the study correlate the observed frequency characteristics with observed transient behavior. The laboratory arrangement for these frequency studies was essentially the same as that used for the measurement of the static characteristics, with

1. Fitzgerald, A.D., "Magnetic Amplifier Characteristics-Neutral Type," J.F.I., 246, (1947), 415-433.

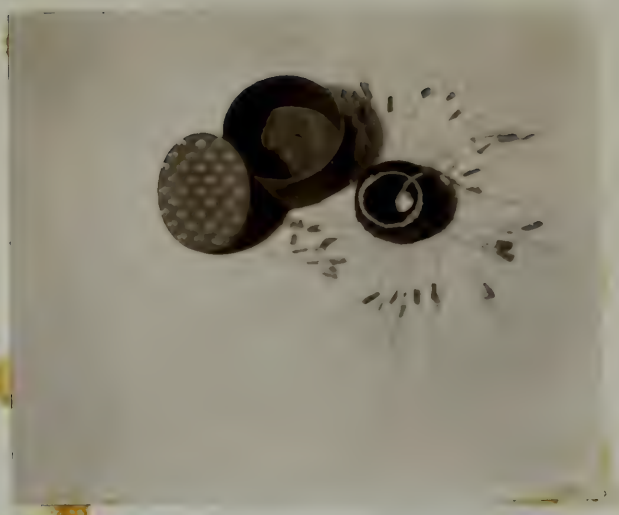

(a) TOROIDAL CORE AND CONTAINER

(b) PAIR OF EXPERIMENTAL SATURABLE REACTORS

FIGURE 3-22

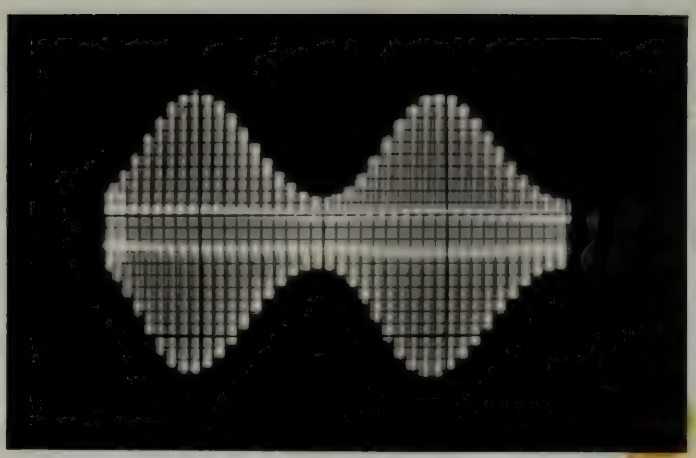

MODULATED CARRIER-CIRCUIT WAVEFORM
WITH SINUSOIDAL SIGNAL APPLIED TO INPUT.

FIGURE 3-23(A).

the exception that a sinusoidal voltage is applied in series in the control circuit, and is thereby superimposed on a direct-current biasing level. This alternating-signal voltage was held constant and the amplitude of the response was observed on an oscilloscope. A typical modulation pattern obtained with a sinusoidal driving voltage is shown in Figure 3-28(A).

A few remarks will be made concerning the frequency response of first-order linear systems in order that a comparative study can be made with the frequency response of the magnetic amplifier. The sinusoidal response of a first-order linear system is characterized by the performance operator

$$[P] = \frac{1}{1 + j2\pi f(CT)} \qquad (3\text{-}28)$$

where

(AR) = ratio of response amplitude to input excitation amplitude,

f = input excitation frequency,

(CT) = time constant

ϕ = phase angle of the response

The relation in Equation 3-28 can further be broken down as

$$[P] = (AR) \angle \phi \qquad (3\text{-}29)$$

where

$$(AR) = \frac{1}{\sqrt{1 + [2\pi f(CT)]^2}} \qquad (3\text{-}30)$$

and

$$\phi = \tan^{-1}[-2\pi f(CT)] \qquad (3\text{-}31)$$

Figure 3-23 shows amplitude ratio and phase angle as a function of the normalized input-excitation frequency. The bandwidth of such a system is measured to the half-power point where the response is down 3db. The frequency at which this occurs is the critical frequency, f_c, and is related to the time constant by the relation

$$(CT) = 1/2\pi f_c \qquad (3\text{-}32)$$

The asymptote of the amplitude ratio at the high end of the frequency spectrum has a negative slope of 6 db/octave passing through the zero db line at the critical frequency when plotted on semi-logarithmic coordinates. The total associated change of phase is ninety degrees.

As seen from Figures 3-24 to 3-30, the magnetic amplifier has a frequency response which approximates a first-order linear system, as can be observed by the initial flat characteristic and the ultimate slope of negative 6 db/octave. The fact that the basic magnetic amplifier is a first-order system can be ascertained by inspection of the equations, or by noting that only one energy storage is involved. The important fact is that linear behavior is approximated. A plot of the transfer function of the magnetic amplifier on the complex plane is shown in Figure 3-31.

The effect of the various circuit parameters on bandwidth has been studied one at a time, and the observations plotted in Figures 3-24 to 3-30 respectively. From

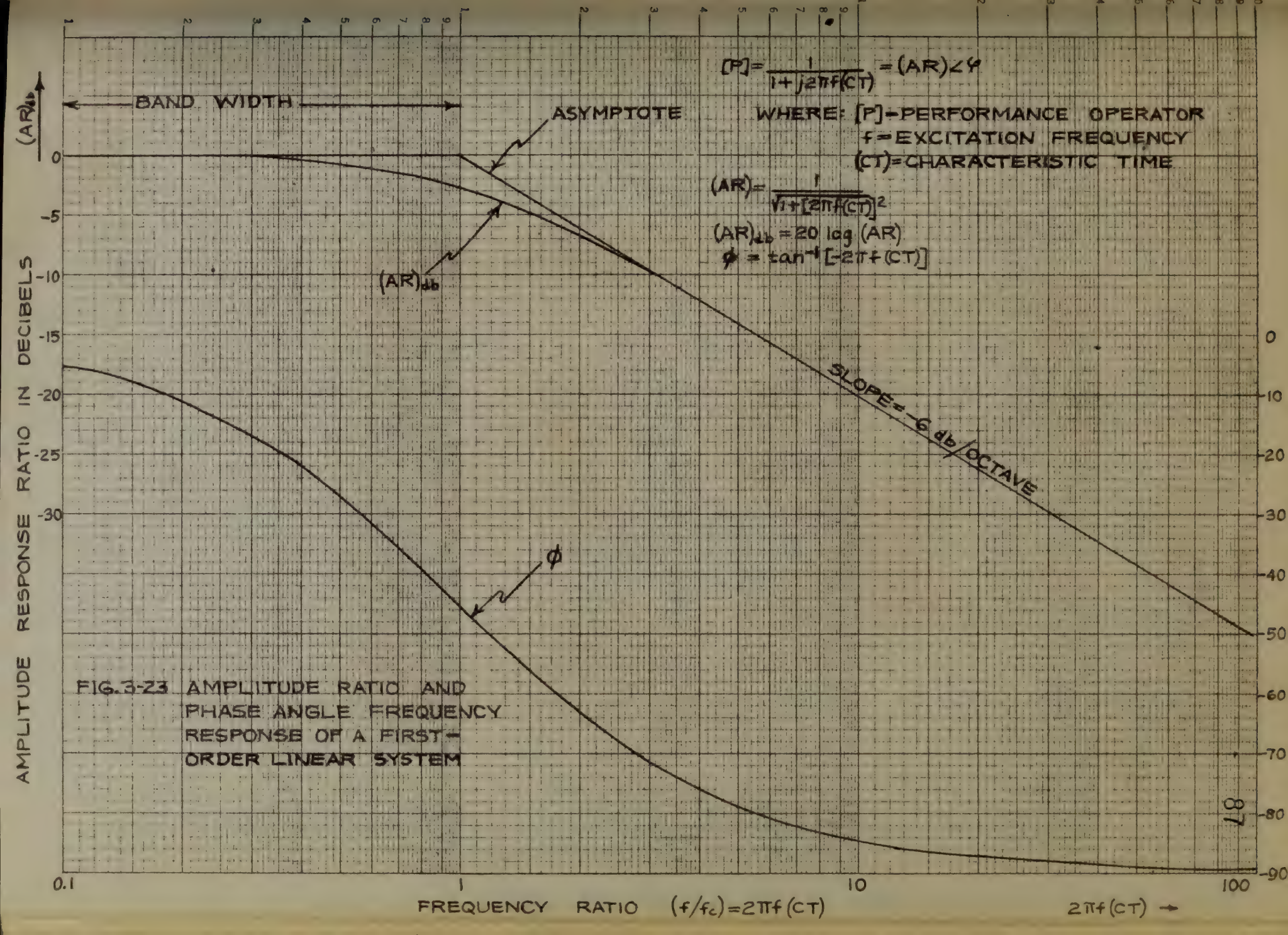

FIG. 3-23 AMPLITUDE RATIO AND PHASE ANGLE FREQUENCY RESPONSE OF A FIRST-ORDER LINEAR SYSTEM

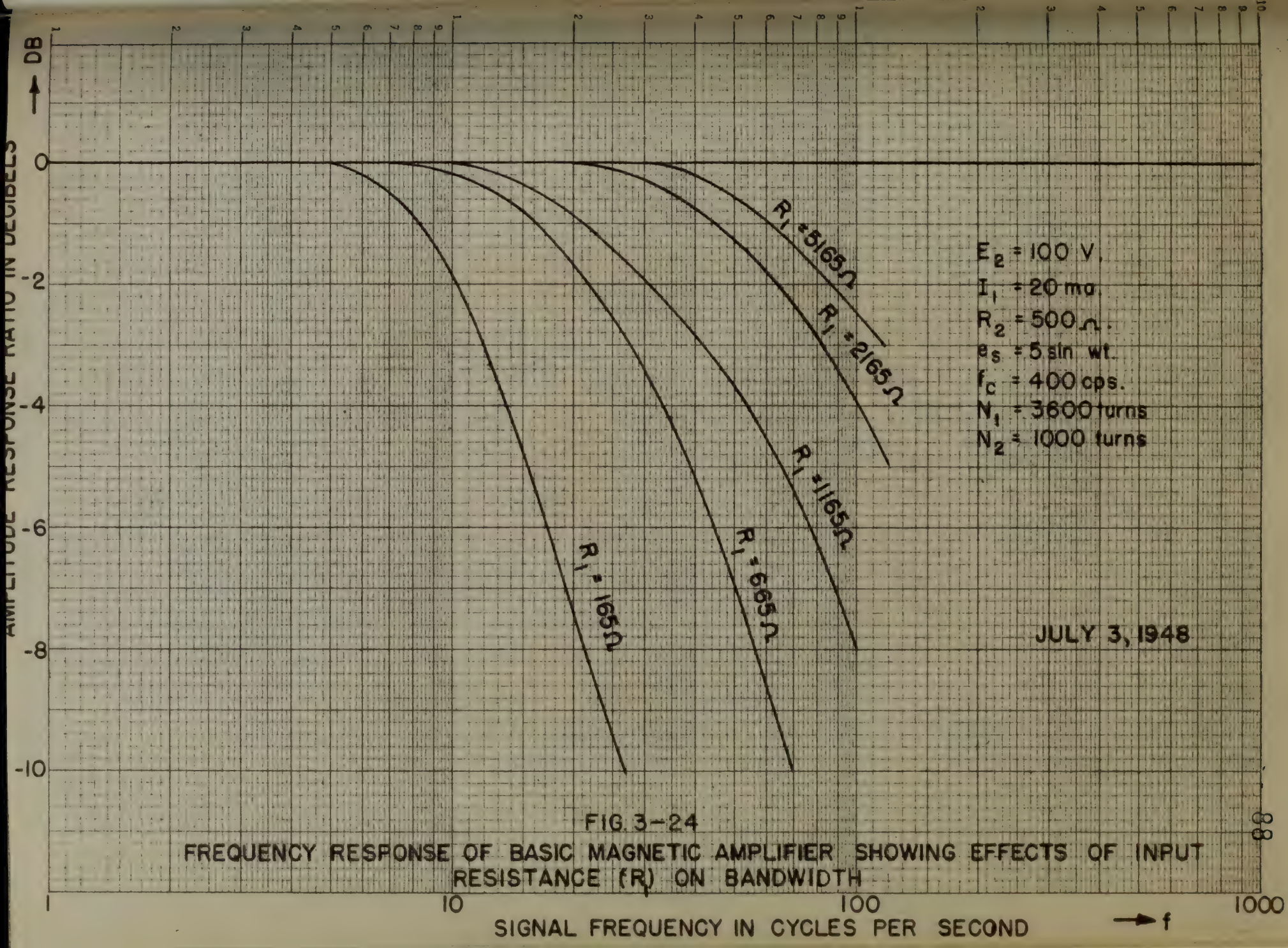

FIG. 3-24

FREQUENCY RESPONSE OF BASIC MAGNETIC AMPLIFIER SHOWING EFFECTS OF INPUT RESISTANCE (R) ON BANDWIDTH

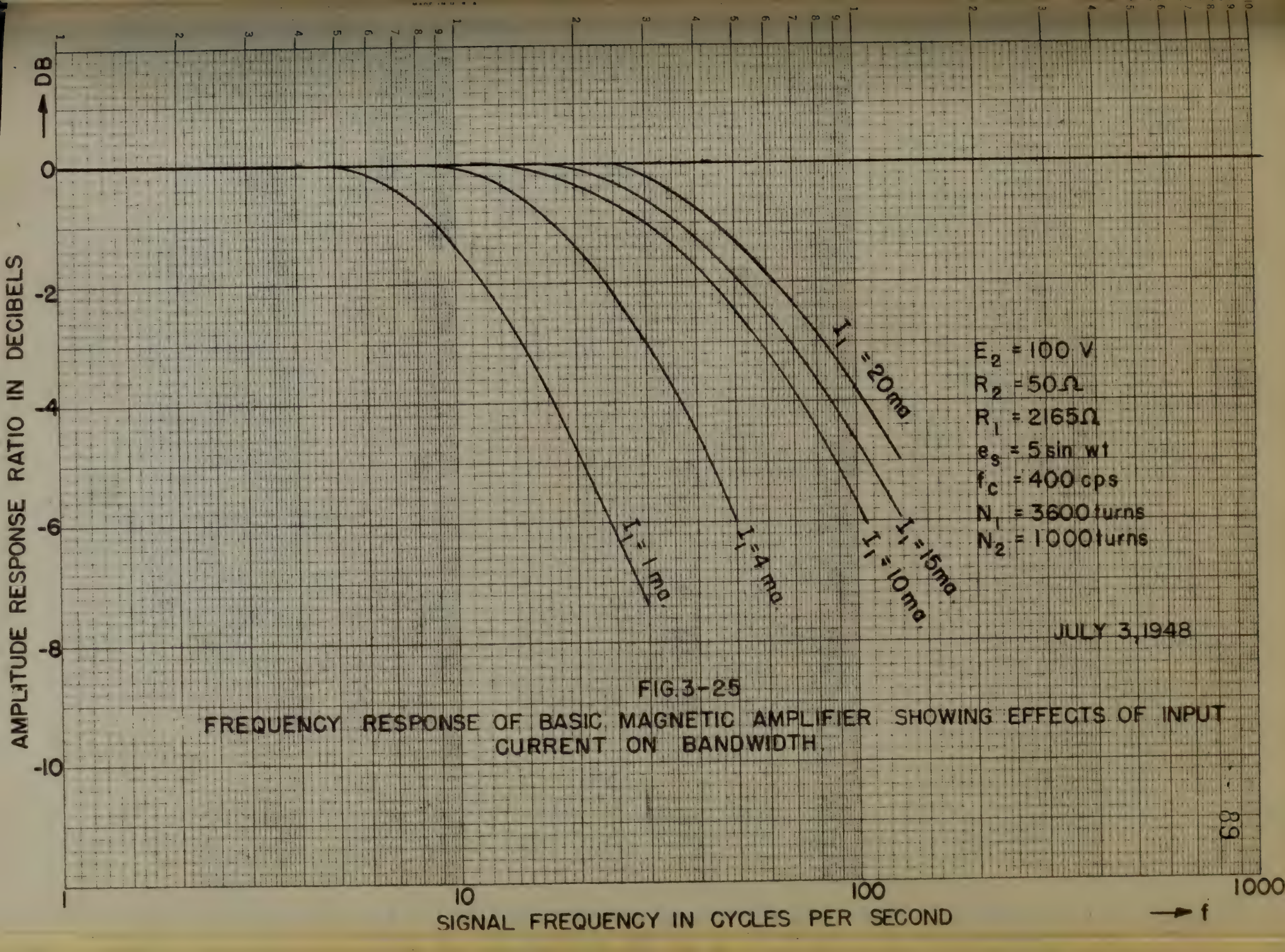

FIG. 3-25

FREQUENCY RESPONSE OF BASIC MAGNETIC AMPLIFIER SHOWING EFFECTS OF INPUT CURRENT ON BANDWIDTH

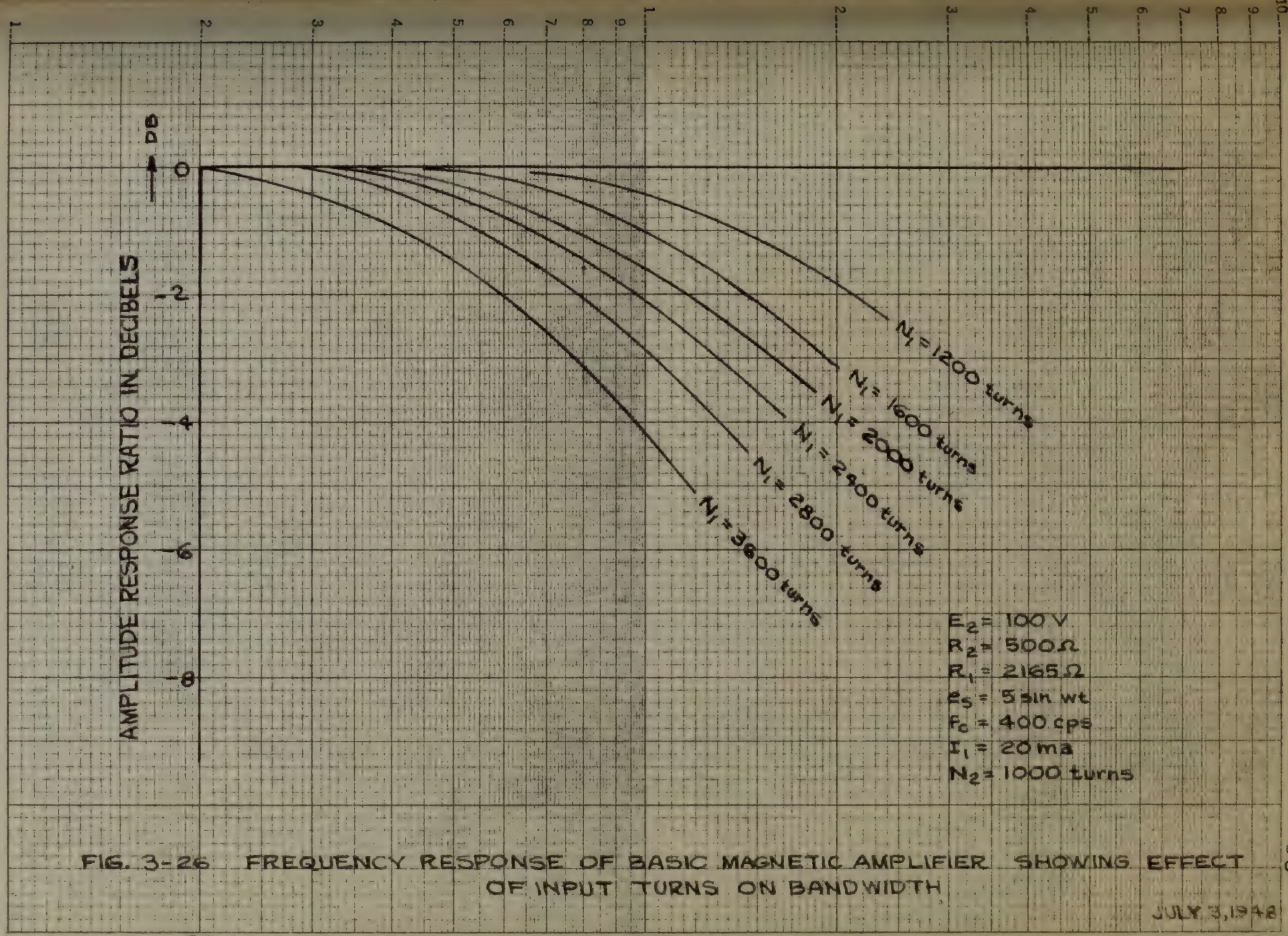

FIG. 3-26 FREQUENCY RESPONSE OF BASIC MAGNETIC AMPLIFIER SHOWING EFFECT OF INPUT TURNS ON BANDWIDTH

JULY 3, 1948

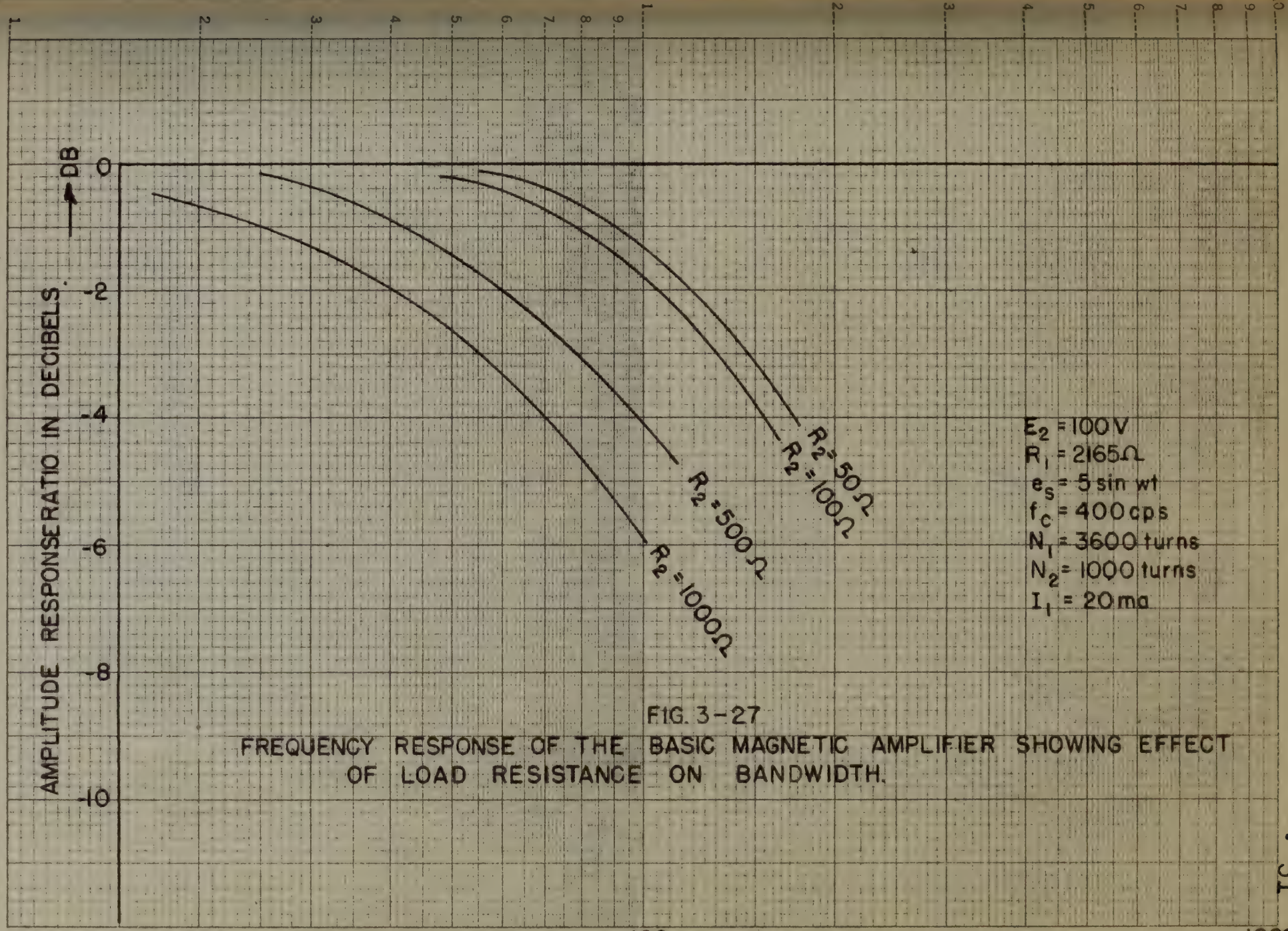

FIG. 3-27

FREQUENCY RESPONSE OF THE BASIC MAGNETIC AMPLIFIER SHOWING EFFECT OF LOAD RESISTANCE ON BANDWIDTH.

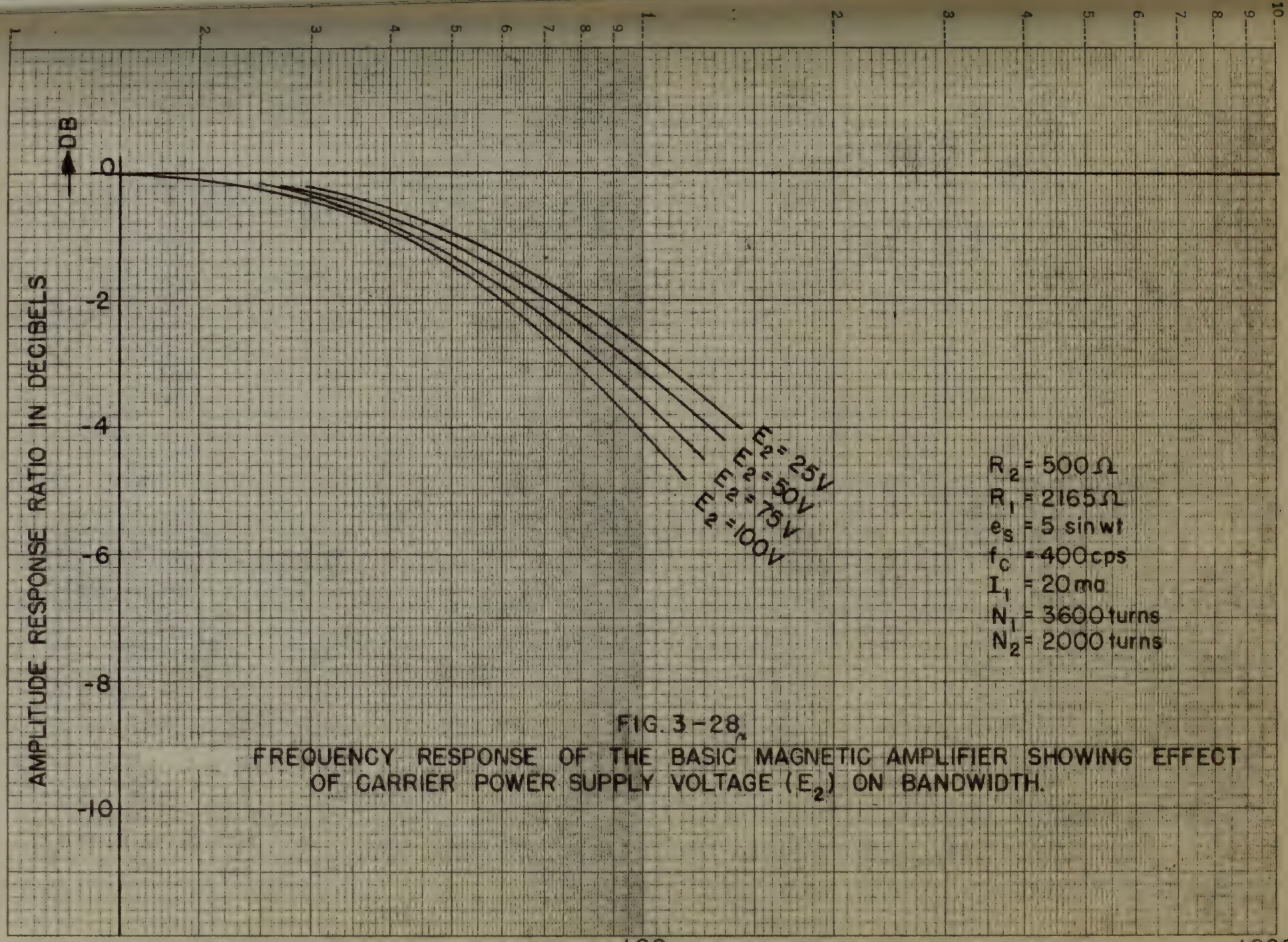

FIG. 3-28.
FREQUENCY RESPONSE OF THE BASIC MAGNETIC AMPLIFIER SHOWING EFFECT OF CARRIER POWER SUPPLY VOLTAGE (E_2) ON BANDWIDTH.

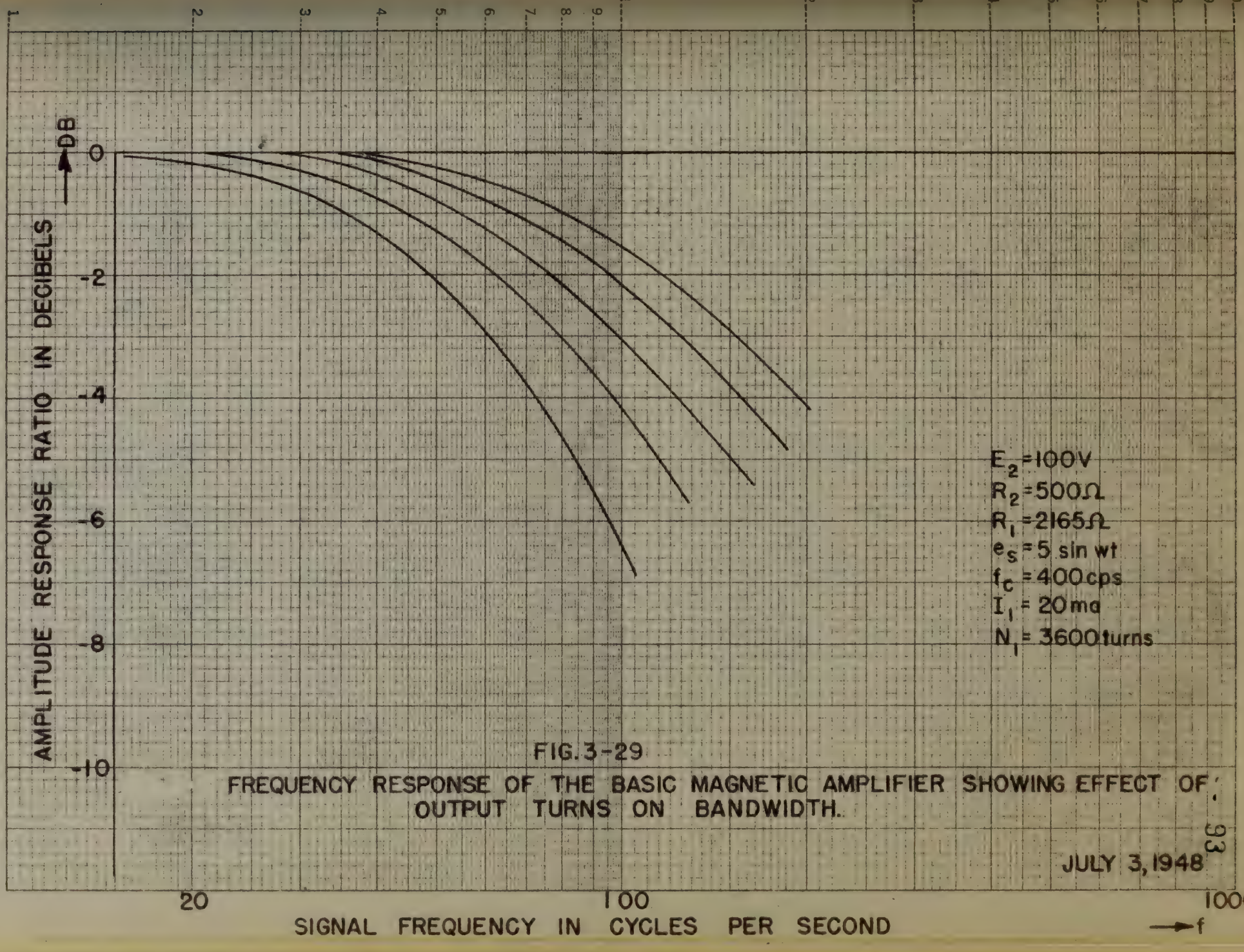

FIG. 3-29

FREQUENCY RESPONSE OF THE BASIC MAGNETIC AMPLIFIER SHOWING EFFECT OF OUTPUT TURNS ON BANDWIDTH.

JULY 3, 1948

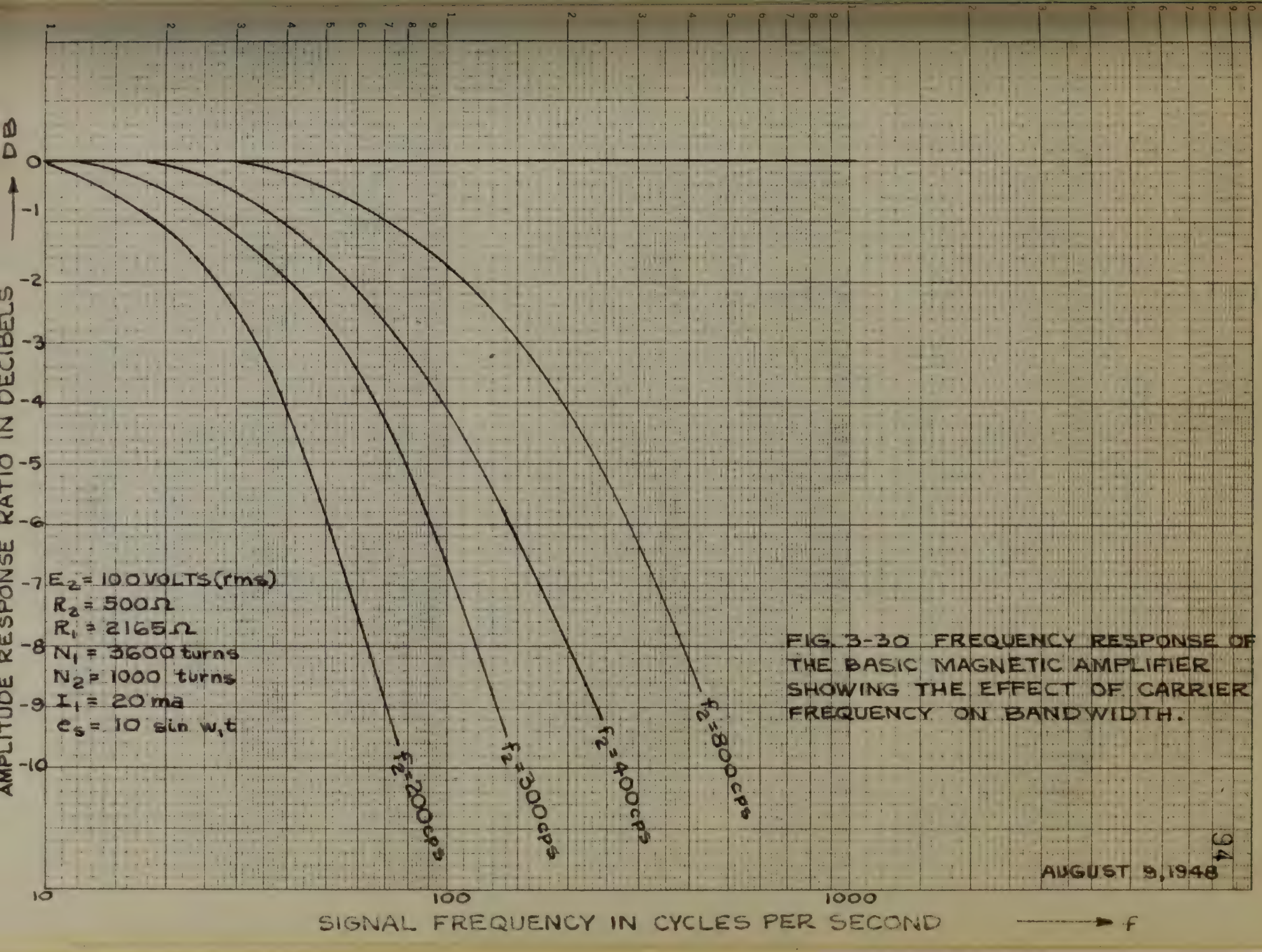

FIG. 3-30 FREQUENCY RESPONSE OF THE BASIC MAGNETIC AMPLIFIER SHOWING THE EFFECT OF CARRIER FREQUENCY ON BANDWIDTH.

AUGUST 9, 1948

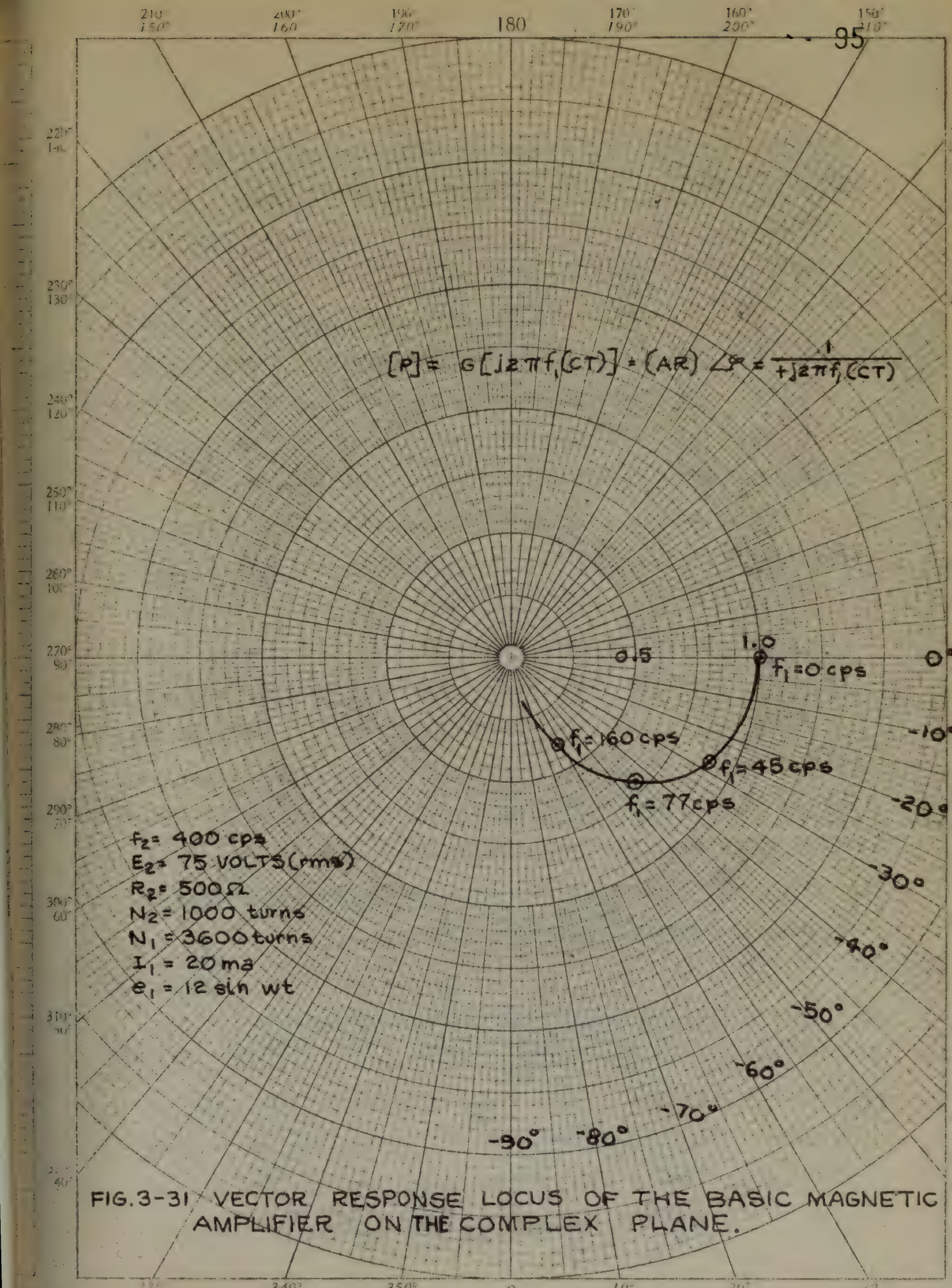

FIG. 3-31 VECTOR RESPONSE LOCUS OF THE BASIC MAGNETIC AMPLIFIER ON THE COMPLEX PLANE.

bandwidth measurements the characteristic time was computed using the Equation 3-32. Logarithmic plots of these results were then prepared for both control and carrier-circuit parameters, the former being shown in Figure 3-32 and the latter in Figure 3-33. As seen from the plots, (CT) was observed to be directly proportional to N_1, and inversely proportional to R_1 and to the square-root of I_1, thus confirming the results obtained from the transient studies.

The effects caused by variations of the carrier-circuit parameters, as observed by frequency response methods, are in general agreement with those obtained from transient studies with some noticeable deviation. The variation of (CT) with E_2 and N_2 was identical. Whereas transient studies gave the result that (CT) depended very little upon f_2, and almost not at all on R_2, sinusoidal studies showed that (CT) varies directly with the one-third power of R_2 and inversely as f_2. These differences are attributable to the fact that in the transient studies I_1 changes from zero to some discrete value, whereas in the sinusoidal studies I_1 varies periodically about a constant level.

The results of the dynamic studies, both transient and sinusoidal steady-state, indicate that in order to widen the bandwidth or shorten the characteristic time, it is desirable to increase R_1, I_1, f_2, and N_2, and to decrease N_1 and E_2. In any case, f_2 would have to be sufficiently high to carry the intelligence as a modulated signal.

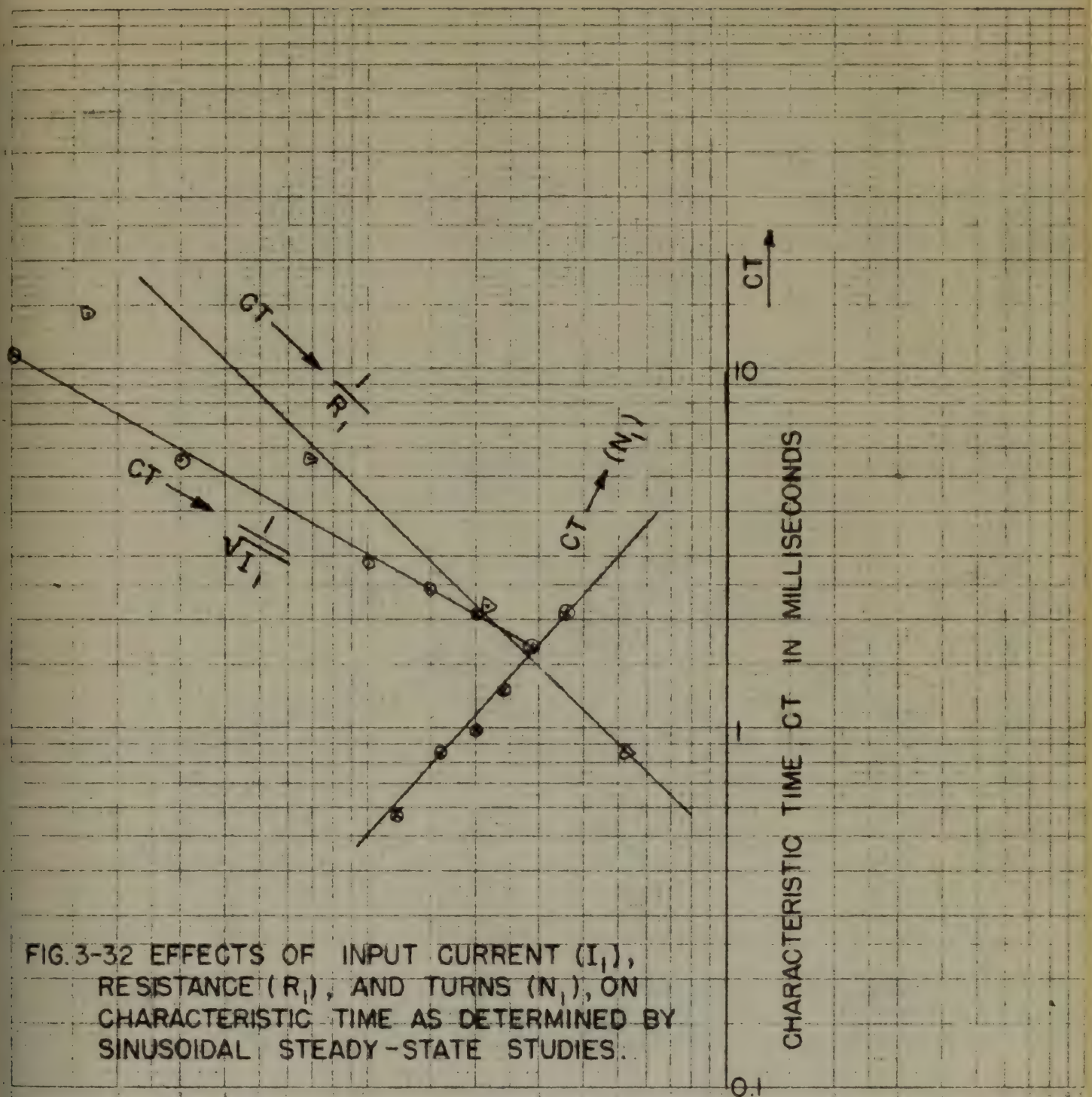

FIG. 3-32 EFFECTS OF INPUT CURRENT (I_1), RESISTANCE (R_1), AND TURNS (N_1), ON CHARACTERISTIC TIME AS DETERMINED BY SINUSOIDAL STEADY-STATE STUDIES.

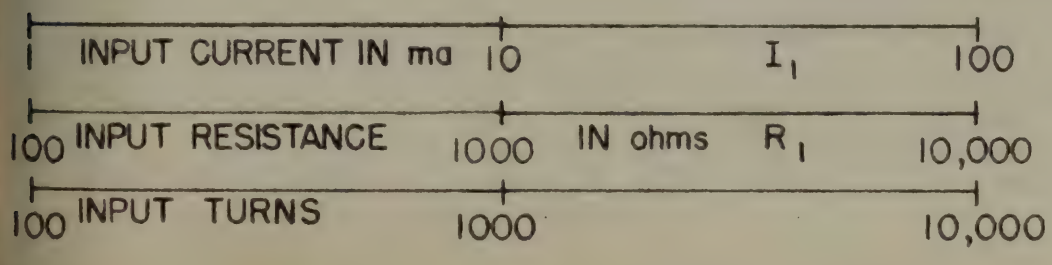

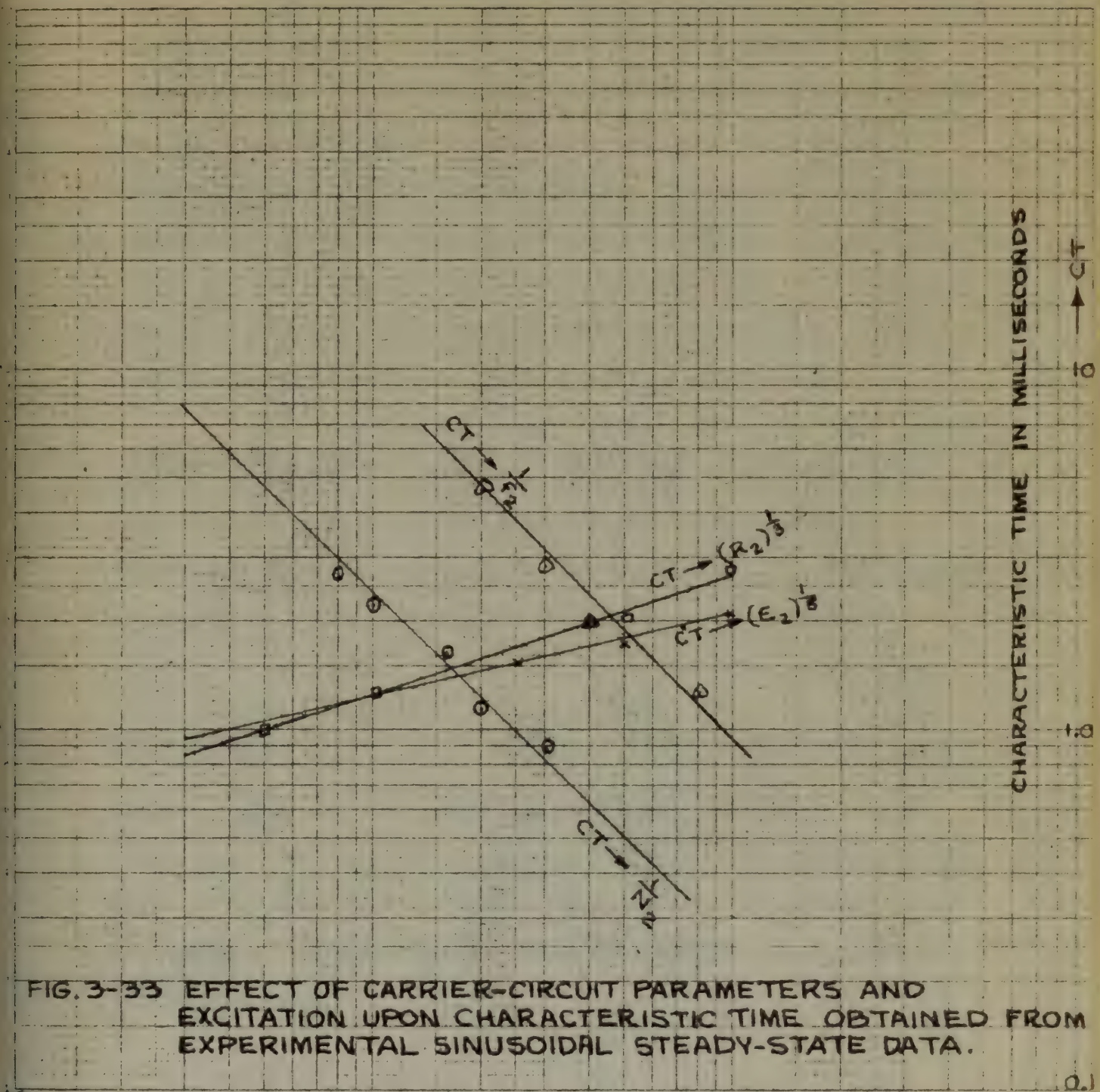
CHARACTERISTIC TIME IN MILLISECONDS
CT
10
1.0
0.1
CT → $(R_2)^{\frac{1}{3}}$
CT → $(E_2)^{\frac{1}{3}}$
CT → $N_2^{\frac{1}{2}}$
CT → $N_2^{\frac{1}{2}}$
10 CARRIER FREQUENCY 100 IN CYCLES/SECOND 1000 → f_2
1 RMS CARRIER VOLTAGE 10 IN VOLTS 100 → E_2
100 OUTPUT WINDING 1000 IN TURNS 10,000 → N_2
10 LOAD RESISTANCE 100 IN OHMS 1000 → R_2

FIG. 3-33 EFFECT OF CARRIER-CIRCUIT PARAMETERS AND EXCITATION UPON CHARACTERISTIC TIME OBTAINED FROM EXPERIMENTAL SINUSOIDAL STEADY-STATE DATA.

Summary

The results of the experimental study of the basic magnetic-amplifier circuit reveal that a compromise must be made between gain and bandwidth. The adjustment of parameters in a direction to increase the gain is seen to simultaneously narrow the bandwidth. The design of a magnetic amplifier to meet a given specification is based first upon the selection of the core material. Once the material has been chosen, experimental data can be taken on a model, and the design scaled to meet specific requirements.

The carrier frequency is determined by the highest signal-frequency of interest. Amplifier bandwidth, sufficiently broad to pass the highest signal-frequency of interest, must be attained by increasing R_1, I_1, and by decreasing N_1. The effects of E_2 and R_2 upon bandwidth appear to be small. To improve gain, however, exclusive of feedback techniques to be discussed later, R_1, I_1, and N_2 must be decreased, and N_1 and R_2 increased. A compromise between gain and bandwidth is obviously necessary. The fact that the magnetic amplifier, despite its nonlinearity, can approximate a first-order system, offers possibilities in certain applications in which electronic amplifiers are currently used.

Summary

CHAPTER IV

THE MATHEMATICAL ANALYSIS OF THE MAGNETIC AMPLIFIER

Introduction to the Analytical Problem

The nonlinear character of the normal magnetizing curve of iron-cored saturable reactors has long placed a restraint on rigorous mathematical analysis of magnetic amplifiers. Since differential equations involving nonlinearities do not yield to ordinary methods of solution, a rigorous approach to this problem implies the use of machine methods of solution.

In the past, several approaches to the analysis and synthesis of the magnetic amplifier have been undertaken. Each method requires certain approximations. The two most important of these approaches are the linear-approximation technique, based on the division of the normal magnetization curve into linear regions,[1] and the reactor design technique developed at the Servomechanisms Laboratory at the Massachusetts Institute of Technology.[2]

Each of these techniques involves approximations which contribute to loss of rigor in the solution. In spite of these limitations, these approaches to the problem have been used with some success to predict and explain the steady-state performance of the magnetic amplifier. Unfortunately, neither technique is readily adaptable to the

---

1. Boyajian, A., "Mathematical Analysis of Nonlinear Circuits," G.E.Rev., 34, (1931), 531-539.
2. Pease, W.M., "Design of a 400 Cycle Servomechanism," M.I.T. MS Thesis (1943).

CHAPTER IV

THE MATHEMATICAL ANALYSIS OF THE MAGNETIC AMPLIFIER

Introduction to the analytical problem

The nonlinear character of the normal magnetizing curve of iron-cored saturable reactors has long placed a restraint on rigorous mathematical analysis of magnetic amplifiers. Since differential equations involving nonlinearities do not yield to ordinary methods of solution, a rigorous approach to this problem implies the use of machine methods of solution.

In the past, several approaches to the analysis and synthesis of the magnetic amplifier have been undertaken. Each method requires certain approximations. The two most important of these approaches are the linear-approximation techniques, based on the division of the normal magnetization curve into linear regions,[1] and the reactor design techniques developed at the Servomechanisms Laboratory at the Massachusetts Institute of Technology.[2]

Each of these techniques involves approximations which contribute to loss of rigor in the solution. In spite of these limitations, these approaches to the problem have been used with some success to predict and explain the steady-state performance of the magnetic amplifier. Unfortunately, neither technique is readily adaptable to the

---

1. Ruyajian, A., "Mathematical Analysis of Nonlinear Circuits," M.S. Rev., 16, (1951), 532-539.
2. Fenes, W.K., "Design of a MOC Cycle Servomechanism," M.I.T. MS Thesis (1945).

prediction of the dynamic performance of the magnetic amplifier.

The use of the differential analyzer to solve the nonlinear differential equations of the magnetic amplifier circuit has offered an original method of attacking this important problem. Since there is no constraint on the nonlinearity of the character of the equations, the use of the analyzer has permitted a rigorous solution of the dynamic problem as well as the steady-state problem. The principal limitation imposed on the analytical solution is the necessity for neglecting hysteretic and eddy-current losses in the cores. If the cores used are of high quality, the neglect of hysteresis and eddy-current losses, as will be shown, is of no great consequence in the static or steady-state solution. The dynamic analytical solution will, however, suffer if losses are not considered. The physical effect of hysteretic loss in an iron-cored coil under excitation by fluxes of two or more different frequencies has not been fully explained, but in spite of this important fact, it was possible to make a semi-quantitative investigation of the effect of hysteresis in the magnetic-amplifier circuit. As has been described in Chapter III, and will be further considered later, hysteresis and eddy-current loss have a definite influence on the dynamic performance of the amplifier at different excitation-flux values, and consequently, the neglect of these phenomena

has somewhat hampered the mathematical investigation of the effects of certain parameters on the time-response of the amplifier. Variations in most of the circuit parameters have, however, been investigated satisfactorily by the analytical approach.

Formulation of the Equations

An investigation of the effect of fundamental parameters of the magnetic-amplifier circuit was established as the primary purpose of the analytical study. Accordingly, analytical investigations have been conducted, on the basic magnetic-amplifier circuit. The clarification of the fundamental behavior of the amplifier under the action of the various parameters which influence this behavior is intended to establish criteria which will then be applicable to the more complex magnetic-amplifier circuits involving feedback.

Experimental studies of the basic magnetic amplifier have indicated that the following circuit parameters influence the transient and steady-state performance of the amplifier: (1) Input-circuit resistance, R_1, (2) Input-circuit coil turns, N_1, (3) Input-circuit current, I_1, (4) Output-circuit resistance, R_2, (5) Output-circuit coil turns, N_2, (6) Peak value of the output-circuit alternating voltage, E_2, and (7) Frequency, ω, of the output-circuit alternating-voltage. These parameters are further identified in Figure 4-1. Analytical

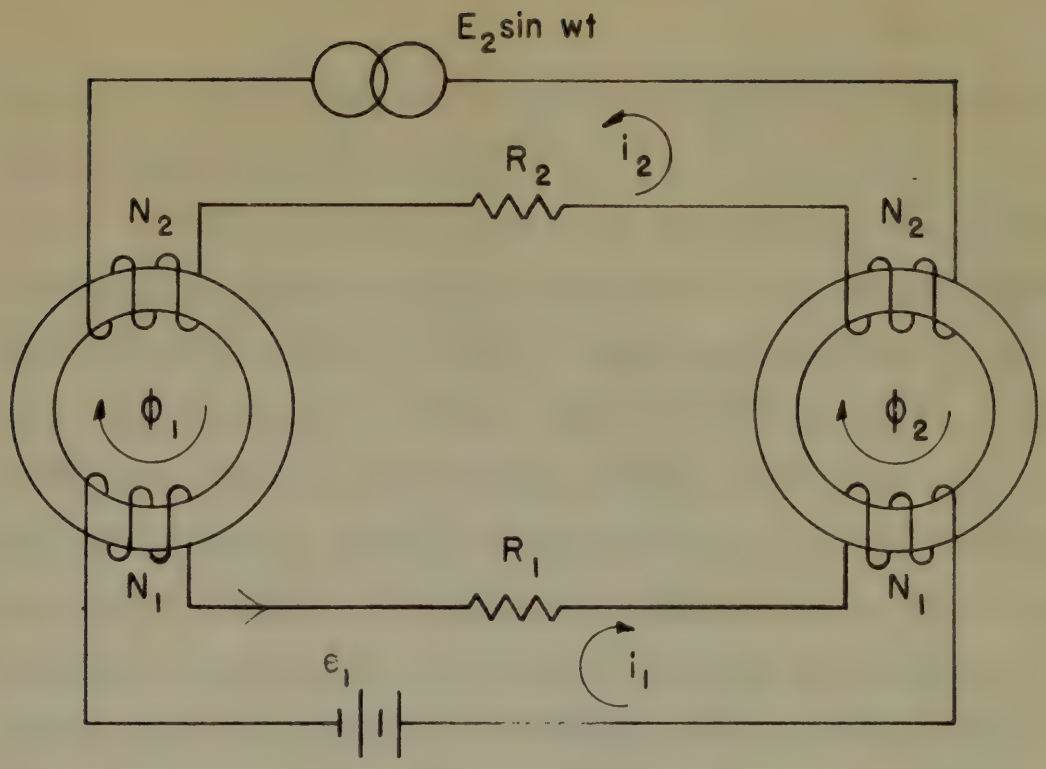

FIG. 4-1 BASIC MAGNETIC AMPLIFIER CIRCUIT

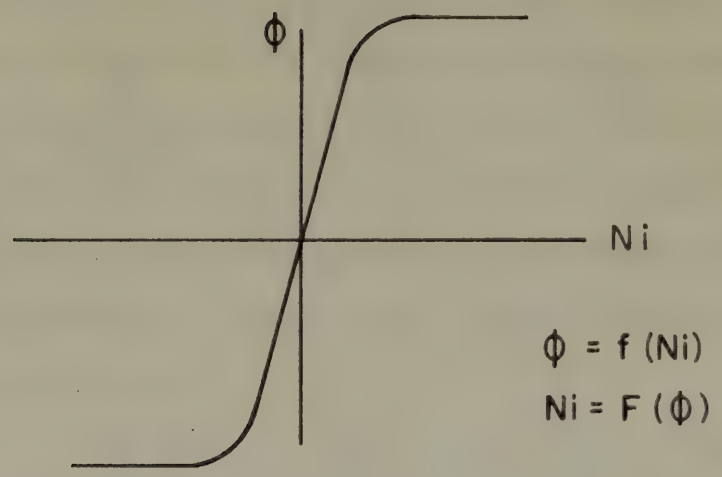

FIG. 4-2 NON-LINEAR RELATIONSHIP BETWEEN FLUX AND MAGNETIZING FORCE.

studies are conducted in a manner designed to indicate the effects of these parameters.

The analytical transient response of the magnetic amplifier is studied through the medium of a step function applied to the input circuit. This step function is applied as a voltage, e_1, across the input terminals of the amplifier. The applied step voltage causes a current, i_1, to flow in the input circuit, and a current, i_2, to flow in the output circuit. In each case solved by the differential analyzer, the solution is carried through the transient period until steady-state conditions are reached. The even-harmonic currents, i_1, which flow in the input circuit, and the odd-harmonic currents, i_2, which flow in the output circuit, were recorded for each solution of the problem. The rate of buildup of current in the output circuit during the transient state establishes the characteristic time of the amplifier circuit for each condition observed. As was the case in the experimental studies described in Chapter III, the characteristic time of the amplifier is defined as the time required for the output current to reach 63% of its steady-state value after the application of the step function input.

In summary, then, the values of i_1, i_2 and characteristic time, (CT), were observed for step function-input variations of e_1 for various conditions on the parameters R_1, R_1, R_2, N_2, E_2, and ω. Minor deviations from this procedure will be discussed subsequently.

The equations used in the analytical solution are based upon the circuit of Figure 4-1, and the non-linear function of Figure 4-2. In Figure 4-1, the flux in Core 1 is defined as ϕ_1 while the flux in Core 2 is defined as ϕ_2. The positive directions of these fluxes are shown by the arrows on the figure. Similarly, the positive directions of the currents i_1 and i_2 are indicated by arrows. The remaining parameters of this circuit have been identified. Figure 4-2 is a sketch of the normal magnetization curve of the core material used in the study. This figure is based on empirical data which was measured as described in Chapter II. In the figure, the flux in the cores, ϕ, in webers, is plotted against the magnetizing force, Ni, expressed in ampere-turns. The studies were conducted using the MKS system of units with all voltages expressed in volts, all currents expressed in amperes, resistances expressed in ohms, and time expressed in seconds.

From the circuit of Figure 4-1, it is possible to write the equilibrium equations of the system on the loop basis for the input and output circuits, respectively:

$$e_1 = R_1 i_1 + N_1 \frac{d\phi_1}{dt} - N_1 \frac{d\phi_2}{dt} \qquad (4-1)$$

$$e_2 = R_2 i_2 + N_2 \frac{d\phi_1}{dt} + N_2 \frac{d\phi_2}{dt} \qquad (4-2)$$

From Figures 4-1 and 4-2, the relationships between flux and magnetizing force are established:

$$\phi = f(Ni) \qquad (4\text{-}3)$$

$$Ni = f(\phi) \qquad (4\text{-}4)$$

$$\phi_1 = f(N_2 i_2 + N_1 i_1) \qquad (4\text{-}5)$$

$$\phi_2 = f(N_2 i_2 - N_1 i_1) \qquad (4\text{-}6)$$

Equations 4-1 and 4-2 are next manipulated as shown in the following series of expressions:

$$e_1 - i_1 R_1 = N_1 \left(\frac{d\phi_1}{dt} - \frac{d\phi_2}{dt}\right) \qquad (4\text{-}7)$$

$$e_2 - i_2 R_2 = N_2 \left(\frac{d\phi_1}{dt} + \frac{d\phi_2}{dt}\right) \qquad (4\text{-}8)$$

If Equation 4-7 is divided by N_1, and Equation 4-8 is divided by N_2, the expressions may be added and subtracted to yield Equations 4-9 and 4-10 respectively:

$$\left(\frac{e_1 - i_1 R_1}{N_1}\right) + \left(\frac{e_2 - i_2 R_2}{N_2}\right) = 2\frac{d\phi_1}{dt} \qquad (4\text{-}9)$$

$$-\left(\frac{e_1 - i_1 R_1}{N_1}\right) + \left(\frac{e_2 - i_2 R_2}{N_2}\right) = 2\frac{d\phi_2}{dt} \qquad (4\text{-}10)$$

or

$$\frac{d\phi_1}{dt} = \frac{1}{2}\left[\left(\frac{e_2 - i_2 R_2}{N_2}\right) + \left(\frac{e_1 - i_1 R_1}{N_1}\right)\right] \qquad (4\text{-}11)$$

$$\frac{d\phi_2}{dt} = \frac{1}{2}\left[\left(\frac{e_2 - i_2 R_2}{N_2}\right) - \left(\frac{e_1 - i_1 R_1}{N_1}\right)\right] \qquad (4\text{-}12)$$

Integrating Equations 4-11 and 4-12 with respect to time, and combining these expressions with Equations 4-5 and 4-6, gives:

$$\phi_1 = f(N_2 i_2 + N_1 i_1) = \frac{1}{2}\int_0^t \left[\frac{e_2 - i_2 R_2}{N_2} + \frac{e_1 - i_1 R_1}{N_1}\right] dt \tag{4-13}$$

$$\phi_2 = f(N_2 i_2 - N_1 i_1) = \frac{1}{2}\int_0^t \left[\frac{e_2 - i_2 R_2}{N_2} - \frac{e_1 - i_1 R_1}{N_1}\right] dt \tag{4-14}$$

By applying Equation 4-4 to Equations 4-13 and 4-14, the following expressions which define the behavior of the magnetic amplifier are obtained:

$$H_1 = N_2 i_2 + N_1 i_1 = F_1\left\{\frac{1}{2}\int_0^t \left[\frac{e_2 - i_2 R_2}{N_2} + \frac{e_1 - i_1 R_1}{N_1}\right] dt\right\} \tag{4-15}$$

$$H_2 = N_2 i_2 - N_1 i_1 = F_2\left\{\frac{1}{2}\int_0^t \left[\frac{e_2 - i_2 R_2}{N_2} - \frac{e_1 - i_1 R_1}{N_1}\right] dt\right\} \tag{4-16}$$

In Equations 4-15 and 4-16, the functions H_1 and H_2 are defined for convenience in the differential analyzer solution. From these expressions, it is now possible to define i_1 and i_2 in terms of H_1 and H_2:

$$i_1 = \frac{H_1 - H_2}{2N_1} \tag{4-17}$$

$$i_2 = \frac{H_1 + H_2}{2N_2} \tag{4-18}$$

Recalling that the input voltage is applied as a step function, and that the output voltage is sinusoidal, the following equations are written:

$$e_1 = E_1 u(t) \tag{4-19}$$

$$e_2 = E_2 \sin \omega_2 t \tag{4-20}$$

The differential analyzer problem is formulated from Equations 4-15 through 4-20 inclusive.

$$\beta_{\mu}^{\alpha} = \frac{1}{2\pi i} \int_{0}^{\infty} \left[\frac{\mu^{\alpha} - \nu^{\alpha}}{\mu^{\alpha}} - \frac{\sigma^{\alpha} - \tau^{\alpha}}{\sigma^{\alpha}} \right] d\sigma \qquad (\mu-23)$$

$$\beta_{\mu}^{\alpha} = \frac{1}{2\pi i} \int_{0}^{\infty} \left[\frac{\mu^{\alpha} - \nu^{\alpha} \tau^{\alpha}}{\mu^{\alpha}} - \frac{\sigma^{\alpha} - \tau^{\alpha} \nu^{\alpha}}{\sigma^{\alpha}} \right] d\sigma \qquad (\mu-24)$$

In substituting Equation $\mu-23$ into Equations $\mu-13$ and $\mu-14$, the Poisson reciprocal relation between the potential and the magnetic susceptibility are obtained.

$$\mu^{\alpha} = \mu_0 \tau^{\alpha} + \mu^{\alpha} \nu^{\alpha} = \mu^{\alpha} \left\{ \frac{2}{\pi} \int_{0}^{\infty} \left[\frac{\mu^{\alpha} - \tau^{\alpha} \nu^{\alpha}}{\mu^{\alpha}} - \frac{\sigma^{\alpha} - \tau^{\alpha} \nu^{\alpha}}{\sigma^{\alpha}} \right] d\sigma \right\} \qquad (\mu-25)$$

$$\nu_{\alpha} = \mu_{\alpha} \tau_{\alpha} - \mu^{\alpha} \tau^{\alpha} = \mu^{\alpha} \left\{ \frac{2}{\pi} \int_{0}^{\infty} \left[\frac{\mu^{\alpha} - \tau^{\alpha} \nu^{\alpha}}{\mu^{\alpha}} - \frac{\sigma^{\alpha} - \tau^{\alpha} \nu^{\alpha}}{\sigma^{\alpha}} \right] d\sigma \right\} \qquad (\mu-26)$$

In Equations $\mu-25$ and $\mu-26$, the functions μ^{α} and ν^{α} are defined for measurement in the electromagnetic medium. Since these observations, it is now possible to define β^{α} and τ^{α} in terms of μ^{α} and ν^{α};

$$\tau^{\alpha} = \frac{\mu^{\alpha} - \nu^{\alpha}}{\mu^{\alpha}} \qquad (\mu-27)$$

$$\tau^{\alpha} = \frac{\mu^{\alpha} + \nu^{\alpha}}{\mu^{\alpha}} \qquad (\mu-28)$$

Identifying these index values is validating as a wave function, for that the natural variable is electromagnetic the Poisson equations $\mu-25$ and $\mu-26$ are obtained.

$$\mu^{\alpha} = \mu^{\alpha} \tau(\beta) \qquad (\mu-29)$$

$$\mu^{\alpha} = \mu^{\alpha} \sin \omega \delta_{\beta} \qquad (\mu-30)$$

Then Equations $\mu-25$ through $\mu-30$ together is Laplacian

Preparation of the Differential Analyzer Problem

The M.I.T. Differential Analyzer No. 1 was employed for the solution of the equations of the magnetic amplifier. The operation of this machine is totally mechanical, in that all process of integration, addition and subtraction, multiplication, the generation and introduction of functions, and the recording of results, are accomplished by mechanical means. The machine has been described in detail in the literature[1,2] and no further description will be attempted in this report. Similarly, the nature of the development of scale factors for use on this analyzer has been discussed in detail, and will not be dealt with further here. The reader is referred to the references given for further study of the analyzer and for further understanding of the method by which the scale factors were established for this problem.

After the equations of the problem have been formulated, limits over which the various parameters of the equations may be expected to vary are established. The knowledge of these limits permits the selection of scale factors which will allow the greatest flexibility of the parameters with minimum requisite changes in the layout of the machine. A schematic diagram of the analyzer layout is then constructed. Gear boxes, differ-

---

1. Bush, V., "The Differential Analyzer," J.F.I., 212, (1931), 447-488.
2. Bush, V. and Caldwell, S.H., "A New Type Differential Analyzer," J.F.I., 240, (1945), 255-326.

Preparation of the Differential Analyzer Problem

The M.I.T. Differential Analyzer No. 1 was employed for the solution of the equations of the magnetic amplifier. The operation of this machine is totally mechanical, in that all process of integration, addition and subtraction, multiplication, the generation and introduction of functions, and the recording of results, are accomplished by mechanical means. The machine has been described in detail in the literature[1,2] and no further description will be attempted in this report. Similarly, the nature of the development of scale factors for use on this analyzer has been discussed in detail, and will not be dealt with further here. The reader is referred to the references given for further study of the analyzer and for further understanding of the method by which the scale factors were established for this problem.

After the equations of the problem have been formulated, limits over which the various parameters of the equations may be expected to vary are established. The knowledge of these limits permits the selection of scale factors which will allow the greatest flexibility of the parameters with minimum requisite changes in the layout of the machine. A schematic diagram of the analyzer layout is then constructed. Gear boxes, differ-

---

1. Bush, V., "The Differential Analyzer," J.F.I., 212, (1931), 447-488.
2. Bush, V. and Caldwell, S.H., "A New Type Differential Analyzer," J.F.I., 240, (1945), 255-326.

ential units and integrator units are provided to perform the necessary functions of the equations. Scale factors are then established to meet the conditions of the equations and these factors are fitted to a schematic diagram. The selection of scale factors is restricted somewhat by the actual gear-ratios available, but, in general, there is sufficient flexibility that scale factors may be chosen in a manner which very closely approximates any desired physical condition. Figure 4-3 shows the actual schematic diagram which was made for the initial problem applied to the machine in this study. In this figure, integrators are identified by number, differentials are identified by number, and gear boxes are identified by letters. In this problem, the sinusoidal voltage of the output circuit, E_2, is generated by integrators No. 3 and 4. The fluxes in each core are integrated in accordance with equations (15) and (16) in integrator units No. 1 and 2. The nonlinear relationship between flux and magnetizing force is inserted by the manually-operated input tables No. 1 and 2, and the resultant currents, i_1 and i_2, are plotted on the output table. The step voltage, e_1, is applied to the lead screws of the integrators No. 1 and 2.

The problem shown in Figure 4-3 represents the conditions which obtained during Runs 1-13 inclusive of the analyzer study. The actual values of the parameters

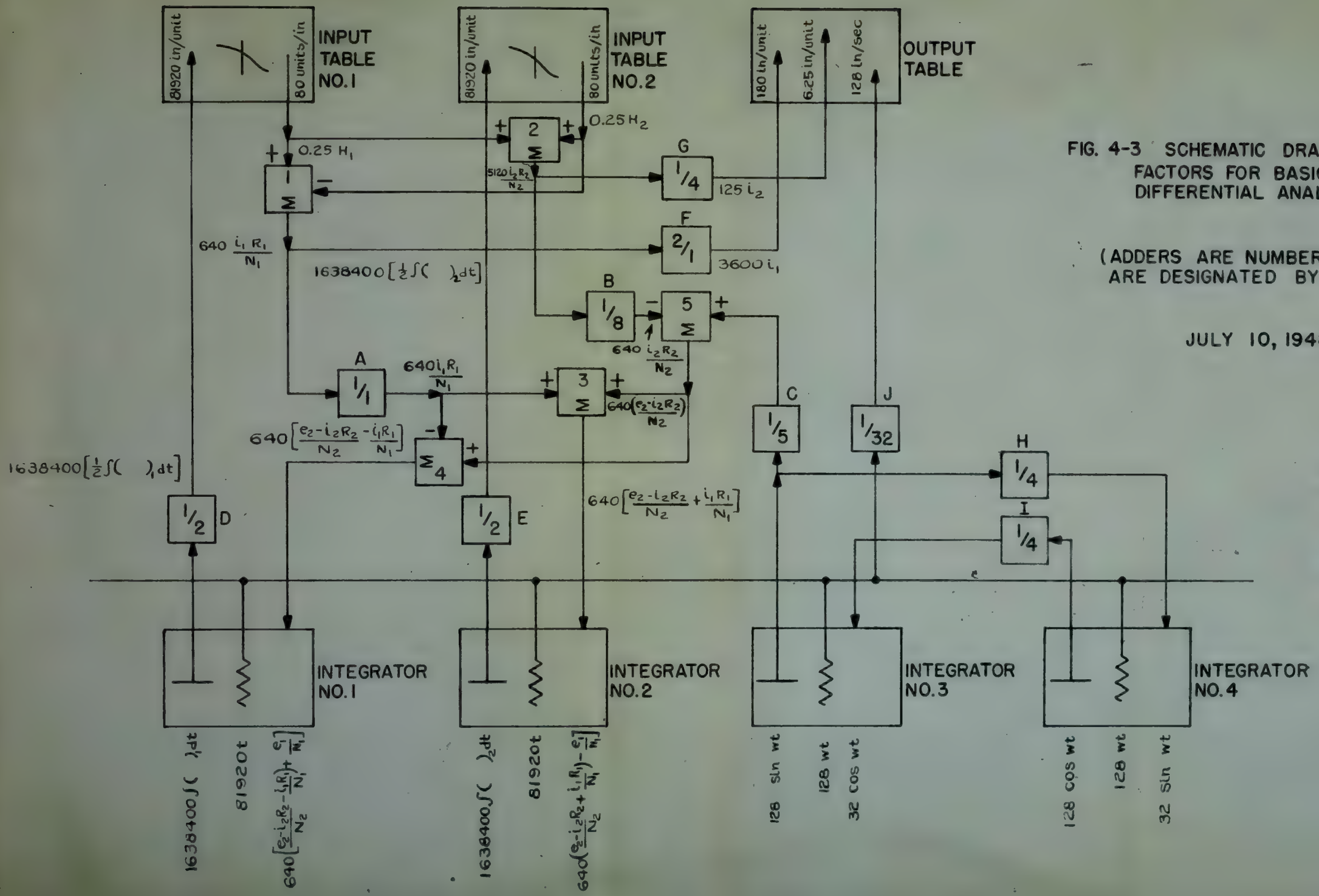

FIG. 4-3 SCHEMATIC DRAWING AND SCALE FACTORS FOR BASIC MECHANICAL DIFFERENTIAL ANALYZER PROBLEM.

(ADDERS ARE NUMBERED; GEAR BOXES ARE DESIGNATED BY LETTERS.)

JULY 10, 1948

f_c = 102 c.p.s.
R_1 = 97.8 ohms
R_2 = 10125 ohms
E_2 = 40 sinωt
N_1 = 3600 T
N_2 = 1000 T

for these runs are tabulated on Chart 4-1. On this chart the parameters and the scale factors, as well as the gear ratios which provide the scale factors, are tabulated for each solution of the equations. The scale factors, and the means by which these were obtained, are shown on Figure 4-3, and may be correlated with the tabulated data of Chart 4-1.

After the schematic diagram and the scale factors have been determined, it is necessary to formulate the actual layout of the problem on the differential analyzer. This phase is subject to limitations on the physical positioning of the various problem components within the machine structure. In the layout used for this problem, a special effort was made to provide a maximum of flexibility to permit the variation of the several parameters with a minimum of required changes of the actual physical layout. With this objective in mind, an effort was made to anticipate the changes in scale factors occasioned by the parameter changes, and wherever possible, additional gear ratios were set up in the gear boxes, and these were left disconnected except when actually in use. Considerable saving in time is enabled by a procedure of this type. The physical layout of the differential analyzer for the problems shown in the schematic drawing of Figure 4-3, Runs 1-13, is shown in Figure 4-4. Changes in the layout for the remaining solutions are tabulated on Charts 4-1 and 4-2.

JULY 1943 — METZEL WERNER GROSSIMON — M.I.T. DIFFERENTIAL ANALYZER NO 1 — D.A. 131

RUN NO.	w	E_2 VOLTS	R_1 OHMS	R_2 OHMS	N. TURNS	N_2 TURNS	GEAR BOX RATIOS A	B	C	D	E	F	G	H	I	J	SCALE FACTORS THE SHAFT	WHEEL I	WHEEL II	LEAD SCREW I	LEAD SCREW II	OUTPUT SCALE FACTORS i_1	i_2	t	STEP FUNCTION E_1 TURNS	STEP FUNCTION E_1 VOLTS	REMARKS
1	640	40	10125	97.7	3600	1000	1	1	8	1	5	1	2	2	1	4	4	4	32	B1920	16 38 400	16 38 400	640	640	180	6.25	128	2.0	11.23	
2	640	40	10125	97.7	3600	1000	1	1	8	1	5	1	2	2	1	4	4	4	32	B1920	16 38 400	16 38 400	640	640	180	25	128	3.0	16.88	
3	640	40	10125	97.7	3600	1000	1	1	8	1	5	1	2	2	1	4	4	4	32	B1920	16 38 400	16 38 400	640	640	180	25	128	3.5	19.68	
4	640	40	10125	97.7	3600	1000	1	1	8	1	5	1	2	2	1	4	4	4	32	B1920	16 38 400	16 38 400	640	640	180	25	128	4.0	22.50	
5	640	40	10125	97.7	3600	1000	1	1	8	1	5	1	2	2	1	4	4	4	32	B1920	16 38 400	16 38 400	640	640	180	25	128	4.5	25.30	
6	640	40	10125	97.7	3600	1000	1	1	8	1	5	1	2	2	1	4	4	4	32	B1920	16 38 400	16 38 400	640	640	180	25	128	5.5	30.90	
7	640	40	10125	97.7	3600	1000	1	1	8	1	5	1	2	2	1	4	4	4	32	B1920	16 38 400	16 38 400	640	640	180	50	128	2.0	11.23	
8	640	40	10125	97.7	3600	1000	1	1	8	1	5	1	2	2	1	4	4	4	32	B1920	16 38 400	16 38 400	640	640	180	50	128	6.5	36.55	
9	640	40	10125	97.7	3600	1000	1	1	8	1	5	1	2	2	1	4	4	4	32	B1920	16 38 400	16 38 400	640	640	180	50	128	7.5	42.20	
10	640	40	10125	97.7	3600	1000	1	1	8	1	5	1	2	2	1	4	4	4	32	B1920	16 38 400	16 38 400	640	640	180	50	128	8.5	47.75	
11	640	40	10125	97.7	3600	1000	1	1	8	1	5	1	2	2	1	4	4	4	32	B1920	16 38 400	16 38 400	640	640	180	50	128	9.5	53.40	
12	640	40	10125	97.7	3600	1000	1	1	8	1	5	1	2	2	1	4	4	4	32	B1920	16 38 400	16 38 400	640	640	180	50	128	10.5	59.00	
13	640	40	10125	97.7	3600	1000	1	1	8	1	5	1	2	2	1	4	4	4	32	B1920	16 38 400	16 38 400	640	640	180	50	128	11.5	64.60	
14	2560	80	10125	97.7	3600	1000	1	2	16	2	5	1	2	2	1	2	2	2	64	16 38 400	16 38 400	16 38 400	320	320	180	50	128	1.0	11.24	
15	2560	80	10125	97.7	3600	1000	1	2	16	2	5	1	2	2	1	2	2	2	32	16 38 400	16 38 400	16 38 400	320	320	180	50	256	2.0	22.50	
16	2560	80	10125	97.7	3600	1000	1	2	16	2	5	1	2	2	1	2	2	2	32	16 38 400	16 38 400	16 38 400	320	320	180	50	256	3.0	33.75	
17	2560	80	10125	97.7	3600	1000	1	2	16	2	5	1	2	2	1	2	2	2	32	16 38 400	16 38 400	16 38 400	320	320	180	50	256	4.0	45.00	
18	2560	80	10125	97.7	3600	1000	1	2	16	2	5	1	2	2	1	2	2	2	32	16 38 400	16 38 400	16 38 400	320	320	180	50	256	5.0	56.25	
19	2560	80	10125	97.7	3600	1000	1	2	16	2	5	1	2	2	1	2	2	2	32	16 38 400	16 38 400	16 38 400	320	320	180	50	256	6.0	67.50	
20	2560	80	10125	97.7	3600	1000	1	2	16	2	5	1	2	2	1	2	2	2	32	16 38 400	16 38 400	16 38 400	320	320	180	50	256	3.0	33.75	Hysteresis
21	2560	80	10125	97.7	3600	1000	1	2	16	2	5	1	2	2	1	2	2	2	32	16 38 400	16 38 400	16 38 400	320	320	180	50	256	1.0	11.24	Hysteresis
22	2560	100	10125	97.7	3600	1000	1	2	16	2	5	1	2	2	1	2	2	2	32	16 38 400	16 38 400	16 38 400	320	320	180	50	256	1.0	11.24	
23	2560	100	10125	97.7	3600	1000	1	2	16	2	5	1	2	2	1	2	2	2	32	16 38 400	16 38 400	16 38 400	320	320	180	50	256	2.0	22.50	
24	2560	100	10125	97.7	3600	1000	1	2	16	2	5	1	2	2	1	2	2	2	32	16 38 400	16 38 400	16 38 400	320	320	180	50	256	3.0	33.75	
25	2560	100	10125	97.7	3600	1000	1	2	16	2	5	1	2	2	1	2	2	2	32	16 38 400	16 38 400	16 38 400	320	320	180	50	256	4.0	45.00	
26	2560	100	10125	97.7	3600	1000	1	2	16	2	5	1	2	2	1	2	2	2	32	16 38 400	16 38 400	16 38 400	320	320	180	50	256	5.0	56.25	
27	2560	100	10125	97.7	3600	1000	1	2	16	2	5	1	2	2	1	2	2	2	32	16 38 400	16 38 400	16 38 400	320	320	180	50	256	5.75	64.70	
28	2560	100	10125	977	3600	1000	1	2	5	8	1	2	1	2	2	1	2	2	32	16 38 40	16 38 400	16 38 400	320	320	180	50	256	1.0	11.24	
29	2560	100	10125	977	3600	1000	1	2	5	8	1	2	1	2	2	1	2	2	32	16 38 40	16 38 400	16 38 400	320	320	180	50	256	2.0	22.50	
30	2560	100	10125	977	3600	1000	1	2	5	8	1	2	1	2	2	1	2	2	32	16 38 40	16 38 400	16 38 400	320	320	180	50	256	3.0	33.75	
31	2560	100	10125	977	3600	1000	1	2	5	8	1	2	1	2	2	1	2	2	32	16 38 40	16 38 400	16 38 400	320	320	180	50	256	4.0	45.00	
32	2560	100	10125	977	3600	1000	1	2	5	8	1	2	1	2	2	1	2	2	32	16 38 40	16 38 400	16 38 400	320	320	180	50	256	5.0	56.25	
33	2560	100	10125	977	3600	1000	1	2	5	8	1	2	1	2	2	1	2	2	32	16 38 40	16 38 400	16 38 400	320	320	180	50	256	5.75	64.70	
34	2560	100	10125	1954	3600	1000	1	2	5	4	1	2	1	2	2	1	2	2	32	16 38 40	16 38 400	16 38 400	320	320	180	50	256	1.0	11.24	
35	2560	100	10125	1954	3600	1000	1	2	5	4	1	2	1	2	2	1	2	2	32	16 38 40	16 38 400	16 38 400	320	320	180	50	256	2.0	22.50	
36	2560	100	10125	1954	3600	1000	1	2	5	4	1	2	1	2	2	1	2	2	32	16 38 40	16 38 400	16 38 400	320	320	180	50	256	3.0	33.75	
37	2560	100	10125	1954	3600	1000	1	2	5	4	1	2	1	2	2	1	2	2	32	16 38 40	16 38 400	16 38 400	320	320	180	50	256	4.0	45.00	
38	2560	100	10125	1954	3600	1000	1	2	5	4	1	2	1	2	2	1	2	2	32	16 38 40	16 38 400	16 38 400	320	320	180	50	256	5.0	56.25	
39	2560	100	10125	1954	3600	1000	1	2	5	4	1	2	1	2	2	1	2	2	32	16 38 40	16 38 400	16 38 400	320	320	180	50	256	5.75	64.70	
40	2560	100	10125	1954	3600	1000	1	2	5	4	1	2	1	2	2	1	2	2	32	16 38 40	16 38 400	16 38 400	320	320	180	50	256	1.0	11.24	
41	2560	100	10125	488.5	3600	1000	1	2	5	16	1	2	1	2	2	1	2	2	32	16 38 40	16 38 400	16 38 400	320	320	180	50	256	2.0	22.50	
42	2560	100	10125	488.5	3600	1000	1	2	5	16	1	2	1	2	2	1	2	2	32	16 38 40	16 38 400	16 38 400	320	320	180	50	256	3.0	33.75	
43	2560	100	10125	488.5	3600	1000	1	2	5	16	1	2	1	2	2	1	2	2	32	16 38 40	16 38 400	16 38 400	320	320	180	50	256	4.0	45.00	
44	2560	100	10125	488.5	3600	1000	1	2	5	16	1	2	1	2	2	1	2	2	32	16 38 40	16 38 400	16 38 400	320	320	180	50	256	5.0	56.25	
45	2560	100	10125	488.5	3600	1000	1	2	5	16	1	2	1	2	2	1	2	2	32	16 38 40	16 38 400	16 38 400	320	320	180	50	256	5.75	64.70	
46	2560	100	10125	488.5	3600	2000	1	1	5	32	1	2	1	4	2	1	1	2	32	16 38 40	32 76 800	32 76 800	640	640	180	50	256	1.0	5.62	
47	2560	100	10125	488.5	3600	2000	1	1	5	32	1	2	1	4	2	1	1	2	32	16 38 40	32 76 800	32 76 800	640	640	180	50	256	2.0	11.25	
48	2560	100	10125	488.5	3600	2000	1	1	5	32	1	2	1	4	2	1	1	2	32	16 38 40	32 76 800	32 76 800	640	640	180	50	256	3.0	16.88	
49	2560	100	10125	488.5	3600	2000	1	1	5	32	1	2	1	4	2	1	1	2	32	16 38 40	32 76 800	32 76 800	640	640	180	50	256	4.0	22.50	
50	2560	100	10125	488.5	3600	2000	1	1	5	32	1	2	1	4	2	1	1	2	32	16 38 40	32 76 800	32 76 800	640	640	180	50	256	5.0	28.13	
51	2560	100	10125	488.5	3600	2000	1	1	5	32	1	2	1	4	2	1	1	2	32	16 38 40	32 76 800	32 76 800	640	640	180	50	256	5.75	32.35	
52	2560	100	10125	488.5	3600	500	1	4	5	8	1	2	1	1	2	1	4	1	2	2	32	B1920	160	160	180	50	256	1.0	22.50	
53	2560	100	10125	488.5	3600	500	1	4	5	8	1	2	1	1	2	1	4	1	2	2	32	B1920	160	160	180	50	256	2.0	45.00	
54	2560	100	10125	488.5	3600	500	1	4	5	8	1	2	1	1	2	1	4	1	2	2	32	B1920	160	160	180	50	256	0.5	11.24	
55	2560	100	10125	488.5	3600	500	1	4	5	8	1	2	1	1	2	1	4	1	2	2	32	B1920	160	160	180	50	256	1.5	33.75	
56	2560	100	10125	488.5	3600	500	1	4	5	8	1	2	1	1	2	1	4	1	2	2	32	B1920	160	160	180	50	256	2.5	56.25	
57	2560	100	10125	488.5	1800	1000	2	1	5	16	1	2	1	2	4	1	2	1	2	2	32	16 38 40	16 38 400	16 38 400	320	320	180	50	256	1.0	5.62	
58	2560	100	10125	488.5	1800	1000	2	1	5	16	1	2	1	2	4	1	2	1	2	2	32	16 38 40	16 38 400	16 38 400	320	320	180	50	256	2.0	11.23	
59	2560	100	10125	488.5	1800	1000	2	1	5	16	1	2	1	2	4	1	2	1	2	2	32	16 38 40	16 38 400	16 38 400	320	320	180	50	256	5.0	16.88	
60	2560	100	10125	488.5	1800	1000	2	1	5	16	1	2	1	2	4	1	2	1	2	2	32	16 38 40	16 38 400	16 38 400	320	320	180	50	256	4.0	22.50	
61	2560	100	10125	488.5	1800	1000	2	1	5	16	1	2	1	2	4	1	2	1	2	2	32	16 38 40	16 38 400	16 38 400	320	320	180	50	256	5.0	28.13	
62	2560	100	10125	488.5	1800	1000	2	1	5	16	1	2	1	2	4	1	2	1	2	2	32	16 38 40	16 38 400	16 38 400	320	320	180	50	256	5.75	32.35	

CHART 4-1

BETZER
WERNER
GROSSNICKLE

JULY 1948

M I T CAPACITRONIC ANALYZER No. 1

DH 131

RUN No	W	E_2 VOLTS	R_1 OHMS	R_2 OHMS	N_1 TURNS	N_2 TURNS	GEAR BOX RATIOS F	B	C	D	E	F	G	H	I	J	LINE FACTORS I	II	III	IV	OHMS PER VOLT FACTORS (IN AMPS) L_1	L_2	L_T	TURNS	VOLTS	REMARKS
63	2560	100	10125	488.5	2543	1000	1	5	16	2	2	2	2	2	1	1						150	50	256	1.0	7.95	
64	2560	100	10125	488.5	2543	1000	1	5	16	2	2	2	2	2	1	1						150	50	256	2.0	15.90	
65	2560	100	10125	488.5	2543	1000	1	5	16	2	2	2	2	2	1	1						150	50	256	3.0	23.85	
66	2560	100	10125	488.5	2543	1000	1	5	16	2	2	2	2	2	1	1						150	50	256	4.0	31.80	
67	2560	100	10125	488.5	2543	1000	1	5	16	2	2	2	2	2	1	1						150	50	256	5.0	39.75	
68	2560	100	5063	488.5	2530	1000	1	4	5	16	2	2	2	2	2	1						320	150	256	1.0	11.74	
69	2560	100	5063	488.5	2530	1000	1	4	5	16	2	2	1	2	2	1						320	150	256	2.0	22.50	
70	2560	100	5063	488.5	2530	1000	1	4	5	16	2	2	1	2	2	1						320	150	256	3.0	33.75	
71	2560	100	5063	488.5	3600	1000	1	4	5	16	2	2	1	2	2	1						320	150	256	4.0	45.00	
72	2560	100	5063	488.5	3600	1000	1	4	5	16	2	2	1	2	2	1						320	150	256	5.5	28.10	
73	2560	100	5063	488.5	3600	1000	1	4	5	16	2	2	1	2	2	1						320	150	256	1.5	16.88	
74	2560	100	2531	488.5	3600	1000	1	8	5	16	2	2	1	2	2	1						320	150	256	1.0	11.24	
75	2560	100	2531	488.5	3600	1000	1	8	5	16	2	2	1	2	2	1						320	150	256	1.5	16.88	
76	2560	100	2531	488.5	3600	1000	1	8	5	16	2	2	1	2	2	1						320	150	256	2.0	22.50	
77	2560	100	2531	488.5	3600	1000	1	8	5	16	2	2	1	2	2	1						320	150	256	.50	5.62	
78	2560	100	1265	488.5	3600	1000	1	16	5	16	2	2	1	2	2	1						320	150	256	1.00	11.24	
79	2560	100	1265	488.5	3600	1000	1	16	5	16	2	2	1	2	2	1						320	150	256	.75	8.44	
80	2560	100	1265	488.5	3600	1000	1	16	5	16	2	2	1	2	2	1						320	150	256	.50	5.62	
81	2560	100	1265	488.5	3600	1000	1	16	5	16	2	2	1	2	2	1						320	150	256	.25	2.81	
82	2560	100	10125	488.5	3600	1000	1	2	5	32	1	4	1	4	2	1						320	150	512	5.0	56.25	30 TIMING ANGLE = 0
83	2560	100	10125	488.5	3600	1000	1	2	5	16	2	2	1	2	2	1						320	150	256	1705	56.25 MAX	NO STOP FLUX PLOT
84	2560	100	10125	488.5	3600	1000	1	2	5	16	2	2	1	2	2	1						320	150	256	2.0	22.50	FLUX PLOT
85	2560	150	10125	488.5	3600	1000	1	3	5	24	1	2	2	4	2	1						213	150	256	1.0	16.88	
86	2560	150	10125	488.5	3600	1000	1	3	5	24	1	2	2	4	2	1						213	150	256	2.0	33.80	
87	2560	150	10125	488.5	3600	1000	1	3	5	24	1	2	2	4	2	1						213	150	256	4.0	67.50	
88	2560	300	10125	488.5	3600	1000	1	6	5	48	1	2	2	4	2	1						160	150	256	0	0	
89	2560	300	10125	488.5	3600	1000	1	6	5	48	1	2	2	4	2	1						160	150	256	.75	8.44	
90	2560	300	10125	488.5	3600	1000	1	6	5	48	1	2	2	4	2	1						160	150	256	.50	5.62	
91	2560	300	10125	488.5	3600	1000	1	6	5	48	1	2	2	4	2	1						160	150	256	1.0	11.24	
92	5120	200	10125	488.5	3600	1000	1	4	5	32	1	4	1	4	2	1	64	65536	32768	16384		160	150	512	2.0	45.00	
93	5120	200	10125	488.5	3600	1000	1	4	5	32	1	4	1	4	2	1						160	150	512	3.0	67.50	
94	5120	200	10125	488.5	3600	1000	1	4	5	32	1	4	1	4	2	1						160	150	512	1.0	22.50	
95	5120	200	10125	488.5	3600	1000	1	4	5	32	1	4	1	4	2	1						160	150	512	4.0	90.00	

CHART 4-2

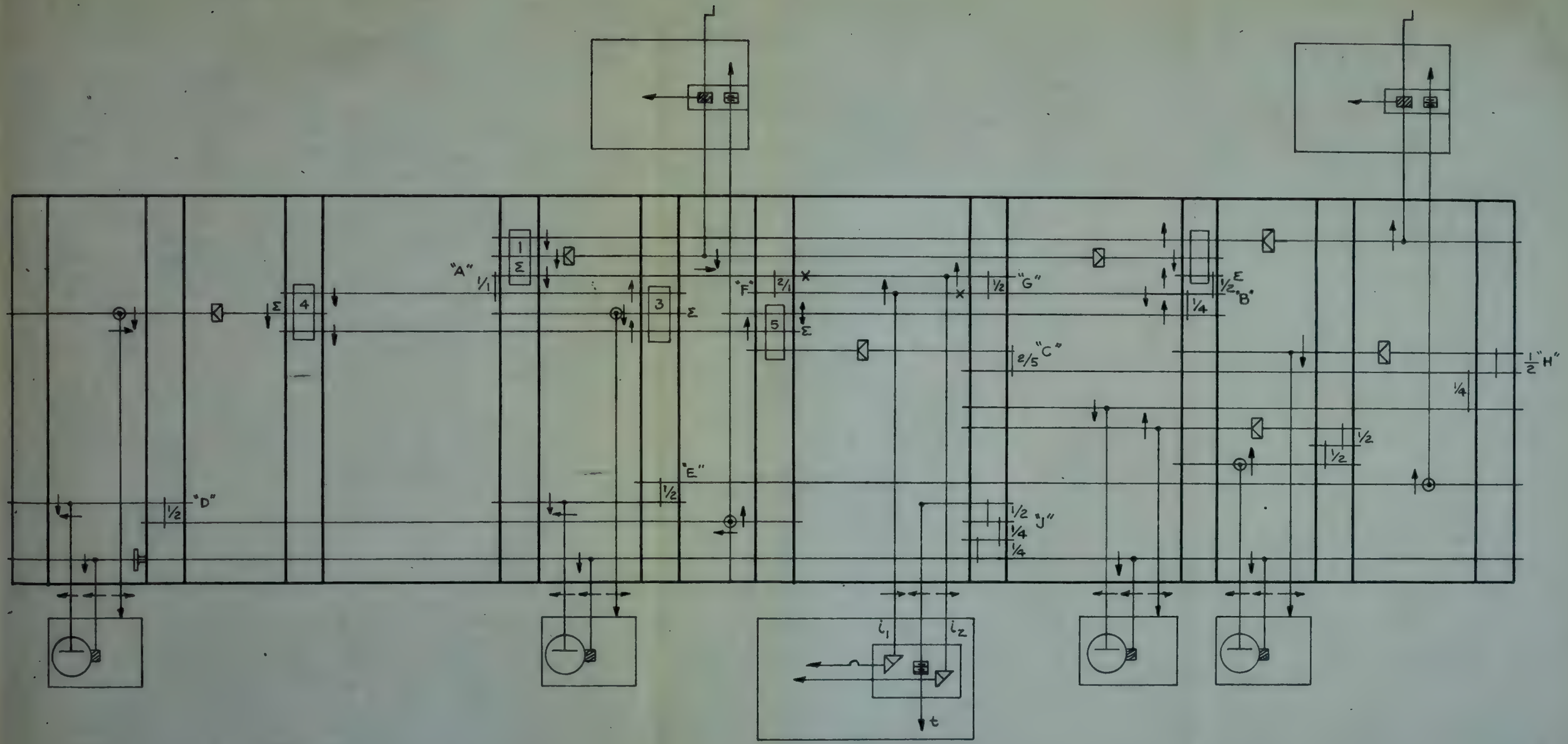

FIG. 4-4 DIFFERENTIAL ANALYZER LAYOUT FOR BASIC PROBLEM OF FIGURE 4-3.

JULY 11, 1948

Approximations, Limitations, and Difficulties

As has been stated, the effects of eddy-current and hysteresis losses have been neglected in this study. For all observations of parametric variations in the input circuit, the neglect of the losses in the core has imposed no serious limitation. The nature of the effect of eddy-current and hysteresis loss on the dynamic behavior of the amplifier when the output-circuit parameters are varied will be discussed.

The magnetic amplifier has an inherently long time-response. The nature of this long response requires that a large number of cycles of the fundamental applied voltage must occur before the final steady-state conditions are reached. When the differential analyzer is operated through a large number of cycles, the cumulative error resulting from the backlash in the many gears in the system can be of serious consequence, and may cause considerable error in the output of the machine. Furthermore, in the machine solution of the simultaneous equation-pair used in this problem, the cumulative error in the mechanical circuit which operates basically on one equation of the pair may be greatly in variance with the cumulative error which builds up in the circuit which operates primarily on the other equation. The accuracy of the solution will be seriously impaired when there is a definite unbalance in the mechanical error arising in different sections of the machine.

Approximations, Limitations, and Difficulties

As has been stated, the effects of eddy-current and hysteresis losses have been neglected in this study. For all observations of parametric variations in the input circuit, the amplitude of the losses in the core has imposed no serious limitation. The nature of the effect of eddy-current and hysteresis loss on the dynamic behavior of the amplifier when the output-circuit parameters are varied will be discussed.

The magnetic amplifier has an inherently long time-response. The nature of this long response requires that a large number of cycles of the fundamental applied voltage must occur before the final steady-state conditions are reached. When the differential analyzer is operated through a large number of cycles, the cumulative error resulting from the backlash in the many gears in the system can be of serious consequence, and may cause considerable error in the output of the machine. Furthermore, in the machine solution of the simultaneous equation-pair used in this problem, the cumulative error in the mechanical circuit which operates basically on one equation of the pair may be greatly in variance with the cumulative error which builds up in the circuit which operates primarily on the other equation. The accuracy of the solution will be seriously impaired when there is a definite unbalance in the mechanical error arising in different sections of the machine.

The mechanical differential analyzer is provided with frontlash units which are inserted judiciously in the layout in a manner designed to compensate for the errors which result from backlash over a period of many cycles of operation. A total of seven frontlash units, as shown in Figure 4-4, were employed in this problem. The adjustment of these units to compensate for the backlash errors is accomplished mainly by trial-and-error, and requires a great deal of skill which, it seems, is acquired mainly by practice. The adjustment of error compensation was perhaps the largest single difficulty encountered by the authors in their work on the differential analyzer. The initial adjustment of the machine required a great deal of time and some rather substantial rearrangement of components to minimize backlash. Each time the circuit parameters were changed with resultant changes in the scale factors and, of course, in the gears and gear-ratios in the system, it was necessary to readjust the frontlash units. The time required to readjust the compensating units seems to be an inverse function of the experience of the operators. Actually, the later adjustments were made quite readily and with a minimum loss in time. In general, however, since the machine was required to operate through many cycles, the adjustment of frontlash units was found to be very critical and extremely important in obtaining accurate, precise solutions.

Before the analytical problem was formulated, experimental work had shown that the characteristic time of the magnetic amplifier is an inverse function of the input-circuit resistance, R_1. In order to keep the number of cycles through which the machine was required to operate at a minimum, most of the analytical observations were made with a large value of the input-circuit resistance. The exception to this condition was a set of observations which were made to determine the effect of R_1 on the dynamic and steady-state operation of the analyzer for smaller values of the input resistance. It has been pointed out in Chapter III that the gain of the amplifier is inversely proportional to the input-circuit resistance. Since the value of R_1 used in the analytical study was quite large, many of the observations made on the differential analyzer were made under conditions in which the power-gain of the amplifier was less than unity. Actually, this situation imposed no limitation whatever on the worth of the observations made, and mention of this condition is made here only to justify the choice of a large value of input resistance as imposed by mechanical considerations of the differential-analyzer performance.

The nonlinear relationship between the flux in the cores and the applied magnetizing force was inserted by two input tables. The input functions, drawn to scale, are shown in Figure 4-5. This curve, of course, represents the normal magnetization curve of the core material, and

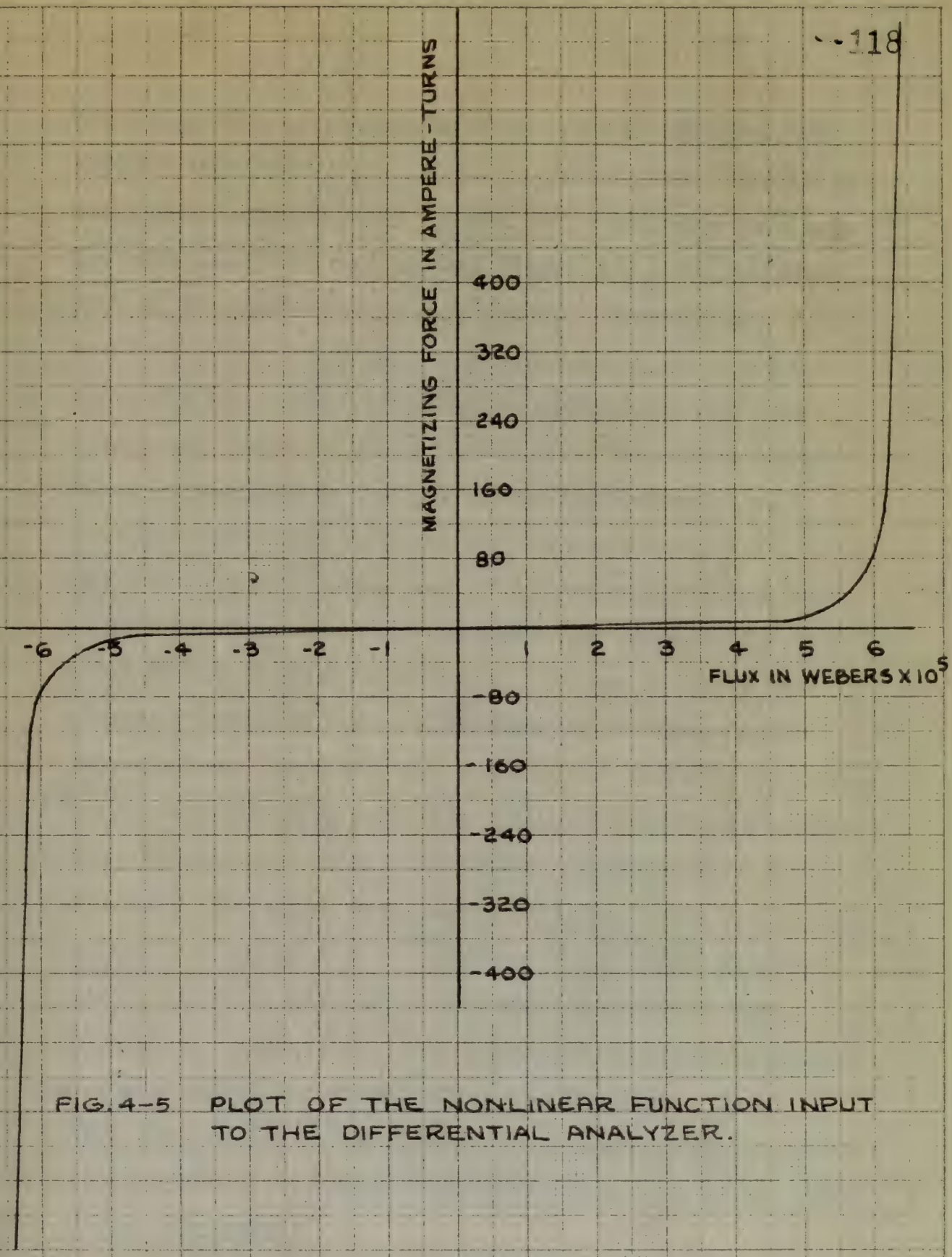

FIG. 4-5 PLOT OF THE NONLINEAR FUNCTION INPUT TO THE DIFFERENTIAL ANALYZER.

the unconventional coordinates of the plot were necessitated by the mechanical layout of the machine. Recalling that the coordinates are rotated 90°, reference to Figure 4-5 will show that the initial slope, i.e., the ratio of flux to ampere-turns, is very great. Mechanically, the abcissas of this function were inserted by the analyzer, while the ordinates were inserted manually by the operators. In practice, it was found that the errors introduced by backlash in the gears when the ordinates were manually introduced were greater than the changes in magnetizing force introduced by following the curve, and it was therefore necessary to assume an infinite initial slope of the magnetization curve in order to avoid the effect of backlash when small input magnetizing forces were applied. Consequently, the initial slope of the curve was assumed infinite (actually zero, as viewed on Figure 4-5); the initial permeability and inductance were then infinite. The slope was assumed infinite until the flux reached a value of 4×10^{-5} webers, after which the empirical curve of the normal magnetization of the core material was followed. This approximation actually imposes no great limitation on the solutions observed. It is clear from Figure 4-5 that the changes in magnetizing force are very minute over the range from the origin to the value of flux mentioned.

It has been shown in the discussions of empirical results in Chapter III that the output ampere-turns over

the normal range of the amplifier or modulation characteristic are very nearly equal to the input ampere-turns. Reference to Equation 4-16 will then indicate another rather serious limitation for the mechanical solution, namely, the measurement of the small difference:

$$N_1 i_1 - N_2 i_2$$

between two relatively large quantities. Again, the necessity for careful error compensation is implied by the nature of the equations to be solved.

It has been the purpose of this section of the report to emphasize the nature of the difficulties anticipated and encountered in solution of the analytical equations of the differential analyzer, and to describe the methods used to minimize these difficulties.

Nature of the Analytical Solutions

Conditions for the various analytical problems were formulated to closely simulate conditions existent during experimental observations. In the case of transient analytical observations, actual oscilloscopic photographs of equivalent experimental situations were made. Throughout the study, all analytical solutions were matched by a series of experimental observations in which circuit conditions were made as nearly identical as possible. The results of all analytical observations are tabulated in Charts 4-3 and 4-4.

As has been stated, the currents i_1 and i_2 which

CHART 4-3

RESULTS OF ANALYTICAL STUDIES

RUN NO.	W PRI SEC	E_2 VOLTS	R_1 OHMS	R_2 OHMS	N_1 TURNS	N_2 TURNS	i_1 SCALE IN/AMP	i_1 MEAS IN²	i_1 AVER INPUT MA	i_1 INPUT MA	$N_1 I_1$	i_2 SCALE IN/AMP	i_2 MEAS IN²	i_2 AVER OUTPUT MA	$N_2 I_2$	SCALE IN/SEC	MEAS IN	(CT) M-SEC
1	640	40	10125	977	3600	1000	180	0.17	1.47	1.11	4	6.25	0.004	1.09	1.09	128	2.58	10.1
2								0.21	1.52	1.66	6	25	0.10	6.25	6.25		1.55	9.77
3								0.24	2.08	1.95	7		0.13	8.12	8.12		1.20	9.37
4								0.26	2.26	2.20	8		0.15	9.37	9.37		1.12	8.75
5								0.29	2.51	2.50	9		0.15	9.37	9.37		1.00	7.81
6								0.35	3.04	3.05	11	2.5	0.18	11.25	11.25		0.82	6.4
7								0.15	1.30	1.11	4	50	0.16	5.63	5.63		1.90	14.9
8								0.42	3.64	3.61	13		0.46	14.4	14.4		0.75	5.85
9								0.49	4.25	4.16	15		0.51	15.9	15.9		0.70	5.47
10								0.58	5.02	4.72	17		0.58	18.1	18.1		0.60	4.69
11								0.60	5.20	5.27	19		0.62	19.4	19.4		0.68	5.31
12								0.69	5.98	5.83	21		0.65	20.3	20.3		0.52	4.06
13	640	40						0.77	6.67	6.37	23		0.79	24.7	24.7		0.48	3.75
14	2560	80						—	—	1.11	4		—	—	—	12.8	3.80	2.58
15								0.10	1.15	1.12	8		0.18	11.25	11.25	25.0	3.33	13
16								0.19	3.30	3.33	12		0.21	13.1	13.1		2.35	9.18
17								—	—	4.44	16		—	—	—		1.80	7.03
18								0.32	5.55	5.55	20		0.31	19.4	19.4		1.42	5.55
19								0.39	6.78	6.66	24		0.40	25.0	25.0		1.25	4.88
20								—	—	3.33	12		—	—	—		—	—
21		80						—	—	1.11	4		—	—	—			
22		100						0.06	1.04	1.11	4		0.07	3.13	3.13		4.25	16.62
23								0.15	2.60	2.22	8		0.15	9.37	9.37		2.85	11.11
24								0.17	2.95	3.33	12		0.23	14.28	14.28		2.10	8.20
25								0.24	4.17	4.44	16		0.24	15.0	15.0		1.60	6.25
26								0.31	5.39	5.55	20		0.32	20.0	20.0		1.40	5.47
27				97.7				0.34	5.90	6.39	23		0.38	24.0	24.0		1.25	4.88
28				977				0.05	0.87	1.11	4		0.07	3.13	3.13		4.25	16.55
29								0.13	2.25	2.22	8		0.14	8.80	8.80		2.25	10.00
30								0.19	3.30	3.33	12		0.18	11.3	11.25		2.03	8.16
31								0.24	4.18	4.44	16		0.25	15.9	15.9		1.55	6.25
32								0.29	5.03	5.55	20		0.30	18.8	18.8		1.40	5.47
33				977				0.37	6.43	6.39	23		0.38	24.0	24.0		1.25	4.88
34				1954				0.05	0.87	1.11	4		0.07	3.13	3.13		4.25	16.55
35								0.12	2.08	2.22	8		0.14	8.80	8.80		2.25	10.00
36								0.19	3.30	3.33	12		0.20	12.50	12.50		2.00	7.80
37								0.25	4.34	4.44	16		0.26	16.25	16.25		1.55	6.05
38								0.32	5.40	5.55	20		0.32	20.0	20.0		1.40	5.47
39				1954				0.34	5.90	6.39	23		0.38	24.0	24.0		1.25	4.88
40				489				0.05	0.87	1.11	4		0.05	3.13	3.13		4.25	16.55
41								0.13	2.25	2.22	8		0.11	6.87	6.87		2.40	9.4
42								0.18	3.13	3.33	12		0.18	11.20	11.20		1.70	6.60
43								0.24	4.16	4.44	16		0.265	16.5	16.5		1.55	6.05
44								0.32	5.53	5.55	20		0.31	19.4	19.4		1.41	5.55
45						1000		0.35	6.09	6.39	23		0.375	23.50	23.50		1.34	5.20
46						2000		0.04	0.69	0.55	2		0.015	0.94	0.94		10.4	40.6
47								0.07	1.22	1.11	4		0.03	1.88	1.88		6.4	25.0
48								0.11	1.91	1.66	6		0.05	3.13	3.13		4.2	16.4
49								0.15	2.60	2.22	8		0.078	4.87	4.87		2.7	14.5
50								0.18	3.13	2.78	10		0.08	5.00	5.00		2.7	10.6
51						2000		0.21	3.65	3.19	11.5		0.08	5.00	5.00		2.55	10.0
52						500		0.15	2.60	2.22	8		0.27	16.9	16.9		1.30	5.08
53								0.26	4.51	4.44	16		0.47	29.4	29.4		1.00	3.91
54								0.105	1.80	1.11	4		0.145	9.06	9.06		1.20	1.43
55								0.185	3.21	3.33	12		0.38	24.4	24.4		1.15	4.49
56					3600	500		0.306	5.30	5.55	20		0.59	36.8	36.8		0.85	3.32
57					1800	1000		0.02	0.35	0.56	1		0.015	0.94	0.94		4.00	15.0
58								0.05	0.87	1.11	2		0.045	2.81	2.81		2.30	9.00
59								0.10	1.73	1.66	3		0.055	3.44	3.44		1.55	6.05
60	2560	100	10125	489	1800	1000	180	0.15	2.60	2.22	4	50	0.065	4.1	4.1	25.0	1.25	4.88

CHART 4-4

RESULTS OF ANALYTICAL STUDIES

RUN NO.	ω RAD/SEC	E_2 VOLTS	R_1 OHMS	R_2 OHMS	N_1 TURNS	N_2 TURNS	SCALE IN AMP	MEAS I_1^2	AVER INPUT MA	INPUT MA	$N_1 I_1$	SCALE IN AMP	MEAS I_2^2	AVER OUTPUT MA	$N_2 I_2$	SCALE IN VOLTS	MEAS E_2	(CT) M SEC
61	2560	100	10125	489	1800	1000	180	0.18	3.13	2.77	5	50	0.03	5.65	5.65	256	1.05	4.1
62					1800		180	0.20	3.47	3.19	5.75		[illegible]	7.50	7.50		3.90	3.51
63					2543		159	0.04	0.79	0.79	~		[illegible]	1.88	1.88		4.8	12.8
64								0.10	1.95	1.57	4		[illegible]	3.44	3.44		2.6	9.76
65								[illegible]	2.45	2.36	6		[illegible]	5.20	5.20		1.8	7.03
66								[illegible]	3.15	3.12	8		[illegible]	8.2	8.2		1.4	5.47
67			10125		2543		159	[illegible]	4.03	3.95	10		0.17	10.6	10.6		1.15	4.49
68			5063		3600		150	0.105	1.52	2.22	8		0.12	7.50	7.50		5.25	20.5
69								[illegible]	4.34	4.44	10		0.26	16.3	16.3		3.2	12.5
70								0.38	6.59	6.66	24		0.38	23.8	23.8		2.3	8.98
71								0.505	8.76	8.88	32		0.525	32.8	32.8		1.9	7.43
72								[illegible]	[illegible]	[illegible]	20		[illegible]	[illegible]	[illegible]		2.7	10.6
73			5063					0.155	2.69	3.33	12		[illegible]	11.5	11.5		1.38	15.3
74			2531					0.195	3.88	4.44	10		[illegible]	14.0	14.0		5.8	24.9
75								0.375	6.50	6.66	24		[illegible]	24.3	24.3		4.5	17.0
76								0.505	8.16	8.88	32		0.53	33.1	33.1		3.55	13.1
77			2531					0.09	1.39	2.22	8		0.12	7.50	7.50		10.0	41.0
78			1265					0.975	5.25	8.88	32		0.44	27.5	27.5		3.07	14.52
79								0.315	5.50	6.66	24		[illegible]	22.2	22.2		4.9	34.7
80								0.23	4.00	4.44	16		0.240	15.0	15.0		12.75	47.0
81			1265					0.08	1.39	2.22	8		0.111	6.70	6.70		10.10	37.60
82			10125					—	—	—			—	—	—		1.35	5.26
83								—	—				—	—	—		—	—
84		100						—	—				—		—		—	—
85		150						0.12	2.08	1.50	6		0.155	3.70	3.70		2.55	10.0
86								0.23	4.00	3.32	12		0.22	13.75	13.75		1.63	6.25
87		150						0.325	3.50	5.00	18		0.30	20.8	20.8		1.15	4.41
88		300						0.465	7.90	6.66	24	50	0.42	26.2	26.2		3.84	7.28
89								0	0	0	0	12.5	0.065	16.25	16.25		—	
90								0.05	0.87	0.53	4		0.07	17.5	17.5		[illegible]	0.137
91	2560	300						0.11	1.91	1.66	6		0.105	[illegible]	[illegible]		0.20	0.78
92	5120	200						0.18	3.22	3.32	12	12.5	0.13	32.5	32.5	256	0.20	0.75
93								0.255	4.42	4.44	16	50	0.26	16.2	16.2	512	3.15	6.03
94								0.365	6.69	6.66	24		0.38	23.8	[illegible]		2.38	4.65
95	5120	200	10125	489	3600	1000	180	0.125	2.17	2.22	8		0.12	7.5	7.5		[illegible]	3.80
								—	—	8.88	16	50	—	—	—	512	1.80	3.51

flow in the input and output circuits of the amplifier respectively, were plotted as outputs of the differential analyzer. The magnitudes of these currents were obtained by integrating the area under the curves by use of a planimeter, and then computing the values of the currents by application of the proper scale factors. Actually, the average value of the second-harmonic alternating current in the input circuit, i_1, is equal to the value of current applied to the circuit when the step voltage is connected to the input-circuit terminals. Stated in a different manner: the average value of i_1 is equal to I_1, which is equal to the magnitude of the step voltage divided by the total input-circuit resistance. The comparison of values obtained by planimetric integration and values obtained by division are shown in Charts 4-3 and 4-4. As will be noticed, agreement is quite good.

Figure 4-6 is a tracing of an actual solution plotted by the differential analyzer after steady-state conditions were reached. The nature of the odd-harmonic composition of the output-circuit current, i_2, is apparent in this figure. Similarly, the even-harmonic composition of the input-circuit current, i_1, is shown by the nature of the tracing. For comparison with the curves of Figure 4-6, actual photographs of the face of a cathode-ray oscillograph are shown in Figures 4-7 and 4-8. It should be emphasized that the photographs of Figure 4-7 are not shown to scale.

flow in the input and output circuits of the amplifier respectively, were plotted as outputs of the differential analyzer. The magnitudes of these currents were obtained by integrating the area under the curves by use of a planimeter, and then computing the values of the currents by application of the proper scale factors. Actually, the average value of the second-harmonic alternating current in the input circuit, i_1, is equal to the value of current applied to the circuit when the step voltage is connected to the input-circuit terminals. Stated in a different manner: the average value of i_1 is equal to I_1, which is equal to the magnitude of the step voltage divided by the total input-circuit resistance. The comparison of values obtained by planimetric integration and values obtained by division are shown in Charts 4-3 and 4-4. As will be noticed, agreement is quite good.

Figure 4-6 is a tracing of an actual solution plotted by the differential analyzer after steady-state conditions were reached. The nature of the non-harmonic composition of the output-circuit current, i_2, is apparent in this figure. Similarly, the even-harmonic composition of the input-circuit current, i_1, is shown by the nature of the tracing. For comparison with the curves of Figure 4-6, actual photographs of the face of a cathode-ray oscillograph are shown in Figures 4-7 and 4-8. It should be emphasized that the photographs of Figure 4-7 are not shown to scale.

OUTPUT CIRCUIT CURRENT i_2

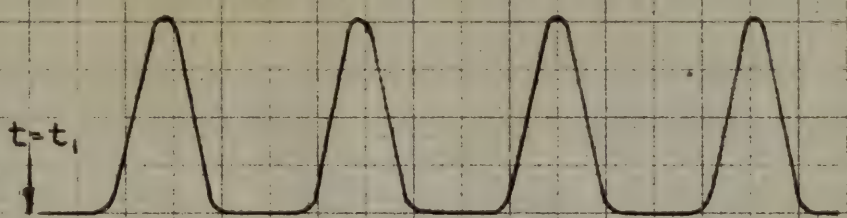

INPUT CIRCUIT CURRENT i_1

FIG. 4-6 FORM OF THE PLOTTED SOLUTIONS OF THE DIFFERENTIAL ANALYZER PROBLEM. (NOTICE THAT THE DISSYMETRY OF THE EXPERIMENTAL CURRENTS IS ABSENT BECAUSE LOSSES ARE NEGLECTED IN THE ANALYTICAL SOLUTION.)

Figure 4-7(a) shows the flow of current in the output circuit when the input current is zero. The square wave obtained is due almost wholly to the effects of hysteresis which have been neglected in the analyzer solution. The frequency of the square wave is that of the applied alternating flux. As the input current increases to a small value, small peaks appear on the output-current waveform when the flux excursions begin to extend into the knee of the magnetization curve. This effect is shown on Figure 4-7(b). A further slight increase in input current yields the waveform of Figure 4-7(c). When the input current is increased to a larger value and flux excursions extend well into the knee, as shown in Figure 4-7(d), the hysteresis current becomes a relatively small portion of the total waveform, and the overall effect is merely to cause a slight difference in the levels of the shoulders of the output waveform. Figure 4-7(d) is analogous to the differential analyzer output-wave shown in Figure 4-6. The dissymmetry of the levels of the shoulders does not, of course, appear in the analytical solution because hysteresis was neglected. If the input current is made sufficiently great, the flux excursion in one core of the amplifier may extend above the knee of the magnetization curve at the same time the flux excursion in the other core is also on the knee. Under these conditions, the output waveform is

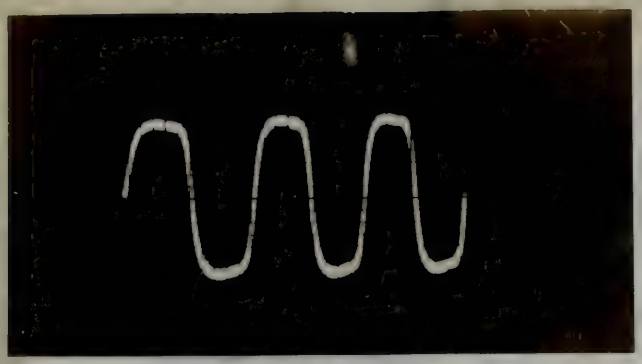

(a)

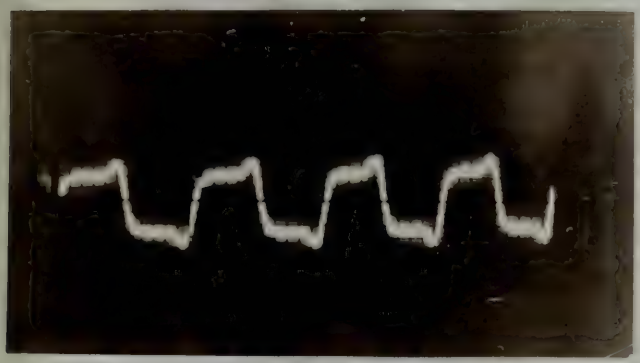

(b)

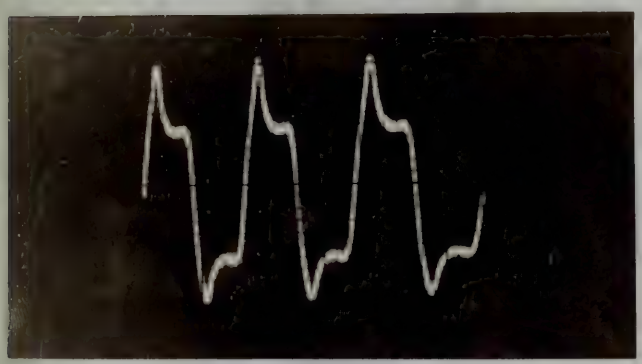

(c)

(d)

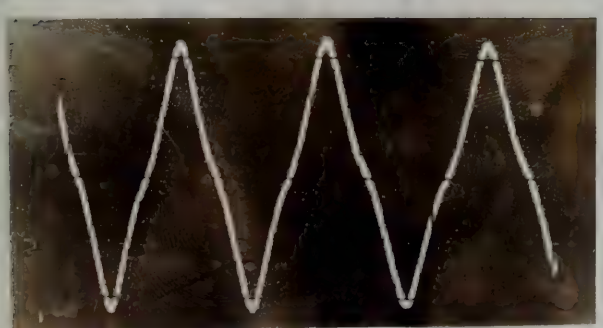

(e)

FIGURE 4-7

OSCILLOSCOPIC PHOTOGRAPHS WHICH SHOW THE INCREASE IN THE STEADY-STATE VALUE OF THE OUTPUT CURRENT, i_2, FOR INCREASING VALUES OF THE INPUT CURRENT, i_1.

f = 100 cps.
N_1 = 3600 T.
N_2 = 1000 T.
R_1 = 10125 ohms.
R_2 = 100 ohms.
e_2 = 40 sin wt.

KEY TO FIGURES

(a) i_1 = 0.
i_2 = 1.8 ma. (Hysteresis only)

(b) i_1 = 0.1 ma.
i_2 = 1.85 ma.

(c) i_1 = 0.3 ma.
i_2 = 1.90 ma.

(d) i_1 = 2.5 ma.
i_2 = 5.4 ma.

(e) i_1 = 10.0 ma.
i_2 = 12.5 ma.

The Photographs are not Shown to Scale

(a)

(b)

(c)

(d)

(e)

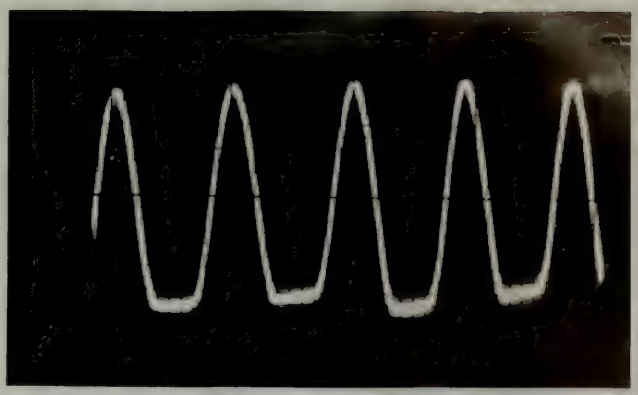

(a)

INPUT CURRENT, i_1 = 5.0 ma.

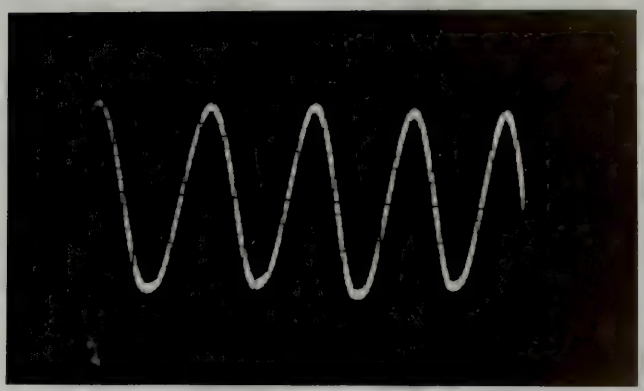

(b)

INPUT CURRENT, i_1 = 10.0 ma.

FIGURE 4-8

OSCILLOSCOPIC PHOTOGRAPHS SHOWING THE INPUT-CIRCUIT CURRENT, i_1, AT THE SECOND-HARMONIC FREQUENCY OF THE APPLIED ALTERNATING VOLTAGE.

(a)

(b)

shaped as shown in Figure 4-7(e). The shoulder has virtually disappeared, because there is no period in the cycle when current ceases to flow because the fluxes in each core are simultaneously passing over the knee of the magnetization curve.

The path of the flux and magnetizing force in an iron core is, of course, affected by the presence of the hysteresis loop. Since the number of loops formed by hysteresis is infinite, it is difficult to determine the proper value of the loop path to follow when the value of the flux versus magnetizing-force function is applied manually as an input to the differential analyzer. It was considered, however, very important to observe, if possible, the effects of hysteresis on the analytical waveform, and consequently, the particular member of the hysteresis loop family shown for 4750 Alloy in Figure 2-7 was utilized as an input to the differential analyzer for several solutions. The observed effect was, of course, qualitative, since it has been pointed out that an infinite number of loops will actually exist, but it is extremely significant to note that output-current curves exactly similar to the experimental waveforms of Figure 4-7 were obtained through the simulated hysteresis method. It may then be stated that much of the current which flows in the output circuit when the input-circuit current is zero is due to hysteresis. Furthermore, the difference in levels of the shoulders of

of the output waveforms is definitely attributable to hysteresis effect, and not to unbalance in the cores, as was previously thought. It is questionable whether these statements could have been made without the aid of the differential analyzer observations.

Figure 4-6(b) shows a tracing of an analytical solution of the second-harmonic input-circuit current, i_1. Similar oscilloscope photographs are shown in Figure 4-8. It is worth noticing that just as the shoulders disappear from the output current waveform when the input current becomes large, so do the flat portions disappear from the lower portions of the input-circuit current waveform when the input circuit current becomes greater. This effect may be seen by comparing Figure 4-8(a), which was made for the conditions which prevailed for the analytical solution shown in Figure 4-6(b), with the waveform of Figure 4-8(b), which was made for a somewhat larger input current. The disappearance of these flat portions is attributed to the same reason given for disappearance of the shoulders of the output-circuit waveform, namely: there is no time in the cycle during which the flux excursions in the two cores are simultaneously on the linear portion of the magnetization curve.

A tracing of the buildup of output-circuit current, i_2, as produced by a solution of the differential analyzer, is shown in Figure 4-9(a). The nature of the

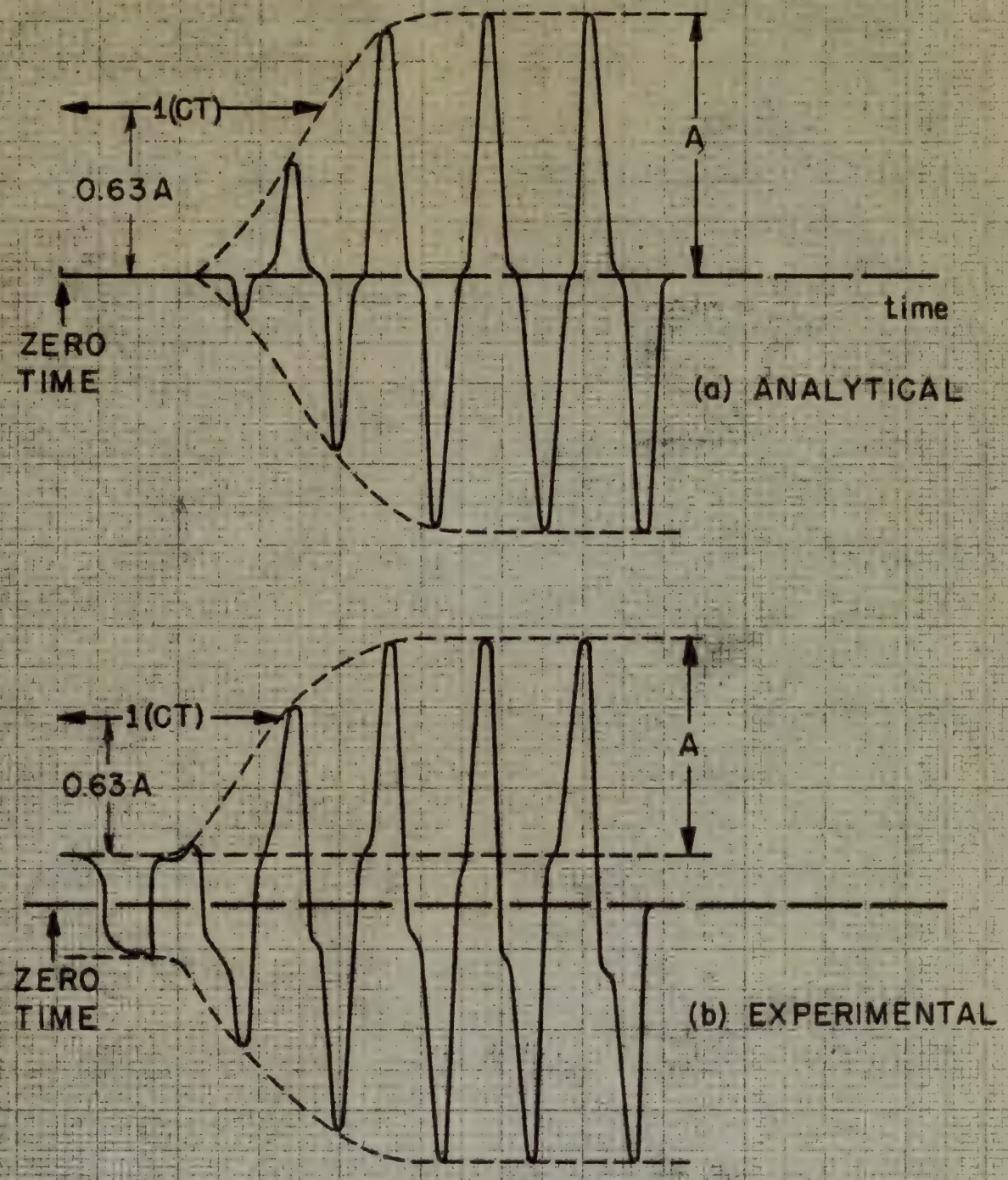

FIG. 4-9
COMPARISON OF THE BUILDUP OF OUTPUT CIRCUIT CURRENT, i, FOR ANALYTICAL AND EXPERIMENTAL OBSERVATIONS.

defined characteristic time has been discussed previously, and is shown pictorially on this figure. Figure 4-9(b) is a drawing made from an oscilloscopic photograph of the output current of the amplifier when the conditions of operation were identical to those shown on the analytical solution. The effect of hysteresis is apparent in the practical case, and the definition of characteristic time for the practical case is apparent from the drawing. It is clear from Figure 4-9(a) that initially, since infinite permeability was assumed, and since hysteresis was neglected, there is no flow of current. A waveform identical to the analytical waveform of Figure 4-9(a) can be simulated experimentally if the input current is made very large; this results in such a large output current that the hysteresis current is negligible by comparison, and the flat line shown initially in Figure 4-9(a) for an analytical solution can be very neatly shown on the oscilloscope for an experimental situation.

The Concept of Buildup of Flux Bias.

There is a certain intangible benefit that may be obtained from working with the mechanical differential analyzer that is difficult to describe. The effect is related somewhat to an intuitive feeling that is acquired while actually observing mechanical parts operate on the differential equations, and this intuitive feeling is of value in understanding the actual behavior of the physical circuit which is represented by the motion of mechanical

parts. This "intangible" benefit, so-called, does not appear in the tabulated solutions of the analyzer problem, and seems to depend principally on actually observing the behavior of the various integrators, differentials, gears, and input tables, as the problem is carried through. It was this type of observation which led to an appreciation of the theoretical behavior of the magnetic amplifier under transient conditions.

Since initial permeability was assumed to be infinite and hysteresis was neglected, no current flows in the input circuit immediately after the application of the step voltage to the input terminals, unless the initial flux applied to the cores is sufficiently great to cause excursions above the break of the knee of the magnetization curve. Under these conditions of zero initial current flow in the input circuit, there is, of course, no current flow in the output circuit. When the step voltage is applied, the flux in each core begins to be biased outward toward the region of the knee. Once the flux excursion extends into the knee, current begins to flow in both the input and output circuits; these currents contribute nonlinearly to the further buildup of flux, in accordance with Equations 4-15 and 4-16, and it becomes difficult to reason the behavior from physical concepts after current flow starts, because of the nonlinear nature of the equations. During the interval of time, however, before the flux excursions extend

into the knee, the theoretical system, since infinite initial permeability was assumed, behaves as a linear system and linear concepts are applicable. This fact was first recognized while actually observing the behavior of the differential analyzer, and probably would not have been recognized from experimental observations alone. In many cases of magnetic-amplifier operation, the original buildup of flux consumes a large portion of the total characteristic time, and, therefore, is of importance when considerations of the transient behavior of the theoretical amplifier are made. The time of flux-bias buildup, t, is defined as the time after the application of the voltage step-function to the input terminals until current begins to flow in the output and input circuits.

The development of the equation which defines flux buildup in the theoretical case follows. It is first necessary to define certain quantities, and in each case the defined quantities refer to only a single core of the magnetic amplifier core-pair. It is possible to deal with a single core because the rise in d-c flux is identical in each core of an amplifier, although the directions of rise are opposite in phase. Let

ϕ_{dc} = applied direct flux as supplied by the input circuit.

ϕ_s = the value of flux at which permeability becomes finite, i.e., the value of flux required to cause flow of currents. Designated as saturation flux.

ϕ_p = the peak value of the applied alternating flux as supplied by the output circuit.

N_1, E_1, N_2, $\hat{E}_2$ - Defined as previously.

Since permeability was initially assumed to be infinite in the theoretical case, there is, as has been pointed out, no initial flow of current in the output circuit. Consequently, the total alternating voltage applied to the output circuit appears across the reactor system, and half of this voltage appears across a single reactor. Similarly, no current flows initially in the input circuit, and half of the total applied stop voltage appears across the control coils of a single reactor. In order to establish the time of bias building, the applied flux, ϕ_{dc}, must equal the difference between the value of flux required for flow of current and the peak magnitude of the applied alternating flux. This is the flux required to bias the alternating flux to a position sufficiently high that peak excursions extend into the nonlinear region of the magnetization curve during some portion of the cycle. Therefore

$$\phi_{dc} = \phi_s - \phi_p \qquad (4-21)$$

By the law of induction

$$\phi = -\frac{1}{N}\int e\,dt \qquad (4-22)$$

Thus, from Equations 4-19 and 4-22

$$\phi_{dc} = \frac{E_1}{2N_1}\,t \qquad (4-23)$$

and similarly, from Equations 4-22 and 4-20 (which assume a sinusoidal flux in the output circuit):

ϕ_a = the peak value of the applied alternating flux as supplied by the output circuit.

ϕ_1, ϕ_2, $\hat{\phi}_1$, $\hat{\phi}_2$ - Defined as previously.

Since permeability was initially assumed to be infinite in the theoretical case, there is, as has been pointed out, no initial flow of current in the output circuit. Consequently, the total alternating voltage applied to the output circuit appears across the reactor system, and half of this voltage appears across a single reactor. Similarly, no current flows initially in the input circuit, and half of the total applied amp voltage appears across the control coils of a single reactor. In order to establish the time of bias building, the applied flux, ϕ_{dc}, must equal the difference between the value of flux required for flow of current and the peak magnitude of the applied alternating flux. This is the flux required to bias the alternating flux to a position sufficiently high that peak excursions extend into the nonlinear region of the magnetization curve during some portion of the cycle. Therefore

$$\phi_{dc} = \phi_a - \phi_p \qquad (4\text{-}21)$$

By the law of induction

$$\phi = -\frac{1}{2}\int e\,dt \qquad (4\text{-}22)$$

Thus, from Equations 4-10 and 4-20

$$\phi_{dc} = \frac{2I}{\pi N_1} \qquad (4\text{-}23)$$

and similarly, from Equations 4-24 and 4-20 [illegible] a sinusoidal flux in the output circuit:

$$\phi_p = \frac{\hat{E}_2}{2\omega N_2} \qquad (4-24)$$

In each case the factor of 2 appearing in the denominator is made necessary because only one coil of the pair is under consideration. By combining Equations 4-21, 4-23 and 4-24, the following expression is written:

$$\phi_{dc} = \phi_s - \phi_p = \frac{E_1}{2N_1} t = \phi_s - \frac{\hat{E}_2}{2\omega N_2} \qquad (4-25)$$

or

$$t = \frac{N_1}{2E_1}\left[\phi_s - \frac{\hat{E}_2}{2\omega N_2}\right] \qquad (4-26)$$

Equation 4-26 has been checked analytically for all of the differential analyzer solutions and agreement has been found to be excellent. ϕ_s is found empirically from the measured magnetization curve, and in this problem, in accordance with Figure 4-5, ϕ_s was found to equal 4×10^{-5} webers. The value of Equation 4-26 will become more apparent later in this chapter.

The Analytical Steady-State Behavior of the Magnetic Amplifier

The experimental behavior of the magnetic amplifier has been examined quite thoroughly in Chapter III. The remainder of Chapter IV will be devoted to (1) presentation of analytical results, and (2) correlation of the experimental results with the analytical results which were obtained through use of the differential analyzer.

Throughout this report, all considerations of the steady-state characteristics of the magnetic amplifier

$$\phi_s = \frac{\hat{E}_c}{2\omega B_s} \qquad (4\text{-}24)$$

In each case the factor of 2 appearing in the denominator is made necessary because only one coil of the pair is under consideration. By combining Equations 4-21, 4-23 and 4-24, the following expression is written:

$$\phi_{dc} = \phi_s - \phi_s = \frac{E_1}{2B_1} t = \phi_s - \frac{\hat{E}_c}{4\omega B_s} \qquad (4\text{-}25)$$

or

$$t = \frac{E_1}{2B_1}\left[\phi_s - \frac{\hat{E}_c}{4\omega B_s}\right] \qquad (4\text{-}26)$$

Equation 4-25 has been observed analytically for all of the differential analyzer solutions and agreement has been found to be excellent. ϕ_s is found empirically from the measured magnetization curve, and in this section, in accordance with Figure 4-9, ϕ_s was found to equal 4×10^{-5} webers. The value of Equation 4-26 will become more apparent later in this chapter.

<u>The Analytical Steady-State Behavior of the Magnetic Amplifier</u>

The experimental behavior of the magnetic amplifier has been examined quite thoroughly in Chapter III. The remainder of Chapter IV will be devoted to (1) presentation of analytical results, and (2) correlation of the experimental results with the analytical results which were obtained through use of the differential analyzer.

Throughout this report, all considerations of the steady-state characteristics of the magnetic amplifier

have been based upon consideration of the modulation characteristic of the magnetic amplifier. This approach has been continued in the analytical studies.

In Figure 4-10, modulation characteristics for experimental and analytical observations are plotted. The circuit parameters for these observations were identical for each case. It will be noticed from Figure 4-10 that the modulation characteristic observed experimentally lies above the analytical characteristic by a constant value of approximately 2 ampere-turns. The fact that the average value of the output ampere-turns is larger by a constant factor in the experimental case is directly attributed to two factors: (1) the fact that infinite initial-permeability was assumed in the theoretical case while in the practical case the initial permeability is not infinite and some current will surely flow in the output circuit, and (2) the more important fact that hysteresis and eddy-current losses were neglected in the theoretical case while in the practical case it has been pointed out that the initial hysteresis current is of a definitely measurable magnitude. Since measured magnetization characteristics for the cores employed have indicated that the initial permeability, while certainly not approaching infinity, is very great, the assumption of infinite initial permeability in the analytical case is construed to be of less importance than the neglect of hysteresis in the analyzer problem, and, therefore, the major part of

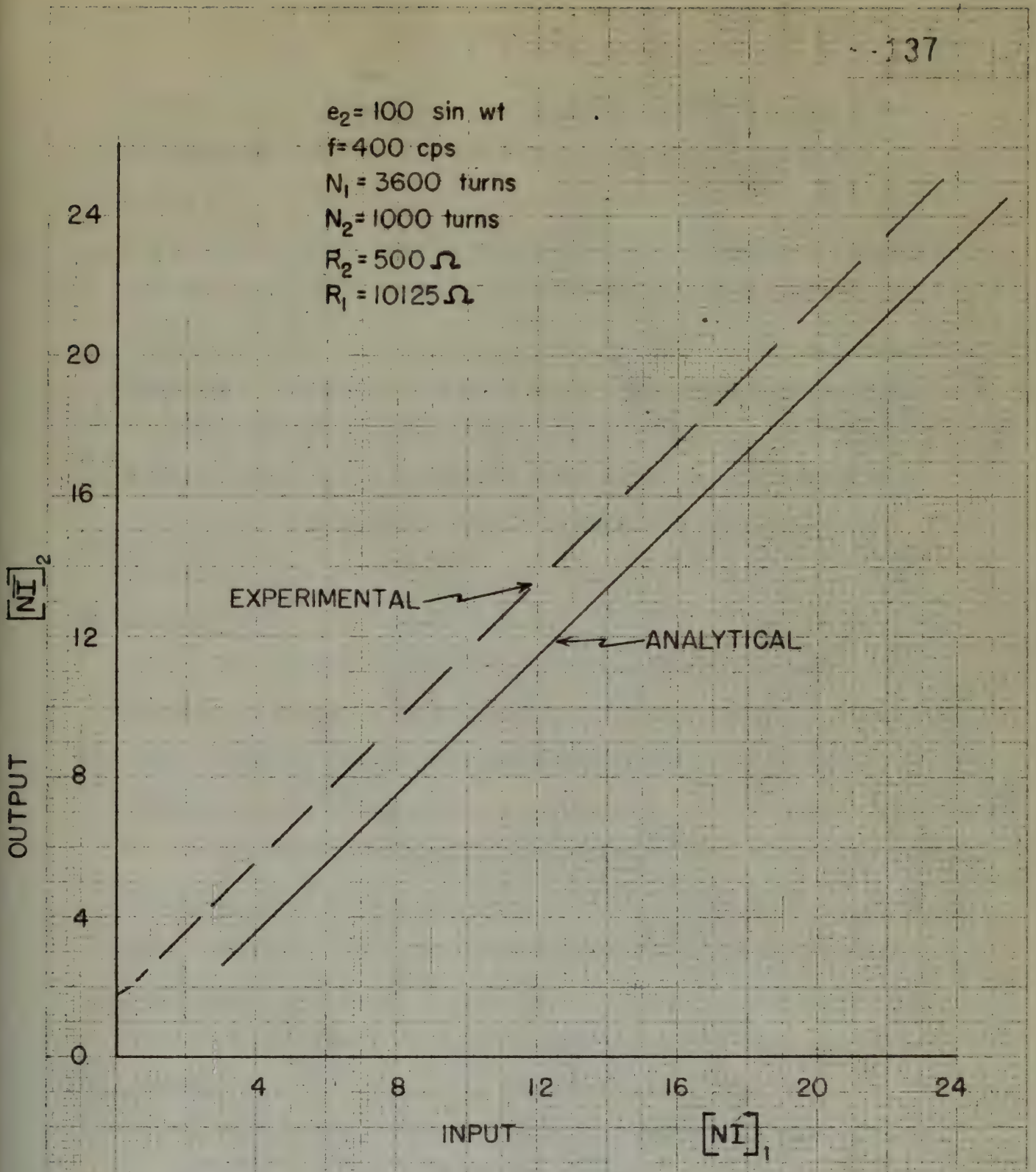

FIG. 4-10 COMPARISION OF ANALYTICAL AND EXPERIMENTAL MODULATION CHARACTERISTICS AT 400 CPS

the variation between observed and analytical cases is assigned to hysteresis effects. As is shown in Figure 4-10, the neglect of hysteresis has not had a marked derogatory effect on the analytical steady-state solution and the error introduced is constant and does not affect the usefulness of the theoretical observations. In further discussions of the effects of the various parameters on the analytical modulation characteristics, the observed variations from experimental conditions which result from neglect of losses are exactly similar to the variation shown in Figure 4-10. It may be stated that the neglect of losses and the assumption of infinite initial permeability in the analytical solutions have not materially affected the value of the data obtained from these solutions, insofar as the steady-state modulation characteristics are concerned.

The discussion of the steady-state and transient response of the analytical amplifier is best divided into discussions of the input-circuit parameters and of the output-circuit parameters. The modulation characteristics obtained analytically will be discussed in these two categories.

(a) The Effects of Input Circuit Parameters on the Modulation Characteristic --- The reader will recall that all output currents were measured with a planimeter and thence calculated by the application of scale factors. Since the planimeter is not a precise instrument, it is conceivable

ratios are concerned.

The discussion of the steady-state and transient response of the analytical monitor is best carried into effective control-circuit parameters. The monitoring electrocardiograph will be discussed in Part III-C-4-a-(3) The effects of finite input-impedance on the amplifier.

tion Characteristic --- The reader will recall that all actual circuits have associated with a finite non-zero impedance, as is shown in Figure C-10, the output of physiologic transducers is usually considered either as the ideal steady-state solution and the stock instrument is considered not affect the physiological operations. In practice the distortion of the signals by the various instruments on the analytical monitoring characteristics, the observed variations from ordinary amplifiers arise largely from changes in figure C-10. It may be stated that the output depends at least one steady signal in the monitoring circuit. Input impedance of physiologic transducers may be considered to vibrate as is shown in Figure C-10, the output of physiologic transducers may be considered either as the analytical

that errors may be present in some measurements which may cause inconsistencies in the results. In general, these inconsistencies have been relatively unimportant.

The measured analytical modulation-characteristic showing the effect of the input-circuit resistance, R_1, is shown on Figure 4-11. It will be noticed on this figure that the effect of R_1 on the analytical modulation characteristic is virtually negligible, as would be expected from the form of the equations, because it is the input-circuit current, which determines the magnitude of the current flowing in the output circuit. In the analytical studies, the magnitude of the input step-voltage was adjusted as R_1 was varied, such that the input current was maintained at an equivalent level for the various observations of the effects of different values of R_1. It may be concluded, therefore, that in accordance with both analytical and experimental observations, the input circuit resistance does not materially affect the shape of the modulation characteristic as long as the input current is maintained unaffected by changes in this resistance. If the input current is to be unaffected by changes in R_1, changes in the magnitude of the input step-voltage are implied.

The effect of the number of turns on the input coils of the amplifier is shown by the modulation characteristics of Figure 4-12. The bending and cross-over of the characteristic at 1000 turns is attributed to inaccuracy of

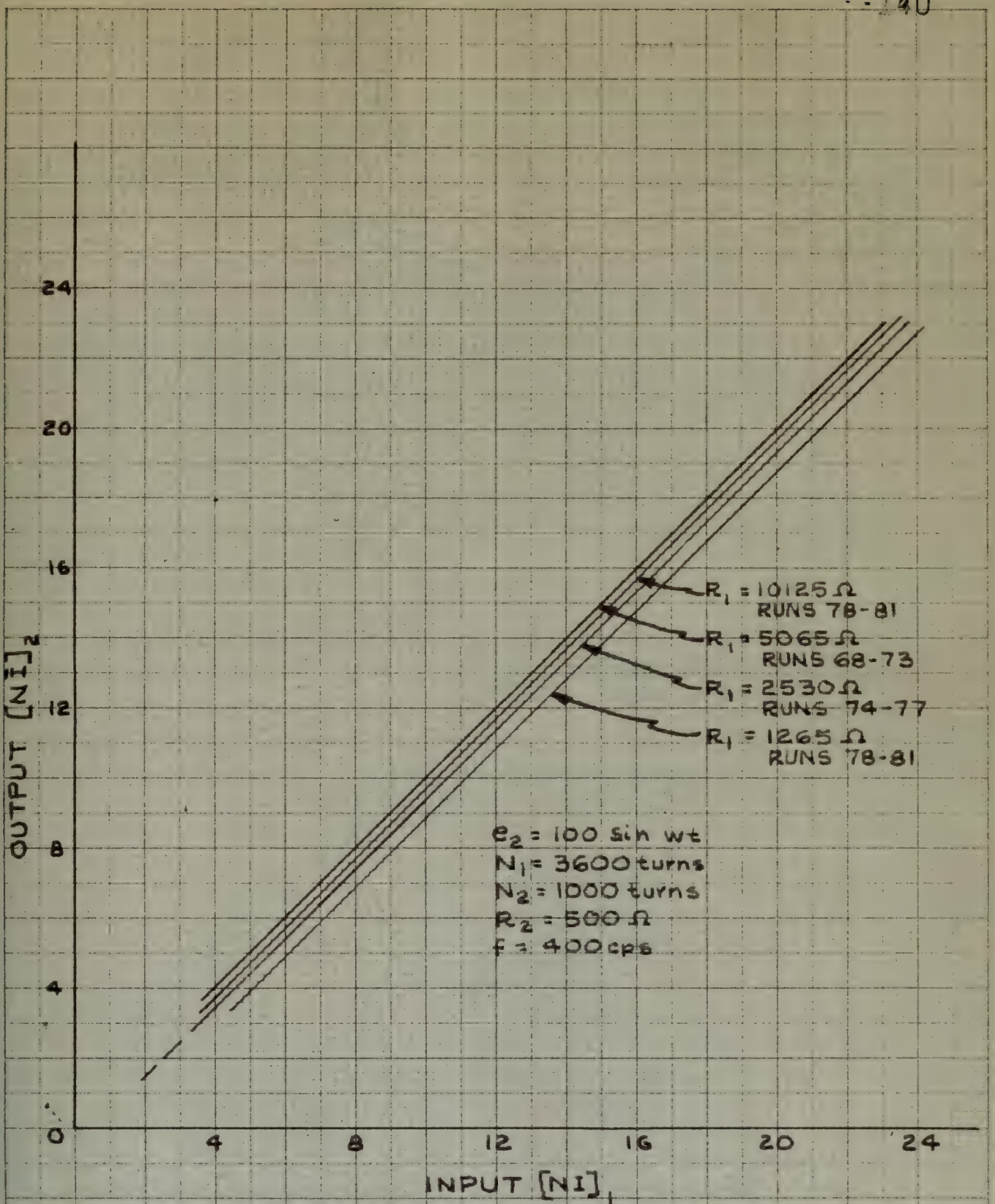

FIG. 4-11 ANALYTICAL OBSERVED EFFECT OF INPUT RESISTANCE, R_1, ON STEADY-STATE OPERATION.

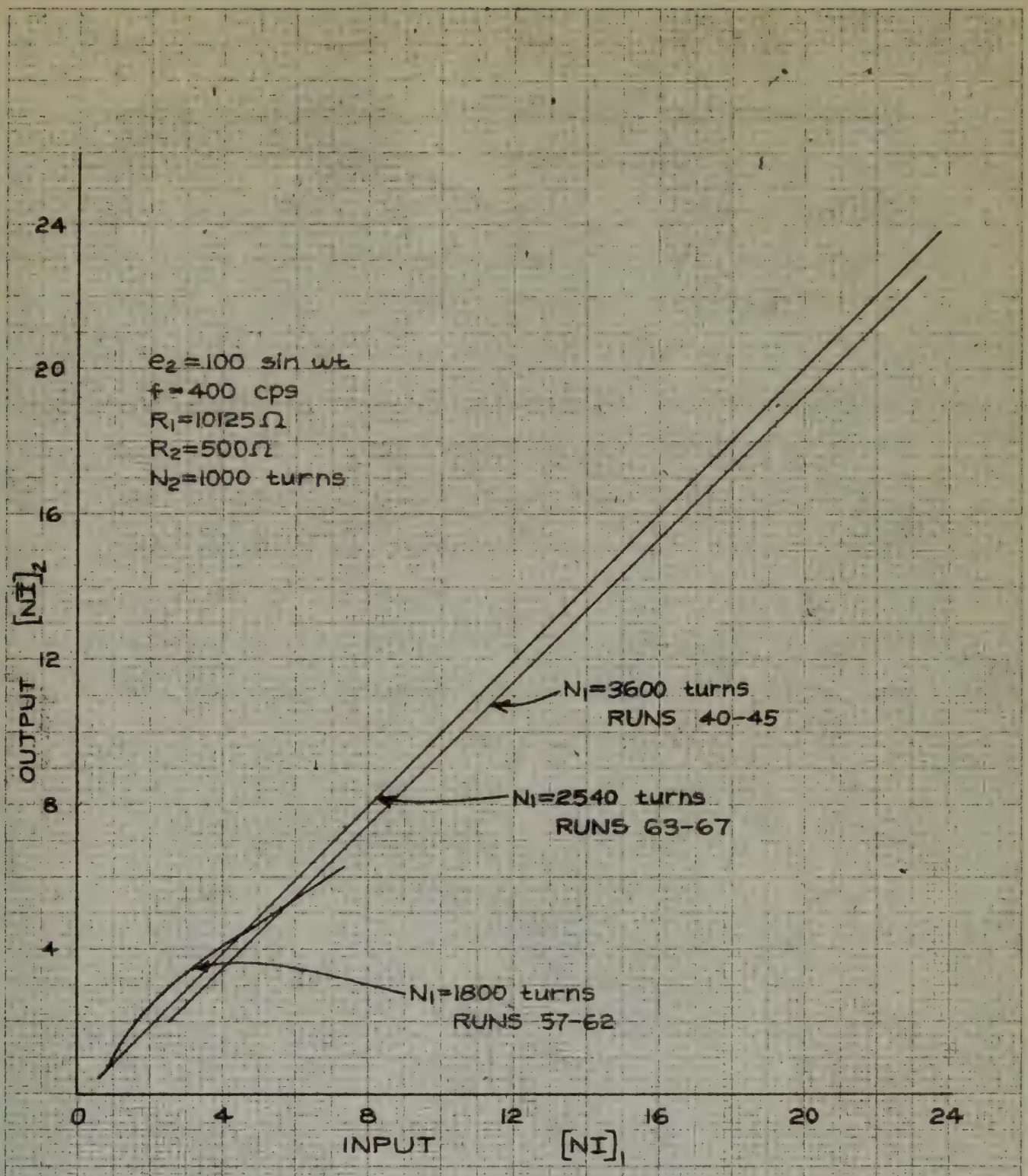

FIG. 4-12 ANALYTICAL OBSERVED EFFECT OF INPUT CIRCUIT TURNS, N_1, ON STEADY STATE OPERATION

of measurement with the planimeter at the lower values of input current. Actually, this characteristic would be expected to be similar to those shown at 2540 turns and at 3600 turns. The modulation characteristics are plotted in ampere-turns and, therefore, the characteristics for the lower values of N_1 actually require larger values of input currents to produce the same amount of ampere-turns in the output circuit. It is therefore apparent that the input power required to produce a given ampere-turn output is greater when the input turns are decreased because larger input-currents are required. The analytical effect of the input turns on the modulation characteristic, as expressed in ampere-turns, is virtually negligible, and this observation is in agreement with experimental investigations.

(b) The Effects of the Output Circuit Parameters on the Modulation Characteristic --- The experimental effect of the output-circuit resistance, R_2, which is largely composed of the system-load resistance, has been considered in detail in Chapter III. As explained previously, the manner in which the load resistance affects static behavior is contingent upon simultaneous magnetic effects and electrical effects in the output circuit. The flattening of the modulation characteristic in the higher ranges of input ampere-turns for large values of R_2 has been explained on the basis of the voltage distribution in the carrier circuit and will not be considered further at this time. Figure 4-13

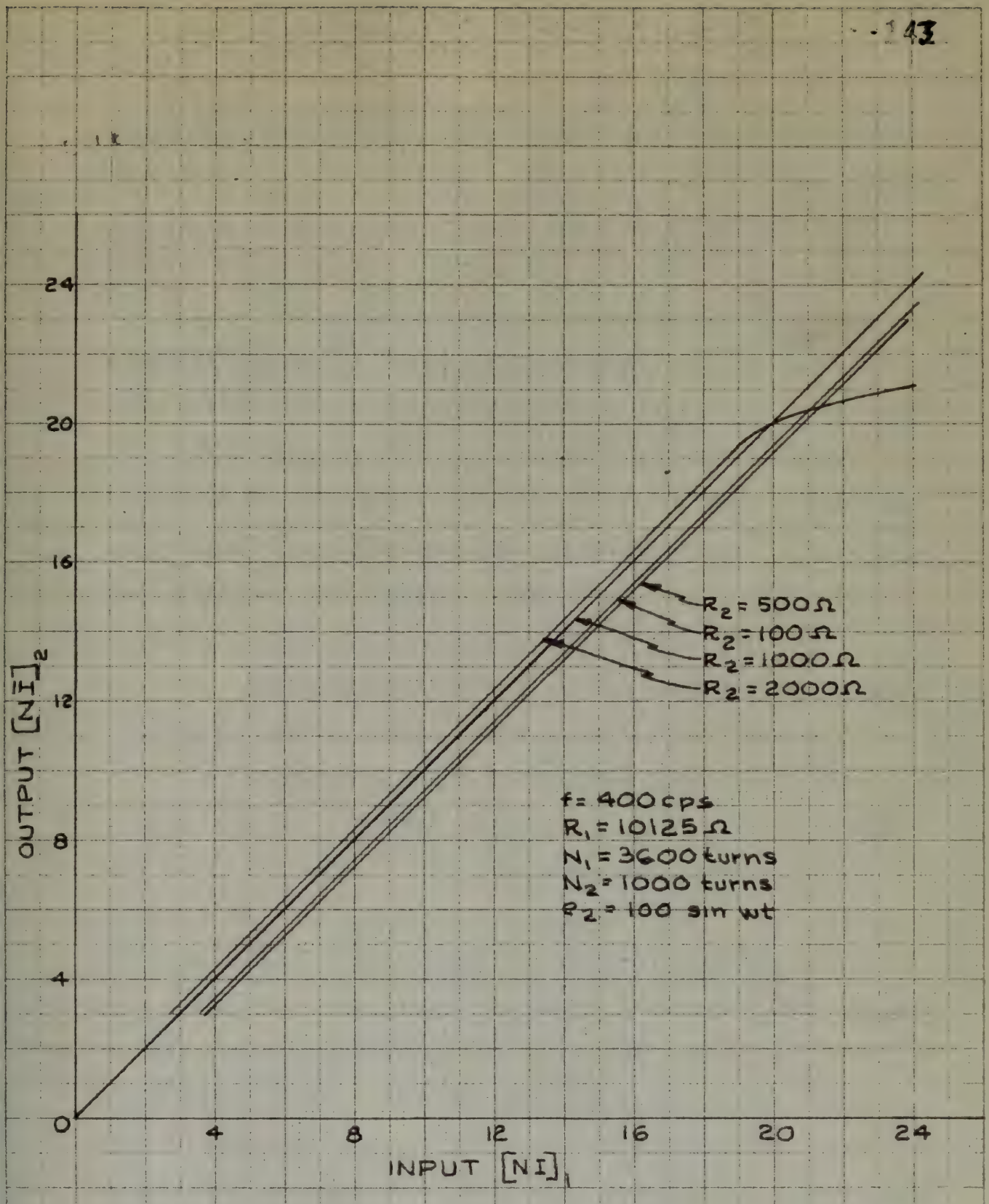

FIG. 4-13 ANALYTICAL OBSERVED EFFECT OF OUTPUT CIRCUIT RESISTANCE, R_2, ON STEADY-STATE OPERATION.

shows the analytically observed effect of the output-circuit resistance on the modulation characteristic. Notice that at the value of R_2 = 2000 ohms the modulation characteristic has commenced to fall off and the effect of saturation of the modulation characteristic is becoming apparent. The other values of R_2, being of lower magnitude, do not exhibit this effect within the range of the observations which were made. The behavior of the analytical circuit is again analogous to the experimentally-observed behavior and tends to confirm the conclusions made previously with regard to the nature of the effect of increasing values of load resistance on the static behavior of the amplifier.

Similarly, the nature of the analytically-observed effects of the variation of the output-circuit turns confirms the observations and conclusions drawn from experimental evidence in the previous chapter. The analytical results for turns variations in the output circuit are shown in Figure 4-14. As was the case experimentally, there is no definite trend of the effect. A definite flattening of the modulation characteristic occurs when the N_2 is reduced to the value of 500 turns per coil, and comparison of this result with Figure 3-10, in which similar characteristics are plotted for similar parameters, will show the marked similarity between analytical and experimental observations. As was the case empirically, so does the analytical solution indicate an optimum value of N_2 for maximum ampere-

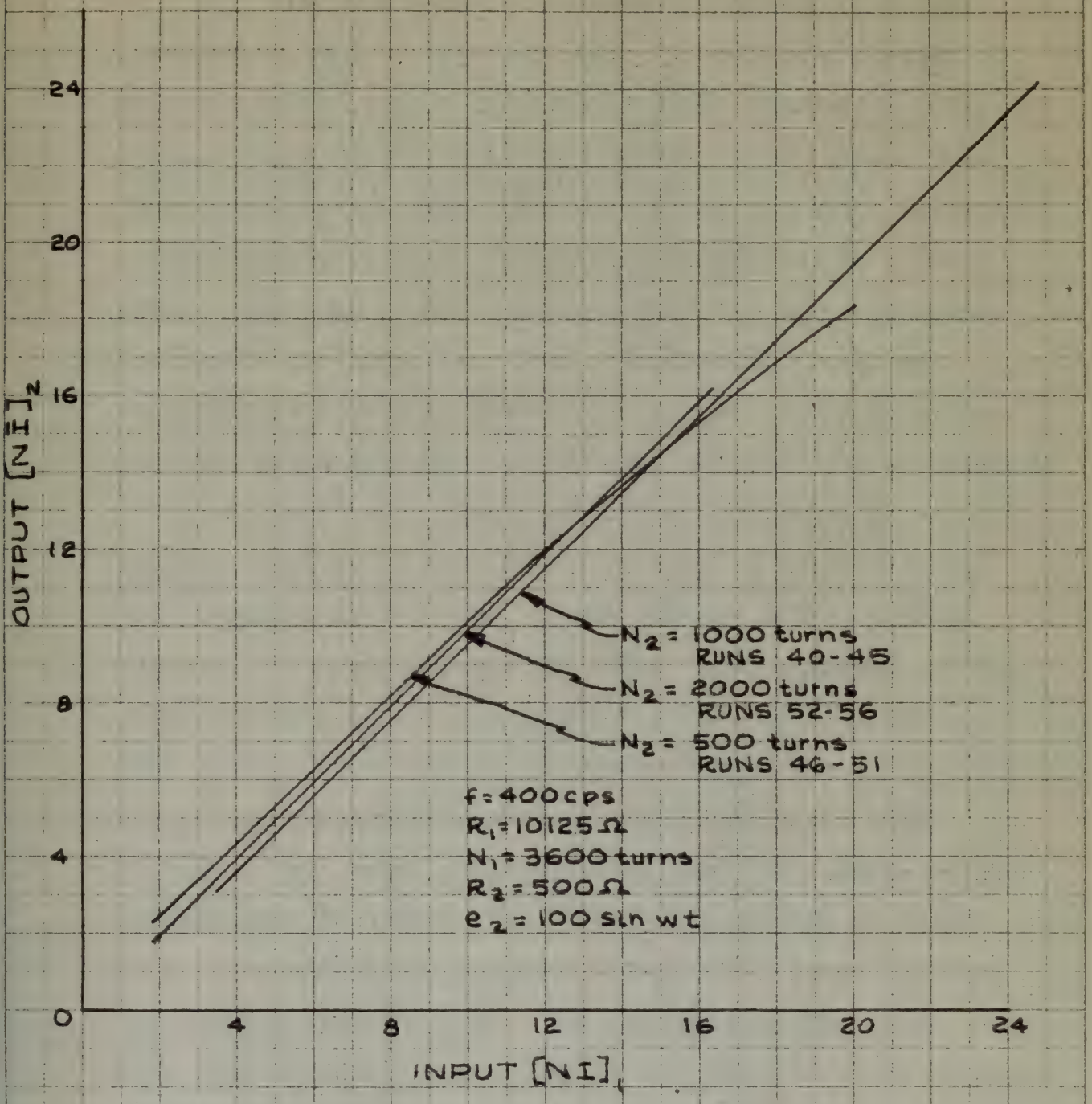

FIG. 4-14 ANALYTICAL OBSERVED EFFECT OF OUTPUT CIRCUIT TURNS, N_2, ON STEADY-STATE PERFORMANCE.

turn sensitivity of the amplifier. The semi-quantitative procedure for optimizing N_2 was discussed in Chapter III.

The peak value of alternating flux in a single core was defined by Equation 4-24. It has been pointed out that if the peak value of this flux exceeds the saturation flux, a current will flow in the output circuit although the applied input circuit current is zero. Analytically, because of scale factor limitations on the differential analyzer, it was not practicable to decrease either the secondary turns, N_2, or the alternating frequency, 2, sufficiently to obtain fluxes of adequate magnitude to exceed the saturation flux at the peak value of the alternating flux. A simple computation made from Equation 4-24 will indicate that if ϕ_s is 4×10^{-5} webers, N_2 is 1000 turns and frequency is 400 cps., a peak voltage of 102.4 volts per coil, or approximately 205 volts total supplied to the secondary circuit, is required to produce an alternating flux sufficient to exceed the value of ϕ_s. The differential analyzer was readily adapted to produce an alternating voltage of 300 volts peak amplitude, and the results of the observations made with this voltage are plotted on Figure 4-15. The output ampere-turns are noted to exceed 16 when the input current is zero. For various reasons, which have been discussed previously in this report and in detail in the literature,[1] the presence of a large initial output current is highly undesirable, and it is, therefore, essen-

---

1. Fitzgerald, A.S., "Magnetic Amplifier Circuits," J.F.I., 244, (1947), 249-263.

turn sensitivity of the amplifier. The semi-quantitative procedure for optimizing N_2 was discussed in Chapter III.

The peak value of alternating flux in a single core was defined by Equation 4-26. It has been pointed out that if the peak value of this flux exceeds the saturation flux, a current will flow in the output circuit although the applied input circuit current is zero. Analytically, because of small factor limitations on the differential analyzer, it was not practicable to decrease either the secondary turns, N_2, or the alternating frequency, β, sufficiently to obtain fluxes of adequate magnitude to exceed the saturation flux at the peak value of the alternating flux. A single computation made from Equation 4-26 will indicate that if β_s is 4×10^{-5} webers, N_2 is 1000 turns and frequency is 400 cps., a peak voltage of 1[illegible].4 volts per coil, or approximately [illegible] volts total supplied to the secondary circuit, is required to produce an alternating flux sufficient to exceed the value of β_s. The differential analyzer was readily adapted to produce an alternating voltage of 300 volts peak amplitude, and the results of the observations made with this voltage are plotted as figure 4-15. The output ampere-turns are noted to exceed 16 when the input current is zero. For various reasons, which have been discussed previously in this report and in detail in the literature,[1] the presence of a large initial output current is highly undesirable, and it is, therefore, essen-

1. Fitzgerald, A.R., "Magnetic Amplifier Circuits," *A.I.E.E. Trans.* (1947), 248-263.

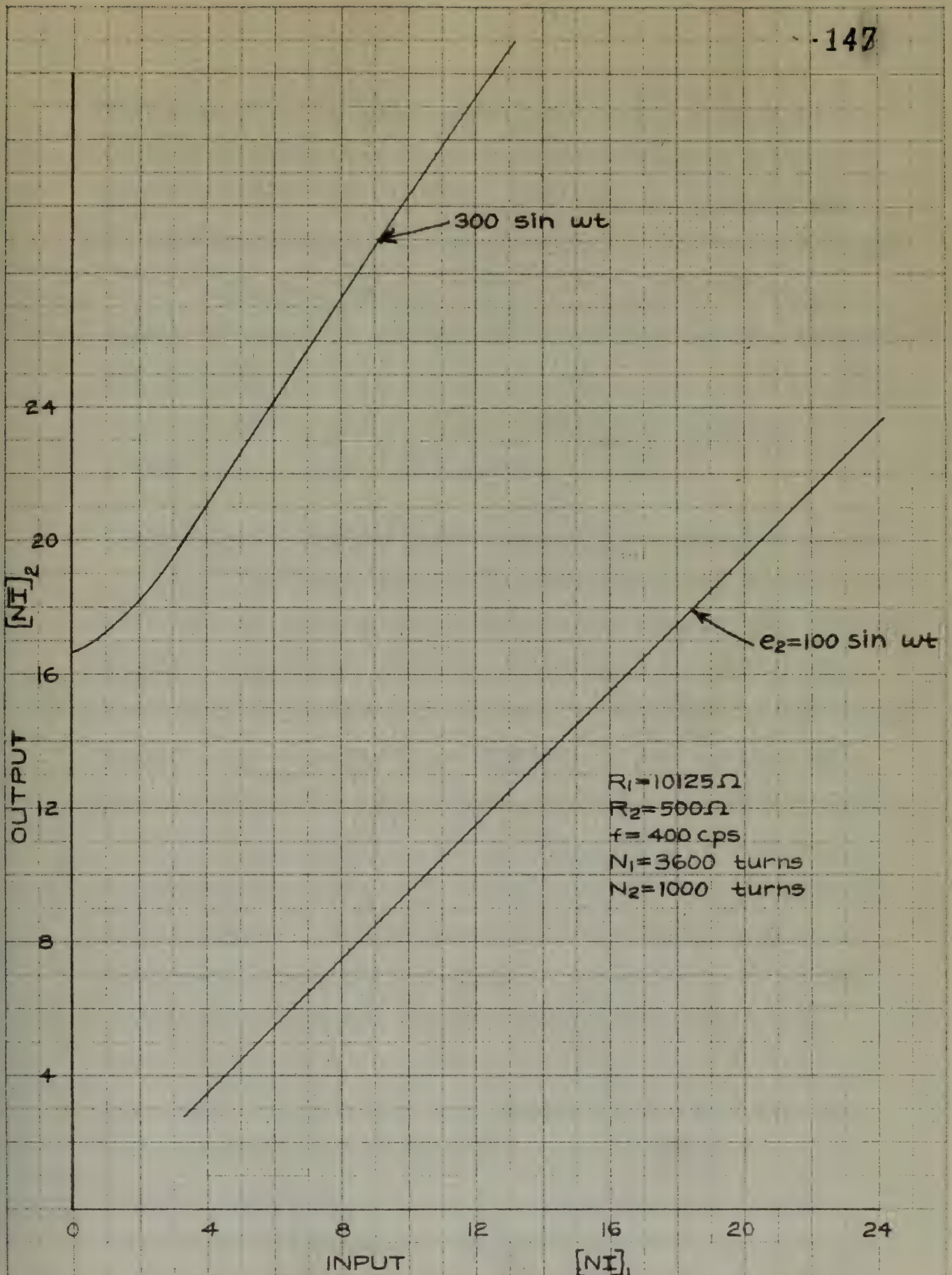

FIG. 4-15 ANALYTICAL OBSERVED EFFECT OF ALTERNATING VOLTAGE, e_2, ON STEADY-STATE OPERATION

tial that the flux excursions of the output circuit be restricted to less than ϕ_s if the effect of large initial output-circuit currents is to be minimized. Limitations of the voltage-generating and amplifying equipment available in the laboratory made it difficult to create an experimental situation having the same circuit parameters used in the analytical observation at 300 volts, and again, the value of the machine solution in observing the fundamental behavior of the circuit is apparent.

The Analytical Transient Behavior of the Magnetic Amplifier

The Elmen theory regarding the nature of hysteresis loss in iron-cored reactors under excitation at more than one frequency has been discussed previously. The theory has been further confirmed by analytical studies of the transient behavior of the magnetic amplifier. In review, the Elmen theory states that if a core is excited at separate circuits in which the frequencies of the alternating parameters are different, the major portion of hysteresis loss is supplied by the higher frequency source. In accordance with this hypothesis, the effect of hysteresis loss would be expected to be more pronounced in the output circuit than in the input circuit of the magnetic amplifier. Such is, indeed, the case. Analytically, the effects of variations in the input-circuit parameters on the transient response of the magnetic amplifier are very nearly exactly equal to the corresponding effects of variations of these parameters as

tial that the flux excursions of the output circuit be restricted to less than B_s if the effect of large initial output-circuit currents is to be minimized. Limitations of the voltage-generating and amplifying equipment available in the laboratory made it difficult to create an experimental situation having the same circuit parameters used in the analytical observation at 300 volts, and again, the value of the machine solution in observing the fundamental behavior of the circuit is apparent.

<u>The Analytical Transient Behavior of the Magnetic Amplifier</u>

The Kleen theory regarding the nature of hysteresis loss in iron-cored reactors under excitation at more than one frequency has been discussed previously. The theory has been further confirmed by analytical studies of the transient behavior of the magnetic amplifier. In review, the Kleen theory states that if a core is excited at separate circuits in which the frequencies of the alternating parameters are different, the major portion of hysteresis loss is supplied by the higher frequency source. In accordance with this hypothesis, the effect of hysteresis loss would be expected to be more pronounced in the output circuit than in the input circuit of the magnetic amplifier. Such is, indeed, the case. Analytically, the effects of variations in the input-circuit parameters on the transient response of the magnetic amplifier are very nearly exactly equal to the corresponding effects of variations of these parameters as

observed experimentally. Quite on the contrary, the effects of analytical variations of the output-circuit parameters on the transient response of the amplifier are very different from the effects observed experimentally. The difference, as was pointed out in Chapter III, is almost totally due to loss effects which are very pronounced in the output circuit.

As was done in the preceding section, the output and input circuits will be dealt with separately in discussions of the analytical transient behavior of the magnetic amplifier.

(a) The Effects of the Input-Circuit Parameters on the Transient Behavior of the Magnetic Amplifier -- The characteristic time of the response of the magnetic amplifier to an applied step voltage for variations in the input-circuit current, i_1, was shown experimentally to be inversely proportional to the square-root of the input current. The nature of this variation has been discussed in Chapter III. The effect of i_1 upon the transient-time of the amplifier was confirmed by the analytical equations, and the inverse square-root function was shown to hold in the theoretical case. In Figure 4-16 the variation of characteristic time with increasing values of input circuit current is plotted from observed analytical data as obtained from the analyzer solutions for a particular set of circuit parameters, as indicated on the figure. The curve of Figure 4-16 is replotted on log-log coordinates in Figure

observed experimentally. While on the contrary, the effects of analytical variations of the output-circuit parameters on the transient response of the amplifier are very different from the effects observed experimentally. The difference, as was pointed out in Chapter III, is almost totally due to loop effects which are very pronounced in the output circuits.

As was done in the preceding section, the output and input circuits will be dealt with separately in discussions of the analytical transient behavior of the magnetic amplifier.

(a) The Effects of the Input-Circuit Parameters on the Transient Behavior of the Magnetic Amplifier -- The characteristic time of the response of the magnetic amplifier to an applied step voltage for variations in the input-circuit current, i_1, was shown experimentally to be inversely proportional to the square-root of the input current. The nature of this variation has been discussed in Chapter III. The effect of i_1 upon the transient-time of the amplifier was verified by the analytical equations, and the inverse square-root function was shown to hold in the theoretical case. In Figure 4-12 the variation of characteristic time with increasing values of input circuit current is plotted from observed analytical data on obtained from the analyzer solutions for a particular set of circuit parameters, as indicated on the figure. The curve of Figure 4-13 is replotted on log-log coordinates in Figure

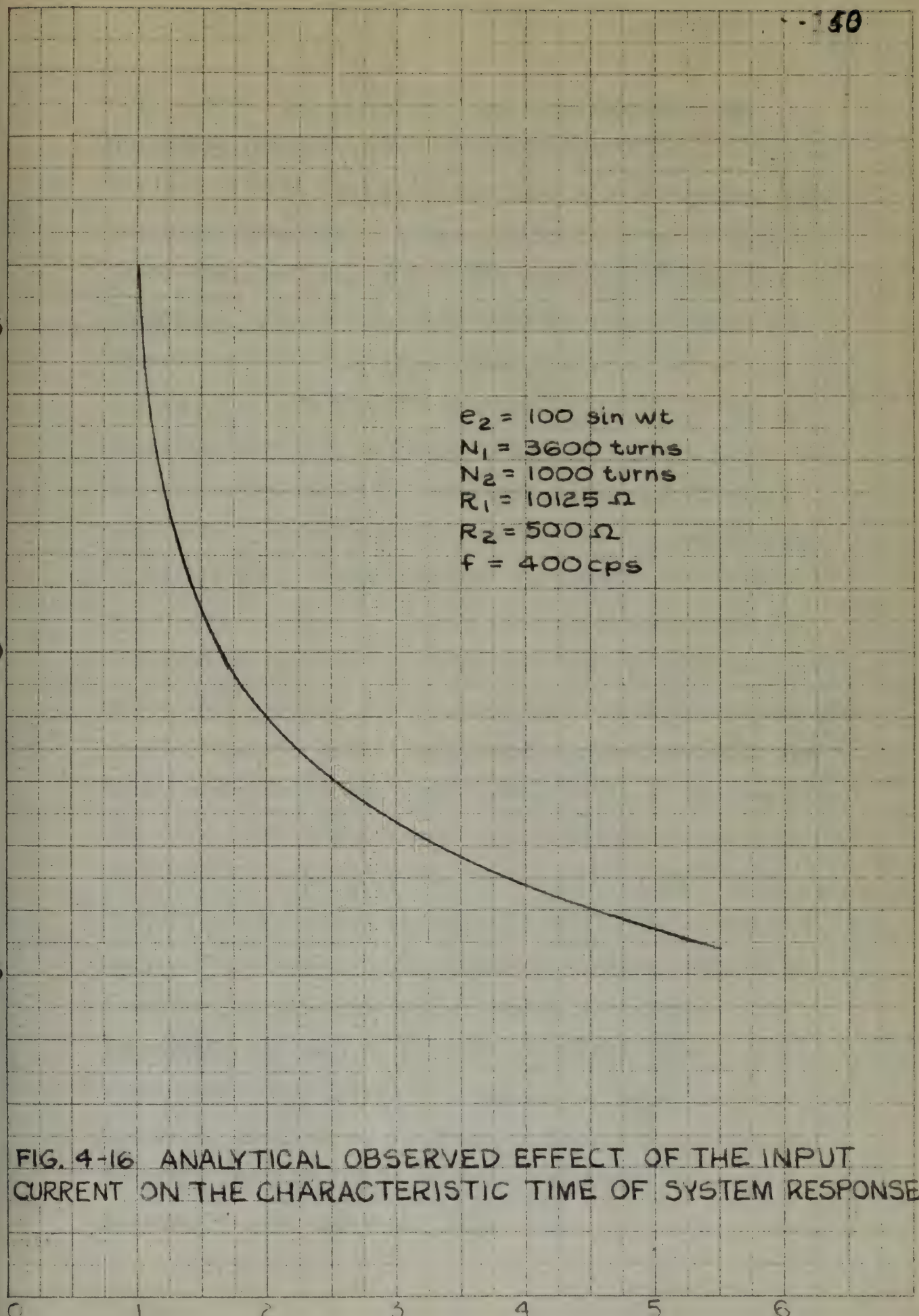

FIG. 4-16 ANALYTICAL OBSERVED EFFECT OF THE INPUT CURRENT ON THE CHARACTERISTIC TIME OF SYSTEM RESPONSE.

4-17, which also shows the experimentally observed variation for equivalent parametric conditions. The experimental data used for comparison with analytical data was taken by photographing a single sweep of an oscilloscope when the transient in the amplifier circuit was in progress. This technique has proved very valuable for observations of this type. The effects of increasing values of i_1 are shown by the series of photographs of transient behavior in Figure 4-18. It will be noted that the characteristic-time variation plots as a straight line with a slope of minus $\frac{1}{2}$ on the log-log coordinates of Figure 4-17, which confirms the inverse square-root variation due to i_1. It will also be noticed that the experimentally observed curve lies beneath the analytical curve, or, in other words, the experimental variations indicate somewhat lesser magnitudes of characteristic time than were observed for equal values of i_1 in the analytical case. This phenomena is attributed to the presence of a small additional variable resistor in the input circuit which appears as a result of the hysteresis and eddy-current losses. The magnitude of this resistor is dependent on the magnitude of the i_1 and changes with increasing currents in a manner which maintains a constant difference between the curves of Figure 4-17. Actually, as shown by the figure, the difference is small over the observed range and might be caused by normal fluctuations of the data.

fluctuations of the data.

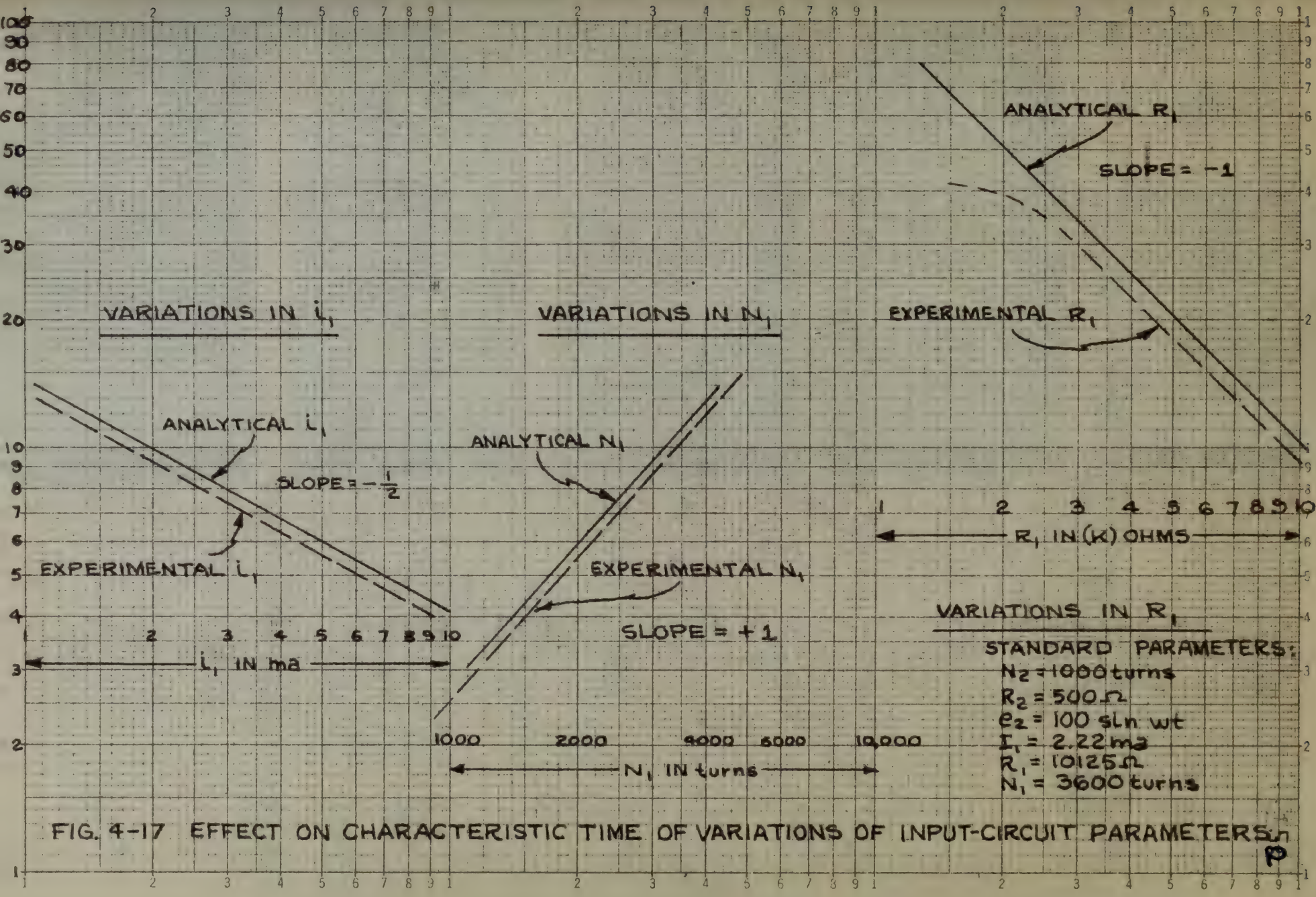

FIG. 4-17 EFFECT ON CHARACTERISTIC TIME OF VARIATIONS OF INPUT-CIRCUIT PARAMETERS.

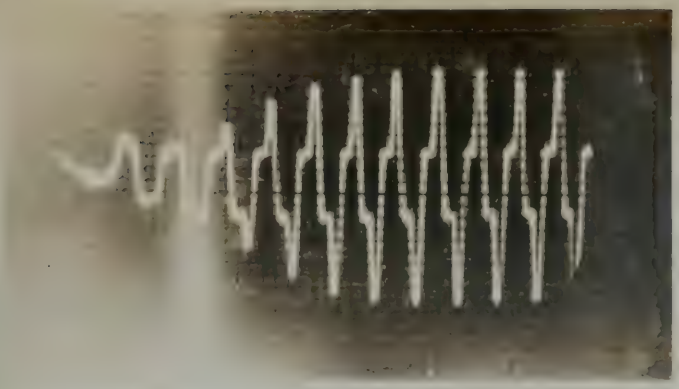

(a)

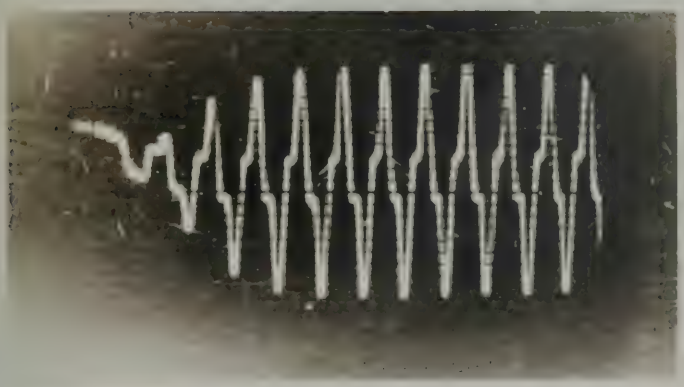

(b)

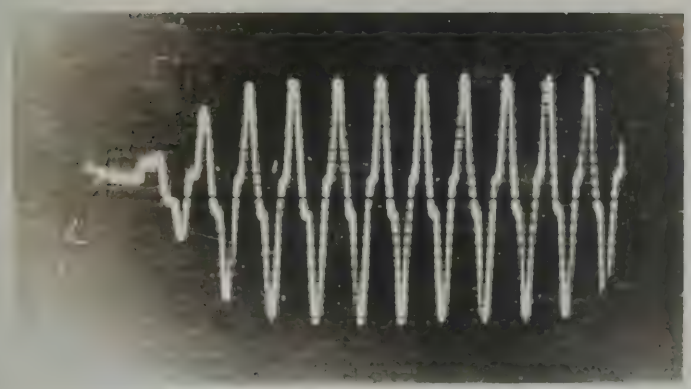

(c)

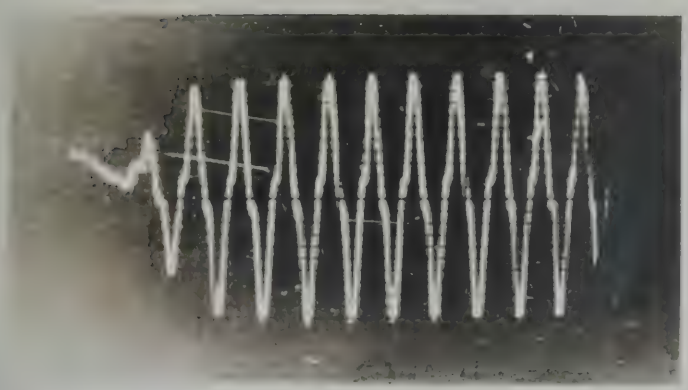

(d)

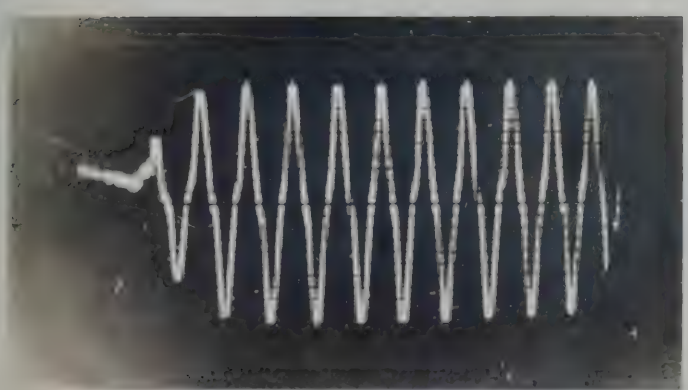

(e)

FIGURE 4-18

OSCILLOSCOPIC PHOTOGRAPHS SHOWING THE BUILDUP OF THE OUTPUT-CIRCUIT CURRENT, i_2, FOR INCREASING VALUES OF THE INPUT CURRENT, i_1, WHEN A STEP-FUNCTION OF VOLTAGE IS APPLIED TO THE INPUT-CIRCUIT TERMINALS

f = 400 cps.
N_1 = 3600 T
N_2 = 1000 T
R_1 = 101.5 ohms
R_2 = 500 ohms
e_2 = 100 sin ωt volts

KEY

(a) i_1 = 1.11 ma.
(CT) = 12.5 msec.

(b) i_1 = 2.22 ma.
(CT) = 8.6 msec.

(c) i_1 = 3.33 ma.
(CT) = 7.2 msec.

(d) i_1 = 4.44 ma.
(CT) = 6.0 msec.

(e) i_1 = 5.55 ma.
(CT) = 5.25 msec.

Observations made analytically have permitted the plotting of families of curves similar to those in Figure 4-16 with the various parameters of the circuit represented by different curves of the family. The data from which each of these analytical curves was plotted are tabulated in Charts 4-3 and 4-4. The families of curves show the variation of characteristic time with i_1 for different values of each parameter. It is then possible to select a constant value of the input-circuit current and to determine the variation of characteristic time as any individual parameter is varied. In these studies the value of I_1 of 2.22 milliamperes has been selected as a standard for observation of parametric effects.

The variation of the characteristic time of amplifier-response with changes in the input-circuit resistance when the other parameters are held constant is shown plotted on log-log coordinates in Figure 4-17. Also plotted on this figure is the experimentally observed variation in characteristic time for the same circuit conditions as were existent in the analytical case. The experimental characteristic times were obtained from the series of oscilloscopic photographs shown in Figure 4-19. As was the case with the analytical and experimental variations of i_1, the comparison of analytical and experimental variations of R_1 also indicates the presence of a small additional variable resistance in the input

Observations made analytically have permitted the plotting of families of curves similar to those in Figure 4-16 with the various parameters of the circuit represented by different curves of the family. The data from which each of these analytical curves was plotted are tabulated in Charts 4-3 and 4-4. The families of curves show the variation of characteristic time with i_1 for different values of each parameter. It is then possible to select a constant value of the input-circuit current and to determine the variation of characteristic time as any individual parameter is varied. In these studies the value of I_1 of 2.52 milliamperes has been selected as a standard for observation of parametric effects.

The variation of the characteristic time of amplifier-response with changes in the input-circuit resistance when the other parameters are held constant is shown plotted on log-log coordinates in Figure 4-17. Also plotted on this figure is the experimentally observed variation in characteristic time for the same circuit conditions as were existent in the analytical case. The experimental characteristic times were obtained from the series of oscilloscopic photographs shown in Figure 4-19. As was the case with the analytical and experimental variations of i_1, the comparison of analytical and experimental variations of R_1 also indicates the presence of a small additional variable resistance in the input

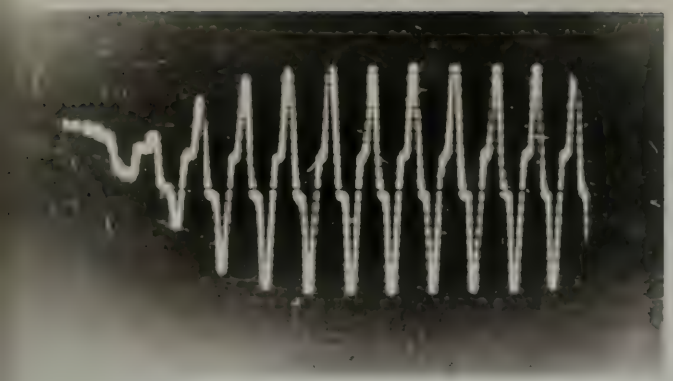

(a)

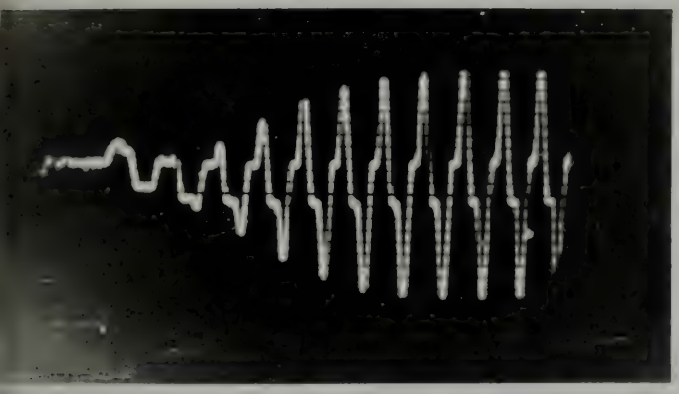

(b)

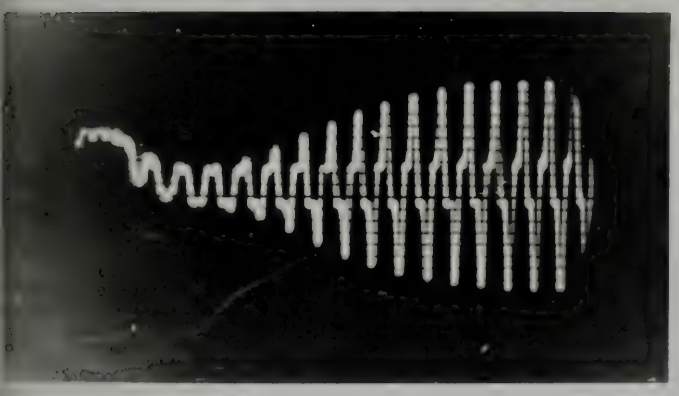

(c)

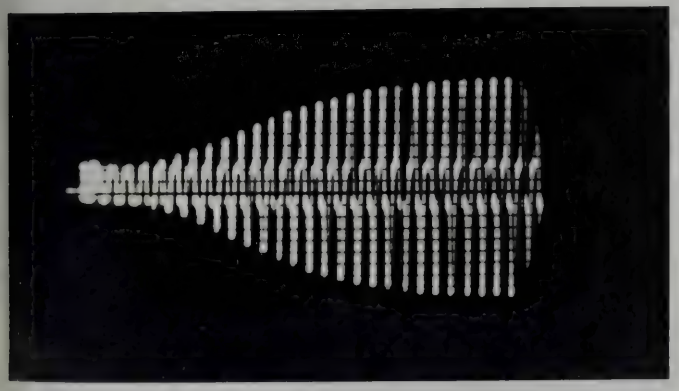

(d)

FIGURE 4- 19

OSCILLOSCOPIC PHOTOGRAPHS SHOWING THE BUILDUP OF THE OUTPUT-CIRCUIT CURRENT, i_2, FOR INCREASING VALUES OF THE INPUT-CIRCUIT RESISTANCE, R_1, WHEN A STEP-FUNCTION OF VOLTAGE IS APPLIED TO THE INPUT-CIRCUIT TERMINALS.

f = 400 cps.
N_1 = 3600 T
N_2 = 1000 T
R_2 = 500 ohms
i_1 = 2.22 ma.
e_2 = 100 sinωt volts

KEY

(a) R_1 = 10125 ohms
$(C\bar{T})$ = 8.6 msec.

(b) R_1 = 5065 ohms
$(C\bar{T})$ = 15.0 msec.

(c) R_1 = 2530 ohms
$(C\bar{T})$ = 33.0 msec.

(d) R_1 = 1265 ohms
$(C\bar{T})$ = 40.0 msec.

circuit as caused by hysteresis and eddy-current effects. In general, however, the agreement between experimental and analytical data is excellent. The variation of characteristic time, (CT), with R_1 plots as a straight line with a slope of negative one on log-log coordinates, confirming the fact that the response time of the amplifier is an inverse function of the total input-resistance of the magnetic-amplifier circuit.

The effects of variations of the input-circuit turns were observed in a similar manner. The points plotted in log-log coordinates in Figure 4-17 were selected from the N_1 family of curves for variations of characteristic time with input-circuit current. The experimental points, also plotted on this figure, were derived from the oscilloscope photographs shown in Figure 4-20. Again agreement between experimental and analytical observations is good, with the expected effect of hysteresis apparent for experimental cases. The slope of the straight line variation of characteristic time with input turns is observed to be equal to positive unity. The nature of this variation has been discussed in Chapter III and the analytical observations confirm the experimentally observed trend.

The effects of input-circuit parameter variations on the characteristic time of the magnetic amplifier have been shown analytically to agree very closely with experimental data. The neglect of losses has imposed no serious limitation to the analytically rigorous approach to the

circuit as caused by hysteresis and eddy-current effects. In general, however, the agreement between experimental and analytical data is excellent. The variation of characteristic time, (CT), with R_1 plots as a straight line with a slope of negative one on log-log coordinates, confirming the fact that the response time of the amplifier is an inverse function of the total input-resistance of the magnetic-amplifier circuit.

The effects of variations of the input-circuit turns were observed in a similar manner. The points plotted in log-log coordinates in Figure 4-17 were selected from the R_1 family of curves for variations of characteristic time with input-circuit current. The experimental points, also plotted on this figure, were derived from the oscilloscope photographs shown in Figure 4-[illegible]. Again agreement between experimental and analytical observations is good, with the expected effect of hysteresis apparent for experimental cases. The slope of the straight line variation of characteristic time with input turns is observed to be equal to positive unity. The nature of this variation has been discussed in Chapter III and the analytical observations confirm the experimentally observed trend.

The effects of input-circuit parameter variations on the characteristic time of the magnetic amplifier have been shown analytically to agree very closely with experimental data. The neglect of losses has imposed no serious limitation to the analytically rigorous approach to the

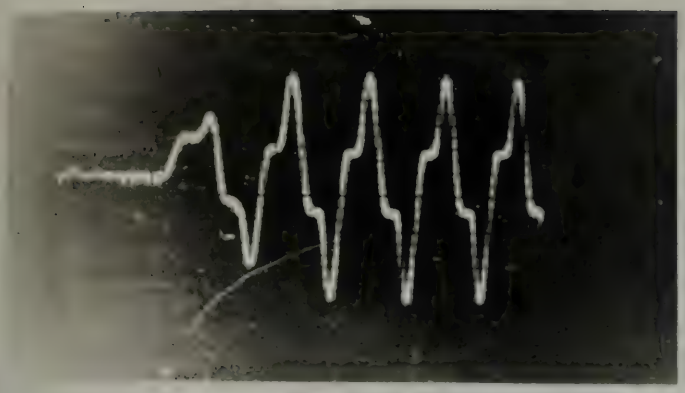

(a)

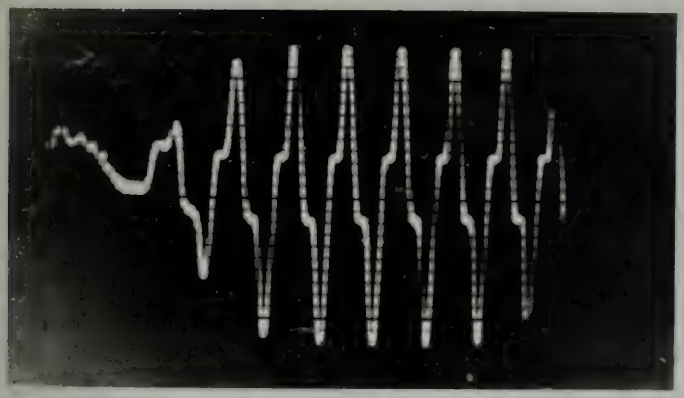

(b)

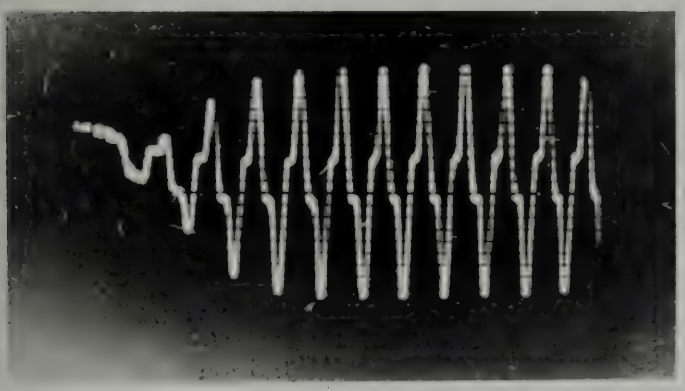

(c)

FIGURE 4- 20

OSCILLOSCOPIC PHOTOGRAPHS SHOWING THE BUILDUP OF THE OUTPUT-CIRCUIT CURRENT, i_2, FOR INCREASING VALUES OF THE INPUT-CIRCUIT TURNS, N_1, WHEN A STEP-FUNCTION OF VOLTAGE IS APPLIED TO THE INPUT-CIRCUIT TERMINALS.

f = 400 cps.
N_2 = 1000 T
R_1 = 10125 ohms
R_2 = 500 ohms
i_1 = 2.22 ma.
e_2 = 100 $\sin \omega t$ volts

KEY

(a) N_1 = 1800 T
$(C\bar{T})$ = 4.7 msec.

(b) N_1 = 2600 T
$(C\bar{T})$ = 6.6 msec.

(c) N_1 = 3600 T
$(C\bar{T})$ = 8.6 msec.

solution of the equations of the magnetic amplifier insofar as variations in the input-circuit parameters are concerned.

(b) The Effects of the Output-Circuit Parameters on the Transient Behavior of the Magnetic Amplifier. -- The concept of the buildup of biasing flux has been introduced previously. Since the buildup of flux bias consumes an appreciable portion of the total characteristic time of the amplifier, the amplitude of the flux in the coils of the output circuit is of great importance in the transient behavior of the magnetic amplifier. Ideally, the alternating flux-amplitude should be initially equal to the saturation flux. It is necessary that the flux amplitude not exceed this value because, as has been pointed out in the discussion of the static effects of flux, large initial currents will flow if the initial flux extends into the nonlinear region of the curve. It is, however, desirable that currents begin to flow as soon as possible after the application of the step function to the input terminals, and in order to accomplish this end, the excursions of the alternating flux should be as great as possible initially without exceeding the break value. Since the flux amplitude plays an important part in the transient behavior of the amplifier, it is convenient to discuss the effects of output-circuit parameters through the medium of the effect of these parameters on the alternating flux.

The effects of losses in the output circuit are pronounced in the practical case, and in general, the agreement between analytical and experimental variations

solution of the equations of the magnetic amplifier insofar as variations in the input-circuit parameters are concerned.

(b) The Effects of the Output-Circuit Parameters on the Transient Behavior of the Magnetic Amplifier. -- The concept of the buildup of biasing flux has been introduced previously. Since the buildup of flux bias consumes an appreciable portion of the total characteristic time of the amplifier, the amplitude of the flux in the coils of the output circuit is of great importance in the transient behavior of the magnetic amplifier. Ideally, the alternating flux-amplitude should be initially equal to the saturation flux. It is necessary that the flux amplitude not exceed this value because, as has been pointed out in the discussion of the static effects of flux, large initial currents will flow if the initial flux extends into the nonlinear region of the curve. It is, however, desirable that currents begin to flow as soon as possible after the application of the step function to the input terminals, and in order to accomplish this end, the excursions of the alternating flux should be as great as possible initially without exceeding the break value. Since the flux amplitude plays an important part in the transient behavior of the amplifier, it is convenient to discuss the effects of output-circuit parameters through the medium of the effect of these parameters on the alternating flux.

The effects of losses in the output circuit are pronounced in the practical case, and in general, the agreement between analytical and experimental variations

of the output-circuit parameters has been poor. The nature of the effects of losses on the magnetic-electric circuit has been considered in detail in the chapter devoted to discussion of experimental results.

As shown by Equation 4-24, the flux in the output circuit is directly proportional to E_2, and inversely proportional to frequency and to N_2. Since large initial flux-excursions lead to small values of characteristic time, it would seem apparent that an increase in E_2 would, in the analytical case, lead to reduction of the characteristic time. As shown on the plot of characteristic time versus E_2 on log-log coordinates of Figure 4-22, the expected decrease of characteristic time with increases in E_2 does not occur. As is consistent with the linear-circuit theory defined by Equation 4-26, the initial drop in characteristic time with E_2 is an inverse function of this parameter. After the value of E_2 becomes sufficiently great to produce fluxes of amplitude in excess of ϕ_s, nonlinear effects of the circuit take place, the buildup of flux is aided by the flow of currents, and the drop in characteristic time becomes much more rapid. The variation ceases to follow linear theory. The value of voltage required to produce ϕ_s was shown to be approximately 205 volts peak, or 145.5 volts rms, for the standard-parameter conditions, and therefore, above this flux value the nonlinear characteristics become apparent. Because of the losses in the out-

of the output-circuit parameters has been poor. The nature of the effects of losses on the magnetic-electric circuits has been observed in detail in the preliminary to discussion of experimental results.

We shown by equation 4-4', the flux in the output circuit is directly proportional to E_g, and inversely proportional to frequency and to R_g. Since large initial flux-excursions tend to small values of characteristic time, it would seem apparent that an increase in R_g would, in the multiplicant case, lead to reduction of the characteristic time. We shown on the plot of characteristic time versus R_g and log-log ordinates of Figure 4-6, the expected variation of characteristic time with increase in R_g does not occur. We is consistent with the linear-element theory defined by equation 4-36, the initial drop in characteristic time with R_g is an inverse function of this parameter. After the value of R_g becomes sufficiently great by comparison with the value of R_1, the multiple of flux is found by the flow of current, and the drop in characteristic time becomes much more rapid. The variation nearly follows the circuit time plane, the multiple of flux is found by one figure of magnitude in excess of R_g, beginning slightly after the value of R_g becomes sufficiently great by comparison with R_1 so as to be effectively R_g equal zero, or Fig.3 value two, for the short-circuit condition, and R_g was shown to be effectively R_g equal zero, or Fig.3 linear theory. The value of voltage required to produce becomes much more rapid. The variation nearly follows the flow of current, and the drop in characteristic time

latter because important. Despite of the losses in the output circuit, above this flux value the magnetic saturation, and therefore, above this flux value the magnetic saturation, and valve two, for the short-circuit condition, and R_g was shown to be effectively R_g equal zero, or Fig.3 linear theory. The value of voltage required to produce becomes much more rapid. The variation nearly follows the flow of current, and the drop in characteristic time of the output-circuit parameters has been poor. The nature of the effects of losses on the magnetic-electric circuits has been observed in detail in the preliminary to discussion of experimental results.

We shown by equation 4-4', the flux in the output circuit is directly proportional to E_g, and inversely proportional to frequency and to R_g. Since large initial flux-excursions tend to small values of characteristic time, it would seem apparent that an increase in R_g would, in the multiplicant case, lead to reduction of the characteristic time. We shown on the plot of characteristic time versus R_g and log-log ordinates of Figure 4-6, the expected variation of characteristic time with increase in R_g does not occur. We is consistent with the linear-element theory defined by equation 4-36, the initial drop in characteristic time with R_g is an inverse function of this parameter. After the value of R_g becomes sufficiently great by comparison with R_1, the multiple of flux is found by the flow of current, and the drop in characteristic time

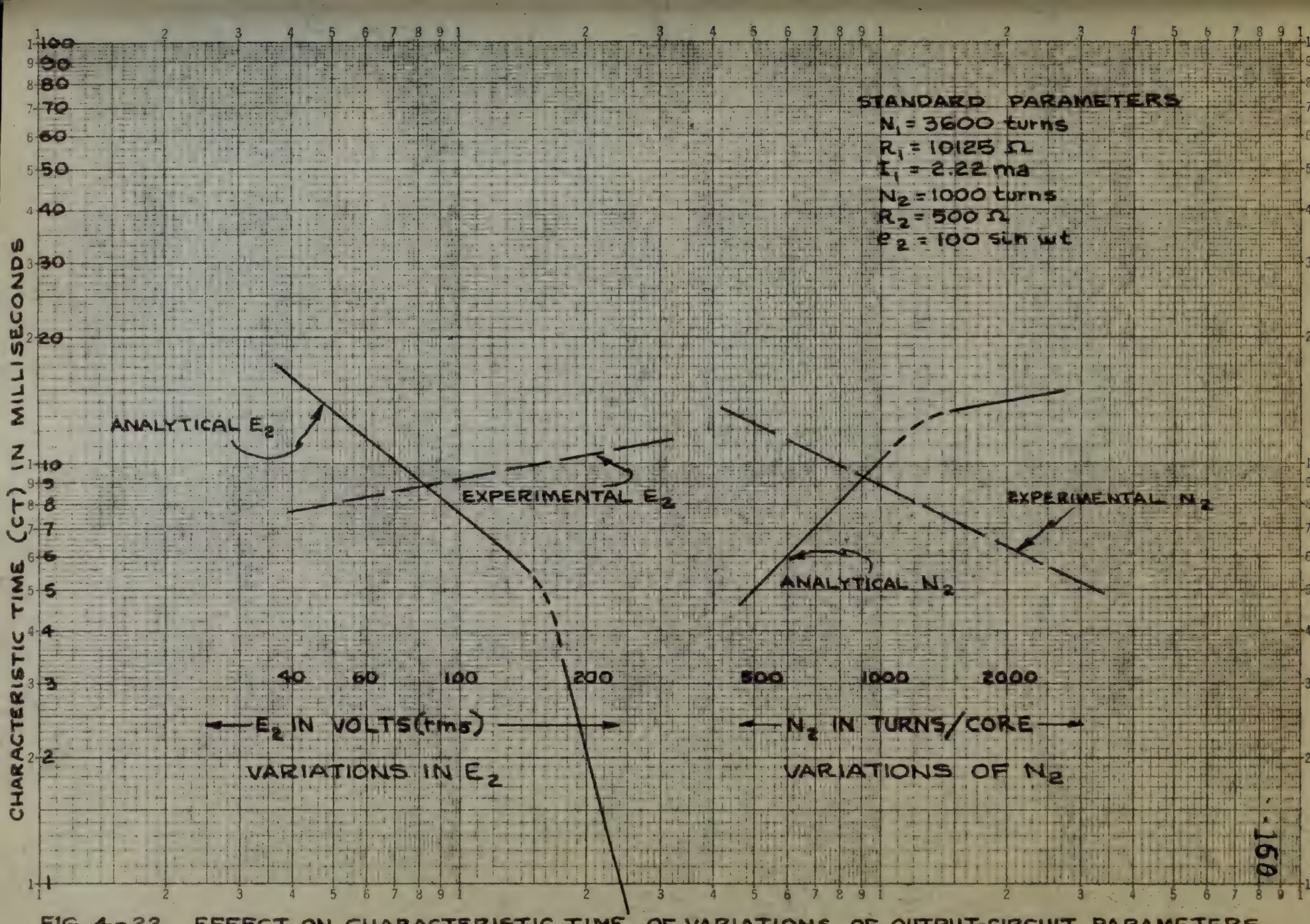

FIG. 4-22 EFFECT ON CHARACTERISTIC TIME OF VARIATIONS OF OUTPUT-CIRCUIT PARAMETERS.

put circuit, the effect of experimental variation of E_2 is radically different, having a positive slope of approximately 1/5, as plotted on Figure 4-22, from the data represented by the photo-oscillographs of Figure 4-21. Since the reasons for this behavior were discussed in Chapter III, it is only necessary to state here that the analytical approach, because of core losses, does not adequately indicate the nature of the effects of variations in E_2 upon the transient characteristics of the magnetic amplifier in the practical case.

The effect of the output-circuit resistance on characteristic time was observed analytically and experimentally to be negligible. This result is to be expected because the effect of the output-circuit resistance on the amount of voltage available to the reactors is constant and independent of the output-circuit losses. Examination of the photographs of Figure 4-23 shows quite clearly that the transient time of the amplifier is practically constant regardless of the magnitude of the load resistor. The results of differential analyzer Runs 27-45 inclusive, as tabulated on Charts 4-3 and 4-4, confirm analytically the lack of effect of R_2 upon transient behavior in the region observed.

The flux-bias buildup concept, Equation 4-26 and Equation 4-24, would indicate that an increase in the output-circuit turns would result in an increase in characteristic time. This expected trend was found to be true in

put circuit, the effect of experimental variation of E_g is radically different, having a positive slope of approximately 1/3, as plotted on Figure 4-22, from the data represented by the photo-oscillographs of Figure 4-21. Since the reasons for this behavior were discussed in Chapter III, it is only necessary to state here that the analytical approach, because of core losses, does not adequately indicate the nature of the effects of variations in E_g upon the transient characteristics of the magnetic amplifier in the practical case.

The effect of the output-circuit resistance on characteristic time was observed analytically and experimentally to be negligible. This result is to be expected because the effect of the output-circuit resistance on the amount of voltage available to the reactors is constant and independent of the output-circuit losses. Examination of the photographs of Figure 4-23 shows quite clearly that the transient time of the amplifier is practically constant regardless of the magnitude of the load resistor. The results of differential analyzer Runs 27-45 inclusive, as tabulated on Charts 4-3 and 4-4, confirm analytically the lack of effect of E_g upon transient behavior in the region observed.

The fine-bias tailing concept, Equation 4-26 and Equation 4-24, would indicate that an increase in the output-circuit turns would result in an increase in characteristic time. This expected trend was found to be true in

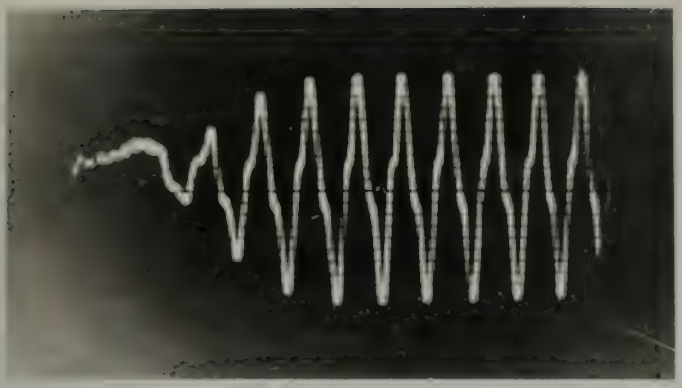

(a)

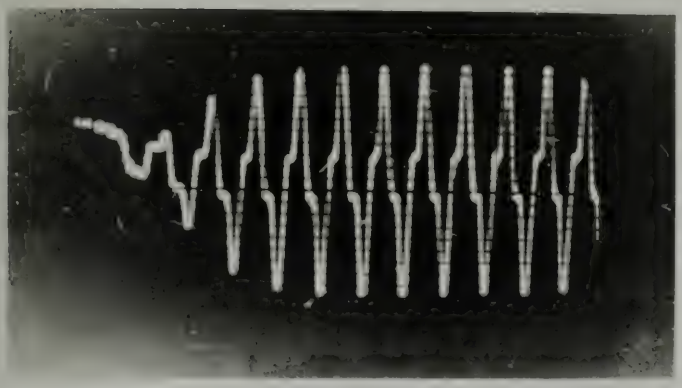

(b)

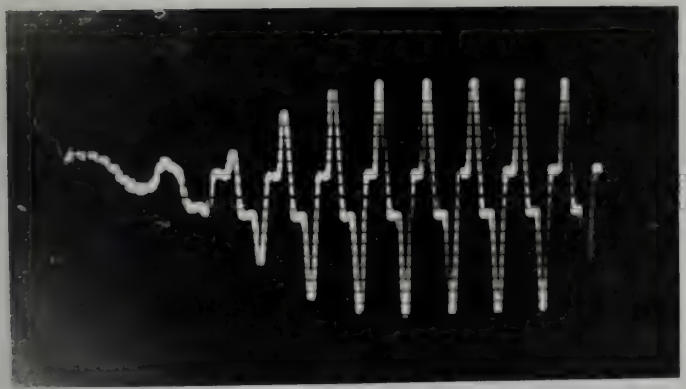

(c)

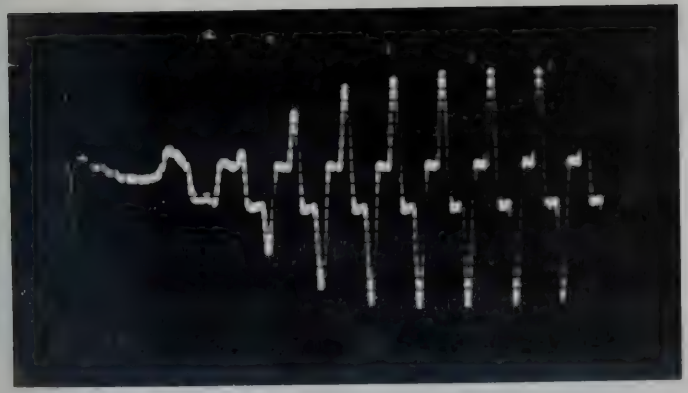

(d)

FIGURE 4-21

OSCILLOSCOPIC PHOTOGRAPHS SHOWING THE BUILDUP OF THE OUTPUT-CIRCUIT CURRENT, i_2, FOR INCREASING VALUES OF THE PEAK VALUE OF THE APPLIED ALTERNATING VOLTAGE, E_2, WHEN A STEP-FUNCTION VOLTAGE IS APPLIED TO THE INPUT-CIRCUIT TERMINALS.

f = 400 cps.
N_1 = 3600 T
N_2 = 1000 T
R_1 = 10125 ohms
R_2 = 500 ohms
i_1 = 2.22 ma.

KEY

(a) E_2 = 80 volts
(CT) = 8.0 msec.

(b) E_2 = 100 volts
(CT) = 8.6 msec.

(c) E_2 = 150 volts
(CT) = 9.2 msec.

(d) E_2 = 185 volts
(CT) = 11.9 msec.

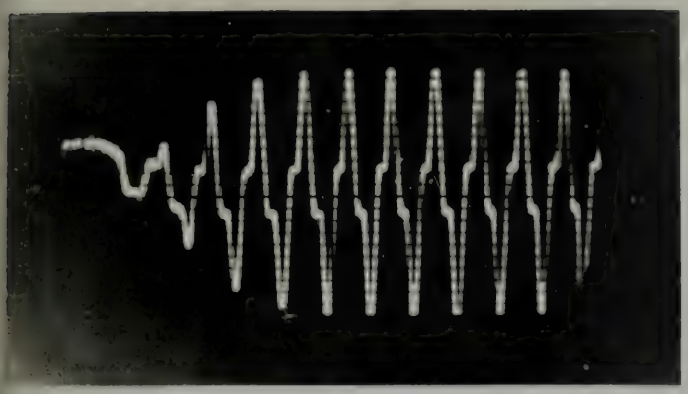

(a)

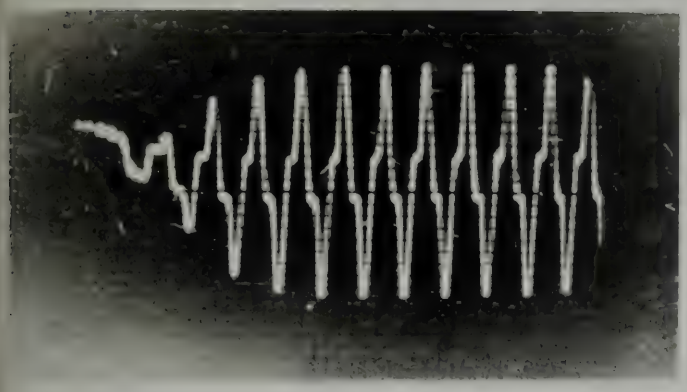

(b)

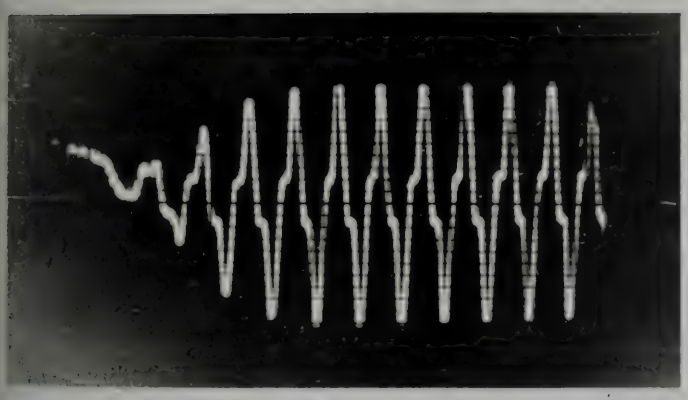

(c)

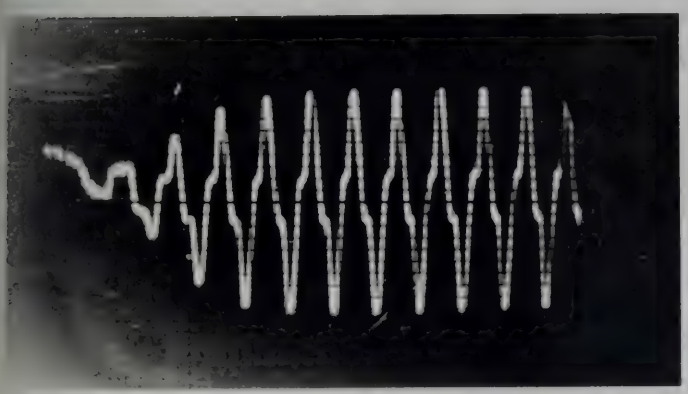

(d)

FIGURE 4-23

OSCILLOSCOPIC PHOTOGRAPHS SHOWING THE BUILDUP OF THE OUTPUT-CIRCUIT CURRENT, i_2, FOR INCREASING VALUES OF THE OUTPUT-CIRCUIT RESISTANCE R_2, WHEN A STEP-FUNCTION OF VOLTAGE IS APPLIED TO THE INPUT-CIRCUIT TERMINALS. (NOTICE THAT THE EFFECT OF VARIATIONS IN R_2 IS VERY SMALL.)

f = 400 cps.
N_1 = 3600 T
N_2 = 1000 T
R_1 = 10125 ohms
i_1 = 2.22 ma.
e_2 = 100 $\sin\omega t$ volts

KEY

(a) R_2 = 100 ohms
($C\bar{T}$) = 8.65 msec.

(b) R_2 = 500 ohms
($C\bar{T}$) = 8.60 msec.

(c) R_2 = 1000 ohms
($C\bar{T}$) = 8.70 msec.

(d) R_2 = 2000 ohms
($C\bar{T}$) = 8.73 msec.

the analytical case, and in accordance with Equation 4-26, the time response increases, analytically, approximately with the number of turns in the output circuit windings. The observed analytical effect, as well as the experimental effect, are shown plotted on log-log coordinates in Figure 4-22. The experimental effect of increasing N_2, as obtained from the photographs of Figure 4-24, shows that the characteristic time is an inverse function of the square-root of N_2. The wide deviation between experimental and analytical results must again be attributed to output-circuit losses, and it is necessary to conclude that the analytical approach, because of these losses, does not present a true picture of the actual transient behavior of a practical magnetic-amplifier circuit.

Time limitations did not permit investigation of the effect of the output-circuit alternating-frequency on the transient behavior of the amplifier, but since the frequency, in accordance with Equation 4-24, affects the flux amplitude in the same manner as the output turns, N_2, it is anticipated that frequency effects observed analytically would be similar to the observed analytical effects of N_2. Since the analytical effects of N_2 are not confirmable experimentally, it is presumed that the analyzer would not show correct frequency effects, again as a result of the circuit losses of hysteresis and eddy-currents.

the analytical case, and in accordance with Equation 4-26, the time response increases, analytically, approximately with the number of turns in the output circuit windings. The observed analytical effect, as well as the experimental effect, are shown plotted on log-log coordinates in Figure 4-27. The experimental effect of increasing N_p, as obtained from the photographs of Figure 4-24, shows that the characteristic time is an inverse function of the square-root of N_p. The wide deviation between experimental and analytical results must again be attributed to output-circuit losses, and it is necessary to conclude that the analytical approach, because of these losses, does not present a true picture of the actual transient behavior of a practical magnetic-amplifier circuit.

Time limitations did not permit investigation of the effect of the output-circuit alternating-frequency on the transient behavior of the amplifier, but since the frequency, in accordance with Equation 4-24, affects the flux amplitude in the same manner as the output turns, N_p, it is anticipated that frequency effects observed analytically would be similar to the observed analytical effects of N_p. Since the analytical effects of N_p are not confirmable experimentally, it is presumed that the analyzer would not show correct frequency effects, again as a result of the circuit losses of hysteresis and eddy-currents.

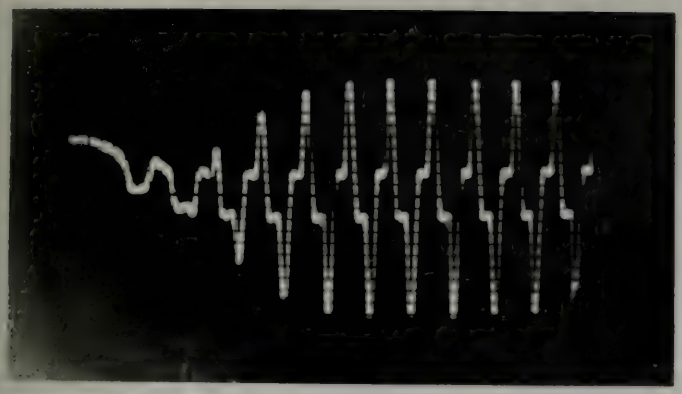

(a)

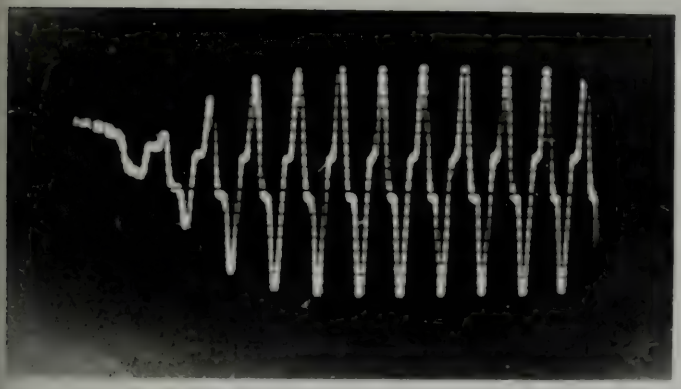

(b)

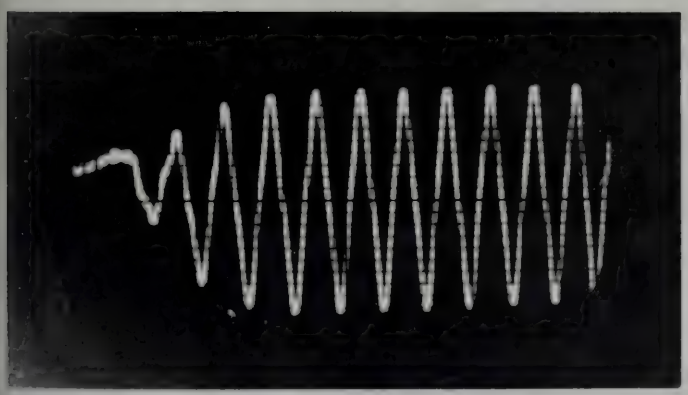

(c)

FIGURE 4-24

OSCILLOSCOPIC PHOTOGRAPHS SHOWING THE BUILDUP OF OUTPUT-CIRCUIT CURRENT, i_2, FOR INCREASING VALUES OF THE OUTPUT-CIRCUIT TURNS, N_2, WHEN A STEP-FUNCTION OF VOLTAGE IS APPLIED TO THE INPUT-CIRCUIT TERMINALS.

f = 400 cps.
N_1 = 3600 T
R_1 = 10125 ohms
R_2 = 500 ohms
i_1 = 2.22 ma.
e_2 = 100 $\sin\omega t$ volts

KEY

(a) N_2 = 600 T
(CT) = 11.6 msec.

(b) N_2 = 1000 T
(CT) = 8.6 msec.

(c) N_2 = 2000 T
(CT) = 6.1 msec.

Conclusions Regarding the Analytical Studies

The analytical approach to the magnetic amplifier problem has given excellent indications of the steady-state performance which might be expected from a given magnetic-amplifier design. It has further indicated the nature of choice of parameters which might be selected to permit optimum operation in the steady-state to meet the requirements of a particular situation. The analytical approach has also indicated the nature of the effects of the input-circuit parameters upon the transient performance of the magnetic amplifier. Unfortunately, the analytical solution fails to give true indications of the effects of the output-circuit parameters which affect the magnitude of the alternating flux in affecting the transient performance of the device.

It should be remembered that the analytical studies were made using the most simple magnetic-amplifier circuit. In general, usable magnetic-amplifier circuits are further complicated by feedback windings and by rectifier-demodulator units which will contribute decidedly toward complicating the equations of amplifier performance, and would seem to make the analytical approach extremely difficult.

This particular investigation was, however, devoted to examination of the fundamentals which affect magnetic-amplifier performance, and as such, the use of

Conclusions Regarding the Analytical Studies

The analytical approach to the magnetic amplifier problem has given excellent indications of the steady-state performance which might be expected from a given magnetic-amplifier design. It has further indicated the nature of choice of parameters which might be selected to permit optimum operation in the steady-state to meet the requirements of a particular situation. The analytical approach has also indicated the nature of the effects of the input-circuit parameters upon the transient performance of the magnetic amplifier. Unfortunately, the analytical solution fails to give true indications of the effects of the output-circuit parameters which affect the magnitude of the alternating flux in affecting the transient performance of the device.

It should be remembered that the analytical studies were made using the most simple magnetic-amplifier circuit. In general, usable magnetic-amplifier circuits are further complicated by feedback windings and by rectifier-demodulator units which will contribute decidedly toward complicating the equations of amplifier performance, and would seem to make the analytical approach extremely difficult.

This particular investigation was, however, devoted to examination of the fundamentals which affect magnetic-amplifier performance, and as such, the use of

the mechanical differential analyzer has been very valuable, both in indicating the precise nature of the amplifier performance, and in crystallizing concepts which affect magnetic-amplifier performance.

the mechanical differential analyzer has been very valuable, both in indicating the precise nature of the amplifier performance, and in crystallizing concepts which affect magnetic-amplifier performance.

CHAPTER V

REGENERATIVE FEEDBACK IN MAGNETIC AMPLIFIERS

The Use of Regenerative Feedback in Magnetic Amplifiers

As a means of improving the gain of the magnetic amplifier, the use of regenerative feedback has proved valuable. Since the magnetic amplifier is limited in time-response to relatively low values, conceivably part of the additional gain obtainable by feedback circuitry might well be sacrificed in an effort directed toward reduction of characteristic time, with a resultant over-all improvement in the performance of the feedback circuit as contrasted with the performance of the basic circuit.

The first noted use of regenerative-feedback techniques was that of P. H. Dowling of the Union Switch and Signal Company, who patented a positive-feedback amplifier in 1929. The techniques used by Dowling were greatly extended by two German engineers, Theodor Buchhold and Wilhelm Geyger, during and in the few years preceding World War II. Recently, under the auspices of the Navy Department, Bureau of Ordnance, experimental investigations of positive feedback techniques have been continued in detail at the Naval Ordnance Laboratory, White Oak, Maryland.

In view of the interest being currently shown in the use of regenerative feedback, it was deemed advisable to examine briefly the use of positive feedback in magnetic amplifiers as an extension of the basic studies which were defined as the primary objective of this research.

CHAPTER V

REGENERATIVE FEEDBACK IN MAGNETIC AMPLIFIERS

The Use of Regenerative Feedback in Magnetic Amplifiers

As a means of improving the gain of the magnetic amplifier, the use of regenerative feedback has proved valuable. Since the magnetic amplifier is limited in time-response to relatively low values, successively part of the additional gain obtainable by feedback circuitry might well be sacrificed in an effort directed toward reduction of characteristic time, with a resultant over-all improvement in the performance of the feedback circuit as contrasted with the performance of the basic circuit.

The first noted use of regenerative-feedback techniques was that of F. H. Bowling of the Union Switch and Signal Company, who patented a positive-feedback amplifier in 1929. The techniques used by Bowling were greatly extended by two German engineers, Theodor Rudhold and Wilhelm Geyger, during and in the few years preceding World War II. Recently, under the auspices of the Navy Department, Bureau of Ordnance, experimental investigations of positive feedback techniques have been continued in detail at the Naval Ordnance Laboratory, White Oak, Maryland.

In view of the interest being currently shown in the use of regenerative feedback, it was deemed advisable to examine briefly the use of positive feedback in magnetic amplifiers as an extension of the basic studies which were defined as the primary objective of this research.

Theory of Regenerative Feedback in Magnetic Amplifiers*

Let us consider for a moment a basic magnetic amplifier in which an additional set of windings have been applied to each core. The additional set of windings is to be wound with exactly the same number of turns as employed on the output circuit of the basic amplifier; that is

$$N_2 = N_3 , \qquad (5\text{-}1)$$

where N_3 is the number of turns per core of the additional winding. The tertiary windings are connected in a manner which will cause the fluxes produced by currents in these windings to be additive to the fluxes produced by currents in the input-circuit coils. The current flowing in the output circuit of the amplifier is rectified in an ordinary full-wave-rectifier bridge, and the rectified current is applied to the tertiary or feedback windings. The nature of the connections required is shown in Figure 3-1.

It has been pointed out previously that the average value of the output ampere-turns of the basic amplifier is approximately equal to the average value of the input ampere-turns over the region of normal amplification. When the output current is rectified and applied to the feedback windings, which, we recall, have the same turns as the output circuit, it is clear that the ampere-turns of magnetizing force in the feedback circuit are approximately equal to the ampere-turns of the input circuit.

---

*The basic theory in the next 2½ pages is adapted from Buchhold, T., "Über Gleichstromvormagnetisierte Wechselstromdrosselspulen und der Ruckkopplung," A.f.E., 36, (1942), p. 514-534.

Theory of Degenerative Feedback in Magnetic Amplifiers*

Let us consider for a moment a basic magnetic amplifier in which an additional set of windings have been applied to each core. The additional set of windings is to be wound with exactly the same number of turns as employed on the output circuit of the basic amplifier; that is

$$N_2 = N_3 \; ; \qquad (5\text{-}1)$$

where N_3 is the number of turns per core of the additional winding. The tertiary windings are connected in a manner which will cause the fluxes produced by currents in these windings to be additive to the fluxes produced by currents in the input-circuit coils. The current flowing in the output circuit of the amplifier is rectified in an ordinary full-wave-rectifier bridge, and the rectified current is applied to the tertiary or feedback windings. The nature of the connections required is shown in Figure 5-1.

It has been pointed out previously that the average value of the output ampere-turns of the basic amplifier is approximately equal to the average value of the input ampere-turns over the region of normal amplification. When the output current is rectified and applied to the feedback windings, which, we recall, have the same turns as the output circuit, it is clear that the ampere-turns of magnetizing force in the feedback circuit are approximately equal to the ampere-turns of the input circuit.

---

*The basic theory in the next 2½ pages is adapted from Buchholz, T., "Über Gleichstromvormagnetisierte Wechselstromdrosselspulen und der Rückkopplung," A.f.E., 36, (1942), p. 314-334.

Since the fluxes produced by the magnetizing force in the feedback circuit are additive to those produced by the input-circuit magnetizing force, it is possible to state that the feedback magnetizing force may be represented by the distance $(NI)_3$ on the modulation characteristic of Figure 5-1. It will be noted that $(NI)_3$ is of sufficient magnitude to provide the magnetizing force necessary to extend just to the 45° slope line, which represents the ideal case. If the amplifier is to be operated at the point "P", it is then necessary that the input circuit provide only the magnetizing force represented by the distance $(NI)_1'$. The magnitude of $(NI)_1'$ depends upon the permeability of the core material, and can be made very small if the permeability is great. Since $(NI)_1'$ is of much lesser magnitude than $(NI)_1$, the power gain of the amplifier operating at point "P" is much improved by the addition of the feedback windings. The new condition in the amplifier input circuit may be expressed

$$(NI)_1 = (NI)_3 + (NI)_1' . \qquad (5-2)$$

The average value of the output ampere-turns remains unchanged although the required input ampere-turns have been reduced. It may be seen in the exaggerated drawing of Figure 5-1 that below the point "A", the value of $(NI)_1'$ required to operate along the modulation characteristic is measured in the negative direction. At point "A", $(NI)_1'$ becomes zero and above this point the feedback input-magnetizing-force, $(NI)_1'$, becomes positive, eventually

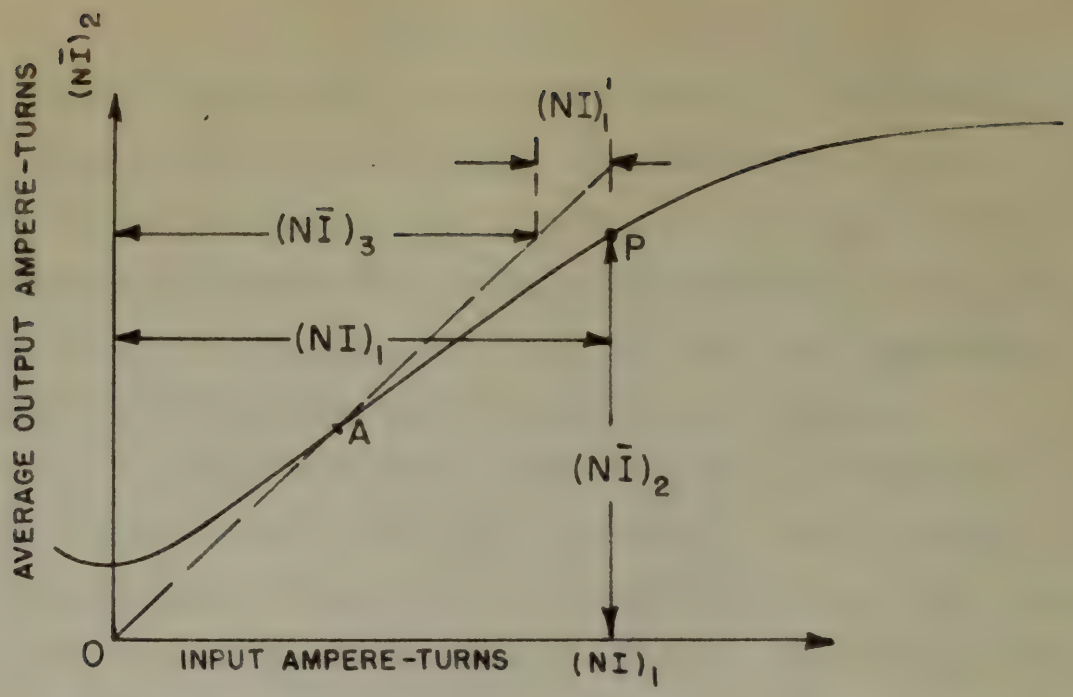

FIG. 5-1 (a) FULLY-COMPENSATED FEEDBACK.

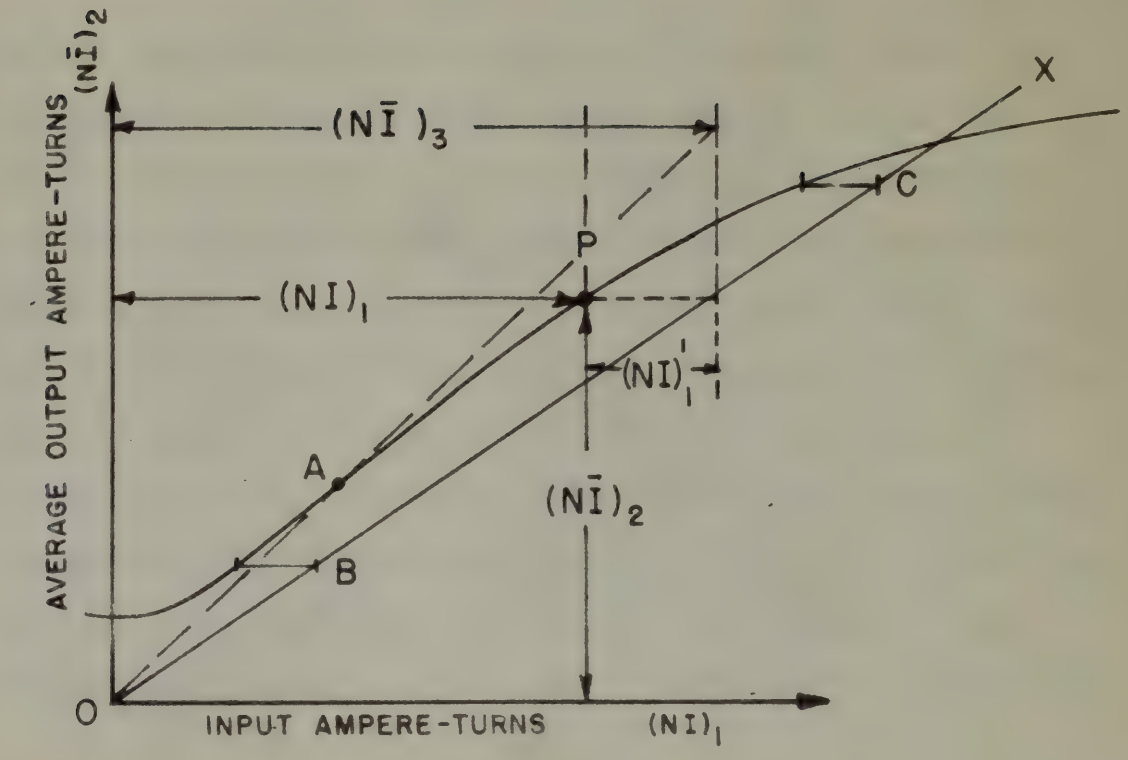

FIG. 5-1 (b) OVER-COMPENSATED FEEDBACK.

becoming very great as saturation occurs. From these considerations it is possible to construct a revised modulation characteristic for the feedback case. Such a revised characteristic is shown in Figure 5-7. The case which has been discussed, i.e., $N_2 = N_3$, has been designated as fully-compensated regenerative-feedback.

If the feedback turns, N_3, are increased to some value greater than N_2, the value of $(NI)_3$ becomes greater than $(NI)_2$, since the currents are the same. Consequently, $(NI)_3$ is of greater magnitude than $(NI)_1$. On a modulation characteristic, as shown in Figure 5-1(b), it is seen that $(NI)_3$ is measured to the line O-X which has a slope of less than 45°, the actual value of this slope being dependent on the ratio of N_3 to N_2 and defined by

$$\tan \theta = \frac{N_2}{N_3} \qquad (5\text{-}3)$$

Under these conditions the point "A" is seen to occur at an increased value of output ampere-turns. Above the point "A", saturation occurs rapidly, and consequently, the usable portion of the characteristic is represented by that portion lying below "A". In this region $(NI)_1'$ is at all times measured in the negative direction. It will be noticed that at two points, "B" and "C", the values of $(NI)_1'$ are equal. This equality results in an instability in the amplifier performance and in a discontinuity in the revised modulation characteristic. The nature of this singularity is shown more clearly in Figure 5-7, where it

$$\tan\theta = \frac{M_2^3}{M_1^3} \qquad (5\text{-}3)$$

Under these conditions the point "A" is seen to occur at an increased value of output temperature. Above the point "A_o" saturation ceases to exist, and consequently the usable portion of the characteristic is terminated at that position lying below "A". In this region $(XI)_2^3$ is at all times measured in the negative direction. It will be noticed that at the points, "B" and "C", the values of $(XI)_1^3$ are equal. This equality inevitably results in an instability in the amplifier performance and is a disadvantage in the desired modulation characteristic. The nature of this instability is shown more clearly in Figure 5-7, where it is clearly to be seen that $(XI)^3$ is of greater magnitude when M_2^3 is of greater magnitude than M_1^3, since the output is the same. Conversely, $(XI)^3$ is of greater magnitude when M_1^3 is of greater magnitude than M_2^3, the value of $(XI)^3$ becomes a modulation characteristic, as shown in Figure 5-7(b), it is seen that $(XI)^3$ is measured on the line O-C which has a slope of less than β_0^0, the actual value of this slope depending on the ratio of M^3 to M^3 and defined by

If the feedback terms, M^3, are increased so some value greater than B^3, the value of $(XI)^3$ becomes mutually, $(XI)^3$ is of greater magnitude when $(XI)^3$. On greater than $(XI)^3$, since the outputs are the same. Considering the fully-compensated temperature-feedback.

mated as fully-compensated temperature-feedback.

ratio has been changed, i.e., $M_2^3 = M_1^3$, has been investigated in the amplifier performance and is a distinct disadvantage in the desired modulation characteristic. The nature of this instability is shown more clearly in Figure 5-7, where it is clearly to be seen that $(XI)^3$ is of greater magnitude when M_2^3 is of greater magnitude than M_1^3, since the outputs are the same. Conversely, $(XI)^3$ is of greater magnitude when M_1^3 is of greater magnitude than M_2^3, the value of $(XI)^3$ becomes a modulation characteristic, as shown in Figure 5-7(b), it is seen that $(XI)^3$ is measured on the line O-C which has a slope of less than β_0^0, the actual value of this slope depending on the ratio of M^3 to M^3 and defined by

$$\tan\theta = \frac{M_2^3}{M_1^3} \qquad (5\text{-}3)$$

Under these conditions the point "A" is seen to occur at an increased value of output temperature. Above the point "A_o" saturation ceases to exist, and consequently the usable portion of the characteristic is terminated at that position lying below "A". In this region $(XI)_2^3$ is at all times measured in the negative direction. It will be noticed that at the points, "B" and "C", the values of $(XI)_1^3$ are equal. This equality inevitably results in an instability in the amplifier performance and is a disadvantage in the desired modulation characteristic. The nature of this instability is shown more clearly in Figure 5-7, where it

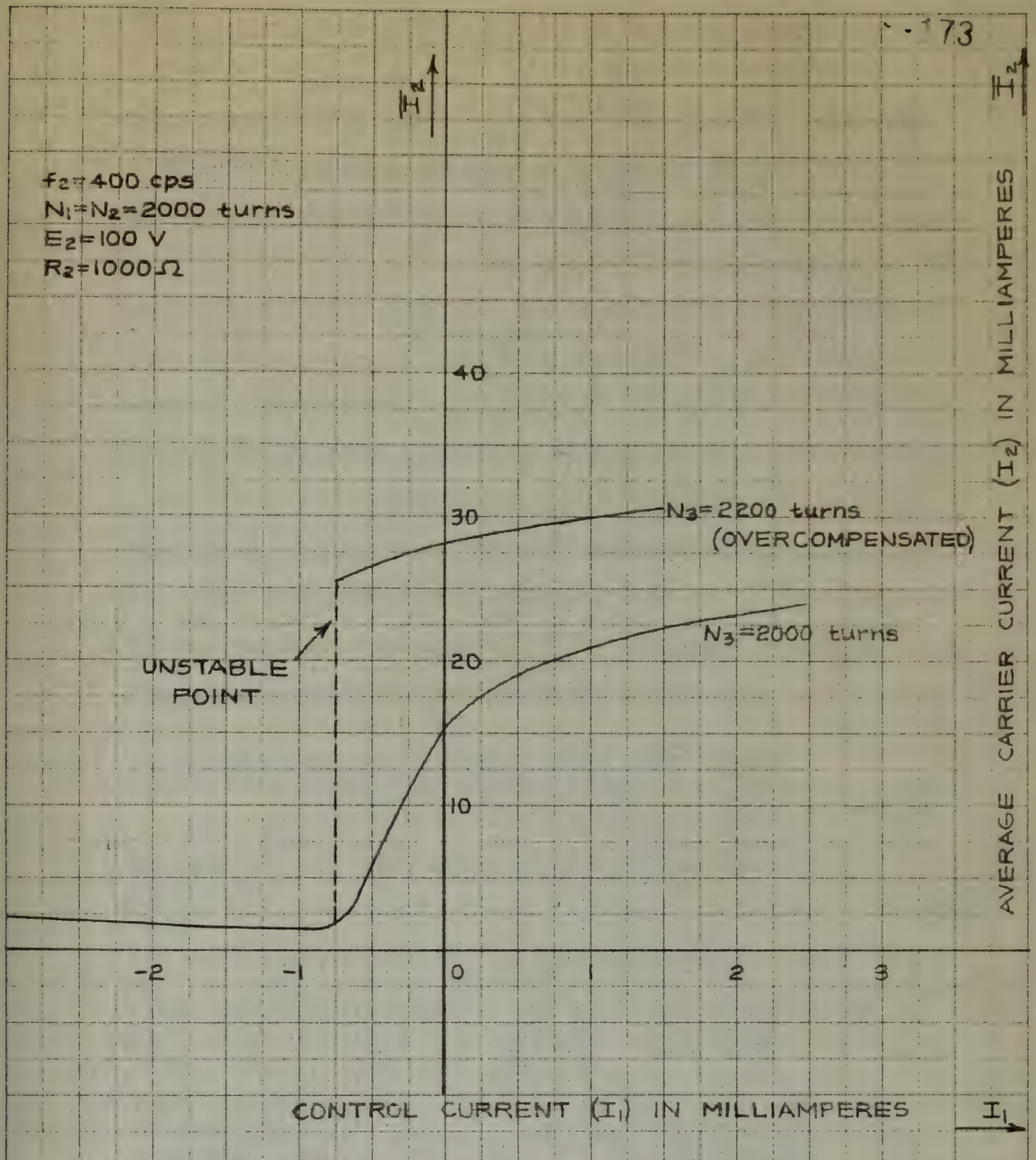

FIG. 5-7 MODULATION CHARACTERISTIC FOR MAGNETIC AMPLIFIER WITH POSITIVE FEEDBACK SHOWING EFFECT OF OVERCOMPENSATION

may be seen that, because of the discontinuity, there is a very rapid rise in $(NI)_2$ for a minute change in the input magnetizing force, corresponding to the double-valued function of $(NI)_2$ at the value of $(NI)_1'$ represented by "B" and "C" of Figure 5-1(a). The value of overcompensated feedback, as this situation is designated, for on-off control, is obvious. Large output currents are controlled by extremely small changes in the input current. It is possible to add a fourth set of windings to the magnetic amplifier, which, when fed with an additional supply, will bias the overcompensated characteristic of Figure 5-7 toward the right in Figure 5-7 in a manner which will cause the singularity to occur at the origin.

Static Characteristics of Feedback Operation

A comparison between practical cases of fully-compensated and overcompensated feedback is shown on Figure 5-7. Actually, there is some question as to whether the case represented by the modulation characteristic for fully compensated feedback does indeed represent the optimum value of 100% compensation. The reader will recall that the windings of the cores used for the study were tapped every 200 turns, and under these conditions, it is thus theoretically possible to make $(NI)_2$ equal to $(NI)_3$. In the practical situation, however, although N_2 is equal to N_3, it is likely that I_3 is slightly less than I_2 because some losses and distortion are inevitable in the rectifier

may be seen that, because of the discontinuity, there is a very rapid rise in $(NI)_2$ for a minute change in the input magnetizing force, corresponding to the double-valued function of $(NI)_2$ at the value of $(NI)_1'$ represented by "B" and "C" of Figure 5-1(a). The value of overcompensated feedback, as this situation is designated, for on-off control, is obvious. Large output currents are controlled by extremely small changes in the input current. It is possible to add a fourth set of windings to the magnetic amplifier, which, when fed with an additional supply, will bias the overcompensated characteristic of Figure 5-7 toward the right in Figure 5-7 in a manner which will cause the singularity to occur at the origin.

Static Characteristics of Feedback Operation

A comparison between practical cases of fully-compensated and overcompensated feedback is shown on Figure 5-7. Actually, there is some question as to whether the case represented by the modulation characteristic for fully compensated feedback does indeed represent the optimum value of 100% compensation. The reader will recall that the windings of the cores used for the study were tapped every 200 turns, and under these conditions, it is thus theoretically possible to make $(NI)_2$ equal to $(NI)_3$. In the practical situation, however, although N_2 is equal to N_3, it is likely that I_3 is slightly less than I_2 because some losses and distortion are inevitable in the rectifier

units. It would, therefore, have been desirable to have provided a means of increasing the turns in the feedback winding by some small amount in order to maintain $(NI)_3$ equal to $(NI)_2$ by compensation for the rectifier distortion and losses. Unfortunately, such a procedure was precluded in this brief study because the toroids were potted in Ceresin Wax in order to increase the breakdown-voltage between windings during studies made of the basic circuit. In general, it is recommended that means be provided in the breadboard circuit to make smaller adjustments of the number of turns in the feedback windings. Perhaps under these conditions, a steeper curve than that shown for fully compensated feedback in Figure 5-7 would then be attainable.

It is essential, whenever regenerative feedback is employed, that the rectifier bridge be perfectly symmetrical. If such symmetry does not exist, an unbalanced waveform will be observed in the current in the feedback windings, which results in an unbalance in the output current waveform. Four Kenwood-Linze Type 32681 selenium rectifier units were available for this study. Dissimilarity between these units made it undesirable to use the dry-disc rectifier bridge, however, because of the unbalanced waveforms produced. Consequently, a rectifier bridge composed of two 6H6 double diodes was constructed. Approximately ten of these tubes were tested before a sufficiently matched pair was found to eliminate asymmetry

in the output waveform of the amplifier. In the practical magnetic amplifier, the use of dry-disc type rectifiers is highly desirable, because the filament-supply problem is eliminated. In the laboratory tests, convenience indicated the use of the diode bridge. A comparison of the modulation characteristics produced by the bridge composed of type 32681 selenium rectifiers and the 6H6 diode bridge is shown in Figure 5-2. The steeper slope associated with the dry-disc rectifier bridge justifies the use of these units when matched pairs are selected. In general, the use of dry-disc rectifiers is desirable because the amplifier circuit is then wholly without tubes.

The subject of the choice of rectifier units for the feedback magnetic-amplifier requires further study.

The shape of the modulation characteristics for magnetic amplifiers utilizing fully-compensated feedback depends on the factors which influence the shape of the modulation characteristics for the basic circuit. This statement is borne out by the measured feedback modulation-characteristics of Figures 5-3, 5-5 and 5-6, which show the effects of R_2, E_2 and N_2 respectively.

The modulation characteristics of Figure 5-3 are quite similar to those of the basic circuit in which a variation in the load resistance R_2 is made. The falling off of the characteristic for large load resistances is again apparent. The nature of this flattening has been discussed in connection with investigations of the basic

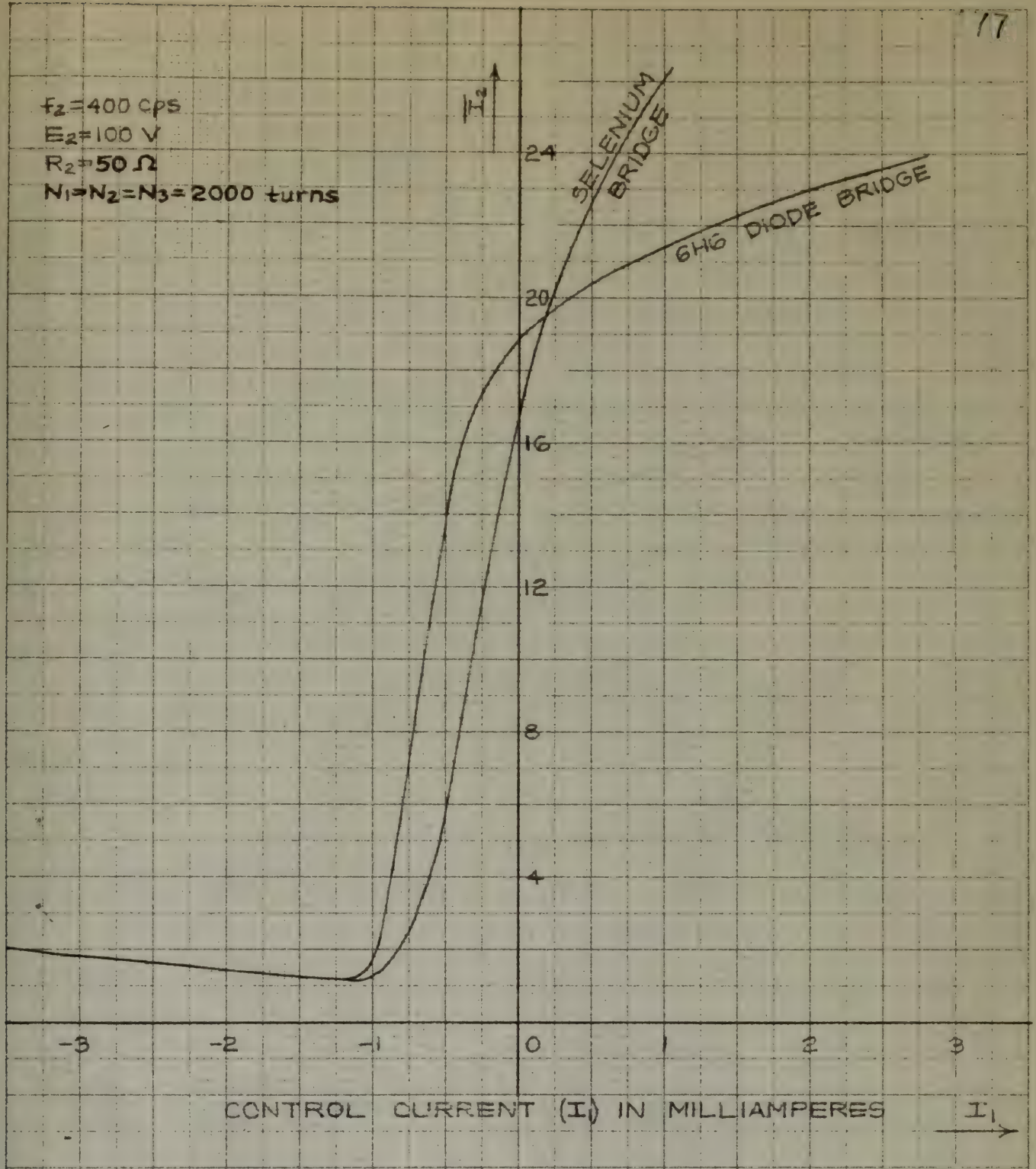

FIG. 5-2 MODULATION CHARACTERISTIC OF MAGNETIC AMPLIFIER WITH POSITIVE FEEDBACK SHOWING COMPARISON OF PERFORMANCE OF A SELENIUM AND A DIODE RECTIFIER BRIDGE.

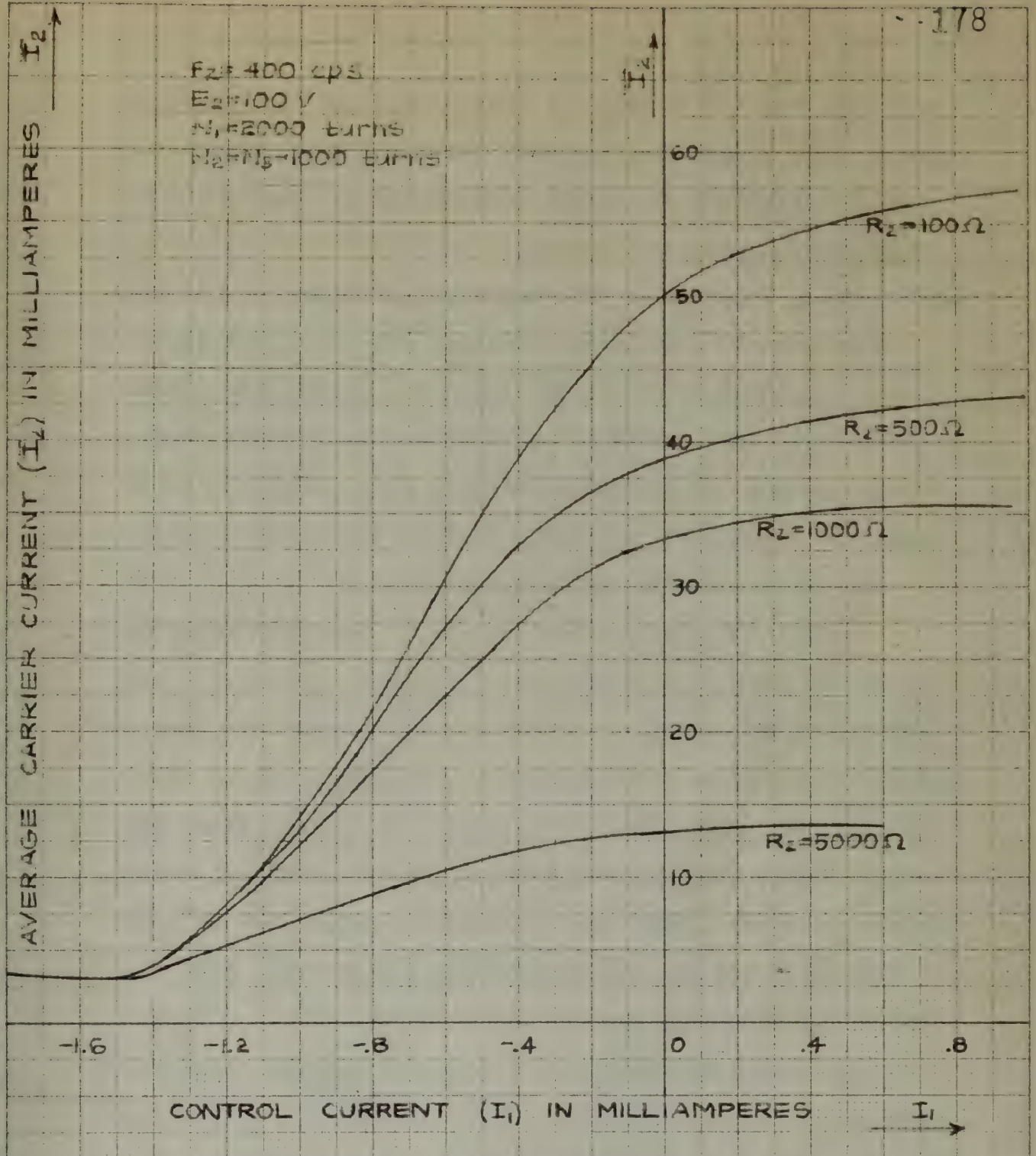

FIG. 5-3 MODULATION CHARACTERISTIC OF MAGNETIC AMPLIFIER WITH POSITIVE FEEDBACK SHOWING EFFECTS OF CHANGING THE LOAD RESISTANCE (R_L).

JULY 29, 1948

circuit, and the discussions in Chapter III are directly extendable to the present feedback situation. The curves of Figure 5-3 attain further practical significance when converted to curves which indicate the power output and gain of the magnetic amplifier at given input power levels. Invariably, when the feedback connection is used in a single amplifier, the additional set of windings, called either biasing or compensation windings, and designed to shift the modulation characteristic to the right, are employed. The shift is made such that the dip of the modulation characteristic occurs at the origin, i.e., for zero input current. In the power-output and gain characteristics shown, it is assumed that such an additional winding has been employed to shift the characteristic to the right by 1.5 milliamperes on the input scale. The power necessary to supply the additional windings is readily available from the a-c power supply after a portion of the supply current is rectified. This conversion has been carried out and the results are shown plotted in Figure 5-4. The power output in watts is plotted versus the input current squared. The input resistance is again omitted, as was the case with similar curves for the basic circuit, in order to allow flexibility in the selection of this parameter, because of the important effect of R_1 in determining the characteristic time of the dynamic performance of the amplifier. On the same figure, the gain of the amplifier times the input circuit resistance is plotted

circuit, and the discussions in Chapter III are directly extendable to the present feedback situation. The curves of Figure 5-3 attain further practical significance when converted to curves which indicate the power output and gain of the magnetic amplifier at given input power levels. Invariably, when the feedback connection is used in a single amplifier, the additional set of windings, called either biasing or compensation windings, and designed to shift the modulation characteristic to the right, are employed. The shift is made such that the dip of the modulation characteristic occurs at the origin, i.e., for zero input current. In the power-output and gain characteristics shown, it is assumed that such an additional winding has been employed to shift the characteristic to the right by 1.5 milliamperes on the input scale. The power necessary to supply the additional windings is readily available from the a-c power supply after a portion of the supply current is rectified. This conversion has been carried out and the results are shown plotted in Figure 5-4. The power output in watts is plotted versus the input current squared. The input resistance is again omitted, as was the case with similar curves for the basic circuit, in order to allow flexibility in the selection of this parameter, because of the important effect of R_1 in determining the characteristic time of the dynamic performance of the amplifier. On the same figure, the gain of the amplifier times the input circuit resistance is plotted

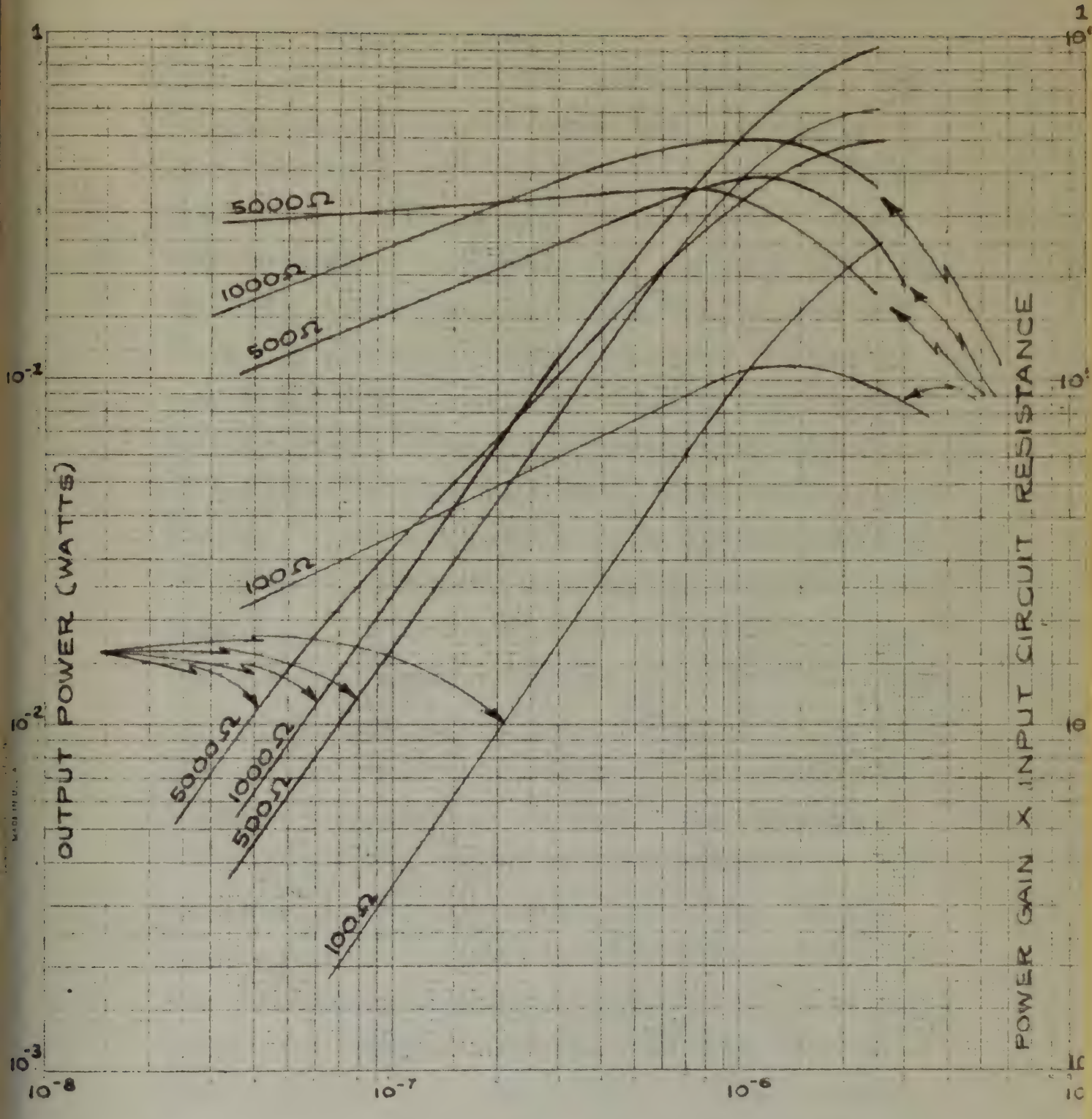

FIG. 5-4 POWER OUTPUT AND GAIN FOR THE FULLY-COMPENSATED FEEDBACK CONNECTION PLOTTED VERSUS (INPUT CURRENT)^2.

versus $(I_1)^2$. It is apparent, from these curves, that there is a definite optimum value of R_2 at which the gain reaches a maximum. This peaking occurs for a value of R_2 of approximately 1000 ohms, and at a value of (input current)^2 equal to 10^{-6} amps.^{2}. The curves indicate that the choice of load resistance must be based upon the level of input power (represented by $(I_1)^2$) and then selected from the optimum gain conditions at this level. In some cases it may be necessary to sacrifice gain in order to obtain larger values of output power. The gain curves of Figure 5-4 were made with 2000 turns on the input windings, while gain curves shown in Figure 3-19 were observed for 3600 turns on the input windings. If the curves of Figure 5-4 are corrected by the squared turns ratio criterion established by Equation 3-17, it may be seen by comparing Figures 3-19 and 5-4 that a gain improvement, depending on the magnitude of the input resistance, of the order of 100 to 150, is possible with regenerative feedback in the region where the squared value of the input current is approximately 10^{-6}. This is the value of $(I_1)^2$ at which the gain of the feedback circuit reaches a maximum, and also is a value at which the basic-circuit gain-characteristic is at its maximum point. For identical conditions, the improvement in power output is of the same order as the improvement in gain with positive feedback. A careful adjustment of the feedback turns as described to obtain perfect 100% feed-

back might permit a better gain improvement than that shown in these limited observations. Both Figure 3-19 and Figure 5-4 emphasize the important and somewhat unfortunate part played by the input resistance in determining the gain available from a given magnetic amplifier. Again, these figures emphasize the significant fact that excellent gains are obtainable with a magnetic amplifier if dynamic response is of sufficiently small importance to permit the use of a minimum input resistance.

The effect of the magnitude of the peak alternating voltage, E_2, in the feedback case is also analogous to this effect in the basic amplifier. The value selected should, for optimum operation, be sufficient to produce a flux with peak amplitude equal to ϕ_s. Values of applied voltage of lesser magnitude result in premature flattening of the modulation characteristic, as shown in Figure 5-5. If E_2 is sufficiently great to produce alternating fluxes of magnitudes greater than ϕ_s, the minimum or dip point of the feedback modulation characteristic will be increased, and the excitation current flowing in the output windings for zero input-current is increased to an undesirable figure. The discussion here implies that the modulation characteristic has been shifted to the right by an additional set of coils so that the minimum of the characteristic occurs at zero input current.

The effects of N_2, which must equal N_3 theoretically, are also similar in the feedback case to those

back might permit a better gain improvement than that shown in these limited observations. Both Figure 3-19 and Figure 3-4 emphasize the important and somewhat unfortunate part played by the input resistance in determining the gain available from a given magnetic amplifier. Again, these figures emphasize the significant fact that excellent gains are obtainable with a magnetic amplifier if dynamic response is of sufficiently small importance to permit the use of a minimum input resistance.

The effect of the magnitude of the peak alternating voltage, E_p, in the feedback case is also analogous to this effect in the basic amplifier. The value selected should, for optimum operation, be sufficient to produce a flux with peak amplitude equal to ϕ_s. Values of applied voltage of lesser magnitude result in premature flattening of the modulation characteristic, as shown in Figure 3-5. If E_p is sufficiently great to produce alternating fluxes of magnitudes greater than ϕ_s, the minimum or dip point of the feedback modulation characteristic will be increased, and the excitation current flowing in the output windings for zero input-current is increased to an undesirable figure. The discussion here implies that the modulation characteristic has been shifted to the right by an additional set of coils so that the minimum of the characteristic occurs at zero input current.

The effects of E_p, which must equal E_s theoretically, are also similar in the feedback case to those

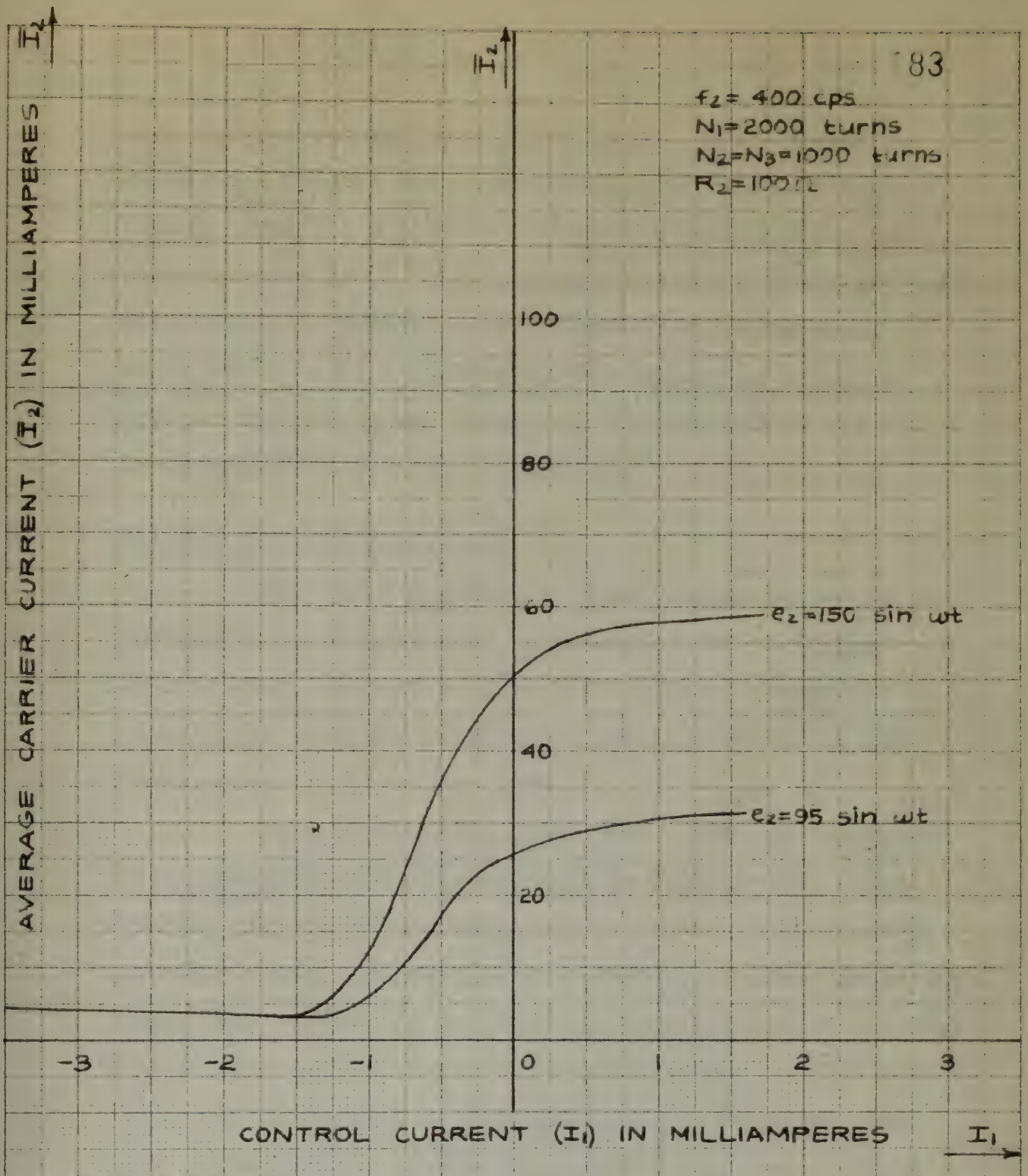

FIG. 5-5 MODULATION CHARACTERISTIC OF MAGNETIC AMPLIFIER WITH POSITIVE FEEDBACK SHOWING EFFECTS OF CHANGING THE APPLIED ALTERNATING VOLTAGE.

effects observed in the basic circuit. N_2 must also be adjusted such that the peak excursion of the alternating flux is equal to ϕ_s, or the minimum points of the modulation characteristic will be raised, as shown in Figure 5-6. This effect is particularly evident in the modulation curve for $N_2 = N_3 = 600$ turns. The selection of N_2, as well as that of E_2 and frequency, is governed by the optimum magnitude of alternating flux.

The Theory of Feedback Gain

The basic concepts of regenerative-feedback, as introduced by Buchhold and discussed in the early pages of this chapter, are extended in the following paragraphs to explain the gain characteristics obtainable with fully-compensated regenerative-feedback.

Formulas for the power gain of the basic amplifier were developed and presented in Chapter III. When dealing with magnetic amplifiers it is also convenient to consider either ampere-turn gain or current gain, since the power gain of the amplifier depends upon the currents in the input and output circuits. The developments of this section will be devoted to consideration of the ampere-turn gain of the basic magnetic amplifier and of the magnetic amplifier with regenerative feedback.

In the idealized magnetic amplifier, as discussed in Chapter III, it has been shown that

effects observed in the basic circuit. N_2 must also be adjusted such that the peak excursion of the alternating flux is equal to ϕ_s, or the minimum points of the modulation characteristic will be raised, as shown in Figure 5-6. This effect is particularly evident in the modulation curve for $N_2 = N_3 = 600$ turns. The selection of N_2, as well as that of N_2 and frequency, is governed by the optimum magnitude of alternating flux.

<u>The Theory of Feedback Gain</u>

The basic concepts of regenerative-feedback, as introduced by Bockhold and discussed in the early pages of this chapter, are extended in the following paragraphs to explain the gain characteristics obtainable with fully-compensated regenerative-feedback.

Formulas for the power gain of the basic amplifier were developed and presented in Chapter III. When dealing with magnetic amplifiers it is also convenient to consider either ampere-turn gain or current gain, since the power gain of the amplifier depends upon the currents in the input and output circuits. The development of this section will be devoted to consideration of the ampere-turn gain of the basic magnetic amplifier and of the magnetic amplifier with regenerative feedback.

In the idealized magnetic amplifier, as discussed in Chapter III, it has been shown that

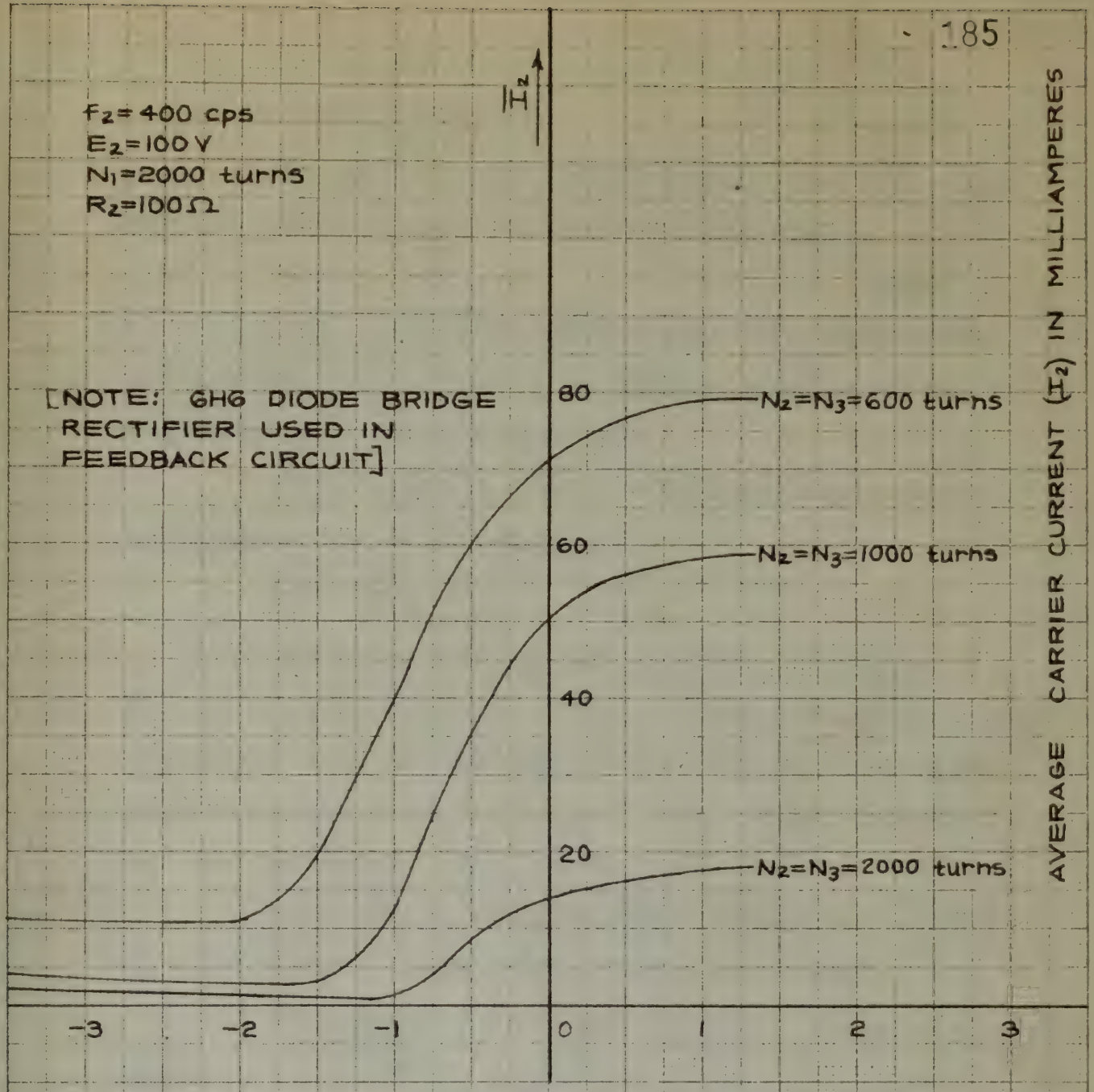

FIG. 5-6 MODULATION CHARACTERISTIC OF MAGNETIC AMPLIFIER WITH POSITIVE FEEDBACK SHOWING EFFECT OF CHANGING THE NUMBER OF TURNS IN OUTPUT (N_2) AND FEEDBACK (N_3) WINDINGS.

JULY 28, 1948

$$(NI)_1 = (N\bar{I})_2 \qquad (5\text{-}4)$$

In the practical basic-amplifier, the equivalent concept, because permeability is not infinite, is

$$(NI)_1 \cong (N\bar{I})_2 \qquad (5\text{-}5)$$

Actually $(NI)_1$ is slightly greater than $(N\bar{I})_2$, the amount greater being, as was shown, an inverse function of the permeability of the core material.

It is possible, then, to define the ampere-turn gain, K_I, of the basic amplifier:

$$K_I = \frac{(N\bar{I})_2}{(NI)_1} \qquad (5\text{-}6)$$

The value of K_I is ideally unity; in the practical case K_I is less than unity. Although the ampere-turn gain is equal to or less than unity, it is still possible to obtain power gains in the basic circuit and the method has been developed. (See Equation 3-17.)

According to accepted feedback-theory, the gain of a system with regenerative feedback is defined

$$K' = \frac{K}{1-\beta K} \qquad (5\text{-}7)$$

where

K' = gain of the feedback system,

K = gain of the system without feedback,

β = feedback ratio.

By reference to Figure 5-1(a) and Equation 5-2, the following relationships for the feedback system are established:

$$(NI)_1 = (N\bar{I})_2 \qquad (5\text{-}4)$$

In the practical basic-amplifier, the equivalent concept, because permeability is not infinite, is

$$(NI)_1 \cong (N\bar{I})_2 \qquad (5\text{-}5)$$

Actually $(NI)_1$ is slightly greater than $(N\bar{I})_2$, the amount greater being, as was shown, an inverse function of the permeability of the core material.

It is possible, then, to define the ampere-turn gain, K_I, of the basic amplifier:

$$K_I = \frac{(N\bar{I})_2}{(NI)_1} \qquad (5\text{-}6)$$

The value of K_I is ideally unity; in the practical case K_I is less than unity. Although the ampere-turn gain is equal to or less than unity, it is still possible to obtain power gains in the basic circuit and the method has been developed. (See Equation 3-17.)

According to accepted feedback-theory, the gain of a system with regenerative feedback is defined

$$K' = \frac{K}{1-\beta K} \qquad (5\text{-}7)$$

where

K' = gain of the feedback system,

K = gain of the system without feedback,

β = feedback ratio.

By reference to Figure 5-1(a) and Equation 5-2, the following relationships for the feedback system are established:

$$K = \frac{(N\bar{I})_2}{(NI)_1} = \frac{(N\bar{I})_2}{(NI)_1' + (N\bar{I})_3} \qquad (5\text{-}8)$$

Ideally for full compensation

$$(N\bar{I})_2 = (N\bar{I})_3 , \qquad (5\text{-}9)$$

but in the practical case $(N\bar{I})_2$ is slightly greater than $(N\bar{I})_3$ because of loss in the rectifier system. The feedback ratio is defined

$$\beta = + \frac{(NI)_3}{(NI)_2} \qquad (5\text{-}10)$$

From Equations 5-7, 5-8 and 5-10

$$K' = \frac{\dfrac{(N\bar{I})_2}{(NI)_1' + (N\bar{I})_3}}{1 - \dfrac{(N\bar{I})_2}{(NI)_1' + (N\bar{I})_3}} \qquad (5\text{-}11)$$

or

$$K' = \frac{(N\bar{I})_2}{(NI)_1' + (N\bar{I})_3 - (N\bar{I})_2} \qquad (5\text{-}12)$$

Let us consider Equation 5-12 in the light of the idealized situation of infinite permeability. Under these conditions $(NI)_1'$ is identically zero, $(N\bar{I})_2$ and $(N\bar{I})_3$ are equal, the denominator is zero and K' becomes infinite. We see that the ampere-turn gain has been increased in the ideal case from unity for the basic circuit to infinity for the case of fully-compensated feedback.

In the practical case, of course, $(NI)_1'$ is a finite value and an inverse function of permeability, while the difference between $(N\bar{I})_2$ and $(N\bar{I})_2$ is small and a direct function of the rectifier losses and distor-

$$K = \frac{(\overline{NI})_2}{(NI)_1} = \frac{(\overline{NI})_2}{(NI)_1' + (\overline{NI})_3} \qquad (5\text{-}8)$$

Ideally for full compensation

$$(\overline{NI})_2 = (\overline{NI})_3 \, , \qquad (5\text{-}9)$$

but in the practical case $(\overline{NI})_2$ is slightly greater than $(\overline{NI})_3$ because of loss in the rectifier system. The feedback ratio is defined

$$\beta = + \frac{(NI)_3}{(NI)_2} \qquad (5\text{-}10)$$

From Equations 5-7, 5-8 and 5-10

$$K' = \frac{\dfrac{(\overline{NI})_2}{(NI)_1' + (\overline{NI})_3}}{1 - \dfrac{(\overline{NI})_2}{(NI)_1' + (\overline{NI})_3}} \qquad (5\text{-}11)$$

or

$$K' = \frac{(\overline{NI})_2}{(NI)_1' + (\overline{NI})_3 - (\overline{NI})_2} \qquad (5\text{-}12)$$

Let us consider equation 5-12 in the light of the idealized situation of infinite permeability. Under these conditions $(NI)_1'$ is identically zero, $(\overline{NI})_2$ and $(\overline{NI})_3$ are equal, the denominator is zero and K' becomes infinite. We see that the ampere-turn gain has been increased in the ideal case from unity for the basic circuit to infinity for the case of fully-compensated feedback.

In the practical case, of course, $(NI)_1'$ is a finite value and an inverse function of permeability, while the difference between $(\overline{NI})_2$ and $(\overline{NI})_3$ is small and a direct function of the rectifier losses and distor-

tion. The value of K' is still very large. Equation 5-12 indicates that high-permeability core-materials and low-loss rectifiers are essential for feedback magnetic-amplifier designs.

Dynamic Performance with Regenerative Feedback

The time available for dynamic feedback studies was very limited, and did not permit a thorough investigation of this subject. A few remarks relative to the effect of regenerative feedback on the dynamic performance of the amplifier are, however, presented here.

It would be desirable to be able to predict the dynamic performance of the feedback amplifier from the dynamic performance of the basic circuit, since it is possible, within reasonable limits, to anticipate the dynamic behavior of the basic circuit by methods which have already been described in the earlier chapters. A means for such a prediction is not, however, apparent to the authors at the present time. The additional feedback windings, and the buildup in current in these windings, involve factors which greatly complicate the dynamic behavior. The effect of input-circuit current on dynamic performance is also complicated by the addition of feedback windings. In the basic circuit, the biasing input-current for an alternating signal may be selected anywhere in a wide range of linear ampere-turn sensitivity. Reference to any of the feedback modulation characteristics in this chapter will show that, in the feedback case, the

tion. The value of K' is still very large. Equation 5-12 indicates that high-permeability core-materials and low-loss rectifiers are essential for feedback magnetic-amplifier designs.

Dynamic Performance with Regenerative Feedback

The time available for dynamic feedback studies was very limited, and did not permit a thorough investigation of this subject. A few remarks relative to the effect of regenerative feedback on the dynamic performance of the amplifier are, however, presented here.

It would be desirable to be able to predict the dynamic performance of the feedback amplifier from the dynamic performance of the basic circuit, since it is possible, within reasonable limits, to anticipate the dynamic behavior of the basic circuit by methods which have already been described in the earlier chapters. A means for such a prediction is not, however, apparent to the authors at the present time. The additional feedback windings, and the buildup in current in these windings, involve factors which greatly complicate the dynamic behavior. The effect of input-circuit current on dynamic performance is also complicated by the addition of feedback windings. In the basic circuit, the biasing input-current for an alternating signal may be selected anywhere in a wide range of linear ampere-turn sensitivity. References to any of the feedback modulation characteristics in this chapter will show that, in the feedback case, the

range of selection is greatly narrowed, and is, in general, limited to somewhere in the range from 0.3 to 1.3 milliamperes. The limitation is a result of the fact that much of the effective "input" magnetizing force is, in effect, supplied by the feedback windings, since these windings are connected in a manner additive to the input circuit windings.

A single sinusoidal band-pass characteristic for a feedback amplifier is shown in Figure 5-8. The input resistance is approximately 7000 ohms plus the resistance of the windings. The biasing current is 0.7 ma., which insures operation over the most linear portion of the feedback modulation-characteristic. The observed bandwidth is seen to be of the order of 12 cycles per second, which is rather low for many applications, and certainly lower than what might be expected from the basic circuit with a 7K input resistance and a moderately large biasing current. The fact that the biasing current may be lower in the feedback case is no specific advantage, since this current can be readily supplied by rectifying a portion of the main supply voltage; the power consumed is thence independent of the signal source. At any rate, a substantial reduction in bandpass is apparent for the feedback circuit as compared with the basic circuit under similar conditions. Of course, the gain has been improved by the use of regenerative feedback.

range of selection is greatly narrowed, and is, in general, limited to somewhere in the range from 0.3 to 1.3 milliamperes. The limitation is a result of the fact that much of the effective "input" magnetizing force is, in effect, supplied by the feedback windings, since these windings are connected in a manner additive to the input circuit windings.

A single sinusoidal band-pass characteristic for a feedback amplifier is shown in Figure 5-8. The input resistance is approximately 7000 ohms plus the resistance of the windings. The biasing current is 0.7 ma., which insures operation over the most linear portion of the feedback modulation-characteristic. The observed bandwidth is seen to be of the order of 12 cycles per second, which is rather low for many applications, and certainly lower than what might be expected from the basic circuit with a 7A input resistance and a moderately large biasing current. The fact that the biasing current may be lower in the feedback case is an specific advantage, since this current can be readily supplied by rectifying a portion of the main supply voltage; the power consumed is thence independent of the signal source. At any rate, a substantial reduction in bandpass is apparent for the feedback circuit as compared with the basic circuit under similar conditions. Of course, the gain has been improved by the use of regenerative feedback.

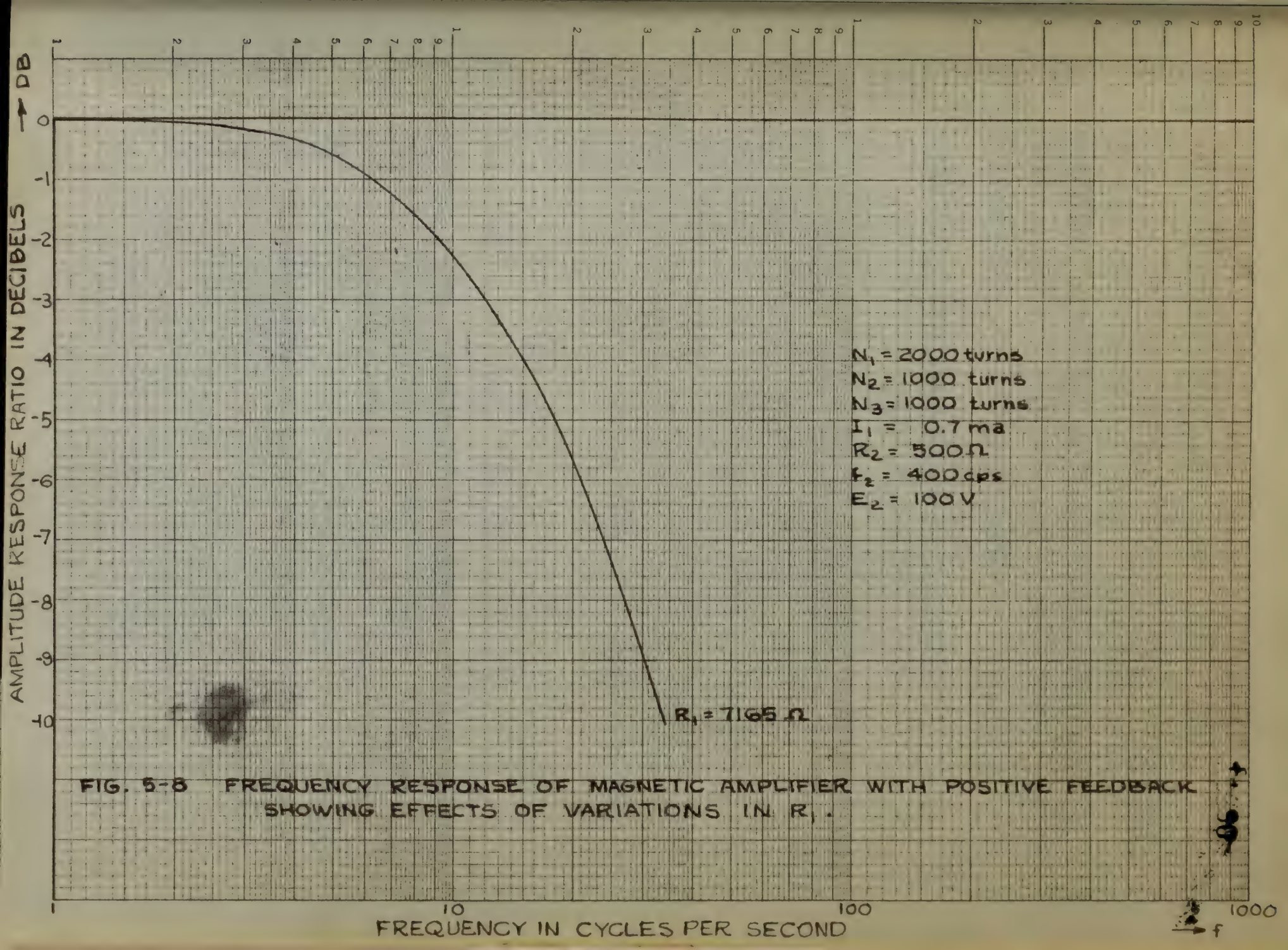

FIG. 5-8 FREQUENCY RESPONSE OF MAGNETIC AMPLIFIER WITH POSITIVE FEEDBACK SHOWING EFFECTS OF VARIATIONS IN R_1.

The proportionate improvement in gain and reduction in dynamic performance should be investigated more thoroughly. The effect of the use of regenerative-ampere-turn feedback on the gain-bandwidth product, rather than on gain alone, is particularly worthy of further study.

Analytical Equations of the Feedback Amplifier

A set of analytical equations, similar to those employed in the solution of the basic magnetic amplifier, may be prepared for the regenerative-feedback amplifier. The regenerative-feedback amplifier-circuit is shown in schematic form in Figure 5-9. New parameters defined by this figure include the resistance of the feedback windings, R_3, the forward resistance of a single rectifier unit, R_f, and the current i_3 which is the rectified value of i_2. Thus

$$i_3 = \pm i_2 \qquad (5\text{-}13)$$

where the signs alternate each half-cycle of the carrier voltage. Ideal rectification is assumed in the rectifier units to the extent that the back resistance is infinite and the forward resistance is a constant independent of the value of i_2. In the practical rectifier, both forward and back resistance are nonlinear functions of the exciting current, and such a function could be readily handled by a differential analyzer. The equivalent circuit of the idealized rectifier and the feedback circuit as seen by i_2 is shown for one half-cycle in Figure 5-10(a), and

The proportionate improvement in gain and reduction in dynamic performance should be investigated more thoroughly. The effect of the use of regenerative-ampere-turn feedback on the gain-bandwidth product, rather than on gain alone, is particularly worthy of further study.

Analytical Equations of the Feedback Amplifier

A set of analytical equations, similar to those employed in the solution of the basic magnetic amplifier, may be prepared for the regenerative-feedback amplifier. The regenerative-feedback amplifier-circuit is shown in schematic form in Figure 5-9. New parameters defined by this figure include the resistance of the feedback windings, R_3, the forward resistance of a single rectifier unit, R_r, and the current i_3 which is the rectified value of i_2. Thus

$$i_3 = \pm i_2 \qquad (5\text{-}13)$$

where the signs alternate each half-cycle of the carrier voltage. Ideal rectification is assumed in the rectifier units to the extent that the back resistance is infinite and the forward resistance is a constant independent of the value of i_2. In the practical rectifier, both forward and back resistance are nonlinear functions of the exciting current, and such a function could be readily handled by a differential analyzer. The equivalent circuit of the idealized rectifier and the feedback circuit as seen by i_2 is shown for one half-cycle in Figure 5-10(a), and

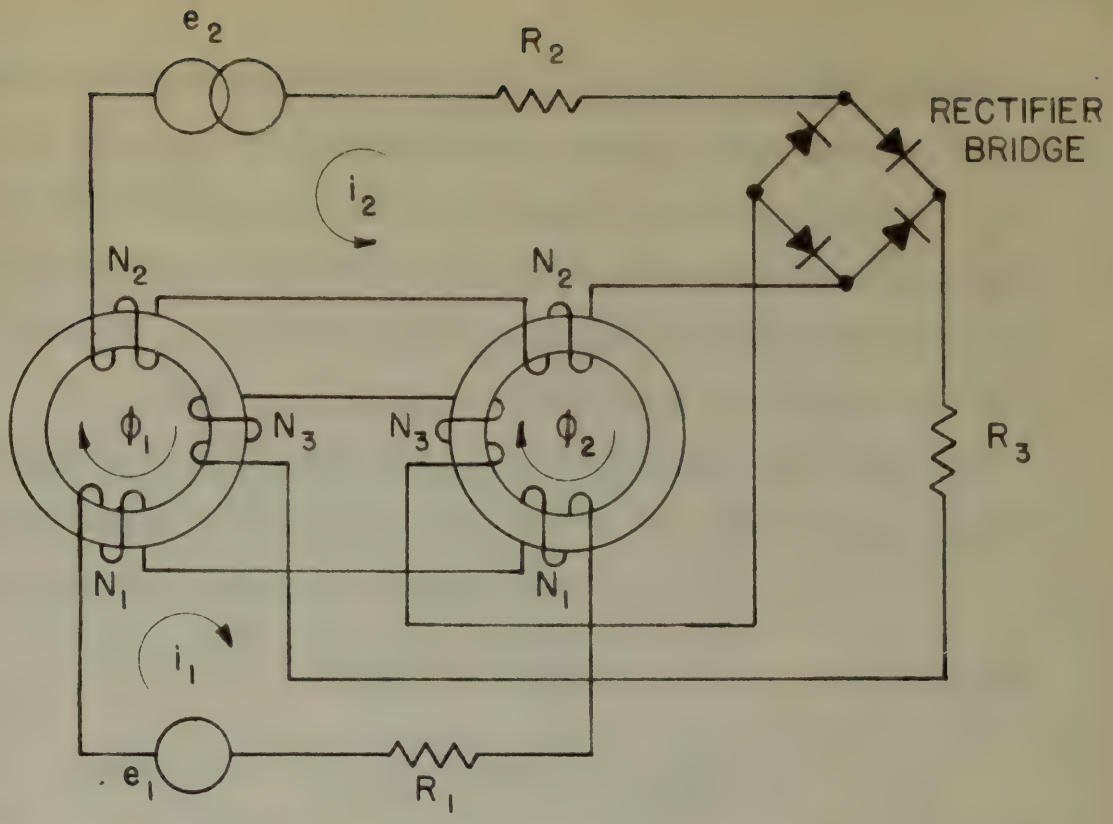

FIG. 5-9 REGENERATIVE FEEDBACK CIRCUIT.

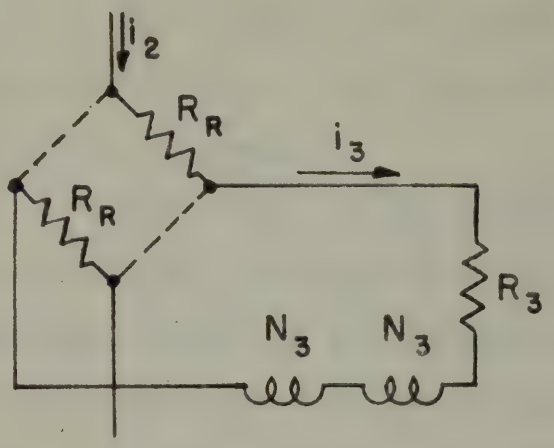

(a) EQUIVALENT RECTIFIER CIRCUIT FOR IST HALF CYCLE.

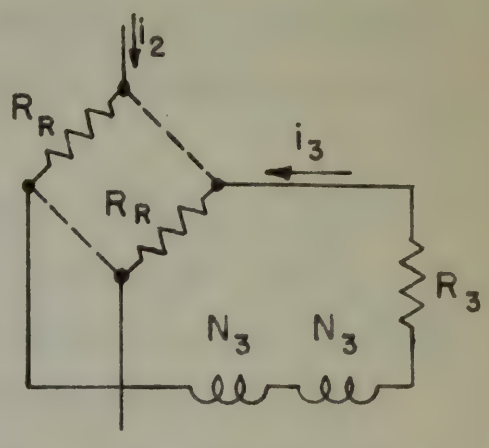

(b) EQUIVALENT RECTIFIER CIRCUIT FOR 2ND HALF CYCLE.

FIG. 5-10 RECTIFIER CIRCUITS.

for the next alternating half-cycle in Figure 5-10(b). The reversal of i_2 each half-cycle as this current flows in the feedback circuit is shown in these figures. It is also apparent that an additional resistance, $2R_r$, is included in the path of i_2 through the feedback circuit.

The system loop-equilibrium equations for the loops defined by i_1 and by i_2 (including the feedback loop and recalling Equation 5-13) are formulated from Figure 5-9 and from Figure 4-2:

$$e_1 = R_1 i_1 + N_1 \frac{d\phi_1}{dt} - N_1 \frac{d\phi_2}{dt} \qquad (5\text{-}14)$$

$$e_2 = (R_2 + 2R_r \pm R_3) i_2 + N_2 \frac{d\phi_1}{dt} + N_2 \frac{d\phi_2}{dt} \pm N_3 \frac{d\phi_1}{dt} \mp N_3 \frac{d\phi_2}{dt} \qquad (5\text{-}15)$$

$$\phi_1 = f(N_2 i_2 + N_1 i_1 \pm N_3 i_3) \qquad (5\text{-}16)$$

$$\phi_2 = f(N_2 i_2 - N_1 i_1 \mp N_3 i_3) \qquad (5\text{-}17)$$

The $\pm$ signs in the above equations are associated with rectification of i_2 when this current is applied to the feedback circuit.

A problem for the differential analyzer could be formulated from Equations 5-14 to 5-17 inclusive. The mechanical layout of the differential analyzer would require provision for reversing the signs each half-cycle, as indicated in the equations. The reversal might be accomplished by including a set of idler gears in each appropriate gear

for the next alternating half-cycle in Figure 5-10(b). The reversal of i_2 each half-cycle as this current flows in the feedback circuit is shown in these figures. It is also apparent that an additional resistance, $2R_r$, is included in the path of i_2 through the feedback circuit.

The system loop-equilibrium equations for the loops defined by i_1 and by i_2 (including the feedback loop and recalling Equation 5-13) are formulated from Figure 5-9 and from Figure 4-2:

$$e_1 = R_1 i_1 + N_1 \frac{d\phi_1}{dt} - N_1 \frac{d\phi_2}{dt} \qquad (5\text{-}14)$$

$$e_2 = (R_2 + 2R_r \pm R_3)\, i_2 + N_2 \frac{d\phi_1}{dt} + N_2 \frac{d\phi_2}{dt} \pm N_3 \frac{d\phi_1}{dt} \mp N_3 \frac{d\phi_2}{dt} \qquad (5\text{-}15)$$

$$\phi_1 = f\,(N_2 i_2 + N_1 i_1 \pm N_3 i_3) \qquad (5\text{-}16)$$

$$\phi_2 = f\,(N_2 i_2 - N_1 i_1 \mp N_3 i_3) \qquad (5\text{-}17)$$

The $\pm$ signs in the above equations are associated with rectification of i_2 when this current is applied to the feedback circuit.

A problem for the differential analyzer would be formulated from Equations 5-14 to 5-17 inclusive. The mechanical layout of the differential analyzer would require provision for reversing the signs each half-cycle, as indicated in the equations. The reversal might be accomplished by including a set of idler gears in each appropriate gear

box. As i_2 passes through zero in the solution, it would then be necessary to stop the machine and reverse the necessary shafts through use of the idlers. The value of an analytical study based upon these equations would be weighed, as was the investigation of the basic circuit of this thesis, against the importance of the losses in the carrier circuit, but would undoubtedly be of significant value in elucidating many of the features of regenerative-feedback magnetic-amplifier performance.

CHAPTER VI

SUMMARY AND CONCLUSIONS

Summary of the Research

This thesis has attempted to investigate the fundamental behavior of the magnetic amplifier both from experimental and analytic studies. Although various articles have appeared in the literature pertaining to the static performance of the amplifier, relatively little has been published concerning circuit dynamics. Both static and dynamic aspects have been explored in this research, with particular emphasis on dynamic studies based upon both transient and frequency-response data. The mathematical analysis of the circuit is complicated by the nonlinear nature of the differential equations which characterize the system. The solution of these equations by means of the differential analyzer is believed to be an original effort. In order to arrive at circuit fundamentals, the simplest case of interest was chosen as the starting point of the investigation. This circuit is the basic magnetic amplifier which involves no feedback techniques. A thorough study was made of the basic circuit correlating experimental and analytical data wherever possible. A rather large amount of experimental characteristics have been included in the thesis because of the paucity of concrete design data in the literature. It is hoped that the inclusion of this data may be of some value to future investigators. After studies of the basic circuit

CHAPTER VI

SUMMARY AND CONCLUSIONS

Summary of the Research

were completed, the remaining available time was devoted to experimental investigations of regenerative ampere-turn feedback.

Results of the Research

A thorough study was made of the basic magnetic amplifier and quantitative design criteria were obtained. The effects of all circuit parameters were studied, a family of curves being plotted for each parametric variation. These curves, as determined experimentally, are reproduced in Chapter III. An analytic formulation of the basic-circuit problem in terms of the differential loop-equilibrium equations was made, neglecting hysteresis and eddy-current losses, and the machine solutions were compared with experimentally determined steady-state and transient response. The results of this study, which are tabulated in Figure 6-1, indicate satisfactory agreement between experimental and theoretical steady-state performance. Important differences were obtained, however, between experimental and theoretical dynamic behavior. Although the effect of the control-circuit parameters upon the effective characteristic time agreed in both cases, the dependence of characteristic time upon carrier-circuit conditions revealed major discrepencies. These inconsistencies are attributable to the functional relation of the core losses upon the carrier-circuit conditions, as expressed by Equation 3-27, and which was neglected in the analytic solutions.

TABULATION OF RESULTS

I STATIC TRENDS - THE EFFECT OF ONE PARAMETER UPON THE MODULATION CHARACTERISTIC, OTHER PARAMATERS CONSTANT.

PARAMETER		EXPERIMENTAL	ANALYTICAL	REMARKS
CONTROL CIRCUIT	R_1	NEGLIGIBLE	NEGLIGIBLE	NATURAL MAGNETIZATION - LOW CONTROL CIRCUIT IMPEDANCE TO CARRIER EVEN - HARMONICS
	N_1	NEGLIGIBLE	NEGLIGIBLE	
CARRIER CIRCUIT	R_2	INCREASING R_2 INCREASES LINEAR RANGE	ANALYTIC RESULTS CHECK EXPERIMENTAL TRENDS OVER THE LOWER INPUT RANGE; NOT EXAMINED OVER HIGHER INPUT RANGE.	AFFECTS ONLY E_L/E_2 CHARACTERISTIC (FIG. 3-5)
	E_2	INCREASING E_2 INCREASES LINEAR RANGE		AFFECTS ONLY A.C. FLUX AMPLITUDE
	f_2	INCREASING f_2 DECREASES LINEAR RANGE		AFFECTS BOTH E_L/E_2 AND FLUX AMPLITUDE
	N_2	OPTIMUM N_2 EXISTS FOR MINIMUM LINEAR RANGE		AFFECTS BOTH E_L/E_2 AND FLUX AMPLITUDE

II DYNAMIC TRENDS - THE EFFECT OF ONE PARAMETER UPON THE EFFECTIVE CHARACTERISTIC TIME, OTHER PARAMETERS CONSTANT.

PARAMETER		EXPERIMENTAL FREQUENCY-RESPONSE	EXPERIMENTAL TRANSIENT	ANALYTICAL TRANSIENT	REMARKS
CONTROL CIRCUIT	I_1	$(CT) \rightarrow \frac{1}{\sqrt{I_1}}$	$(CT) \rightarrow \frac{1}{\sqrt{I_1}}$	$(CT) \rightarrow \frac{1}{\sqrt{I_1}}$	ALL CHECK
	R_1	$(CT) \rightarrow \frac{1}{R_1}$	$(CT) \rightarrow \frac{1}{R_1}$	$(CT) \rightarrow \frac{1}{R_1}$	ALL CHECK
	N_1	$(CT) \rightarrow N_1$	$(CT) \rightarrow N_1$	$(CT) \rightarrow N_1$	ALL CHECK
CARRIER CIRCUIT	R_2	$(CT) \rightarrow (R_2)^{1/3}$	NEGLIGIBLE	NEGLIGIBLE	ANALYSIS NEGLECTED CORE-LOSS FUNCTION THEREFORE DIFFERENT FROM EXPERIMENTAL DATA. FREQUENCY-RESPONSE DATA INVOLVES CONSTANT I_1 BIAS; WHILE I_1 TRANSIENT BUILDS UP FROM ZERO; HENCE THE DIFFERENCE.
	E_2	$(CT) \rightarrow (E_2)^{1/5}$	$(CT) \rightarrow (E_2)^{1/5}$	$(CT) \rightarrow \frac{1}{E_2}$	
	f_2	$(CT) \rightarrow \frac{1}{f_2}$	$(CT) \rightarrow \frac{1}{(f_2)^{1/10}}$	NOT EXAMINED	
	N_2	$(CT) \rightarrow \frac{1}{N_2}$	$(CT) \rightarrow \frac{1}{\sqrt{N_2}}$	$(CT) \rightarrow N_2$	

FIG. 6-1 BASIC CIRCUIT STUDIES.

The differential analyzer was directly responsible for disclosing two effects which otherwise might have escaped observation. These were, first, the concept of flux-bias buildup, and secondly, the relation of hysteresis to the carrier-current waveform. Finally, an approximate expression for power gain, Equation 3-17, was developed. By comparing this relation with the effects of circuit parameters upon characteristic time, tabulated in Figure 6-1, it is evident that a compromise between gain and bandwidth must be accepted.

Results from the studies of the regenerative ampere-turn feedback connection are more of a qualitative nature than quantitative. Lack of time curtailed a more thorough investigation of this circuit. As would be expected from a consideration of feedback-amplifier theory, the sensitivity of this circuit is much greater than that of the equivalent basic circuit, but the bandwidth is much less. Further study should indicate whether or not an overall improvement of the gain-bandwidth product can be obtained with the feedback connection. Experimentation with this circuit revealed that the rectifier bridge must be carefully balanced if a symmetrical carrier-current waveform is to be obtained.

Conclusions

The results indicate that certain design criteria have been obtained which will permit a prediction of both power-gain and amplifier-bandwidth. It has been shown that

The differential analyzer was directly responsible for disclosing two effects which otherwise might have escaped observation. These were, first, the concept of flux-bias buildup, and secondly, the relation of hysteresis to the carrier-current waveform. Finally, an approximate expression for power gain, Equation 3-17, was developed. By comparing this relation with the effects of circuit parameters upon characteristic time, tabulated in Figure 6-1, it is evident that a compromise between gain and bandwidth must be accepted.

Results from the studies of the regenerative ampere-turn feedback connection are more of a qualitative nature than quantitative. Lack of time curtailed a more thorough investigation of this circuit. As would be expected from a consideration of feedback-amplifier theory, the sensitivity of this circuit is much greater than that of the equivalent basic circuit, but the bandwidth is much less. Further study should indicate whether or not an overall improvement of the gain-bandwidth product can be obtained with the feedback connection. Experimentation with this circuit revealed that the rectifier bridge must be carefully balanced if a symmetrical carrier-current waveform is to be obtained.

Conclusions

The results indicate that certain design criteria have been obtained which will permit a prediction of both power-gain and amplifier-bandwidth. It has been shown that

a compromise between the two, consistent with the requirements of the particular application, must be sought. In order to crystallize these concepts, a sample design to meet fixed specifications is outlined in the Appendix. Model theory could then be applied to miniaturize this design, a consideration of importance where space and weight must be minimized.

The value of the analytic approach cannot be overestimated. It has been valuable in disclosing the importance of hysteresis and eddy-current loss in the cores. It has been of assistance in establishing the transient behavior of flux bias. But perhaps the most beneficial result obtained from the solution of the problem on the differential analyzer was the appreciation of the physical significance of the differential equations acquired by watching the relative motion of the shafts which represented the system variables. This intuitive feeling for the fundamentals of the circuit would be most difficult, if not impossible, to acquire from experimental observations alone. Any variable of interest can readily be plotted by the analyzer as a function of time, and both the transient and steady-state behavior simultaneously determined.

A study of the frequency-response characteristics has disclosed that the magnetic amplifier can be characterized by a first-order time constant when an incremental signal is superimposed upon a direct-current

bias. Although the first-order concept is not original with this thesis, it does not appear that the above information has yet been used to clarify certain criteria that Alexanderson established in 1916 for the gain of the magnetic amplifier.[1] According to Alexanderson, the ratio of amplification is roughly proportional to the ratio of the carrier frequency to the signal frequency. The frequency response of the magnetic amplifier has been shown to be flat in the low-frequency range, and subsequently to fall off at 6 db/octave in the higher ranges. The critical frequency of the amplifier is inherently low, as can be observed from the frequency-response characteristics of Chapter III. The reason Alexanderson observed the gain to be inversely proportional to the audio frequency can be attributed to the fact that the bandwidth of his amplifier was very low and that he was actually operating in the cutoff region of the amplitude response where the slope is, indeed, inversely proportional to the frequency - in other words, in the region where the response falls off at 6 db/octave.

The magnetic amplifier has been used for a number of years in automatic-control,[2] measuring,[3] and audio systems.[1] The principal limitation of this highly inductive

---

1. Alexanderson, E.F.W. and S.F. Nixdorf, "A Magnetic Amplifier for Radio Telephony," I.R.E. Proc., 4, (1916), 101-129.
2. Giroz, H.E., "Application of Magnetic Amplifiers to the Control and Automatic Regulation of Furnace Temperatures," Bull. Soc. Franc. Elec., 1, (1941), 459-497.
3. Geyger, W., "Magnetische Verstärker fur die Mess und Regeltechnik," E.T.Z., 62, (1941), 849-853, 891-898.

bias. Although the first-order concept is not original with this thesis, it does not appear that the above information has yet been used to clarify certain criteria that Alexanderson established in 1916 for the gain of the magnetic amplifier.[1] According to Alexanderson, the ratio of amplification is roughly proportional to the ratio of the carrier frequency to the signal frequency. The frequency response of the magnetic amplifier has been shown to be flat in the low-frequency range, and subsequently to fall off at 6 db/octave in the higher ranges. The critical frequency of the amplifier is inherently low, as can be observed from the frequency-response characteristics of Chapter III. The reason Alexanderson observed the gain to be inversely proportional to the audio frequency can be attributed to the fact that the bandwidth of his amplifier was very low and that he was actually operating in the cutoff region of the amplitude response where the slope is, indeed, inversely proportional to the frequency - in other words, in the region where the response falls off at 6 db/octave.

The magnetic amplifier has been used for a number of years in automatic-control,[2] measuring,[3] and audio systems.[1] The principal limitation of this highly inductive

---

1. Alexanderson, S.F.W. and S.E. Sindorf, "A Magnetic Amplifier for Radio Telephony," I.R.E. Proc., 4, (1916), 101-129.
2. Girez, H.E., "Application of Magnetic Amplifiers to the Control and Automatic Regulation of Furnace Temperatures," Bull. Soc. Franc. Elec., 1, (1941), 459-497.
3. Geyger, W., "Magnetische Versterker für die Mess und Regeltechnik," E.T.Z., 62, (1941), 649-653, 691-698.

device is its inherently narrow bandwidth. The future value of the amplifier in applications other than direct-current instruments lies in the success with which bandwidth can be increased while still maintaining reasonable gain. The use of the magnetic amplifier in automatic control has thus far been limited to medium and low-speed servomechanisms having bandwidths in the order of 1 cycle per second.[1] Within the last few months a recent development has occurred which indicates that higher bandwidths combined with reasonable gain can be obtained. This event was the announcement of a two-stage magnetic audio-amplifier having a 3kc. bandwidth, a power gain of about 10 per stage, and a 10.6 kc. power supply.[2] The saturable-reactor cores used in the design were made of improved magnetic material.

The attractive feature of long life under adverse operating conditions enjoyed by the magnetic amplifier has been the motivating force behind recent magnetic amplifier development, and results of this thesis indicate that some improvement of bandwidth while retaining reasonable gain is possible. Where high gain is desired and bandwidth is of little consequence, the magnetic amplifier has already proved its value.

Suggestions for Further Work

This thesis has investigated only the fundamentals of magnetic-amplifier performance, and a great

---

1. Rodemann, W.B., "A Study of the Magnetic Amplifier as a Servo Controller," E.E. Thesis, (M.I.T., 1947).
2. Logan, F.W., "Saturable Reactor and Magnetic Amplifier Circuits," N.O.R.L. 1091, Naval Ordnance Laboratory, White Oak, Md. (1948), 7-20.

deal of work yet remains to be done before the potentialities are fully exploited and the limitations fully understood. A thorough investigation of regenerative ampere-turn feedback is essential to the development of high-gain amplifiers. Bandwidth and stability considerations of such a circuit should be put on a quantitative basis. The performance of the feedback varistor-bridge has, in the past, been a source of trouble since the varistors are affected by changes of voltage, frequency, and particularly of temperature. Such fluctuation results in considerable variation of amplifier sensitivity.[1] The solution of this problem would increase the accuracy of magnetic-amplifier instruments. Shock and fatigue studies should be conducted to give specific data on the ability of the magnetic amplifier to maintain uniform performance over long uninterrupted periods under adverse operating conditions. The problem of noise appears completely untouched, and information as to its importance should prove valuable in establishing performance limitations. The Barkhausen effect, or discrete reversals of electron spins, is somewhat analogous to the shot effect in electronic amplifiers. This and other sources of noise should be investigated. Rigorous theoretical studies could profitably be made taking into account core loss. These studies could be extended to the feedback case. The mathematics involved in rigorous analyses is, in general, too involved for practical design engineering, and

---

1. Geyger, W., "Magnetisch Verstärker für die Mess und Regeltechnik," E.T.Z., 62, (1941), 849-853.

hence, performance criteria should be reduced wherever possible to permit linear-system approximations. Further extension of familiar amplifier configurations, such as the cascaded circuit, balanced circuit, and push-pull circuit, will undoubtedly yield other useful designs.

APPENDIX

SAMPLE DESIGN PROCEDURE

Specifications

Let us assume that the following specifications for a magnetic amplifier are given:

f = 400 cps.

BW = 40 cps.

Core type - Allegheny #4750 alloy of dimensions shown in Figure 2-4.

The amplifier is to employ the basic circuit, and is to be designed to produce maximum gain. The design will be based on empirical data, developed equations and the information of Figure 6-1.

Flux-Adjustment for Static Linear Operation

The applied alternating voltage is selected as 75 volts, rms, and the load resistance is chosen as 500 ohms from Figure 3-8. The optimum empirical value of N_2 is selected from Figure 3-10 as 1200 turns per core. The turns are to be made of No. 30 Formvar wire which has an approximate average resistance of 0.025 ohms per turn on the chosen cores.

It is desirable to use a large number of input turns in order to increase the gain, since the gain increases with the square of N_1 in accordance with Equation 3-17, whereas the bandwidth decreases directly with N_1. The principal limitation on the maximum value of N_1 is the

APPENDIX

SAMPLE DESIGN PROCEDURE

Specifications

Let us assume that the following specifications for a magnetic amplifier are given:

f = 400 cps.

BW = 40 cps.

Core type - Allegheny #4750 alloy of dimensions shown in Figure 2-4.

The amplifier is to employ the basic circuit, and is to be designed to produce maximum gain. The design will be based on empirical data, developed equations and the information of Figure 6-1.

Flux-Adjustment for Static Linear Operation

The applied alternating voltage is selected as 75 volts, rms, and the load resistance is chosen as 500 ohms from Figure 3-8. The optimum empirical value of N_2 is selected from Figure 3-10 as 1200 turns per core. The turns are to be made of No. 30 Formvar wire which has an approximate average resistance of 0.025 ohms per turn on the chosen cores.

It is desirable to use a large number of input turns in order to increase the gain, since the gain increases with the square of N_1 in accordance with Equation 3-17, whereas the bandwidth decreases directly with N_1. The principal limitation on the maximum value of N_1 is the

available core window-space. For purposes of this design, there is ample window space for 8000 turns per core for the input windings. The windings are again made of No. 30 Formvar and the total winding resistance is therefore approximately 400 ohms.

From Equation 3-17

$$K_p R_1 = \left(\frac{8000}{1200}\right)^2 \times 500 = 22.25 \times 10^3.$$

Design for Dynamic Operation

The choice of R_1 for use in the gain equation must be based on the desired bandwidth. From Figure 3-28, the following conditions are established for a particular observation:

R_1 = 2165 ohms
BW = 77 cps.
f = 400 cps.
E_2 = 75 volts rms.
R_2 = 500 ohms
N_1 = 3600 T.
N_2 = 1000 T.
I_1 = 20 ma.

The values of R_2 and E_2 for this design are identical to the above, and hence, need no further consideration. The variation of bandwidth with the effective parameters, R_1, N_1, N_2, and I_1, can be selected from Figure 6-1, recalling that bandwidth is the inverse of the defined characteristic time. The following equation may then be written:

available core window-space. For purposes of this design, there is ample window space for 8000 turns per core for the input windings. The windings are again made of No. 30 Forever and the total winding resistance is therefore approximately 400 ohms.

From Equation 3-17

$$K_2 R_1 = \left(\frac{8000}{1200}\right)^2 \times 500 = 23.25 \times 10^3.$$

Design for Dynamic Operation

The choice of R_1 for use in the gain equation must be based on the desired bandwidth. From Figure 3-28, the following conditions are established for a particular observation:

R_1 = 2165 ohms

BW = 77 cps.

f = 400 cps.

E_2 = 75 volts rms.

R_2 = 500 ohms

M_1 = 3600 T.

N_2 = 1000 T.

I_1 = 20 ma.

The values of R_2 and E_2 for this design are identical to the above, and hence, need no further consideration. The variation of bandwidth with the effective parameters, R_1, M_1, N_2, and I_1, can be selected from Figure 6-1, recalling that bandwidth is the inverse of the defined characteristic time. The following equation may then be written:

$$BW = \frac{C_1 R_1 N_2 I_1^{\frac{1}{2}}}{N_1}$$

where C_1 is a constant. Substitution of the listed values in the above equation permits solution for C_1:

$$C_1 = \frac{N_1 BW}{R_1 N_2 I_1^{\frac{1}{2}}} = \frac{3600 \times 77}{2165 \times 1000 \times 20^{\frac{1}{2}}} = 28.65 \times 10^{-3}$$

The value of the biasing current, I_1, is chosen to insure operation in the linear range. A satisfactory value is 10.0 milliamperes. The biasing current may be applied in series with the control circuit.

It is now possible to solve for R_1 from the selected parameters

N_1 = 8000 turns

N_2 = 1200 turns

I_1 = 10.0 ma.

BW = 40 cps.

$C_1 = 28.65 \times 10^{-3}$

The expression for R_1 becomes:

$$R_1 = \frac{N_1 \times BW}{C_1 N_2 I_1^{\frac{1}{2}}} = \frac{8000 \times 40}{28.65 \times 10^{-3} \times 1200 \times 10^{\frac{1}{2}}}$$

$$= \underline{2950 \text{ ohms.}}$$

The gain equation is now solvable:

$$K_p = \frac{22.25 \times 10^3}{R_1} = \frac{22.25 \times 10^3}{2950} = \underline{7.52}$$

The gain is relatively low, but the bandwidth of 40 cps. is excellent for this type amplifier.

If bandwidth considerations would permit the use of a minimum input resistance, that is, the resistance of

$$BW = \frac{C_1 R_1 R_2 I_1^{\frac{1}{2}}}{R_1}$$

where C_1 is a constant. Substitution of the listed values in the above equation permits solution for C_1:

$$C_1 = \frac{R_1 BW}{R_1 R_2 I_1^{\frac{1}{2}}} = \frac{1600 \times 77}{2165 \times 1000 \times 20^{\frac{1}{2}}} = 28.65 \times 10^{-3}$$

The value of the biasing current, I_1, is chosen to insure operation in the linear range. A satisfactory value is 10.0 milliamperes. The biasing current may be applied in series with the control circuit.

It is now possible to solve for R_1 from the selected parameters

R_1 = 8000 turns

R_2 = 1200 turns

I_1 = 10.0 ma.

BW = 44 cps.

C_1 = 28.65×10^{-3}

The expression for R_1 becomes:

$$R_1 = \frac{R_1 \times BW}{C_1 R_2 I_1^{\frac{1}{2}}} = \frac{8000 \times 40}{28.65 \times 10^{-3} \times 1200 \times 10^{\frac{1}{2}}}$$

$$= \underline{2950 \text{ ohms.}}$$

The gain equation is now solvable:

$$Kp = \frac{22.25 \times 10^{3}}{R_1} = \frac{22.25 \times 10^{3}}{2950} = \underline{7.55}$$

The gain is relatively low, but the bandwidth of 44 cps. is excellent for this type amplifier.

If bandwidth considerations would permit the use of a minimum input resistance, that is, the resistance of

the windings of the input circuit, which we recall is 2 X 8000 X 0.025, or 400 ohms, the gain becomes

$$K_p = \frac{22.25 \times 10^3}{400} = 55.5 .$$

Under these conditions, the bandwidth is reduced to

$$BW = \frac{40 \times 400}{2950} = 5.43 \text{ cps.}$$

Obviously, further increases in the input turns to entirely fill the window space will result in further increases in the gain-bandwidth product. In this particular design, however, provision is made for the addition of feedback windings.

The Addition of Feedback Windings

Sufficient window space remains to add regenerative-feedback windings to equal the windings of the output circuit for fully-compensated feedback. The improvement in gain with the feedback connection will be of the order of at least 100, and if compensation is accurately made, may be well in excess of this value. A reduction in bandwidth will undoubtedly occur. The extent of this thesis investigation does not permit a prediction to be made as to the extent of this reduction.

the windings of the input circuit, which we recall is 2 X 8000 X 0.025, or 400 ohms, the gain becomes

$$K_p = \frac{22.25 \times 10^3}{400} = 55.5 .$$

Under these conditions, the bandwidth is reduced to

$$BW = \frac{40 \times 400}{2950} = 5.43 \text{ cps.}$$

Obviously, further increases in the input burde to entirely fill the window space will result in further increases in the gain-bandwidth product. In this particular design, however, provision is made for the addition of feedback windings.

<u>The Addition of Feedback Windings</u>

Sufficient window space remains to add regenerative-feedback windings to equal the windings of the output circuit for fully-compensated feedback. The improvement in gain with the feedback connection will be of the order of at least 100, and if compensation is accurately made, may be well in excess of this value. A reduction in bandwidth will undoubtedly occur. The extent of this thesis investigation does not permit a prediction to be made as to the extent of this reduction.

BIBLIOGRAPHY

1. Alexanderson, E.F.W., and Nixdorff, S.P., "A Magnetic Amplifier for Radio Telephony," I.R.E. Proc., 4, (1916), 101-129.

2. Boyajian, A., "Mathematical Analysis of Nonlinear Circuits," G.E.Rev., 34, (1931), 531-745.

3. Buchhold, T., "Für Theorie des Magnetischen Verstärken (On the Theory of the Magnetic Amplifier)," A.f.E., 37, (1943), 197-211.

4. Buchhold, T., "Uber Gleichstromvormagnetisierte Wechselstromdrosselspulen und dern Rückkopplung (On D-C Premagnetized A-C Choke Coils and Their Feedback)," A.f.E., 36, (1942), 221-239, 514.

5. Burton, E.T., "Transformer," U. S. Patent #1,880,412, (1930).

6. Bush, V., "The Differential Analyzer," J.F.I., 212, (1931), 447-448.

7. Bush, V., and Caldwell, S.H., "A New Type Differential Analyzer," J.F.I., 240, (1945), 255-326.

8. Draper, C.S. and McKay, W., "Instrument Analysis," M.I.T. Notes, (1946).

9. Elmen, G.W., "High-Frequency Detector," U. S. Patent, #1,289,418, (1918).

10. Fitzgerald, A.S., "Magnetic Amplifier Characteristics, Neutral Type," J.F.I., 244, (1947), 415-439.

11. Fitzgerald, A.S., "Some Notes on the Design of Magnetic Amplifiers," J.F.I., 244, (1947), 323-362.

12. Fitzgerald, A.S., "Magnetic Amplifier Circuits, Neutral Type," J.F.I., 244, (1947), 249-265.

13. Geyger, W., "Magnetische Verstärken für die Mess und Regeltechnik (Magnetic Amplifiers for Measurement and Control), E.T.Z., 62, (1941), 849-853, 891-898.

14. Giroz, M.E., "Application of Magnetic Amplifiers to the Control and Automatic Regulation of Furnace Temperatures," Bul. Soc. Franc. Elect., 1, (1941), 459-479.

15. Grafinger, L.N., "A Study of Magnetic Amplifiers for Servomechanisms," S.B. Thesis, (M.I.T., 1946).

BIBLIOGRAPHY

1. Alexanderson, E.F.W., and Nixdorff, B.P., "A Magnetic Amplifier for Radio Telephony," I.R.E. Proc., 4, (1916), 101-129.

2. Boyajian, A., "Mathematical Analysis of Nonlinear Circuits," G.E. Rev., 34, (1931), 531-745.

3. Buchhold, T., "Für Theorie des Magnetischen Verstärkers (On the Theory of the Magnetic Amplifier)," A.f.E., 37, (1943), 197-211.

4. Buchhold, T., "Über Gleichstromvormagnetisierte Wechselstromdrosselspulen und deren Rückkopplung (On D-C Premagnetized A-C Choke Coils and Their Feedback)," A.f.E., 36, (1942), 221-239, 514.

5. Burkos, E.F., "Transformer," U. S. Patent #1,680,612, (1930).

6. Bush, V., "The Differential Analyzer," J.F.I., 212, (1931), 447-488.

7. Bush, V., and Gelnzell, S.H., "A-Res Type Differential Analyzer," J.F.I., 240, (1945), 255-326.

8. Draper, C.S. and McKay, W., "Instrument Analysis," M.I.T. Notes, (1946).

9. Klaen, O.W., "High-Frequency Detector," U. S. Patent, #1,269,818, (1918).

10. Fitzgerald, A.E., "Magnetic Amplifier Characteristics, Neutral Type," J.F.I., 244, (1947), 415-439.

11. Fitzgerald, A.E., "Some Notes on the Design of Magnetic Amplifiers," J.F.I., 244, (1947), 323-362.

12. Fitzgerald, A.E., "Magnetic Amplifier Circuits, Neutral Type," J.F.I., 244, (1947), 249-263.

13. Geyger, W., "Magnetische Verstärker für die Mess und Regeltechnik (Magnetic Amplifiers for Measurement and Control)," E.T.Z., 62, (1941), 849-853, 891-892.

14. Giros, H.H., "Application of Magnetic Amplifiers to the Control and Automatic Regulation of Furnace Temperatures," Bul. Soc. Franç. Elect., 1, (1941), 459-479.

15. Grafinger, L.H., "A Study of Magnetic Amplifiers for Servomechanisms," C.E. Thesis, (M.I.T., 1946).

16. Lamm, U., "The Transductor, D.C. Pre-Saturated Reactor," (Stockholm, Esselte Aktiebolag, 1943).

17. Lamson, H.W., "Alternating-Current Measurements of Magnetic Properties," I.R.E. Proc., 36, (1947), 266-277.

18. M.I.T. E.E. Staff, "Magnetic Circuits and Transformers," (New York, John Wiley and Sons, 1943), 198.

19. Naval Ordnance Laboratory Report, "Papers Presented at the Naval Ordnance Laboratory Magnetic Materials Symposium," N.O.L.R. #1091, (1948).

20. Pease, W.M., "Design of a 400 Cycle Servomechanism," E.E. Thesis, (M.I.T., 1943).

21. Rex, H.B., "The Transductor," Instruments, 20, (1947), 1102-1109.

22. Ricker and Tucker, "Electrical Engineering Laboratory Experiments," (New York, McGraw-Hill, 1940), 91-100.

23. Rockett, F., "Improved Material for Magnetic Amplifiers," Electronics, (August, 1948), 128-130.

24. Rodemann, W.B., "A Study of the Magnetic Amplifier as a Servo-Controller," E.E. Thesis, (M.I.T.),(1947).

25. Therkelsen, E.B., "A Low-Power Magnetic Amplifier for Servomechanisms," E.E. Thesis, (M.I.T.),(1946).

26. U. S. Naval Mission to Japan, "Magnetic Development in Japan during World War II," Target Report X-34N, (1946).

16. Lamm, U., "The Transductor, U.C. Pre-Saturated Reactor," (Stockholm, Esselte Aktiebolag, 1943).

17. Lamson, H.W., "Alternating-Current Measurements of Magnetic Properties," I.R.E. Proc., 35, (1947), 255-277.

18. M.I.T. E.E. Staff, "Magnetic Circuits and Transformers," (New York, John Wiley and Sons, 1943), 198.

19. Naval Ordnance Laboratory Report, "Papers Presented at the Naval Ordnance Laboratory Magnetic Materials Symposium," N.O.L.R. #1091, (1948).

20. Pease, W.M., "Design of a 400 Cycle Servomechanism," E.E. Thesis, (M.I.T., 1943).

21. Rex, M.B., "The Transductor," Instruments, 20, (1947), 1102-1109.

22. Ricker and Tucker, "Electrical Engineering Laboratory Experiments," (New York, McGraw-Hill, 1940), 91-100.

23. Rockett, F., "Improved Material for Magnetic Amplifiers," Electronics, (August, 1948), 128-130.

24. Rodemann, P.E., "A Study of the Magnetic Amplifier as a Servo-Controller," E.E. Thesis, (M.I.T.), (1947).

25. Therkelsen, E.S., "A Low-Power Magnetic Amplifier for Servomechanisms," E.E. Thesis, (M.I.T.), (1946).

26. U. S. Naval Mission to Japan, "Magnetic Development in Japan during World War II," Target Report X-34N, (1946).

APR 30
AUG 31
SEP 3
SEP 30
12 SEP 67
244
BINDERY
171
509
15731

Thesis 11256
B48 Betzer
Study of the magnetic amplifier.

12 SEP 67 15731

Thesis 11256
B48 Betzer
Study of the magnetic amplifier.

Library
U. S. Naval Postgraduate School
Monterey, California

ARTISAN
GOLD LETTERING
AND
SMITH BINDERY
OAKLAND, CALIF.

thesB48
A study of the magnetic amplifier /
3 2768 002 13794 5
DUDLEY KNOX LIBRARY